Rotating Electrical Machines

René Le Doeuff
Mohamed El Hadi Zaïm

ISTE
WILEY

Rotating Electrical Machines

Rotating Electrical Machines

René Le Doeuff
Mohamed El Hadi Zaïm

ISTE
WILEY

First published 2010 in Great Britain and the United States by ISTE Ltd and John Wiley & Sons, Inc.
Adapted and updated from *Machines électriques tournantes : de la modélisation matricielle à la mise en œuvre* published 2009 in France by Hermes Science/Lavoisier © LAVOISIER 2009

ISTE Ltd
27-37 St George's Road
London SW19 4EU
UK

www.iste.co.uk

John Wiley & Sons, Inc.
111 River Street
Hoboken, NJ 07030
USA

www.wiley.com

Library of Congress Cataloging-in-Publication Data

Le Doeuff, R.
[Machines electriques tournantes. English]
Rotating electrical machines / René Le Doeuff, Mohamed El Hadi Zaïm .
p. cm.
Includes bibliographical references and index.
ISBN 978-1-84821-169-8
1. Electric motors 2. Electric machinery--Design and construction. 3. Industrial equipment--Design and construction. I. El Hadi Zaom, Mohamed. II. Title.
TK2435.D6413 2009
621.46--dc22

2009039568

British Library Cataloguing-in-Publication Data
A CIP record for this book is available from the British Library
ISBN 978-1-84821-169-8

Printed and bound in Great Britain by CPI Antony Rowe, Chippenham and Eastbourne

Table of Contents

Preface

Rotating electrical machines provide the basis of the electromechanical energy conversion and constitute the core of a wide scientific and technological field called “electrical engineering”. This discipline has seen a very important evolution with the extensive development of related fields: power electronics, analogical and digital control techniques, etc. This revolution has led to the generalization of electrical actuators in every industrial area as well as in everyday life. It has also modified the way the machines are used while, at the same time, simplifying their adaptation to new energy sources. Therefore, this evolution has to be taken into account in the teaching of electrical machinery.

The present text is the result of our long teaching and research experience in various universities’ engineering schools, both in France and Algeria. It is intended mainly for Master’s level students enrolled in electrical engineering programs. Its aims consists of providing readers with the essential knowledge of electrical machines, their structures, the ways they can be modeled and their implementation. This basic understanding should allow them to tackle with relative ease the study of transient phenomenon, speed variation and control of drives, and any other special applications.

This methodological approach was first proposed by Professor E. J. Gudefin in Nancy (France) in the 1960s. It is based on matrix representation of the machine equations using instantaneous values of electromagnetic variables.

This modeling approach is particularly suitable for the study of electrical machines fed by static converters; and it is necessary for the analysis of machines in transient regimes or any other study that uses Concordia and Park transformations, etc. It can also be used to establish classic steady state equations of electrical motors. The calculation of the instantaneous electromagnetic torque leads to a simple and convenient representation of the association machine-converter enabling an easy understanding of the continuous energy conversion phenomenon.

The main preliminary knowledge useful for reading this text (electromagnetism, sinusoidal systems, power electronics) is gathered in Chapter 1 (Main Requirements).

General concepts are established in Chapter 2 (Introduction to Rotating Electrical Machines) and are then used for different analyses of conventional machines: Synchronous Machines (Chapter 3), Induction Machines (Chapter 4) and Direct Current Machines (Chapter 5). Many examples describing the use of these machines with and without converters are also presented. Some traditional aspects (e.g. resistive starters, circle diagrams, etc.), which are of very little use today, are still presented because of their historical and pedagogical interest.

To make this book as factual as possible, we have illustrated it with many photographs that have been graciously provided by industrial firms; most of the curves, diagrams and characteristics are those of machines that really exist. Different field distribution plots describing electromagnetic behaviours of machines have been obtained from software codes developed in our research laboratory.

We would like to acknowledge all the individuals and organizations who took part in the realization of this book:

– Our colleagues from Electrical Engineering Department of Polytech'Nantes (France), particularly Professors M.F. Benkhoris and M. Machmoum.

– Professor Bernard Multon, from École Normale Supérieure de Cachan (France).

– Professor Guy Olivier from École Polytechnique de Montréal (Canada).

– The following firms: ECA EN, Converteam and STX France (previously, Aker Yards) for generously providing most of the photographs illustrating this book.

The authors wish to pay a particular tribute to their mentor, the late Professor Emeritus Edmond J. Gudefin (1923-1996).

Chapter 1

Main Requirements

1.1. Introduction

The study of rotating electrical machines is a science which is linked with several other topics. In order to make this book easier to read, we are going to summarize the main results and concepts used later on in this introductory chapter:

– sinusoidal systems;

– electromagnetism;

– power electronics.

1.2. Sinusoidal variables

1.2.1. *Single-phase variables*

1.2.1.1. *Timed expressions*

An x variable, a timed-sinusoidal function, can be written as:

$$x = X\sqrt{2}\cos\omega t$$

where X is the rms (root-mean-square) value and ω is the angular velocity.

1.2.1.2. *Vector representation*

The x variable defined above can be considered to be the projection on an axis of a vector of length $X\sqrt{2}$ rotating anticlockwise at an angular velocity ω (Figure 1.1).

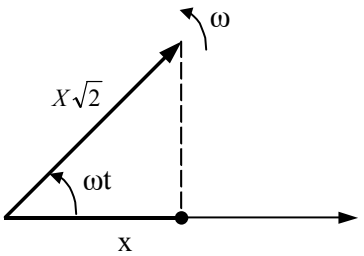

Figure 1.1. *Vector representation of a sinusoidal variable*

1.2.1.3. *Single-phase currents and voltages*

If a sinusoidal single-phase voltage v is applied at a Z impedance terminal, current i in this impedance, at steady state, is also sinusoidal, and can be written:

$$v = V\sqrt{2}\cos\omega t$$

$$i = I\sqrt{2}\cos(\omega t - \varphi)$$

φ being the phase shift between the voltage often chosen as the origin and the current. Conventionally, φ is counted positively when the current is lagging behind the voltage. The instantaneous power supplied to impedance Z is:

$$p = v.i = VI\cos\varphi + VI\cos(2\omega t - \varphi)$$

$$P = VI\cos\varphi \qquad [1.1]$$

is the active power and:

$$P_f = VI\cos(2\omega t - \varphi) \qquad [1.2]$$

is the pulsating power. It must be noted that this variable, which characterizes the fact that the single-phase power supplied to a receiver is time varying, is cancelled with balanced polyphase systems.

Figure 1.2 shows that voltage is changed into current through a similitude of ratio Z and angle φ.

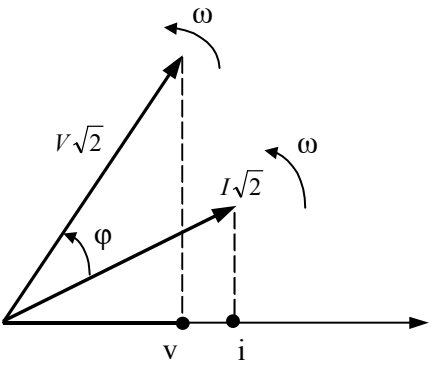

Figure 1.2. *Vector representation of sinusoidal current and voltage*

1.2.1.4. *Complex representation*

Complex numbers are very useful to represent the previous similitude and vector $\vec{V}$ will thus be associated with complex number $\bar{V}$, as well as complex number $\bar{I}$ with vector $\vec{I}$. They can then be written as follows:

$$\bar{V} = Ve^{j\omega t}$$

$$\bar{I} = Ie^{j(\omega t - \varphi)}$$

Complex impedance $\overline{Z}$ is also defined by ratio:

$$\overline{Z} = \frac{\overline{V}}{\overline{I}} = \frac{V}{I} e^{j\varphi} = Ze^{j\varphi}$$

It will be set down:

$$Z \cos \varphi = R$$

$$Z \sin \varphi = X$$

R and X respectively being the resistance and the reactance expressed in Ohms.

$\overline{S}$ is also introduced:

$$\overline{S} = \overline{VI}^* = VIe^{j\varphi} = VI \cos \varphi + jVI \sin \varphi = P + jQ \qquad [1.3]$$

$\overline{S}$ is the apparent power expressed in volt-amperes (VA). Q is the reactive power expressed in volt-amperes reactives (VA_r).

1.2.2. *2-phase voltages and currents*

A 2-phase voltage system is defined by two voltages in quadrature:

$$v_\alpha = V\sqrt{2} \cos(\omega t)$$

$$v_\beta = V\sqrt{2} \sin(\omega t)$$

if it is loaded onto a symmetrical impedance it leads to a balanced 2-phase current system:

$$i_\alpha = I\sqrt{2} \cos(\omega t - \varphi)$$

$$i_\beta = I\sqrt{2} \sin(\omega t - \varphi)$$

There is no pulsating power and the instantaneous power is constant:

$$p = 2VI\cos\varphi = P$$

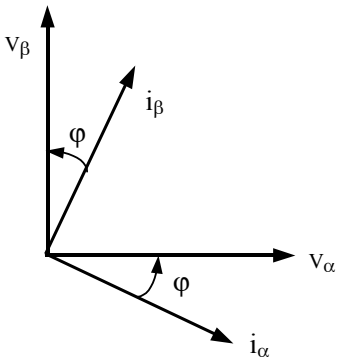

Figure 1.3. *2-phase currents and voltages*

The complex representation can also be introduced:

$$\bar{V}_\alpha = V \qquad \bar{V}_\beta = jV$$

$$\bar{I}_\alpha = Ie^{-j\varphi} \quad I_\beta = jI^{-j\varphi}$$

with the expressions of the active and reactive powers:

$$P = 2VI\cos\varphi$$

$$Q = 2VI\sin\varphi$$

1.2.3. *Balanced 3-phase sinusoidal systems*

1.2.3.1. *Time expressions*

A balanced 3-phase voltage system is composed of three voltages with the same frequency, with the same amplitude and phase shifted by a third of a period with respect to the others. It is thus written as a time expression:

$$v_a = V\sqrt{2}\cos\omega t$$

$$v_b = V\sqrt{2}\cos(\omega t - \frac{2\pi}{3})$$

$$v_c = V\sqrt{2}\cos(\omega t + \frac{2\pi}{3})$$

If this voltage system is connected to a symmetrical load (with a circulating impedance matrix), it leads to a balanced current system (Figures 1.4 and 1.5):

$$i_a = I\sqrt{2}\cos(\omega t - \varphi)$$

$$i_b = I\sqrt{2}\cos(\omega t - \frac{2\pi}{3} - \varphi)$$

$$i_c = I\sqrt{2}\cos(\omega t + \frac{2\pi}{3} - \varphi)$$

with the vector representation shown in Figure 1.4.

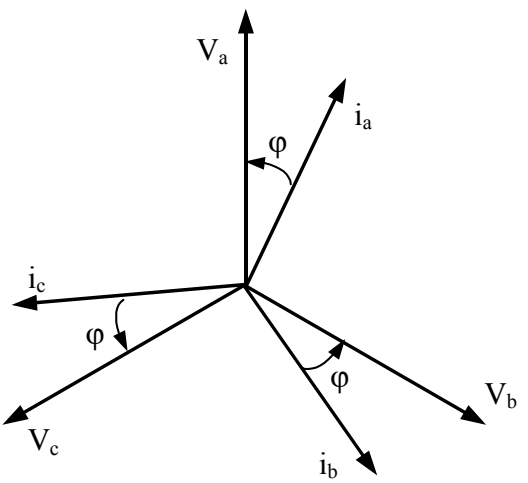

Figure 1.4. *3-phase currents and voltages*

A zero pulsating power is then obtained and the instantaneous power is constant and equal to the active power:

$$p = 3VI\cos\varphi$$

1.2.3.2. *Associated complex notations*

Complex vectors are associated with balanced voltage and current systems:

$$[\bar{V}] = \bar{V}\begin{bmatrix} 1 \\ a^2 \\ a \end{bmatrix} \quad \text{and} \quad [\bar{I}] = \bar{I}\begin{bmatrix} 1 \\ a^2 \\ a \end{bmatrix} \qquad [1.4]$$

where 1, a and a^2 are the cube roots of the unit: $a = e^{j2\pi/3}$, $a^2 = e^{j4\pi/3}$.

If the 3-phase voltage system is applied to a load characterized by a circulating impedance matrix $[\bar{Z}]$ (Figure 1.5) such as:

$$[\bar{Z}] = \begin{bmatrix} \bar{z} & \bar{z}' & \bar{z}'' \\ \bar{z}'' & \bar{z} & \bar{z}' \\ \bar{z}' & \bar{z}'' & \bar{z} \end{bmatrix}$$

the expression $[\bar{V}] = [\bar{Z}][\bar{I}]$ leads to the phase equation:

$$\bar{V} = \bar{Z}\bar{I}$$

in which:

$$\bar{Z} = (\bar{z} + a^2\bar{z}' + a\bar{z}'') \qquad [1.5]$$

is the impedance of the load.

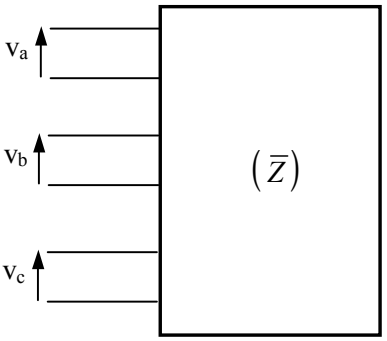

Figure 1.5. *Balanced 3-phase load*

This happens as if each of the three phases was loaded with a $\bar{Z}$ impedance decoupled from the other two (it is in fact a diagonalization of the impedance matrix that has $\bar{Z}$ as an eigenvalue). In those conditions balanced 3-phase systems can be dealt with as independent and decoupled single-phase systems.

1.2.4. *Unbalanced 3-phase sinusoidal systems: Fortescue symmetrical components*

Voltage and current systems may be unbalanced (different amplitudes depending on the phases or phase-shifts different from $2\pi/3$). Expressions [1.4] and [1.5] are no longer valid and 3-phase equations cannot be replaced by single-phase equations. Generally, the analysis of these systems is very difficult.

However there is a system class, fortunately quite commonplace in electrical engineering, for which there is a mathematical simplification. They are the devices described by a circulating impedance matrix $[\bar{Z}]$ and to which dissymmetrical external conditions are imposed. It can be demonstrated that matrix $[\bar{Z}]$ has three eigenvectors:

$$\begin{bmatrix}1\\1\\1\end{bmatrix}, \begin{bmatrix}1\\a^2\\a\end{bmatrix} \text{ and } \begin{bmatrix}1\\a\\a^2\end{bmatrix}$$

respectively associated with the three eigenvalues:

$$\overline{Z}_0 = \overline{z} + \overline{z}' + \overline{z}'' \quad [1.6]$$

$$\overline{Z}_d = \overline{z} + a^2\overline{z}' + a\overline{z}'' \quad [1.7]$$

$$\overline{Z}_i = \overline{z} + a\overline{z}' + a^2\overline{z}'' \quad [1.8]$$

The three above-written impedances are respectively called zero phase-sequence impedance, forward impedance and backward impedance. A transformation matrix can be built from the three eigenvectors:

$$[S] = \begin{bmatrix}1 & 1 & 1\\1 & a^2 & a\\1 & a & a^2\end{bmatrix} \quad [1.9]$$

called “Fortescue’s matrix”. Its backward matrix is:

$$[S]^{-1} = \frac{1}{3}\begin{bmatrix}1 & 1 & 1\\1 & a & a^2\\1 & a^2 & a\end{bmatrix} \quad [1.10]$$

If three variables composing an unbalanced 3-phase system are named G_a, G_b and G_c (voltages, currents, flux, etc.), then the homologous variables G_0, G_d and G_i can be defined by:

$$\begin{bmatrix}\overline{G}_0\\\overline{G}_d\\\overline{G}_i\end{bmatrix} = [S]^{-1}\begin{bmatrix}\overline{G}_a\\\overline{G}_b\\\overline{G}_c\end{bmatrix} \quad [1.11]$$

with, of course, the opposite transition expression:

$$\begin{bmatrix} \overline{G}_a \\ \overline{G}_b \\ \overline{G}_c \end{bmatrix} = [S] \begin{bmatrix} \overline{G}_0 \\ \overline{G}_d \\ \overline{G}_i \end{bmatrix} \qquad [1.12]$$

This last expression shows that if only the forward (positive phase-sequence) part exists, the above-mentioned balanced 3-phase system (Figure 1.4) will be found:

$$\begin{bmatrix} \overline{G}_a \\ \overline{G}_b \\ \overline{G}_c \end{bmatrix} = \overline{G}_d \begin{bmatrix} 1 \\ a^2 \\ a \end{bmatrix}$$

only if the backward (negative phase-sequence) part is not zero:

$$\begin{bmatrix} \overline{G}_a \\ \overline{G}_b \\ \overline{G}_c \end{bmatrix} = \overline{G}_i \begin{bmatrix} 1 \\ a \\ a^2 \end{bmatrix}$$

A balanced 3-phase system is obtained, also known as "backward (negative phase-sequence)", for which components b and c exchange their roles.

Finally, if only $\overline{G}_0$ is different from zero:

$$\begin{bmatrix} \overline{G}_a \\ \overline{G}_b \\ \overline{G}_c \end{bmatrix} = \overline{G}_0 \begin{bmatrix} 1 \\ 1 \\ 1 \end{bmatrix}$$

This is an expression defining a zero phase-sequence 3-phase system in which the three components are identical.

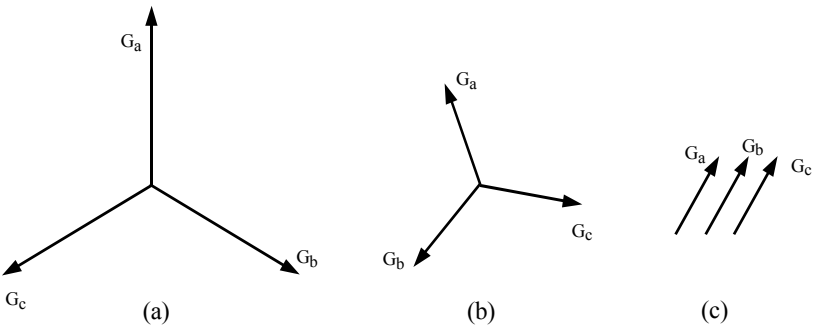

Figure 1.6. *Systems: a) forward (positive phase-sequence); b) backward (negative phase-sequence); c) zero phase-sequence*

This approach therefore consists of replacing an unbalanced 3-phase system with the superposition of three different balanced 3-phase systems of different natures: forward, backward and zero phase-sequence, which can be studied separately and easily.

Matrix equation:

$$[\overline{V}] = [\overline{Z}][\overline{I}]$$

in which $[\overline{V}]$ and $[\overline{I}]$ represent voltage and current unbalanced systems, can be divided into:

$$\overline{V}_0 = \overline{Z}_0 \overline{I}_0$$

$$\overline{V}_d = \overline{Z}_d \overline{I}_d$$

$$\overline{V}_i = \overline{Z}_i \overline{I}_i$$

$\overline{Z}_0, \overline{Z}_d$ and $\overline{Z}_i$ are respectively the impedances of the device in zero phase-sequence, forward and backward modes.

This method, called “Fortescue’s symmetric components”, is very convenient for studying and

calculating unbalanced sinusoidal 3-phase systems. It is also noticeable that it can be used to study non-sinusoidal balanced 3-phase systems. Indeed it can be demonstrated that 3k rank harmonics create zero phase-sequence systems, that 3k + 1 rank harmonics create forward systems and that 3k – 1 rank harmonics create backward systems.

1.3. Electromagnetism

1.3.1. *Primary laws*

1.3.1.1. *Maxwell's equations*

Considering the industrial frequencies used in power systems, displacement currents $\frac{\partial \vec{D}}{\partial t}$ are neglected, and Maxwell's equations can be written as follows:

$$r\vec{o}t\ \vec{E} = -\frac{\partial \vec{B}}{\partial t} \qquad [1.13]$$

$$r\vec{o}t\ \vec{H} = \vec{J} \qquad [1.14]$$

$$div\ \vec{D} = \rho \qquad [1.15]$$

$$div\ \vec{B} = 0 \qquad [1.16]$$

E [V/m] and H [A/m] are respectively electric and magnetic fields. D [C/m^2] and B [T] are the electric flux density and the magnetic flux density. J [A/m^2] is the current density, and ρ [C/m^3] the volume charge density. Equation [1.13] illustrates the coupling between E and B, whereas equation [1.14] leads to $div\ \vec{J} = 0$ (i.e. nodal rule). Equations [1.13] to [1.16] are valid in any fixed or mobile axis systems provided the different variables are measured and their derived values are calculated in the same coordinate system. Considering the

speeds encountered in power systems, H, B and J are unchanged in a reference frame moving at speed $\vec{v}$. Only the electric field is modified as follows:

$$\vec{E}' = \vec{E} + \vec{v} \wedge \vec{B} \qquad [1.17]$$

1.3.1.2. *Ampere's theorem*

Equation [1.14] leads to:

$$\oint_c \vec{H}\, d\vec{l} = \sum_j i_j \qquad [1.18]$$

The magnetic field circulation on a closed circuit (C) is equal to the algebraic sum of the embraced currents.

1.3.1.3. *Faraday's law*

Let's consider circuit (C) in Figure 1.7, first assumed to be fixed. Equation [1.13] leads to:

$$e = \oint_C \vec{E}\, d\vec{l} = -\frac{\partial \phi}{\partial t} = -\frac{d\phi}{dt} \qquad [1.19]$$

ϕ is the magnetic flux through circuit (C)'s surface S and e is the induced electromotive force (emf) on (C)'s terminals. This is a transformation emf.

If (C) is moving at speed $\vec{v}$, equation [1.17] gives:

$$e = = -\frac{d\phi}{dt} = \oint_C \vec{E}\, d\vec{l} + \oint_C (\vec{v} \Lambda \vec{B})\, d\vec{l} = e_T + e_V \qquad [1.20]$$

The induced emf at (C)'s terminals is the sum of the transformation emf e_T and of emf e_V, also called speed emf or emf due to the cut-flux.

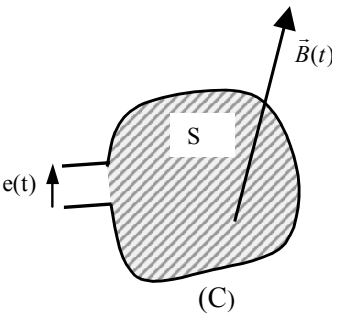

Figure 1.7. *Production of an emf at the circuit's terminals*

1.3.2. *Materials and magnetic circuits*

When a material is subjected to a magnetic field H, each dV element gains a magnetic moment able to oppose or add itself to H. Those magnetic moments can be considerable for ferromagnetic materials. Magnetic flux density within the material is written:

$$\vec{B} = \mu_0 \vec{H} + \mu_0 \vec{M}$$

$\mu_0 \vec{H}$ is the flux density which would have been created into free space, and $\vec{M}$ [A/m] is the magnetization. This is noted:

$$\vec{M} = \chi \vec{\mathrm{H}}$$

The magnetic susceptibility χ usually varies in a very complex way with the field and leads to a B(H) expression presenting a hysteresis (Figure 1.8). Figure 1.8 shows the remanence flux density Br, the coercive field Hc and the initial magnetization characteristics.

According to the hysteresis cycle, "soft" materials can be distinguished from "hard" materials. Soft materials (electrical steel, solid steel, etc.) are characterized by a narrow cycle. Br and Hc are weak. Hc is around 50 to

70 A/m, whereas Br is below 0.1 T. Hard materials (permanent magnets) have a wide cycle. The coercive field Hc is held between 200 and 1,000 kA/m while Br is held between 0.3 T and 1.2 T.

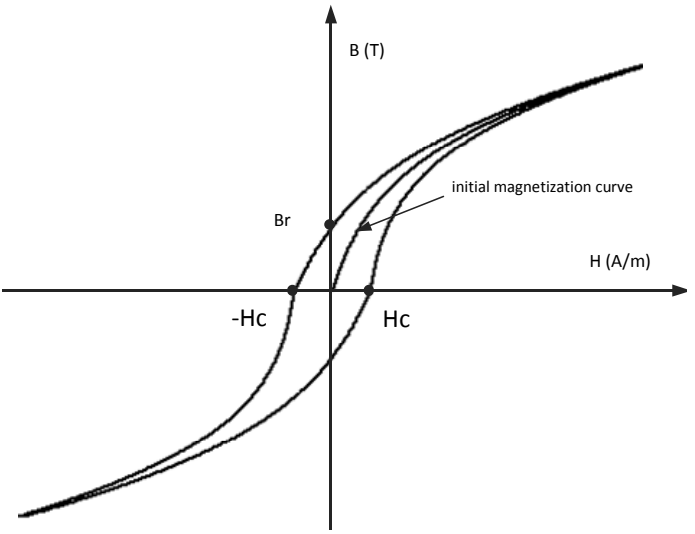

Figure 1.8. *Hysteresis cycle*

1.3.2.1. *Soft ferromagnetic materials*

As the hysteresis cycle is narrow, only the initial magnetization curve is taken into consideration. If the material is characterized by a constant χ:

$$\vec{B} = \mu_0 (1 + \chi) \vec{H} = \mu_0 \mu_R \vec{H} = \mu \vec{H}$$

$\mu_R = 1 + \chi$ is the relative permeability. μ is the material's permeability [H/m]. The ferromagnetic materials are characterized by $\chi \approx \mu_R >> 1$. The magnetic materials have a susceptibility close to zero. This is negative ($\chi \approx -10^{-5}$) for the diamagnetic materials and positive ($\chi = 10^{-3}$) for the paramagnetic materials.

1.3.2.1.1. Saturation

The magnetic permeability of ferromagnetic materials depends on the applied field:

$$\vec{B} = \mu(B)\vec{H}$$

Figure 1.9 shows the initial magnetization curve as well as the relative permeability in terms of the magnetic field of a steel frequently used in electrical machines.

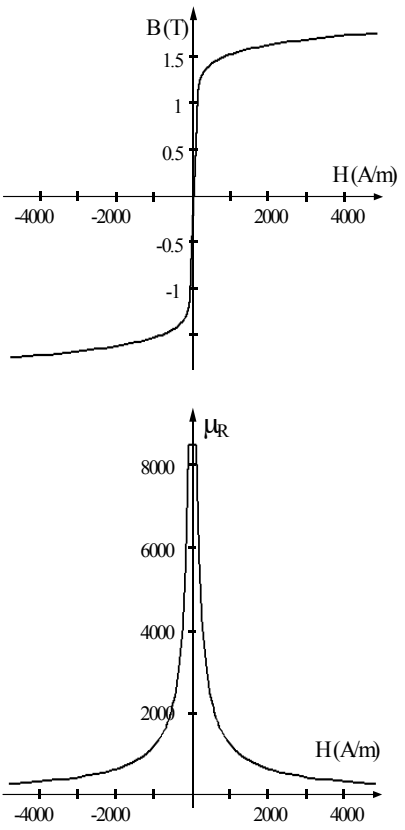

Figure 1.9. *Initial magnetization curve and variation of the relative permeability of FeV 400-50 HA steel in terms of the field*

1.3.2.1.2. Iron losses

Hysteresis losses

When the field in a ferromagnetic material varies with time, losses (called hysteresis losses) appear; they are proportional to the area enclosed by this hysteresis loop. They correspond to the energy required for the orientation of the magnetic moments. Those losses are proportional to frequency f of the excitation currents, as well as to volume V of the magnetic circuit:

$$P_h = K_h V f B_m^n$$

Bm is the maximum value of the magnetic flux density. Constant K_h depends on the material. n is the Steinmetz coefficient; its value is held between 1.8 and 2. The value n = 2 is often accepted.

Eddy current losses

Let us consider the solid ferromagnetic circuit drawn in Figure 1.10.

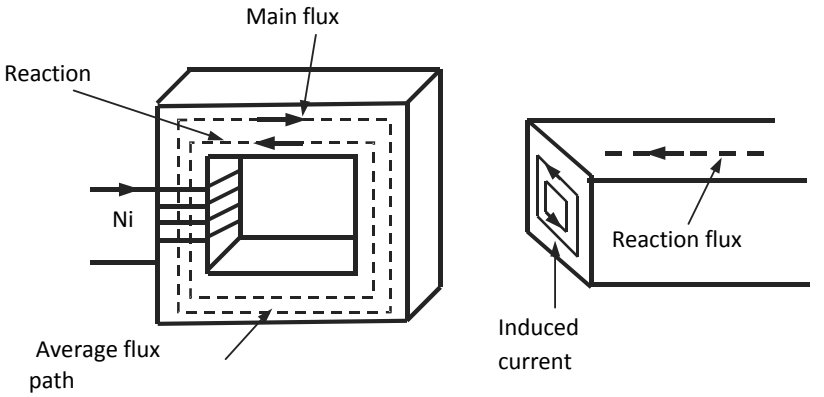

Figure 1.10. *Flux and induced currents in a solid circuit*

When mmf (i.e. magnetomotive force) NI is variable, currents are induced in the conductive iron. The corresponding losses are called “eddy current losses”. In order to reduce those losses the solid material is usually replaced by thin metal sheets insulated from one another. Those losses are given by:

$$P_F = K_F \, Ve \, f^2 B_m^2$$

Constant K_F depends on the material, e is the metal sheet thickness (about 0.5 mm for electrical machines).

Iron losses

The sum of the hysteresis losses and the eddy current losses are usually gathered under the name “iron losses” (P_{fer}):

$$P_{fer} = K_h \, V \, f \, B_m^n + K_F \, Ve \, f^2 B_m^2$$

1.3.2.1.3. Magnetic circuits

We have seen that ferromagnetic materials are characterized by an important permeability which enable the magnetic flux to be canalized.

Hopkinson’s law

Let us consider the circuit characterized by the average closed path (C) of length l (Figure 1.11). Assuming that field $\vec{H}$ and $d\vec{l}$ are colinear, and assuming that H is constant, Ampere’s theorem leads to:

$$\oint_{(c)} \vec{H} d\vec{l} = NI = Hl = \mu HS \frac{l}{\mu S} = \phi \frac{l}{\mu S} = \Re \phi$$

Hopkinson's law is obtained:

$$\varepsilon = NI = \Re\phi = \frac{\phi}{\wp} \qquad [1.21]$$

ε is the magnetomotive force, expressed in [At]. ℜ is the magnetic circuit reluctance, and $\wp$, its permeance, with:

$$\Re = \frac{1}{\wp} = \frac{l}{\mu S} \qquad [1.22]$$

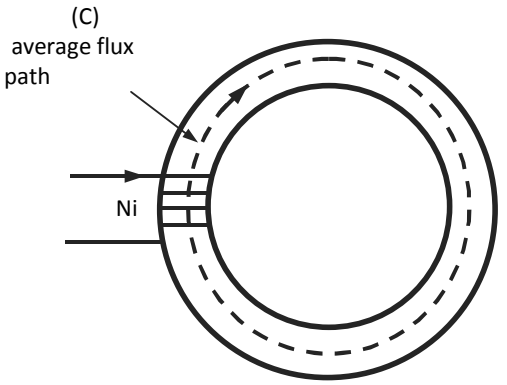

Figure 1.11. *Magnetic field and average flux path*

Analogy between a magnetic circuit and an electrical circuit

Hopkinson's law can be represented by Figure 1.12. The flux ϕ circulates within reluctance ℜ of the magnetic circuit, like current I which circulates within resistance R of the electrical circuit. In comparison to Ohm's law, it is therefore noted that mmf ε, flux ϕ and reluctance ℜ are respectively similar to voltage V, current I and electrical resistance R. However there is no equivalence to the notion of electrical losses associated with a resistance. Moreover at constant temperature, R is constant whereas in the presence of saturation, ℜ varies with flux density B.

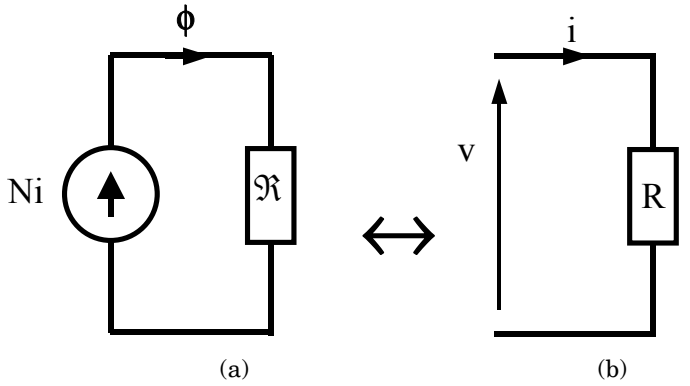

Figure 1.12. *Analogy between a magnetic circuit (a) and an electrical circuit (b)*

Series and parallel magnetic circuits

As for electrical circuits:

– the equivalent reluctance $\Re_{eq}$ of several reluctances $\Re_i$ connected in series (crossed by the same flux) is:

$$\Re_{eq} = \sum_i \Re_i \qquad [1.23]$$

– the equivalent reluctance $\Re_{eq}$ of several reluctances $\Re_i$ connected in parallel (submitted to the same mmf) is:

$$\frac{1}{\Re_{eq}} = \sum_i \frac{1}{\Re_i} \qquad [1.24]$$

1.3.2.2. *Permanent magnets*

1.3.2.2.1. Classification

These are "hard" materials characterized by large hysteresis loops. They operate in plane Ba > 0 and Ha < 0 (Figure 1.13). There are:

– ferrites or ceramics. They are iron oxide-based materials characterized by:

Br = 0.3 to 0.4 T, Hc = 200 to 300 kA/m, $(BH)_{max}$ = 25 to 30 kJ/m^3

– Alnico or metal magnets also called “Ticonal” and mainly constituted of iron, cobalt, nickel, aluminum and copper, with:

Br = 0.8 to 1.1 T, Hc = 100 to 150 kA/m, $(BH)_{max}$ = 60 to 90 kJ/m^3

– rare earth magnets, samarium-cobalt (Sm_2 Co_{17}, Sm Co_5, etc.) and neodymium-iron-boron magnets (NeFeBo). SmCo magnets are characterized by:

Br = 0.8 to 1 T, Hc = 500 to 800 kA/m, $(BH)_{max}$ = 120 to 250 kJ/m^3

NeFeBo magnets are quite sensitive to temperature. In order to avoid their demagnetization they are generally used under 120°C. They are characterized by:

Br = 1 to 1.2 T, Hc = 700 to 900 kA/m, $(BH)_{max}$ = 200 to 300 kJ/m^3

Note that the characteristics of the SmCo, NeFeBo magnets and of the ceramics are quite linear (Figure 1.13). Those magnets are called “rigid magnets”. In this quadrant, this characteristic can be written:

$$B_a = \mu_a H_a + B_R = \mu_a (H_a - H_c)$$

The permeability μ_a of the magnet is near to the free space permeability $\mu_0 = 4\pi\ 10^{-7}$ H/m. In the following, only rigid magnets will be considered.

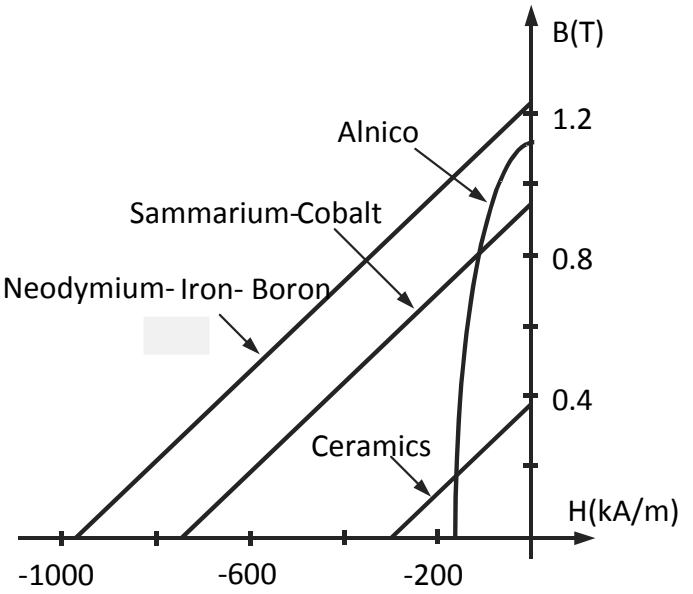

Figure 1.13. *Magnetic characteristics of different permanent magnets*

1.3.2.2.2. Static behavior

Let us consider the magnetic circuit constituted of a rigid magnet inserted into iron (soft ferromagnetic material of very high permeability) with air-gap e (Figure 1.14a). According to the high permeability of iron, the magnetic field can be neglected in it. If the flux leakage is also overlooked, flux density and magnetic field within the magnet are linked by the external characteristic or load curve:

$$B_a = -\wp_e \frac{L_a}{S_a} H_a \qquad [1.25]$$

S_a and L_a are respectively the cross-section and the length of the magnet. $\wp_e$ is the air-gap permeance given by:

$$\wp_e = \mu_0 \frac{S_e}{e}$$

The P operating point (Figure 1.14b) corresponds to the crossing of this load curve with the magnetic characteristic of the magnet. Note that, within the magnet, the field is negative and the useful portion of the cycle is defined by B > 0 and H < 0.

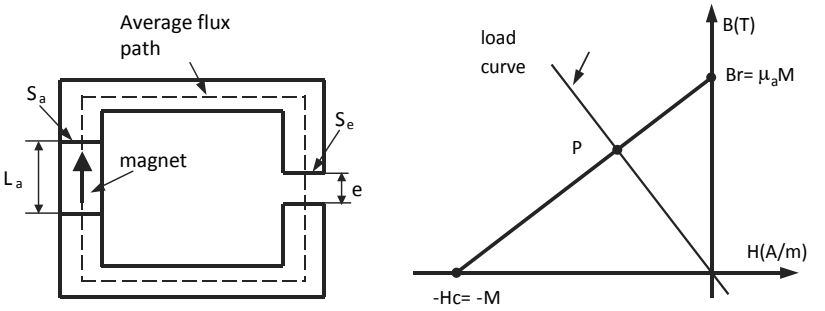

Figure 1.14. *a) Magnetic circuit excited by a magnet; b) operating point P*

1.3.2.2.3. Equivalent circuit

Using the Amperian current model of the magnet and if we neglect the fictitious currents inside the magnet $(\overrightarrow{rot}\,\vec{M} = 0)$ and the flux leakages in the magnet, the equivalent circuit of a rigid magnet consists of a magnetomotive force ε in series with magnet reluctance $\Re_a$ (Figure 1.15). With:

$$\varepsilon = ML_a = H_c L_a, \qquad \Re_a = \frac{L_a}{\mu_a S_a} \text{ with } \mu_a \approx \mu_0$$

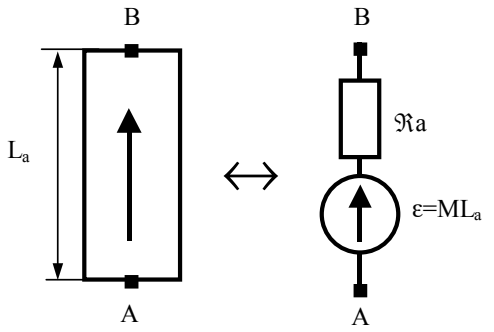

Figure 1.15. *Equivalent circuit of a magnet*

For example, the circuit presented in Figure 1.14a can be replaced by the equivalent circuit given by Figure 1.16.

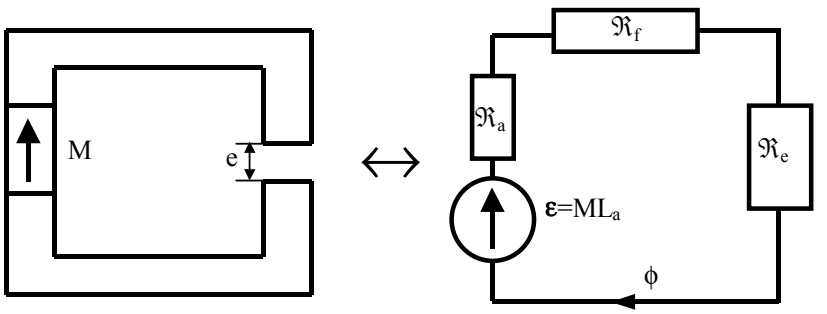

Figure 1.16. *Equivalent circuit of a magnetic circuit excited by a magnet*

R_e and R_f are respectively the reluctances of the air-gap and iron. The magnetic flux Φ is then given by:

$$\phi = \frac{ML_a}{\Re_a + \Re_f + \Re_e}$$

1.3.3. *Inductances*

Electrical circuits are supposed to be in free space.

1.3.3.1. *Mutual inductances*

Let's consider two circuits (C_1) and (C_2) having respectively N_1 and N_2 turns (Figure 1.17). Only (C_1) is supposed to be supplied by current I_1.

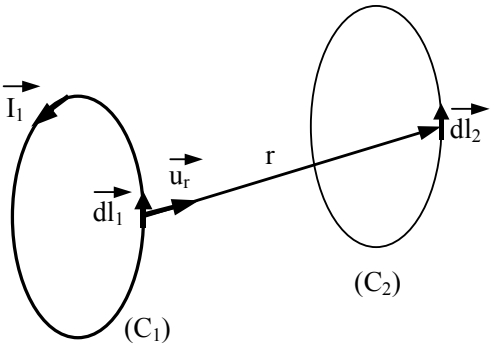

Figure 1.17. *Electrical circuits (C_1) and (C_2)*

The total flux in (C_2) created by I_1 is given by:

$$\Psi_{12} = M_{12} I_1$$

M_{12} is the mutual inductance between (C_1) and (C_2). With:

$$M_{12} = \frac{N_1 N_2 \mu_0}{4\pi} \oint_{C_1} \oint_{C_2} \frac{\vec{dl}_1 \, \vec{dl}_2}{r} \qquad [1.26]$$

M_{12} is therefore proportional to the product N_1N_2. In the same way, if only (C_2) was supplied by I_2, the total flux in (C_1) would be:

$$\Psi_{21} = M_{21} I_2$$

with:

$$M_{12} = M_{21}$$

1.3.3.2. *Self-inductances*

Self-inductance $M_{11} = L_1$ would be obtained by the previous test if C_1 and C_2 were joined. Expression [1.26] cannot be used because of indetermination when r tends to zero. It is thus preferable to determine L_1 from the associated energy. However when the flux flows in a magnetic circuit surrounded by a coil (i.e. case of a winding or a transformer), it can be calculated in restricting the surface to that of the magnetic circuit not including the coil:

$$\phi_1 = \iint_S \vec{B}\, d\vec{S}$$

If the circuit consists of N_1 turns, the total flux is:

$$\Psi_1 = N_1\phi_1 = L_1 I_1$$

The self-inductance is then obtained by:

$$L_1 = \frac{N_1\phi_1}{I_1} \qquad [1.27]$$

Flux ϕ_1 being proportional to N_1, it can be noticed that L_1 is proportional to $(N_1)^2$.

1.3.3.3. *Coupled circuits*

Let us consider two circuits (C_1) and (C_2) from Figure 1.17 again, and let us suppose that they are respectively supplied by currents I_1 and I_2. The total flux created by I_1 equals L_1I_1. A part of this flux, equal to $M_{12}I_1$, crosses circuit (C_2). The total flux crossed by (C_1) and (C_2) is therefore given by:

$$\begin{cases} \Psi_1 = L_1 I_1 + M_{12} I_2 \\ \Psi_2 = M_{21} I_1 + L_2 I_2 \end{cases}$$

with $M_{12} = M_{21} = M$:

$$[\Psi]=\begin{bmatrix}\Psi_1\\ \Psi_2\end{bmatrix} \qquad [I]=\begin{bmatrix}I_1\\ I_2\end{bmatrix} \qquad [L]=\begin{bmatrix}L_1 & M\\ M & L_2\end{bmatrix}$$

It is then written in a matricial form:

$$[\Psi] = [L][I]$$

The co-energy (numerically equal to the energy in a linear case) associated with those two circuits is given by:

$$\tilde{W}_{em} = \frac{1}{2}\sum_{i=1}^{2\,\text{circuits}} \mathrm{I}_i\,\Psi_i = \frac{1}{2}\left(\Psi_1 I_1 + \Psi_2 I_2\right) = \frac{1}{2}\left(\left(L_1 I_1 + M I_2\right)\mathrm{I}_1 + \left(M I_1 + L I_2\right)\mathrm{I}_2\right)$$

and thus:

$$\tilde{W}_{em} = \frac{1}{2}L_1 I_1^2 + \frac{1}{2}L_2 I_2^2 + M I_1 I_2$$

This result can be generalized to n coupled circuits:

$$[\Psi]=\begin{bmatrix}\Psi_1\\ \Psi_2\\ .\\ .\\ \Psi_n\end{bmatrix} \qquad [I]=\begin{bmatrix}I_1\\ I_n\\ .\\ .\\ I_n\end{bmatrix} \qquad [L]=\begin{bmatrix}L_1 & \mathrm{M}_{12} & \mathrm{M}_{13} & \ldots. & \mathrm{M}_{1n}\\ \mathrm{M}_{21} & L_1 & \mathrm{M}_{23} & \ldots. & \mathrm{M}_{2n}\\ . & . & . & . & .\\ . & . & . & . & .\\ \mathrm{M}_{n1} & \mathrm{M}_{n2} & \mathrm{M}_{n3} & \ldots. & L_n\end{bmatrix}$$

$$\tilde{W}_{em} = \frac{1}{2}[I]^t[L][I] \qquad [1.28]$$

$[I]^t = [I_1\ I_2 \ldots\ I_n]$ being the transpose of matrix [I].

1.3.3.4. *Inductances, reluctances, permeances*

A magnetic circuit of reluctance $\mathfrak{R}$, crossed by magnetic flux ϕ (Figure 1.18) is considered.

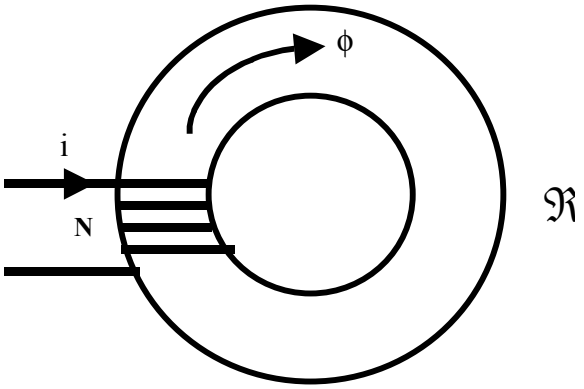

Figure 1.18. *Magnetic circuit of reluctance $\mathfrak{R}$*

We have $Ni = \mathfrak{R}\,\phi$, where:

– ϕ is the flux embraced by one turn of the coil.

– The total flux in the coil is $\Psi_T = N\,\phi$.

– Ψ_T is related to current I by self-inductance L: $\Psi_T = L\,i$.

thus, $N\,\phi = L\,i = N^2\,i/\mathfrak{R}$.

The self-inductance of a coil is therefore bound to reluctance $\mathfrak{R}$ (or to permeance $\wp$) of the corresponding magnetic circuit by:

$$L = \frac{N^2}{\mathfrak{R}} = N^2\,\wp \qquad [1.29]$$

This shows that the self-inductance of a coil is forwardly related to the permeance of its magnetic circuit. This is also the case for the mutual inductances between two coils.

1.3.4. *Skin effect or Kelvin effect*

Let us consider one homogenous conductor with a rectangular cross-section S characterized by permeability μ and conductivity σ, and travelling by current i (Figure 1.19). When i is DC, current density J is constant in the entire cross-section S. J is not constant for an alternating current.

In this case, the field leads to auto-induction phenomena and there is a current concentration on the surface which is all the more important when the frequency is high. The conductor then has a higher electrical resistance than the resistance obtained with forward current; it is sometimes necessary to subdivide the conductors, particularly when frequency increases.

Skin thickness δ is defined as being the thickness of the layer in which most of the current is concentrated.

$$\delta = \sqrt{\frac{2}{\omega \mu \sigma}} \qquad [1.30]$$

As an example, for copper, δ approximately equals 1 cm at 50 Hz, and 2 mm at 1 kHz.

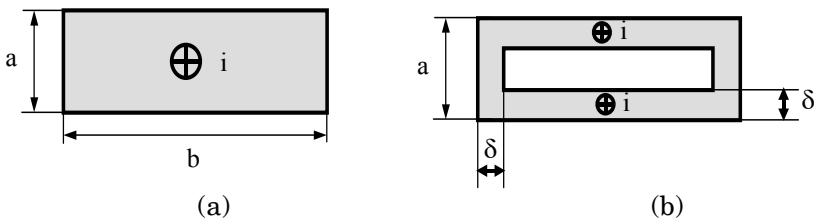

Figure 1.19. *Schematic representation of the current repartition in a conductor: a) forward current; b) alternating current*

1.3.5. *Torque calculation using the virtual work principle*

1.3.5.1. *Single-phase system*

Let us consider a single-phase system (Figure 1.20) converting electrical energy into mechanical energy. Electrical energy W_1 provided by the source is the sum of energy W_p dissipated in losses, of energy W_{em} stored in the electromagnetic field and of converted mechanical energy W_M.

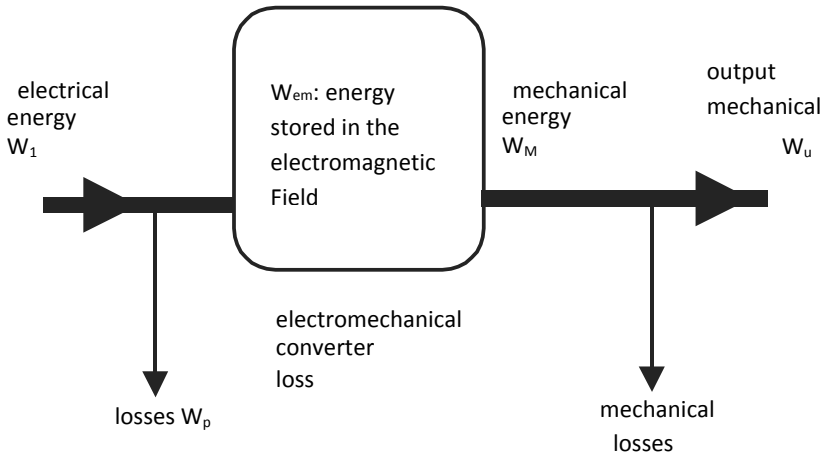

Figure 1.20. *Energy balance in electromechanical energy conversion*

Losses W_p do not affect the conversion process. The diagram of Figure 1.21 in which losses W_p are dissipated in equivalent resistances R_1 and R_2 is adopted. The system is supplied by voltage u and the loss free converter absorbs current i. The energy supplied to the idealized converter can then be expressed in terms of the electromotive force e:

$$W_e = \int eidt = W_1 - W_p$$

It can also be written in a differential way:

$$dW_e = eidt = id\psi = dW_1 - dWp$$

$$dW_e = dW_M + dWem$$

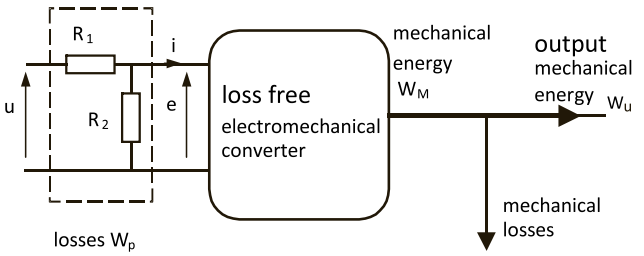

Figure 1.21. *Loss free converter*

Considering a rotating converter, the mechanical energy generated during time dt is linked to the electromagnetic torque Γ_e by:

$$dW_M = \Gamma_e \, d\theta$$

For a system in translation in direction x, this energy is related to force F by:

$$dW_M = Fdx$$

In the following we shall consider that the system is rotating:

$$\mathrm{dW_{em}} = id\Psi - \Gamma_e \, \mathrm{d}\theta$$

This equation shows that energy W_{em} is a function of flux ψ and of position θ. It can then be written:

$$\mathrm{dW_{em}} = \frac{\partial \mathrm{W_{em}}}{\partial \Psi} \, d\Psi + \frac{\partial \mathrm{W_{em}}}{\partial \theta} \, d\theta$$

then:

$$i = \left.\frac{\partial W_{em}}{\partial \Psi}\right|_{\theta \text{ constant}} \quad \text{and} \quad \Gamma_e = -\left.\frac{\partial W_{em}}{\partial \theta}\right|_{\psi \text{ constant}}$$

It is important to note that the electromagnetic torque is obtained by deriving W_{em} in terms of position θ, while keeping a constant flux. This constraint is not easy to achieve. Co-energy $d\tilde{W}_{em}$ is introduced by:

$$d\tilde{W}_{em} + dW_{em} = d(i\,\Psi)$$

thus:

$$d\tilde{W}_{em} = \Psi di + \Gamma_e\, d\theta = \frac{\partial \tilde{W}_{em}}{\partial i}\, di + \frac{\partial \tilde{W}_{em}}{\partial \theta}\, d\theta$$

then:

$$\psi = \left.\frac{\partial \tilde{W}_{em}}{\partial i}\right|_{\theta \text{ constant}} \quad \text{and} \quad \Gamma_e = \left.\frac{\partial \tilde{W}_{em}}{\partial \theta}\right|_{i \text{ constant}}$$

The electromagnetic torque therefore equals the derivative, with constant current, of the co-energy in terms of position θ.

1.3.5.2. *Generalization: polyphase systems*

Let us consider a multiphase system absorbing currents i_1, i_2... i_n with respective voltages v_1, v_2... v_n. If dW_p is the sum of the electrical losses before the electromagnetic transformation, we get:

$$dW_1 = dW_2 + dW_p = v_1 i_1 dt + v_2 i_2 dt + ... + v_n i_n dt$$

with:

$$dW_e = dW_M + dW_{em} = e_1 i_1 dt + e_2 i_2 dt + ... + e_n i_n dt$$

Since:

$$dW_M = \Gamma_e \, d\theta \qquad \text{and} \qquad e_n i_n dt = i_n d\psi_n$$

we get:

$$\mathrm{dW_{em}} = i_1 d\Psi_1 + i_2 d\Psi_2 + ... + i_n d\Psi_n - \Gamma_e \, \mathrm{d}\theta \qquad [1.31]$$

As the state variables are flux ψ and position θ:

$$dW_{em} = \frac{\partial \mathrm{W_{em}}}{\partial \Psi_1} \, d\Psi_1 + \frac{\partial \mathrm{W_{em}}}{\partial \Psi_2} \, d\Psi_2 + ... + \frac{\partial \mathrm{W_{em}}}{\partial \Psi_n} \, d\Psi_n + \frac{\partial \mathrm{W_{em}}}{\partial \theta} \, d\theta$$

thus:

$$i_i = \left. \frac{\partial \mathrm{W_{em}}}{\partial \Psi_i} \right|_{\theta \text{ constant}} \qquad [1.32]$$

$$\Gamma_e = - \left. \frac{\partial \mathrm{W_{em}}}{\partial \theta} \right|_{\psi \text{ constant}} \qquad [1.33]$$

In the same way, co-energy $d\widetilde{W}_{em}$ is introduced by:

$$d\widetilde{W}_{em} + dW_{em} = d(i_1 \Psi_1 + i_2 \Psi_2 + ... + i_n \Psi_n)$$

thus:

$$\mathrm{d\widetilde{W}_{em}} = \Psi_1 di_1 + \Psi_2 di_2 + ... + \Psi_n di_n + \Gamma_e \, \mathrm{d}\theta$$

The state variables are currents i_j and position θ, then:

$$d\tilde{W}_{em} = \frac{\partial \tilde{W}_{em}}{\partial i_1} di_1 + \frac{\partial \tilde{W}_{em}}{\partial i_2} di_2 + ... + \frac{\partial \tilde{W}_{em}}{\partial i_n} di_n + \frac{\partial \tilde{W}_{em}}{\partial \theta} d\theta$$

It can be deduced that:

$$\psi_i = \left.\frac{\partial \tilde{W}_{em}}{\partial i_i}\right|_{\substack{\theta \text{ constant} \\ \psi_j \ (j \neq i) \text{ constant}}} \qquad [1.34]$$

$$\Gamma_e = \left.\frac{\partial \tilde{W}_{em}}{\partial \theta}\right|_{i \text{ constant}} \qquad [1.35]$$

1.3.5.3. *Linear systems*

Fluxes and currents are linked by a linear law. Energy and co-energy are then numerically equal.

1.3.5.3.1. Single-phase systems

We have:

$$\psi = Li \qquad i = \frac{1}{L}\psi = \frac{\Re}{n^2}\psi$$

L is the self-inductance of the phase with n turns, and $\Re$ is the reluctance of the corresponding magnetic circuit. L and $\Re$ can depend upon position θ. With a fixed θ, energy is given by:

$$dW_{em} = \frac{1}{L}\psi d\psi \qquad W_{em} = \frac{1}{2L}\psi^2 = \frac{1}{2}\Re\phi^2$$

ϕ is the flux per turn with $\psi = n\phi$.

In the same way, co-energy is given by:

$$d\widetilde{W}_{em} = Lidi \qquad \widetilde{W}_{em} = \frac{1}{2}Li^2$$

The electromagnetic torque can therefore be calculated indiscriminately by:

$$\Gamma_e = -\frac{1}{2}\psi^2 \frac{\partial}{\partial\theta}\left\{\frac{1}{L(\theta)}\right\}$$

or by:

$$\Gamma_e = \frac{1}{2}i^2 \frac{\partial L(\theta)}{\partial\theta}$$

1.3.5.3.2. Polyphase systems

Fluxes and currents are related by:

$$\begin{bmatrix}\psi_1\\ \psi_2\\ \vdots\\ \psi_n\end{bmatrix} = \begin{bmatrix}L_1 & M_{12} & \cdots & \cdots & M_{1n}\\ M_{21} & L_2 & \cdots & \cdots & M_{2n}\\ \vdots & \vdots & \vdots & \vdots & \vdots\\ M_{n1} & M_{n2} & \cdots & \cdots & L_n\end{bmatrix}\begin{bmatrix}i_1\\ i_2\\ \vdots\\ i_n\end{bmatrix}$$

Co-energy is given by:

$$d\widetilde{W}_{em} = (L_1 i_1 + M_{12} i_2 + \ldots + M_{1n} i_n)di_1 + \ldots + (M_{1n} i_1 + M_{2n} i_2 + \ldots + L_n i_n)di_n$$

which can be written:

$$\widetilde{W}_{em} = \frac{1}{2}[i]^t [L(\theta)][i]$$

In the same way, energy is expressed:

$$W_{em} = \frac{1}{2}[\phi]^t [\Re(\theta)][\phi]$$

The electromagnetic torque can therefore be obtained indiscriminately by:

$$\Gamma_e = -\frac{1}{2}[\phi]^t \left[\frac{\partial \Re(\theta)}{\partial \theta}\right][\phi] \qquad [1.36]$$

or by:

$$\Gamma_e = \frac{1}{2}[i]^t \left[\frac{\partial L(\theta)}{\partial \theta}\right][i] \qquad [1.37]$$

1.4. Power electronics

Since the 1960s, power electronics have made considerable modifications in electrical engineering and particularly in the implementation of electrical machines. Thanks to the development in semi-conductors, motors are mainly supplied by static converters. That is why it is useful to mention in the present chapter the functioning principles and the main characteristics of static converters associated with electrical machines. For simplification we shall restrict the presentation to idealized functioning of the most common converters.

Power electronics are in constant and quick technological evolution, particularly regarding components technology. In order to make writing easy we shall assume that "traditional" components are used: diodes (represented by D) or thyristors (represented by T) for rectifiers or naturally commuted inverters, thyristors for AC power controllers. Concerning choppers and inverters, we shall consider that fully controlled switches (bipolar or field effect transistors, GTO, IGBT, etc.) denoted Tc are used. This does not alter the validity of the results presented in the following.

1.4.1. *Rectifiers and naturally commutated inverters*

1.4.1.1. *Introduction*

Rectifiers ensure an AC-DC energy conversion. They are constituted of diodes (in that case the output voltage is constant in average value) or of thyristors in order to make the output voltage variable or regulated.

1.4.1.2. *3-phase bridge converters*

3-phase bridge rectifiers are largely used for the control of electrical machines. Figure 1.22 represents a thyristor-based 3-phase bridge. The time variation of the output voltage is shown in Figure 1.23a and the currents absorbed from the AC supply are represented on Figure 1.23b. Assuming the bridge conduction to be uninterrupted and neglecting the commutation phenomena, the average value of the rectified voltage is:

$$U_0 = \frac{3V\sqrt{6}}{\pi}\cos\alpha \qquad [1.38]$$

where V is the rms value of the phase voltage of the source, and α, the firing angle of the thyristors.

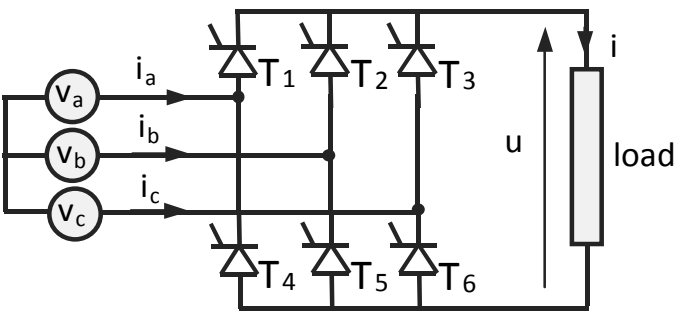

Figure 1.22. *Thyristor bridge*

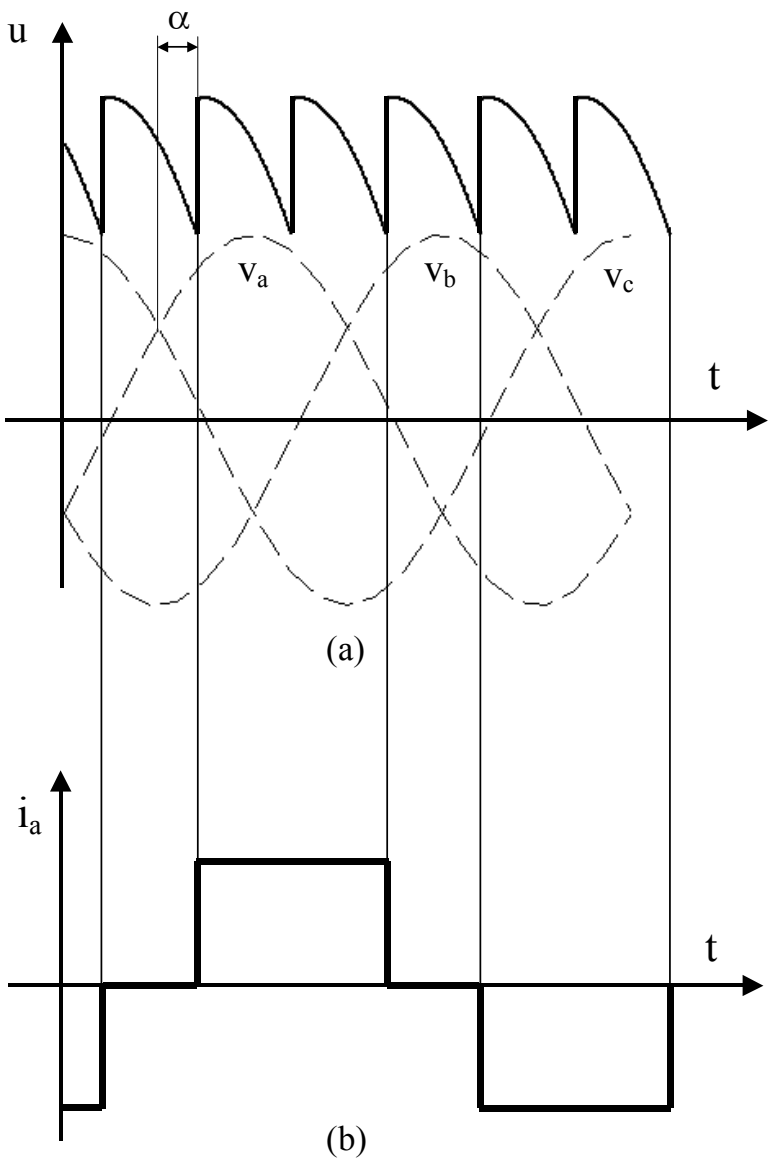

Figure 1.23. *Load voltage (a) and source phase current (b) of a 3-phase thyristor bridge.* i_b *and* i_c *are shifted by* $\pm 2\pi/3$ *with respect to* i_a

1.4.1.2.1. Single-phase bridge

When a 3-phase source is not available, a single-phase bridge is used (Figure 1.24). With the same assumptions, the mean value of its output voltage is:

$$U_0 = \frac{2V\sqrt{2}}{\pi}\cos\alpha \qquad [1.39]$$

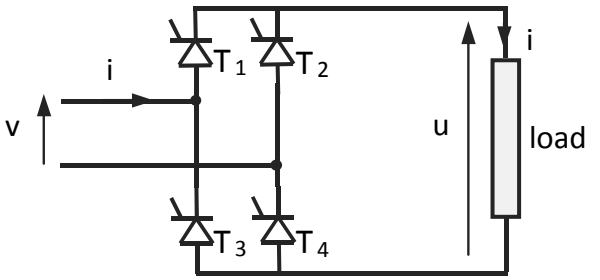

Figure 1.24. *Single-phase bridge*

1.4.1.2.2. Diode bridge

A diode bridge can be considered to be a thyristor bridge with a zero firing angle. The mean value of its output voltage will then be respectively $\frac{3V\sqrt{6}}{\pi}$ and $\frac{2V\sqrt{2}}{\pi}$ for 3-phase and single-phase bridges.

1.4.1.3. *Inverter mode*

Equation [1.38] shows that if α is greater than $\pi/2$, U_0 becomes negative. The output current of the bridge, I_0 (considered as constant in a first approximation) remains positive, the AC to DC power flow becomes negative and the bridge works as an inverter. The DC "load", of course, has to be active in order to become a generator. The DC voltage is then as shown in Figure 1.25.

The inverter mode of thyristor bridges also requires that the AC system has electromotive forces in order to ensure the commutation of the thyristors.

1.4.1.3.1. Maximum firing angle

In order to take into account the components blocking conditions, it is necessary that $\alpha < \pi$, and, to take the various commutation and overlap phenomena into account, the value of the firing angle is limited to $\pi - \beta$, where β is a guarding angle often called "minimum extinction angle".

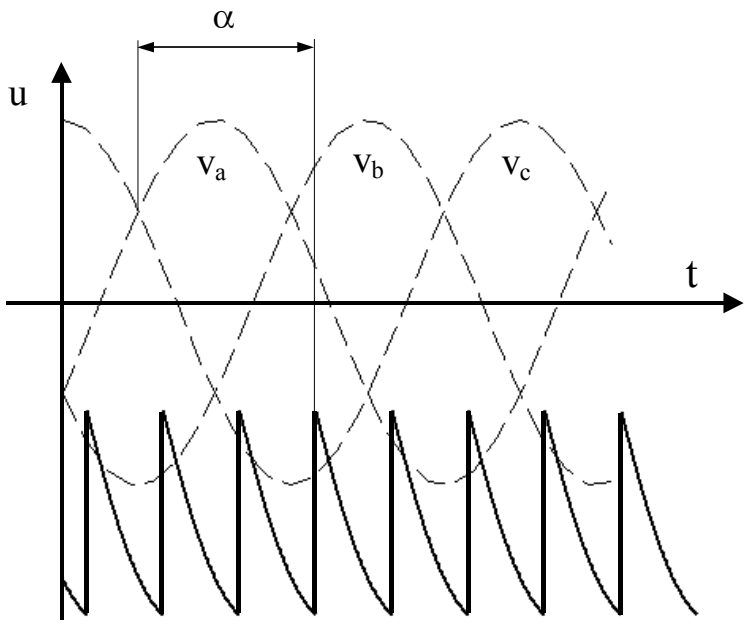

Figure 1.25. *Output voltage of a thyristor bridge (inverter mode)*

1.4.1.3.2. Reversibility

The transition of the thyristor bridge from "rectifier" mode to "inverter" mode allows us to reverse the direction of the energy transfer. However, this reversibility is only partial because only the voltage changes sign; the current remaining

positive. In order to reverse the current in the AC side it is necessary to use two thyristor bridges anti-parallel connected (Figure 1.26), giving a four-quadrant converter.

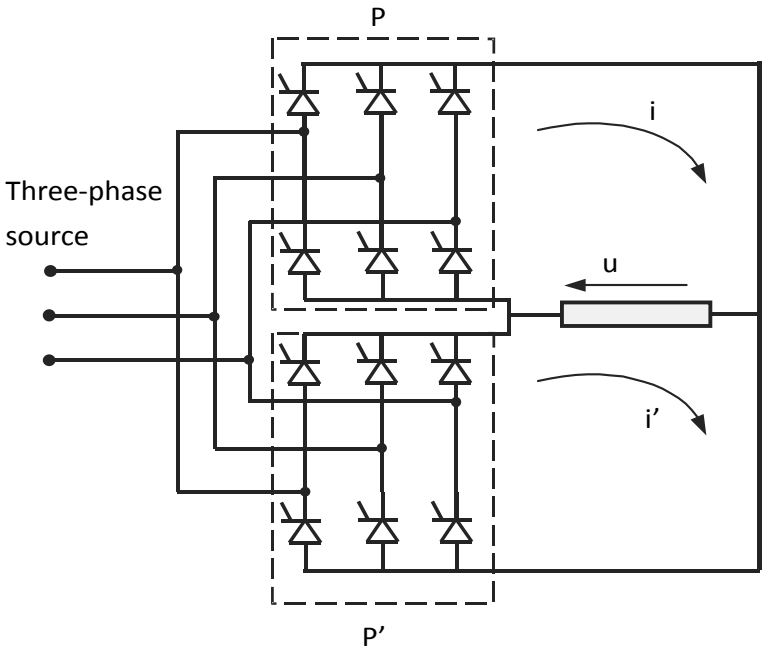

Figure 1.26. *Four-quadrant AC-DC converter*

1.4.2. *AC thyristor controllers*

1.4.2.1. *Single-phase AC controller*

A single-phase AC controller is generally constituted of two anti-parallel connected thyristors. It ensures power transfer from an AC voltage source to an AC load (Figure 1.27).

Thyristors are usually controlled with a firing angle ψ the origin of which is the zero crossing of the source voltage (Figure 1.28).

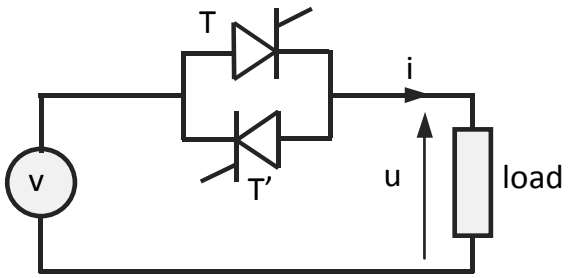

Figure 1.27. *Single-phase AC controller*

Depending on the nature of the load, voltages and currents represented in Figure 1.28 are obtained.

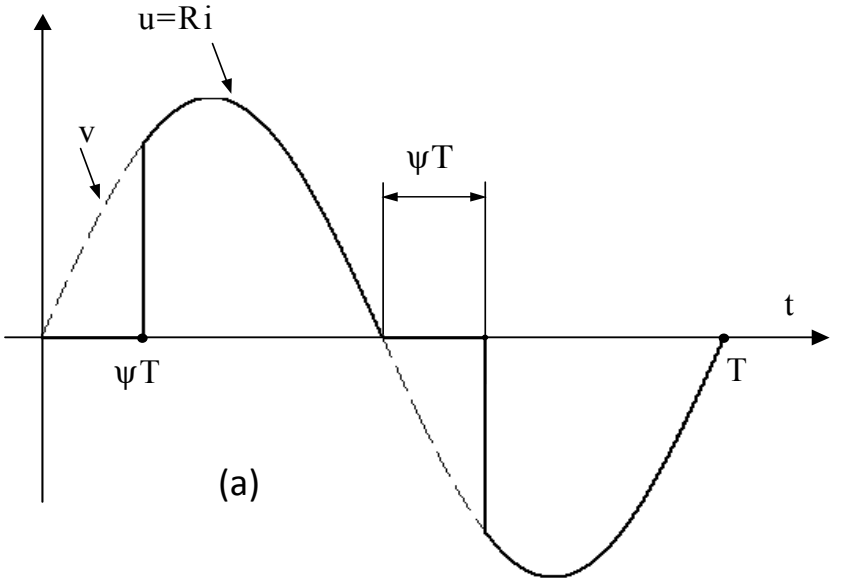

Figure 1.28. *Load voltages and currents. Single-phase AC controller: a) resistance load*

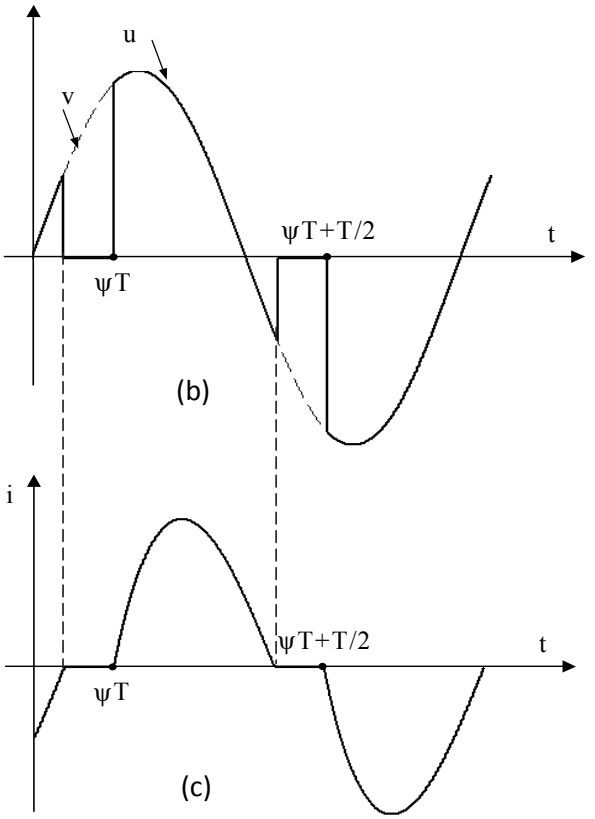

Figure 1.28 (continued). *Load voltages and currents. Single-phase AC controller: b) and c) resistance and inductive load ($\psi > \varphi$), where the current is out of phase by φ with respect to the voltage*

When ψ varies, rms value V_{eff} of the load voltage varies; however, the relation between ψ and V_{eff} is not simple. For example, on the resistance load:

$$V_{eff} = V\sqrt{1 - \frac{\psi}{\pi} + \frac{\sin 2\psi}{2\pi}} \qquad [1.40]$$

If the load is inductive, the calculation of V_{eff} depends on the load parameters and is complicated, but V_{eff} remains a decreasing function of ψ. Furthermore the load voltage and, consequently, the current have important harmonic components.

1.4.2.2. *3-phase AC controllers*

The most common structure (fully controlled star connected load) of an AC controller designed for power supply or motors is represented in Figure 1.29. As there is no connection between the source and the load neutrals there is no circulation of 3k rank harmonics which would give zero sequence currents in the machines.

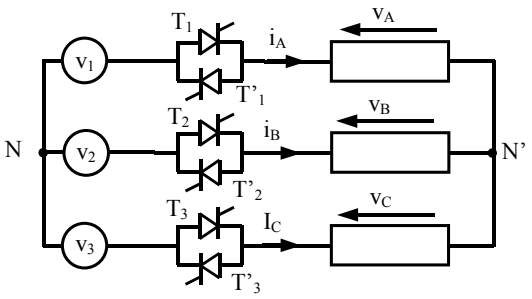

Figure 1.29. *3-phase AC controller*

This converter allows us to supply a 3-phase load by a non-sinusoidal voltages constant frequency and which rms value is controlled by the firing angle ψ. As for the single-phase AC controller, the load voltages (and therefore the currents) have a high harmonic content.

1.4.3. *Choppers*

Choppers ensure energy transfer between two DC systems with different voltages.

1.4.3.1. *Step-down chopper*

The diagram of the basic step-down chopper is represented in Figure 1.30. Its functioning assumes that the source is a "voltage" source (voltage E is a state variable and cannot have any discontinuity) and that the load is a "current type" receiver, the presence of an inductance preventing current discontinuities.

Assuming that T_c is switched on with a period T and switched off after a delay αT ($\alpha \in [0,1]$), the voltage and the current waveforms of Figure 1.31 are obtained. The average value of the load voltage is therefore αE, from which we derive the name "step-down DC to DC converter". The average output DC voltage is adjusted using the variation of α.

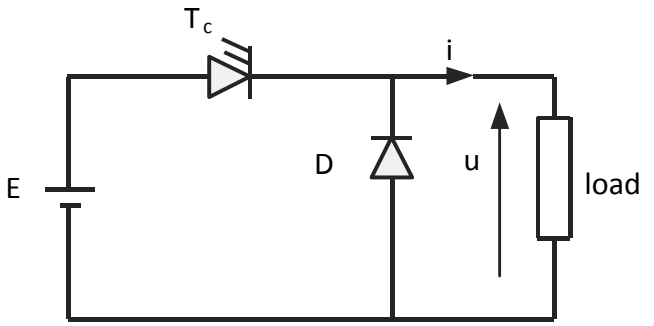

Figure 1.30. *Step-down DC to DC converter*

1.4.3.2. *Boost chopper*

In order to ensure energy transfer between a source with a voltage E and a load of voltage E' (with E' > E), the circuit represented in Figure 1.32 can be used. This matches the previous circuit. The structure including a step-down chopper and a boost chopper (regenerative chopper) enables a bi-directional energy transfer between a DC source and a DC load.

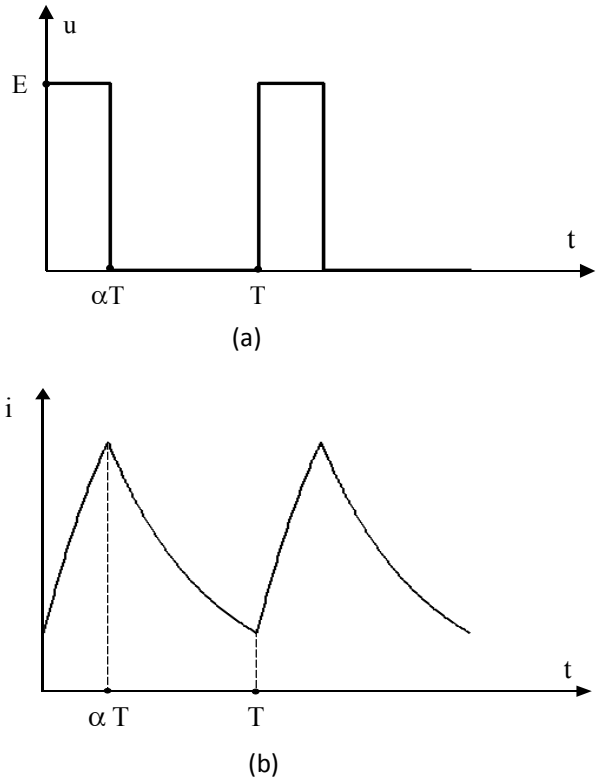

Figure 1.31. *Voltage (a) and load current (b) of a step-down DC to DC converter*

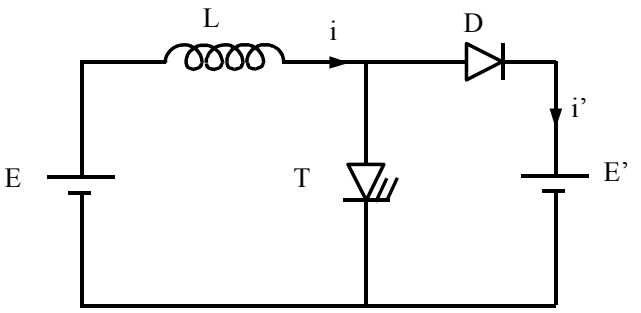

Figure 1.32. *Boost chopper*

1.4.4. *Cycloconverters*

These are AC-AC converters enabling forward variation of the load currents frequency. They are rarely used and only for very high power applications. Interest in cycloconverters is decreasing.

1.4.5. *Force commutated inverters*

These converters ensure energy transfer from a DC source to an AC load (single-phase or 3-phase). They are based on the use of fully controlled switches. The elementary structure includes a fully controlled switch (transistor, GTO, IGBT, etc.) connected in an anti-parallel with a diode. The set of two elementary structures connected to a same phase of the load makes an "inverter leg".

A force commutated 3-phase inverter is generally constituted of three inverter legs, one per phase (Figure 1.33).

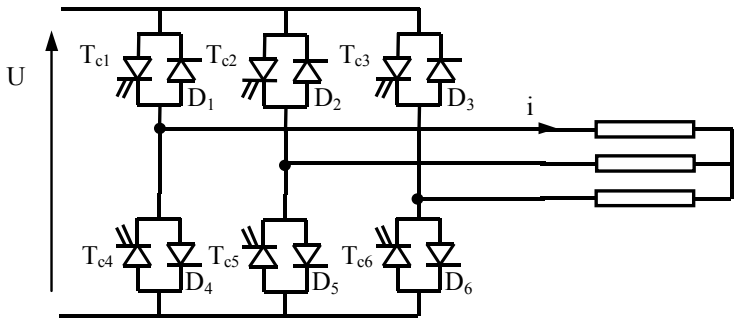

Figure 1.33. *Force commutated 3-phase inverter*

When controlled by pulse width modulation (PWM), force commutated inverters provide load currents with few harmonics (Figure 1.34). The fundamental frequency of voltages and currents imposed by the switch control can vary

over a wide range. Force commutated inverters are therefore very useful for obtaining almost sinusoidal 3-phase systems with variable frequencies.

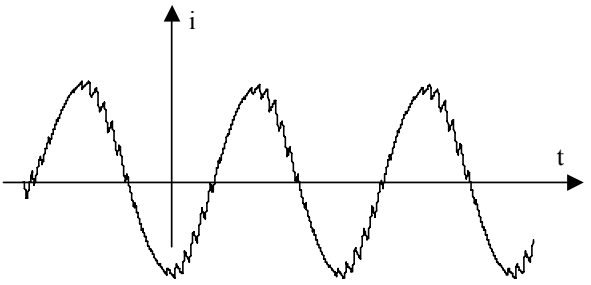

Figure 1.34. *Current in a load supplied by a PWM inverter*

Chapter 2

Introduction to Rotating Electrical Machines

2.1. Introduction

Rotating electrical machines are electromechanical energy converters. Their economic importance is considerable because they provide almost all the electrical energy. In addition, electrical motors, usually associated with power electronics static converters, play an ever-increasing part in all industrial areas as well as in day to day life.

These machines are made of two distinct parts, one fixed (the stator) and the other one, mobile (the rotor). Those two parts are mainly constituted of ferromagnetic materials whose high permeability enables us to lead the field lines; they are separated by an air space (the air-gap) and carry a set of conductors (the windings) usually made of copper, a material chosen for its good electric conductivity. Those two armatures have different and complementary roles, illustrated by the terms of “field system” and of “armature” which are allotted to them.

2.2. Main notations

– B_e: air-gap flux density.

– e: air-gap thickness.

– H_e: field within the air-gap.

– H_f: field within the iron.

– i_i: phase i instantaneous current.

– L: active length of the machine.

– L_i: self-inductance of phase i.

– M_{ij}: mutual inductance between phases i and j.

– n: total number of the machine phases.

– n_s: number of turns per stator phase.

– n_r: number of turns per rotor phase.

– p: number of pole pairs.

– P: active power.

– P_i: instantaneous value of the electrical power.

– P_m: mechanical power.

– Q: reactive power.

– R: radius of the rotor.

– R_i: resistance of phase i.

– v_i: instantaneous voltage at the terminals of phase i.

– μ_0: permeability of free space.

– ψ_i: total flux within phase i.

– τ_p: pole pitch.

– Θ: stator/rotor mechanical angle.

– $\theta = p\,\Theta$: electrical angle.

– $\Omega = d\Theta/dt$: angular speed of the rotor.

– Γ_e: electromagnetic torque.

2.2.1. *Vectors*

– {v}: voltages of the phases vector (dimension n);

– {i}: currents of the phase vector (dimension n);

– {Ψ}: fluxes per phase vector (dimension n);

as well as matrix:

– {R}: diagonal matrix of the resistances of the phases (dimensions n x n);

– {ℒ}: inductance matrix or coupling matrix (dimensions n x n).

It should be noticed that the inductance matrix is naturally symmetrical because $M_{ij} = M_{ji}$.

2.3. Principle of the electromechanical energy conversion

First let us see how it is possible to produce electric energy by moving conductors within a magnetic field: let's consider conductor (C) set in an area where a flux density B appears (Figure 2.1).

Let us assume that this conductor is submitted to a basic movement dl during a time dt. The conductor will trace a surface dS through which the flux (or "flux-cutting") will be noted dϕ. It is known that, under such circumstances, an electromotive force of module $e = \frac{d\phi}{dt}$ appears at the terminals of conductor (C). If this conductor is connected to an external

impedance, a current i will flow within (C) and lead to the production of an instantaneous electrical power $P_i = e\ i$. The movement of the conductor requiring a mechanical power P_m, a conversion of mechanical energy into electrical energy is therefore achieved.

On the contrary if a current i is injected into (C), a force F which will tend to move it will be applied to it, consequently producing a work and therefore a mechanical power P_m (Figure 2.2). A conversion of electrical energy into mechanical energy is then achieved.

Bear in mind that the situation described in Figure 2.2 (field applied directly on the conductors) is rarely encountered in electromechanical converters. Conductors are usually set in slots, as represented in Figure 2.3a. The magnetic field is then canalized in teeth made of a highly permeable ferromagnetic material. At the conductors level (in the slot), the values of the flux density are small because the corresponding flux is a leakage flux. Consequently, as long as the currents do not exceed their nominal value, the electromagnetic force the conductors are submitted to is not important. The main force is indeed located on the slots sides because of the discontinuity of magnetic permeability.

However it can be shown that the real armature (coils, slots, teeth) may be replaced by an equivalent smooth armature (Figure 2.3b) where the conductors would be set down on the surface and would be of a thickness ε. Thickness ε is often made to tend towards zero in order to replace the real current by equivalent superficial currents.

This equivalence enables us to calculate force F, as suggested in Figure 2.2, but obviously doesn't make it possible to determine the local effects due to the slot. The representation in Figure 2.2 is therefore useful for emphasizing in a qualitative way the phenomena of

electromechanical conversion. The example given in Figure 2.2 shows that electromechanical conversion result from the action of magnetic fields in relative movement with one another. This highlights the complementary roles played by the armatures.

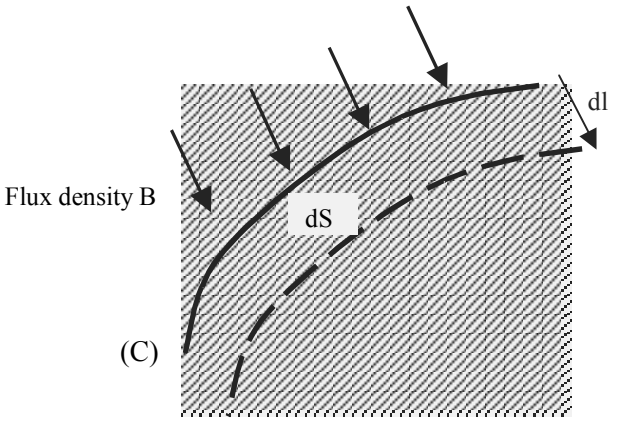

Figure 2.1. *Elementary movement of a conductor*

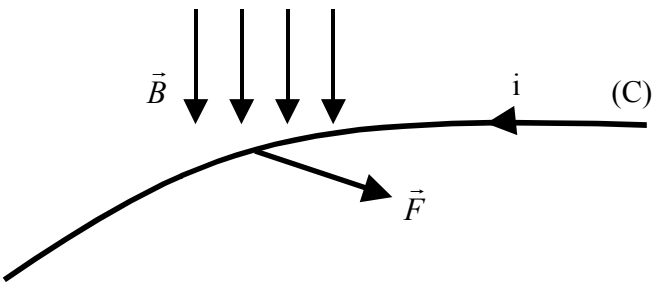

Figure 2.2. *Force created by the interaction between flux density and current*

Considering this, it can be noted that only a relative movement between these armatures, which can be placed indiscriminately at the stator or at the rotor of the machine, is necessary.

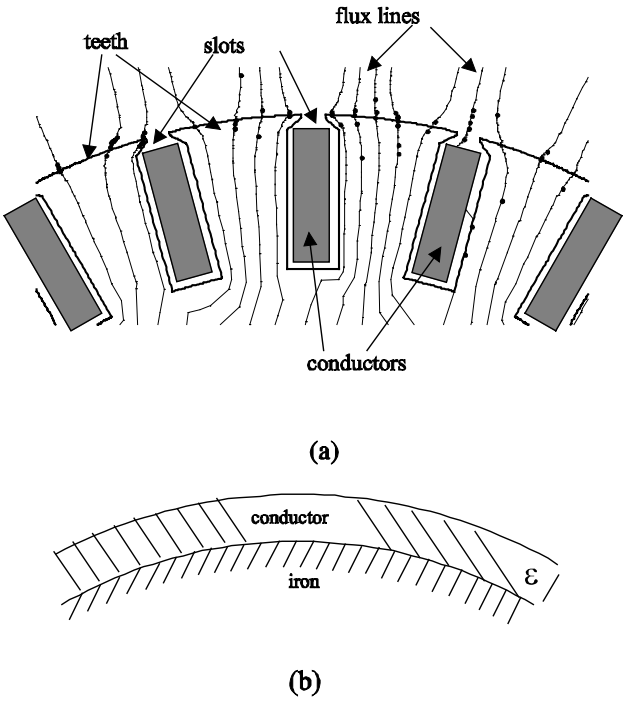

Figure 2.3. *Conductors in slots (a) and layer of equivalent currents (b)*

In most cases, the machines used for electromechanical energy conversion are cylindrical. Indeed, this geometry is particularly convenient, as the example in Figure 2.4 shows.

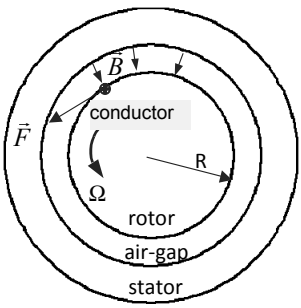

Figure 2.4. *Production of mechanical energy within a cylindrical structure*

A conductor, carrying a current i directed longitudinally, is fixed to a rotor of circular section (radius R) and of length L. It is placed in a radial field (flux density B) which generates a tangential force creating a torque $\Gamma_e = BiLR$ which, if the rotor has a speed Ω, will work and produce a mechanical power ΓΩ.

2.4. Continuous energy conversion

In most applications, electrical rotating machines are designed for "continuous energy conversion". This means that it is desirable for the power produced to have an average value different from zero. For example in the hypothesis of a motor working mode, the average mechanical power Pm produced is given by:

$$P_m = \frac{1}{\mathrm{T}} \int_{\mathrm{T}} \Gamma_e \, \Omega \, \mathrm{dt}$$

where T is the functioning period of the machine (one turn, for example). If it is admitted that speed Ω is constant (functioning in a stationary mode), this expression leads to:

$$\int_T \Gamma_e dt \neq 0 \qquad [2.1]$$

This concept is usually expressed as follows: a machine achieves a continuous energy conversion when the average value of the instantaneous torque is different from zero. This is an important notion which will then enable us to clarify some principles of the construction and of the power supply of electrical machines.

2.5. Non-salient and salient poles

The inductor has to generate a series of "north" poles and "south" poles along the air-gap. This can be achieved in two different ways: in the first method, the conductors are set

inside the slots hollowed out along the field spool, the latter being indiscriminately stator or rotor, and are then connected with one another at the extremities of the machine (those connections are called “end windings”) so as to generate the desired pole alternation (Figure 2.5).

In this case the dimensions of the slots are generally considered to be negligible compared to the other geometrical parameters of the machine, which enables us to admit that the air-gap has a constant thickness. It is then referred to as “non-salient air-gap”, and by extension “non-salient pole machine”.

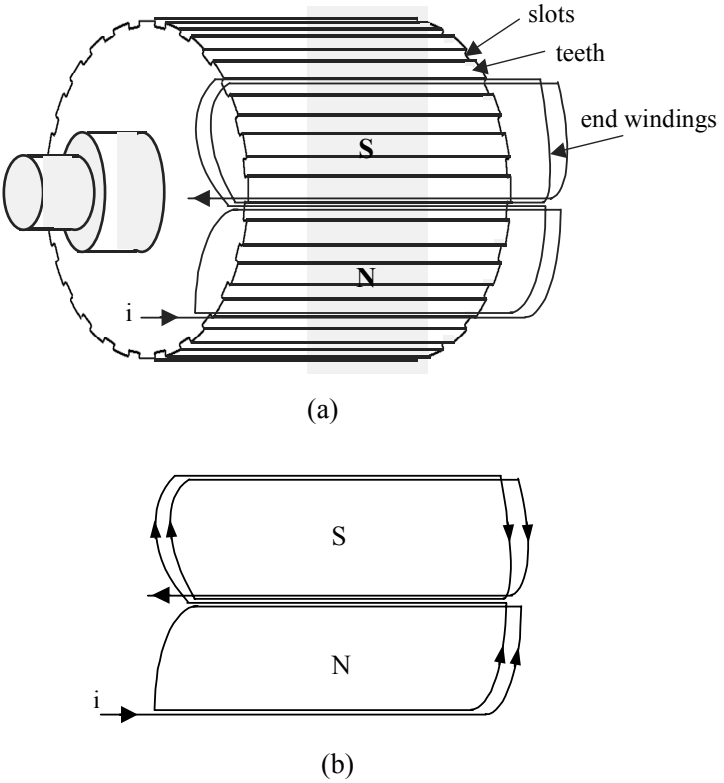

Figure 2.5. *a) Non-salient poles armatures and b) structure and coil of the rotor*

(c)

Figure 2.5 (continued). *Non-salient poles armatures: c) introduction of a coil (section) in the stator (ECA EN document)*

The other approach consists of using (Figure 2.6) windings around salient poles, with the direction it is wound imposing the name of the pole. In this case they will be referred to as "salient poles inductor" and "salient poles machine", and the air-gap cannot be considered to be constant.

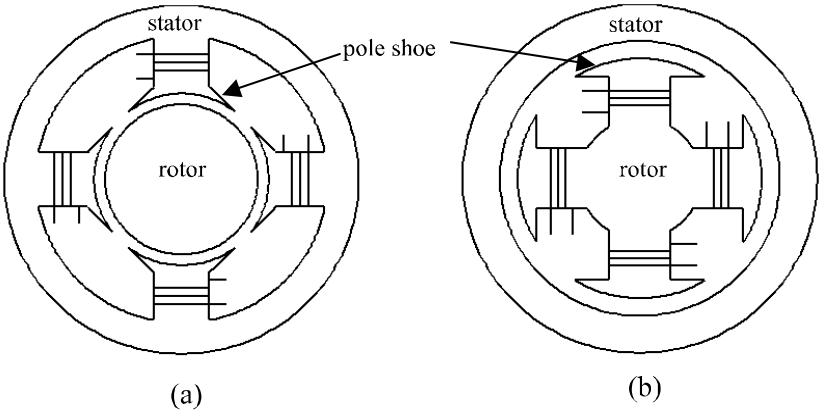

Figure 2.6. *Salient pole machines a)salient stator b) salient rotor*

2.6. Notion of pole pitch

The armatures of an electrical machine generate a series of p "north" poles and p "south" poles, p being the number of pairs of poles along the air-gap, whether the machine is a salient pole one or a non-salient pole one. The pole pitch τ_p is defined by central angle π/p. The "double pole pitch" is therefore the central angle $2\pi/p$ through which consecutive "north" pole and "south" pole are seen. This emphasizes the existence of two different periods: the "mechanical period", which corresponds to one revolution of the rotor, and the "electrical period", which corresponds to the double pole pitch.

If Figure 2.7 which represents a tetrapolar machine is considered, it is clear that the position of a point P located along the air-gap, can be marked by two distinct angles of same origin: the "mechanical angle" Θ and the "electrical angle" θ with the expression:

$$\theta = p\,\Theta \qquad [2.2]$$

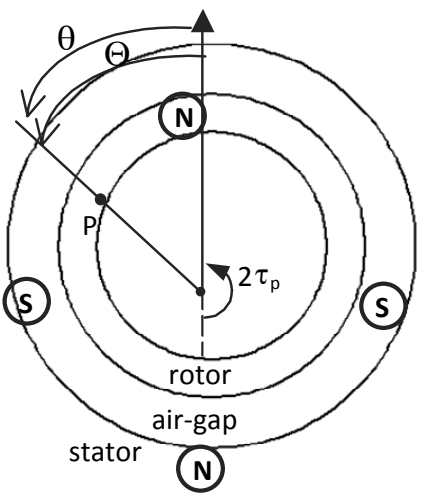

Figure 2.7. *Tetrapolar machine*

Figure 2.8 shows the distribution of the flux density along the air-gap.

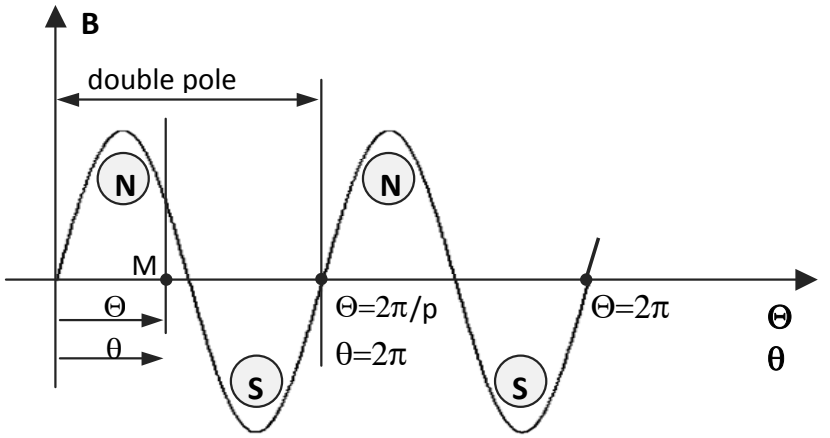

Figure 2.8. *Variation of the air-gap flux density in a tetrapolar machine*

2.7. Stator/rotor coupling: the "basic machine"

In order to attempt an approach of the principles of a "good conversion" of electromechanical energy in machines, we shall consider an elementary structure which shall be called a "basic machine" (Figure 2.9).

The structure is made of a cylindrical ferromagnetic rotor and stator with a circular section, coaxial and a length L. In each one two diametral slots of negligible dimensions have been hollowed out and carry two coils with respectively n_r and n_s turns. The radius of the rotor is named R, and the air-gap thickness e; it is assumed that R >> e, which enables us to consider in what follows that R + e ≈ R.

Considering θ the angle made by the axes of the two coils and ξ the angle spotting the position of a point P of the air-gap in relation to the axis of the rotor coil. In order to

express the mutual inductance in the two coils, we can assume, for instance, that the rotor coil is supplied by a current i_r and calculate the flux induced in the stator coil which is assumed to be without any power supply.

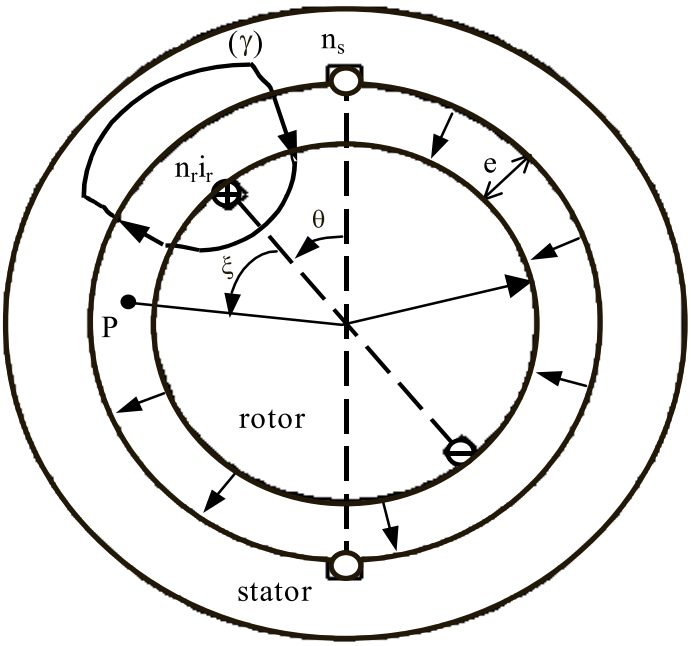

Figure 2.9. *Basic machine*

If the permeability of the iron is assumed to be infinite, and since the air-gap is assumed to be small, it can be stated that field H_f in the iron is zero and that the lines of field H_e in the air-gap are radial. Since they change direction following the plan of the rotor coil (see Figure 2.9), it is arbitrarily set down that:

$$H_e > 0 \text{ for } 0 < \xi < \pi \qquad \text{and} \qquad H_e < 0 \text{ elsewhere}$$

If Ampere's theorem is applied on a contour (γ) including two crossings of the air-gap located on each side of the rotor coil, we get:

$$\oint_{(\gamma)} \vec{H}_e \, d\vec{l} = 2H_e e = \sum n\,i = n_r\, i_r$$

thus the module of H_e:

$$|H_e| = \frac{n_r\, i_r}{2e}$$

and therefore $H_e = \pm \frac{n_r\, i_r}{2e} = \frac{B_e}{\mu_0}$.

The variation of $H_e = B_e/\mu_0$ in terms of ξ is shown in Figure 2.10.

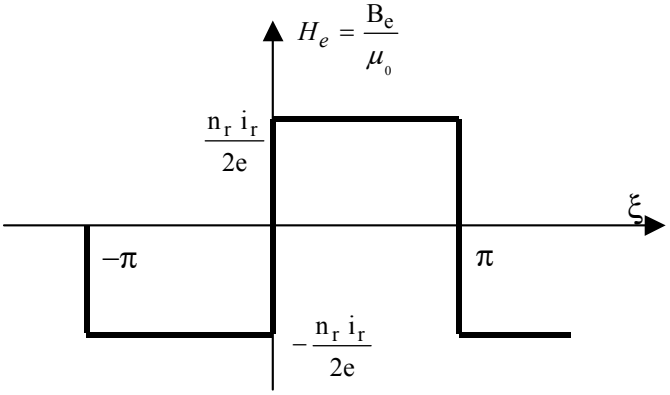

Figure 2.10. *Variation of the air-gap field versus ξ*

Considering the calculation hypotheses, the flux density within the iron is indeterminate. In order to calculate the flux in a stator turn, we shall consider the half-cylinder of length L located in the air-gap as close to the stator as possible and leaning on the turn (Figure 2.11).

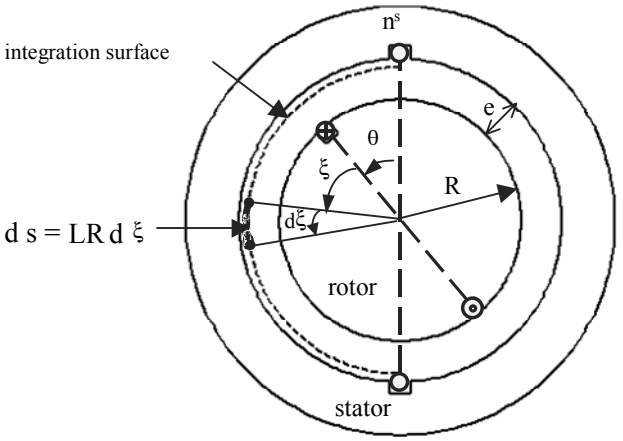

Figure 2.11. *Calculation of the stator flux*

Calling dφ the flux through an elementary surface ds of the cylinder, seen under the central angle dξ, leads to:

$$d\phi = \mathrm{B}\,\mathrm{ds} = \mu_0 \frac{\mathrm{n_r} i_r}{2\mathrm{e}} \mathrm{LR}\,\mathrm{d}\xi$$

$$\phi = \int_{\xi=-\theta}^{\pi-\theta} \mathrm{d}\phi = \mu_0 \frac{n_r i_r}{2\mathrm{e}} \mathrm{LR} \left[\int_{-\theta}^{0} -\mathrm{d}\xi + \int_{0}^{\pi-\theta} \mathrm{d}\xi \right]$$

$$\phi = \mu_0 \frac{n_r i_r}{2\mathrm{e}} \mathrm{LR}\,(\pi - 2\theta)$$

The total flux in the n_s turns of the stator coil is then:

$$\Psi = \mathrm{n_s}\,\phi = \mu_0 \frac{n_s n_r}{2\mathrm{e}} \mathrm{LR}\,(\pi - 2\theta)\,\mathrm{i_r} \qquad \text{for } \theta \in [0, \pi]$$

Mutual inductance M between the two coils is defined by:

$$\Psi = M\,\mathrm{i_r}$$

with:

$$M = \mu_0 \frac{n_s n_r}{2e} \mathrm{LR} \ (\pi - 2\theta)$$

This inductance varies in terms of θ, as shown in Figure 2.12.

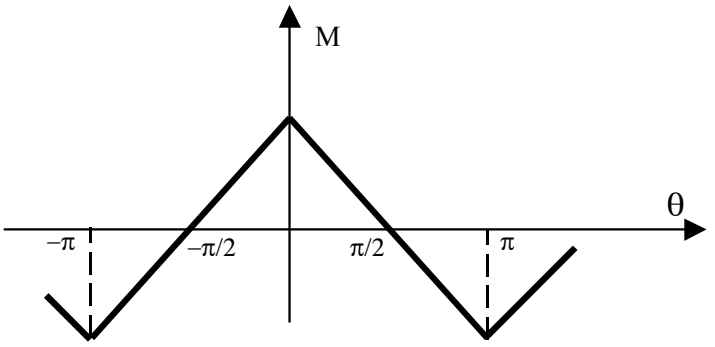

Figure 2.12. *Variation of the mutual M in terms of θ*

The Fourier series of this wave is:

$$M = M_0 \sum_{k} \frac{\cos(2k+1)\theta}{(2k+1)^2} \qquad [2.3]$$

with:

$$M_0 = \frac{2}{\pi} \mu_0 \frac{n_s n_r}{2e} \mathrm{LR}$$

Expression [2.3] highlights the fundamental $M_0 \cos\theta$, corresponding to k = 0, and the "space harmonics" obtained for k ≠ 0. In order to show the respective roles of the fundamental and space harmonics, we shall now assume that the machine is made of three identical stator coils shifted 2π/3 in space in comparison to the previous machine

(Figure 2.13). Let us assume these coils are supplied by a 3-phase balanced current system and the rotor coil by a DC current.

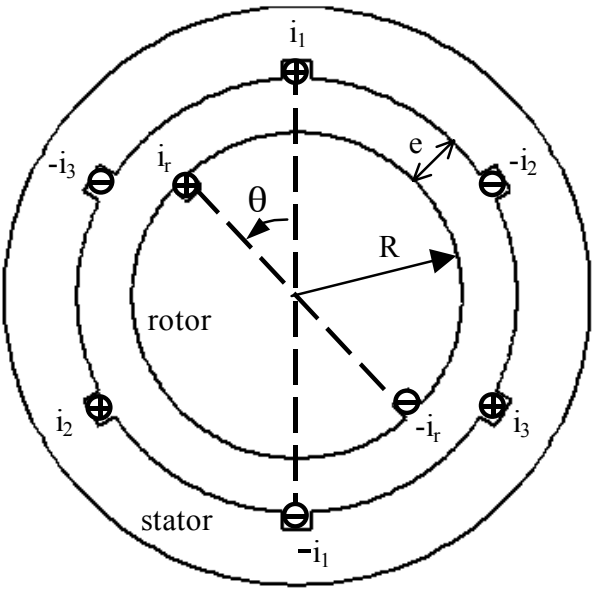

Figure 2.13. *"Basic" 3-phase machine*

Let us calculate, for example, the torque resulting from the interaction of the rotor coil with the stator coil "1" travelled by current i_1:

$$\Gamma_1(i_1, i_r, \theta) = 2 n_s i_1 \, LR \, B_e \qquad \text{for } -\pi < \theta < 0$$

$$\Gamma_1(i_1, i_r, \theta) = -2 n_s i_1 \, LR \, B_e \qquad \text{for } 0 < \theta < \pi$$

where B_e is the air-gap normal flux density generated by the rotor current. Thus:

$$\Gamma_1 = \pm \mu_0 \, n_s \, n_r \, \frac{LR}{e} \, i_1 \, i_r$$

Γ_1 can be written as follows:

$$\Gamma_1 = - K\, i_1 \varepsilon(\theta)$$

with:

$$K = \mu_0\, n_s\, n_r\, \frac{LR}{e}\, i_r$$

The variation of ε ("square wave") is given by Figure 2.14, and its Fourier series is written:

$$\varepsilon(\theta) = \frac{4}{\pi} \sum_{k=1}^{\infty} \frac{\sin(2k+1)\theta}{2k+1}$$

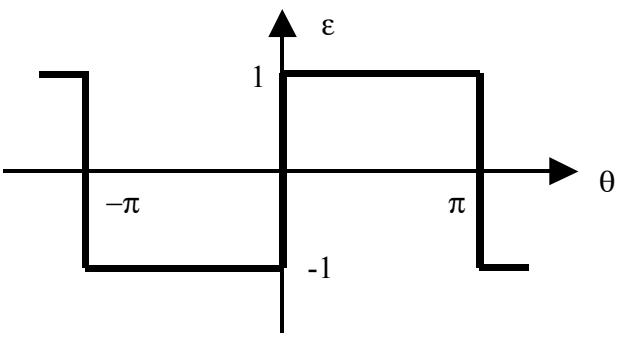

Figure 2.14. *Variation of function ε versus θ*

Naming Γ_1, Γ_2 and Γ_3 the torque contributions of the rotor coil with each of the stator coils, the global electromagnetic torque Γ_e is worth:

$$\Gamma_e = \Gamma_1 + \Gamma_2 + \Gamma_3 = - K\,[i_1\, \varepsilon(\theta) + i_2\, \varepsilon(\theta - \frac{2\pi}{3}) + i_3\, \varepsilon(\theta + \frac{2\pi}{3})]$$

If we set down, for example:

$$i_1 = \mathrm{I}\sqrt{2}\cos\omega t\ ; \qquad i_2 = \mathrm{I}\sqrt{2}\cos(\omega t - \frac{2\pi}{3})\ ; \qquad i_3 = \mathrm{I}\sqrt{2}\cos(\omega t + \frac{2\pi}{3})$$

the resolution of the torque in Fourier series leads to:

$$\Gamma_e = -\frac{4\mathrm{KI}\sqrt{2}}{\pi}\left\{\cos\omega t \sum_{\mathrm{k}\geq 0}\frac{\sin(2\mathrm{k}+1)\theta}{2\mathrm{k}+1} + \cos(\omega t - \frac{2\pi}{3})\sum_{\mathrm{k}\geq 0}\frac{\sin(2\mathrm{k}+1)(\theta - 2\pi/3)}{2\mathrm{k}+1} + \cos(\omega t + \frac{2\pi}{3})\sum_{\mathrm{k}\geq 0}\frac{\sin(2\mathrm{k}+1)(\theta + 2\pi/3)}{2\mathrm{k}+1}\right\}$$

Let us assume that the rotor speed is ω, it is possible to write:

$$\theta = \omega\,\mathrm{t} + \theta_0$$

If this expression of θ is transferred into the expression of the torque, we obtain:

$$\Gamma_e = -\frac{6\mathrm{KI}\sqrt{2}}{\pi}\left\{\sin\theta_0 + \sum_{\mathrm{k}\geq 1}\left[\frac{\sin[6\mathrm{k}\omega\mathrm{t} + (6\mathrm{k}-1)\theta_0]}{6\mathrm{k}-1} + \frac{\sin[6\mathrm{k}\omega\mathrm{t} - (6\mathrm{k}+1)\theta_0]}{6\mathrm{k}+1}\right]\right\}$$

On the one hand this expression shows a constant term:

$$\Gamma_0 = -\frac{6\mathrm{KI}\sqrt{2}}{\pi}\sin\theta_0 \qquad [2.4]$$

which corresponds to the average value of the instantaneous torque produced by the machine, and on the other hand, time related sinusoidal terms or "torque harmonics".

Since these harmonics have a zero average value, they will not lead to continuous energy conversion, but only to losses and vibrations. This calculation therefore shows that if a machine is supplied by sinusoidal currents it is important to reduce the space harmonics as much as possible in order to obtain mutual inductances as near as possible to sinusoidal functions of the relative positions of the coils. This can be obtained by distributing the conductors into several slots, as shown in Figure 2.15.

In the example under consideration, the n_r rotor turns are distributed equally in ten slots, which gives $n_r/5$ conductors per slot, each with a current i_r travelled through them.

Applying Ampere's theorem to the contour γ_1, the embraced Ampere-turns are equal to $\frac{n_r i_r}{5}$, leading to an air-gap field worth:

$$H_1 = \frac{n_r i_r}{10e}$$

If contour γ_2 is used, the Ampere-turns change to $\frac{3n_r i_r}{5}$, hence the new field value:

$$H_2 = 3H_1 = \frac{3n_r i_r}{10e}$$

Likewise contour γ_3 would have led to a field:

$$H_3 = 5H_1 = \frac{n_r i_r}{2e}$$

The flux being conservative, the magnetic field H varies "in steps" between $+\frac{n_r i_r}{2e}$ and $-\frac{n_r i_r}{2e}$ (Figure 2.16).

Determination of mutual inductance M between the rotor and phase 1 of the stator requires a calculation of the magnetic flux travelling through the stator coil. This requires the integration of the field (see previous calculation). Each of the "steps" of H will therefore lead to a variation of M with a slope proportional to the value of H. We obtain the variation of M in relation to θ qualitatively, represented in Figure 2.16.

Thus a sinusoidal approximation of inductance M(θ) for a sufficiently large number of slots can be admitted. In such conditions it will be quite possible to overlook the space harmonics, at least in a first approximation. In this case, the machines are said to have "a sinusoidal repartition of amperes-turns".

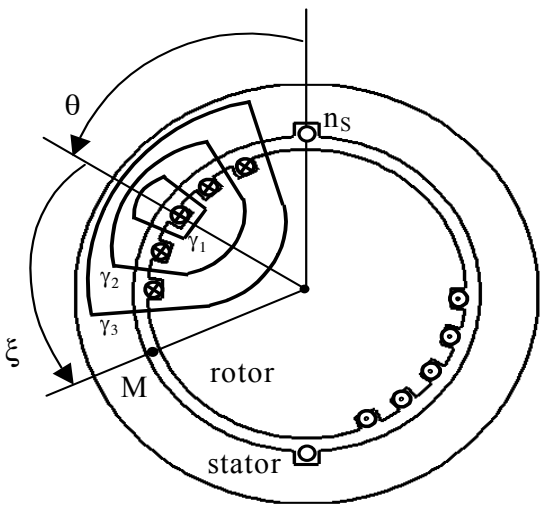

Figure 2.15. *Rotor coil distributed in 10 slots*

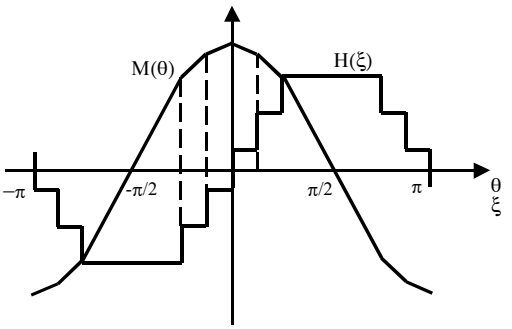

Figure 2.16. *Variations of the field in terms of ξ and of the mutual inductions in terms of θ*

Note that a similar calculation would show that a machine devoid of space harmonics and supplied by non-sinusoidal currents would have a torque with a constant term linked to the fundamental component of current and torque harmonics caused by current harmonics. This explains the fact than when designing static converters, intended to supply sinusoidal distribution rotating machines, considerable attention is paid to the reduction of the harmonics of the output currents.

2.8. Losses within the machines

Rotating machines provide a conversion during which energy takes various successive forms: electric, electromagnetic and mechanical. This process is, at each step, accompanied by energy losses of various natures, which are usually classified as follows.

2.8.1. *Losses due to Joule effect (or "Joule losses")*

These are due to the circulation of currents through conductors having a non-zero resistance. In order to reduce them, good conductive materials are used (usually copper,

but sometimes aluminum for low cost machines). The frequency of the currents can have an influence upon these losses through the skin effect.

2.8.2. *Electromagnetic losses (or "iron losses")*

These are linked to the behavior of ferromagnetic materials submitted to alternating fields. They gather, on the one hand hysteresis losses, and on the other hand losses due to the eddy currents. In order to reduce them, soft materials are used (materials with a narrow hysteresis cycle) in thin laminated steel, insulated from one another. Those losses mainly vary according to the frequency and the amplitude of the fields.

2.8.3. *Mechanical losses*

Gathered under this term are all of the energy losses caused by machine rotation: friction of the axes on the bearings, ventilation and air movement in the air-gap, etc. These losses are functions of the rotation speed of the machine. They are often represented by a losses torque with polynomial expression in terms of the speed ($\Gamma_p = a_0 + a_1\Omega + a_2\Omega^2 + \ldots$, where a_0, a_1, a_2 are constants).

All these losses cause the production of heat within the machine, and therefore an increase in temperature with a risk of deterioration. That is why machines include cooling devices in order to extract the calories as they are produced: fans at the shaft ends, or driven by auxiliary motors, hollow conductors through which a coolant fluid runs, etc.

2.9. Nominal values

The previous considerations (power losses, temperature rises, cooling, etc.) bring about the definition of "nominal

values" of a given machine. This is a set of quantities (power, voltages, currents, torque, speed, etc.) which the considered machine is likely to bear for an indeterminate time. Those values lead to a thermal equilibrium corresponding to the maximum temperature the machine can bear. This equilibrium is reached when the cooling devices extract the calorific energy exactly due to the losses within the machine.

It can be noted, in this connection, that those quantities can be exceeded during a limited time e.g. in transients like the starting of motors. This is possible because the thermal time constants (from several minutes to a few hours) are noticeably bigger than the mechanical time constants (usually about a few seconds) and electrical time constants (several dozen milliseconds) of the machines.

2.10. General sign covenant

Throughout this book, except for some specific cases which will be specified, we shall consider machines as motors: the mechanical power is considered to be positive when it is produced, and the electrical power is positive when it is absorbed. As a consequence, the various coils and windings shall *a priori* be considered as receivers.

2.11. Establishment of matricial equations

In this section, we shall establish a general process to translate the problem into equations for electrical machines, and a general expression of the electromagnetic torque. The approach consists of an overall writing of electrical equations in instantaneous quantities (voltages, currents, flux). A machine shall be considered as a set of coils (rotor and stator coils) the self inductances and mutual inductances of which constitute coupling matrices. The expression of the magnetic co-energy in relation to those coupling matrices and to

instantaneous currents will enable us to establish a general expression of the electromagnetic torque and to examine the possibility of continuous energy conversion.

2.11.1. *Working assumptions*

Later in this section we shall consider a machine made of n coils with 2p poles at the stator and at the rotor. We shall neglect saturation and hysteresis phenomena, as well as induced eddy currents in the ferromagnetic parts.

2.11.2. *Expression of the instantaneous torque*

Let us consider the stator phase I, with R_i its electrical resistance, v_i the voltage applied between its terminals and Ψ_i the total flux through it. The following general equation can be written:

$$v_i = R_i i_i + \frac{d\psi_i}{dt}$$

For all n phases of the machine:

$$\{v\} = \{R\}\{i\} + \left\{\frac{d\psi}{dt}\right\} \qquad [2.5]$$

with:

$$\{\psi\} = \begin{Bmatrix} \psi_1 \\ \psi_2 \\ . \\ . \\ \psi_n \end{Bmatrix} \qquad \{i\} = \begin{Bmatrix} i_1 \\ i_2 \\ . \\ . \\ i_n \end{Bmatrix} \qquad \{R\} = \begin{Bmatrix} R_1 & 0 & . & . & 0 \\ 0 & R_2 & . & . & 0 \\ . & . & . & . & . \\ . & . & . & . & . \\ 0 & 0 & . & . & R_n \end{Bmatrix}$$

The instantaneous power P_i absorbed by the entire circuit is:

$$P_i = \{i\}^t\{v\} = \{i\}^t[R]\{i\} + \{i\}^t\left\{\frac{d\psi}{dt}\right\} \qquad [2.6]$$

The first term of the right-hand member represents the Joule losses while the second represents (see equation [1.31]) the sum of the "accumulated power" in the electromagnetic field $\frac{dW_{em}}{dt}$ and the converted mechanical power $\Gamma_e\Omega$.

In a linear state, the global expression of the flux is written:

$$\{\psi\} = [\mathcal{L}]\{i\}$$

with:

$$[\mathcal{L}] = \begin{bmatrix} L_1 & M_{12} & . & . & M_{1n} \\ M_{21} & L_2 & . & . & M_{2n} \\ . & . & . & . & . \\ . & . & . & . & . \\ M_{n1} & M_{n2} & . & . & L_n \end{bmatrix}$$

L_i is the self inductance of phase i, and M_{ij}, the mutual inductance between phases i and j.

The electromagnetic torque is then obtained from equation [1.37].

$$\Gamma_e = \frac{1}{2}\{i\}^t\left\{\frac{\partial\mathcal{L}}{\partial\Theta}\right\}\{i\} = \frac{p}{2}\{i\}^t\left\{\frac{\partial\mathcal{L}}{\partial\theta}\right\}\{i\} \qquad [2.7]$$

This expression of the torque instantaneous value shall enable us to seek the main structures of machines likely to

lead to a continuous energy conversion, that is to say the ones producing an average value of Γ_e different from zero.

The inductance matrix $\{\mathcal{L}\}$ is broken up in four sub-matrices:

$$\{\mathcal{L}\} = \begin{Bmatrix} [\mathcal{L}_s] & [\mathcal{L}_{sr}] \\ [\mathcal{L}_{rs}] & [\mathcal{L}_r] \end{Bmatrix}$$

$[\mathcal{L}_s]$ and $[\mathcal{L}_r]$ respectively group together the stator and rotor inductances, $[\mathcal{L}_{sr}]$ and $[\mathcal{L}_{rs}]$ group together the stator-rotor and rotor-stator mutual inductances; keep in mind that the last two sub-matrices are the transposed matrices of one another. We shall now analyze the influence of the structure (non-salient or salient poles) of the machines on the instantaneous electromagnetic torque Γ_e, and, more specifically on the possibility of achieving a continuous energy conversion.

2.11.3. *Continuous energy conversion in cylindrical machines*

2.11.3.1. *Instantaneous torque in cylindrical machines*

In a cylindrical machine, the influence of the slots can, in a first approximation, be overlooked, and the air-gap can be considered to be constant. In such conditions the reluctance of the magnetic circuits of stator and rotor phases is independent of the stator-rotor position; it shall thus be the same for the inductances of those phases. It can be deduced that:

$$\left[\frac{\partial \mathcal{L}_s}{\partial \theta}\right] = 0 \qquad \text{and} \qquad \left[\frac{\partial \mathcal{L}_r}{\partial \theta}\right] = 0$$

thus:

$$\left\{\frac{\partial \mathcal{L}}{\partial \theta}\right\} = \begin{Bmatrix} [0] & \left[\frac{\partial \mathcal{L}_{sr}}{\partial \theta}\right] \\ \left[\frac{\partial \mathcal{L}_{rs}}{\partial \theta}\right] & [0] \end{Bmatrix}$$

If this expression is transferred into the equation of the instantaneous electromagnetic torque, we obtain:

$$\Gamma_e = \frac{p}{2}\left\{[i_s]^t \quad [i_r]^t\right\} \begin{Bmatrix} [0] & \left[\frac{\partial \mathcal{L}_{sr}}{\partial \theta}\right] \\ \left[\frac{\partial \mathcal{L}_{rs}}{\partial \theta}\right] & [0] \end{Bmatrix} \begin{Bmatrix} [i_s] \\ [i_r] \end{Bmatrix}$$

which leads to:

$$\Gamma_e = \frac{p}{2}[i_s]^t \left[\frac{\partial \mathcal{L}_{sr}}{\partial \theta}\right][i_r] + \frac{p}{2}[i_r]^t \left[\frac{\partial \mathcal{L}_{rs}}{\partial \theta}\right][i_s]$$

Since $\left[L_{rs}\right] = \left[L_{sr}\right]^t$, the two terms of the above expression are equal, and it can then be written indiscriminately:

$$\Gamma_e = p\,[i_s]^t \left[\frac{\partial \mathcal{L}_{sr}}{\partial \theta}\right][i_r] \qquad [2.8a]$$

or:

$$\Gamma_e = p\,[i_r]^t \left[\frac{\partial \mathcal{L}_{rs}}{\partial \theta}\right][i_s] \qquad [2.8b]$$

2.11.3.2. *Periodicities and angular frequencies*

We shall now consider that all rotor currents have the angular frequency ω_r, and the stator currents, the angular

frequency ω_s. The stator-rotor mutual inductances depend on $\theta = p\Theta$, and, if the machine is assumed to be "well built" (that is to say with a sinusoidal distribution of the Ampere-turns), this dependence will be sinusoidal. The period of variation of those mutual inductances will therefore be the "electrical period" or double pole pitch, which leads to an angular frequency $p\Omega$.

Torque Γ_e is the product of three periodical functions; hence a non-zero average value needs the algebraic sum of the angular frequencies to be equal to zero. It is deduced that:

$$\omega_s \pm \omega_r \pm p\Omega = 0 \qquad [2.9]$$

Now let us see what can be deduced from this expression, in analyzing first the special case when one of the terms of this expression is zero.

2.11.3.2.1. Case of $\omega_r = 0$ (rotor supplied by a DC current)

In this case:

$$\omega_s = p\Omega \qquad [2.10]$$

which corresponds to the functioning of a synchronous machine (rotation speed proportional to the stator angular frequency); this will be studied in Chapter 3.

2.11.3.2.2. Case of $\omega_s = 0$ (stator supplied by a DC current)

In that case:

$$\omega_r = p\Omega \qquad [2.11]$$

This expression corresponds to so-called "inverted" synchronous machines (field system at the stator side and the armature at the rotor side), but also to DC machines. The

currents in the rotor of the latter are AC currents and are mechanically rectified by the brush-commutator system (Chapter 5).

2.11.3.2.3. Case of $\Omega = 0$ (stationary machine)

If $\Omega = 0$, we obviously get $\omega_s = \omega_r$. The stator and rotor angular frequencies will then have to be equal. We shall see that the asynchronous machine (Chapter 4) provides this condition, leading to an initial non-zero torque. The DC machine also respects this expression with $\omega_s = \omega_r = 0$ at a zero speed.

2.11.3.2.4. General case

If none of the three variables (ω_s, ω_r, Ω) are zero, equation [2.9] leads to:

$$\omega_s = \omega_r + p\Omega \qquad [2.12]$$

This equation corresponds to the functioning of the asynchronous machine, whether it is an induction machine or a "doubly fed" machine (Chapter 4).

2.11.4. *Continuous energy conversion in salient pole machines*

2.11.4.1. *Salient pole machine torque*

When one of the two spools (rotor or stator) has salient poles (Figure 2.6), it is not possible to consider the air-gap as constant. For example, let us consider the case of rotor salience (Figure 2.6b): since the stator is cylindrical, the magnetic circuit of the rotor coil has a geometry independent from the stator-rotor position; its reluctance, and as a consequence, its inductance shall be independent from Θ, and therefore from θ. On the contrary, it is clear that as far as the magnetic circuit of the stator phases is concerned,

the air-gap, and therefore the reluctance, are extremely dependent from relative rotor-stator position, which generates a variation of the stator inductances in relation to Θ, and therefore to θ.

So, for a machine with a salient rotor, matrix $[\mathcal{L}_s]$ is a function of Θ, whereas $[\mathcal{L}_r]$ is not. This leads to an inductance matrix derivative in terms of the position:

$$\left\{\frac{\partial \mathcal{L}}{\partial \Theta}\right\} = \begin{Bmatrix} \left[\frac{\partial \mathcal{L}_s}{\partial \Theta}\right] & \left[\frac{\partial \mathcal{L}_{sr}}{\partial \Theta}\right] \\ \left[\frac{\partial \mathcal{L}_{rs}}{\partial \Theta}\right] & [0] \end{Bmatrix}$$

Bringing this expression into the equation of the electromagnetic torque leads to an extra term (with regards to the non-salient machine torque) called "salience torque" or "reluctance torque":

$$\Gamma_s = [i_s]^t \left[\frac{\partial \mathcal{L}_s}{\partial \Theta}\right] [i_s] \qquad [2.13]$$

An identical reasoning would show that for a salient stator machine (Figure 2.6a), it is matrix $[\mathcal{L}_r]$ which is a function of Θ, and this leads to a salience torque as follows:

$$\Gamma_s = [i_r]^t \left[\frac{\partial \mathcal{L}_r}{\partial \Theta}\right] [i_r] \qquad [2.14]$$

2.11.4.2. *Periodicities and angular frequencies*

In the previous sections, the inductances variation period in terms of Θ is the polar pitch (and not the double polar pitch, as for rotor-stator mutuals). Therefore, when in the

case of rotor salience, $\left[\frac{\partial \mathcal{L}_s}{\partial \Theta}\right]$ has a 2pΩ angular frequency. $\left[\frac{\partial \mathcal{L}_r}{\partial \Theta}\right]$ also has an angular frequency of 2pΩ in the case of a stator salience.

2.11.4.3. *Continuous energy conversion*

Expressions [2.13] and [2.14] show that in order to obtain a non-zero average value of Γ_s it would be advisable to have:

$$\omega_s = p\Omega \text{ for a salient rotor}$$

or:

$$\omega_r = p\Omega \text{ for a salient stator}$$

We can deduce that the machines for which it is useful to have salient rotors are the synchronous machines, which will be studied in Chapter 3. In the same way, DC machines (Chapter 5), as well as "inverted" synchronous machines (Chapter 3) can have stator salient poles. On the contrary, asynchronous machines need a non-salient air-gap, that is to say they cannot have any salient pole either at the stator or at the rotor.

2.12. Mechanical equation

Electrical machines have a mechanical interaction with their environment (charge in the case of a motor, driving mechanism in the case of a generator). This is characterized by the dynamics equation applied to rotating solids. In the case of a motor it can be written as:

$$J\frac{d\Omega}{dt} = \Gamma - \Gamma_c \qquad [2.15]$$

where Γ is the torque of the electrical machine, Γ_c that of the charge, and J the moment of inertia of the whole of the

rotating parts. This equation is often called the “mechanical equation” of the rotating machines.

2.13. Conclusion

The matricial formalism introduced in this chapter will later allow the translation into equations of synchronous, asynchronous and DC machines: the analysis of the physical structure of each machine will lead to writing the coupling matrices, and knowing the power supply will enable us to write the current and voltage expressions. Bear in mind that since the equations are written with instantaneous values, the supply by static converters giving out non-sinusoidal currents can be taken into account. The instantaneous electromagnetic torque expression (equation [2.7]) shall be used in the following chapters in order to characterize the electromagnetic energy conversion in each machine.

Chapter 3

Synchronous Machines

3.1. Introduction

The industrial value of synchronous machines is considerable: first, used as generators (called "AC generators"), they provide almost all the production of electric energy.

In addition, associated with static converters (inverters or cycloconverters) functioning on variable frequencies, synchronous motors have become essential during recent decades in a number of industrial areas: rail traction, naval propulsion, manufacturing industry, iron and steel industry, oil exploitation, machine-tools, etc.

In this chapter, we shall mainly consider cylindrical machines, however we will address salient pole machines at the end of the chapter.

3.2. Introduction and equations of the cylindrical synchronous machine

3.2.1. *General description*

We shall consider a machine with cylindrical field spools, each one having 2p poles at the stator as well as at the rotor. In most cases the field system is at the rotor. It is supplied with DC current or provided with permanent magnets. The field current is usually injected in the rotor via slip rings and brushes. The armature (Figure 3.1), which usually is 3-phase, is at the stator and makes exchanges with a source (network or static converter) or with a voltage and current charge assumed to be sinusoidal *a priori*. Depending on the kind of power exchanged by the machine with its environment, we shall either talk about an AC generator or about a synchronous motor.

We shall usually assume the machines to be "well built", that is to say with a sinusoidal repartition of the ampere-turns, enabling us to overlook the space harmonics.

3.2.1.1. *Main notations*

– f: stator currents frequency.

– i_j: instantaneous value of the current in phase j.

– I_j: rms value of current i_j.

– J: moment of inertia.

– L_S: self inductance of a stator phase.

– L_R: self inductance of a rotor coil.

– M_S: mutual inductance between two stator phases.

– M: maximum value of the rotor-stator mutual inductance.

– $L = L_S - M_S$: synchronous inductance.

– p: number of pole pairs.

– P: active power.

– Q: reactive power.

– S: apparent power.

– V: rms value of the voltage per phase.

– $\overline{Z} = Z\, e^{j\xi}$: complex stator impedance.

– ω: stator currents angular frequency.

– Θ: stator/rotor mechanical angle.

– θ: electrical angle (Θ = pθ).

– Ω: speed of rotation.

– φ: voltage/current phase shift.

– ψ_j: total flux in phase j.

– Γ_i: instantaneous value of the torque.

– γ: load angle.

– δ: power angle.

– μ: ampere-turns equivalence factor.

– λ = lω: leakage reactance.

Figure 3.1. *Synchronous machine stator (photo source: Converteam)*

3.2.1.2. *Conventional representation*

We shall describe the machine in the form of three coils A, B and C, representing the stator phases, and representing the rotor field system of a coil R (Figure 3.2).

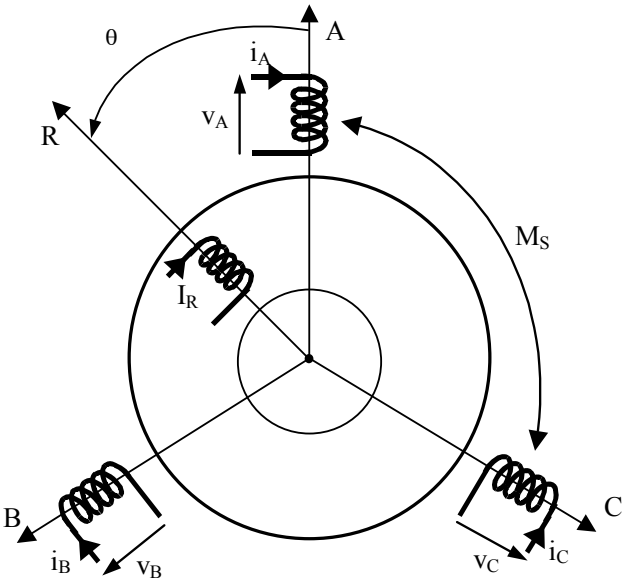

Figure 3.2. *Conventional representation of the synchronous machine*

Conventionally, we will choose the axis of phase A as the origin of the angles which will be counted positively in the trigonometric direction. Phases B and C are then shifted in space respectively by $2\pi/3$ and $4\pi/3$ electric in relation to the origin, and the field system is shifted by an electric angle θ.

3.2.1.3. *Inductances and coupling matrixes*

Let us introduce the stator coupling matrix $\mathcal{L}_S$, the rotor coupling matrix $\mathcal{L}_R$ and the stator-rotor coupling matrixes $\mathcal{L}_{SR}$ and $\mathcal{L}_{RS}$:

$$\{\mathcal{L}_S\} = \begin{Bmatrix} L_S & M_S & M_S \\ M_S & L_S & M_S \\ M_S & M_S & L_S \end{Bmatrix}$$

$$\{\mathcal{L}_R\} = L_R$$

$$\{\mathcal{L}_{SR}\} = \{\mathcal{L}_{RS}\}^t = M \begin{Bmatrix} \cos\theta \\ \cos(\theta - 2\pi/3) \\ \cos(\theta + 2\pi/3) \end{Bmatrix}$$

3.2.2. *Why synchronous?*

In order to justify the name given to this machine, we shall make two calculations: one for a functioning as a generator, and the other, as a motor. Let us assume first that the machine is driven at an angular speed Ω and that only the field system is supplied by a DC current I_R. The stator phases not being supplied, their flux are exclusively caused by the excitatation current I_R.

Since $\theta = \theta_0 + \omega t = \theta_0 + p\Omega t$, it can be written that:

$$\{\psi_S\} = \{L_{SR}\}\ I_R = M\ I_R \begin{Bmatrix} \cos\theta \\ \cos(\theta - 2\pi/3) \\ \cos(\theta + 2\pi/3) \end{Bmatrix} = M\ I_R \begin{Bmatrix} \cos(\theta_0 + \omega t) \\ \cos(\theta_0 + \omega t - 2\pi/3) \\ \cos(\theta_0 + \omega t + 2\pi/3) \end{Bmatrix}$$

Those flux being variable in terms of time, electromotive forces appear in the stator. They are given by:

$$\{e_S\} = -\left\{\frac{d\psi_S}{dt}\right\} = M\omega Ir \begin{Bmatrix} \sin(\theta_0 + \omega t) \\ \sin(\theta_0 + \omega t - 2\pi/3) \\ \sin(\theta_0 + \omega t + 2\pi/3) \end{Bmatrix}$$

which establishes that this machine enables the production of a 3-phase sinusoidal voltage system, for which frequency is proportional to the speed of rotation:

$$f = \frac{\omega}{2\pi} = \frac{p\Omega}{2\pi}$$

Let us now assume that the stator of this machine is supplied with a balanced 3-phase sinusoidal current system as follows:

$$\{i_S\} = I\sqrt{2}\begin{Bmatrix} \cos(\omega t - \varphi) \\ \cos(\omega t - 2\pi/3 - \varphi) \\ \cos(\omega t + 2\pi/3 - \varphi) \end{Bmatrix}$$

As the rotor is still supplied by a DC current I_R, we shall assume that it turns at the angular speed $\Omega' = \omega'/p$, so that $\theta = \theta_0 + \omega' t$.

In using the general expression giving the instantaneous torque of a cylindrical machine:

$$\Gamma_i = p\{i_S\}^t \left\{\frac{\partial \mathcal{L}_{SR}}{\partial \theta}\right\} \{i_R\} \qquad [1.8a]$$

with:

$$\left\{\frac{\partial \mathcal{L}_{SR}}{\partial \theta}\right\} = -M\begin{bmatrix} \sin\theta \\ \sin(\theta - 2\pi/3) \\ \sin(\theta + 2\pi/3) \end{bmatrix} \qquad \text{and} \qquad \{i_R\} = I_R$$

We obtain:

$$\Gamma_i = -\frac{3}{2} pMI_R I\sqrt{2}\sin(\theta - \omega t + \varphi)$$

and finally:

$$\Gamma_i = -\frac{3}{2} p\, M\, I_R I\sqrt{2}\, \sin[(\omega' - \omega)t + \theta_0 + \varphi)]$$

This expression shows that, if and only if ω' = ω, torque Γ_i will have a mean value different from zero. In that case Γ_i will be constant and equal to:

$$\Gamma_i = -\frac{3}{2} p M I_R I\sqrt{2} \sin(\theta_0 + \varphi) \qquad [3.1]$$

In the following, it will be set down:

$$\gamma = \theta_0 + \varphi$$

γ is called the load angle.

It is now clearly illustrated that it is necessary for the speed of rotation to be proportional to the frequency of the armature currents for a synchronous machine to make a continuous energy conversion:

$$\Omega = \frac{\omega}{p} = \frac{2\pi f}{p} \qquad [3.2]$$

Also let us now assume that this machine is supplied by non-sinusoidal stator currents as follows:

$$i_A = \sum_n I_n \sqrt{2} \cos(n\omega t - \varphi_n)$$

$$i_B = \sum_n I_n \sqrt{2} \cos\left(n\omega t - \varphi_n - \frac{2\pi}{3}\right)$$

$$i_C = \sum_n I_n \sqrt{2} \cos\left(n\omega t - \varphi_n + \frac{2\pi}{3}\right)$$

In transferring those expressions to [1.8a], we obtain, after a few calculations:

$$\Gamma_i = \sum_n -\frac{3}{2} p M I_R I_n \sqrt{2} \cos\left[(\omega' - n\omega)t + \theta_0 + \varphi_n\right]$$

This expression clearly shows that only one of the current harmonics (usually, the fundamental) gives a continuous energy conversion; the others generate some torques of zero mean value, which cause vibrations and losses.

This shows the relevance of the reduction of current harmonic factor when synchronous motors are supplied by power electronics converters.

3.2.3. *Rotation speeds at constant frequency*

When a synchronous machine is connected to a fixed frequency network (50 Hz in Europe, 60 Hz on the American continent, for example), its rotation speed expressed in revolutions per minute (rpm) is:

$$N = \frac{60}{2\pi}\Omega = \frac{60}{2\pi}\frac{\omega}{p}$$

Thus, if f = 50 Hz, $N = \frac{3000}{p}$ rpm. The possible speeds for synchronous machines (usually AC generators) connected to a 50 Hz network are therefore sub-multiples of 3,000 rpm.

3.2.4. *Equations of the cylindrical machine*

3.2.4.1. *Assumptions and sign covenant*

We shall consider machines with a constant air-gap in electrical and mechanical stationary states. We neglect the magnetic saturation and hysteresis phenomena. The stator currents are assumed to be sinusoidal, and the rotor current is constant. The only losses taken into account are those due to the Joule effect.

We choose sign covenants relative to a “motor” working, that is to say that the mechanical power is counted positively if it is furnished to a load, and the active and reactive electrical powers are counted positively when they are absorbed by the machine.

3.2.4.2. *Calculation of the flux in a phase*

Let us consider Figure 3.2, which represents the stator and rotor phases of the machine with their respective voltages and currents. We can express the various flux in the machine as follows:

$$\{\psi\} = \{\mathcal{L}\}\{i\}$$

with:

$$\{\psi\} = \begin{Bmatrix} [\psi_S] \\ [\psi_R] \end{Bmatrix} \qquad \{i\} = \begin{Bmatrix} [i_S] \\ I_R \end{Bmatrix}$$

and:

$$\{\mathcal{L}\} = \begin{Bmatrix} [\mathcal{L}_S] & [\mathcal{L}_{SR}] \\ [\mathcal{L}_{RS}] & L_R \end{Bmatrix}$$

hence the total flux in a stator phase:

$$\{\psi_S\} = \{\mathcal{L}_S\}\{i_S\} + \{\mathcal{L}_{SR}\} I_R$$

which, when it is developed, gives:

$$\{\Psi_S\} = \begin{Bmatrix} L_S & M_S & M_S \\ M_S & L_S & M_S \\ M_S & M_S & L_S \end{Bmatrix} \begin{Bmatrix} i_A \\ i_B \\ i_C \end{Bmatrix} + \begin{Bmatrix} M\cos\theta \\ M\cos(\theta - 2\pi/3) \\ M\cos(\theta + 2\pi/3) \end{Bmatrix} I_R \qquad [3.3]$$

assuming that:

$$i_A = I\sqrt{2}\cos(\omega t - \varphi)$$
$$i_B = I\sqrt{2}\cos(\omega t - \varphi - \frac{2\pi}{3})$$
$$i_C = I\sqrt{2}\cos(\omega t - \varphi + \frac{2\pi}{3})$$

If the first row of [3.3] is developed in order to calculate the flux in phase A:

$$\psi_A = L_S\, i_A + M_S\,(i_B + i_C) + M\, I_R \cos\theta$$

hence:

$$\psi_A = (L_S - M_S)\, i_A + M\, I_R \cos\theta$$

$$\psi_A = (L_S - M_S)\, I\sqrt{2}\cos(\omega t - \varphi) + M\, I_R \cos(\omega t + \theta_0)$$

likewise:

$$\psi_B = (L_S - M_S)\, I\sqrt{2}\cos(\omega t - \varphi - \frac{2\pi}{3}) + M\, I_R \cos(\omega t + \theta_0 - \frac{2\pi}{3})$$
$$\psi_C = (L_S - M_S)\, I\sqrt{2}\cos(\omega t - \varphi + \frac{2\pi}{3}) + M\, I_R \cos(\omega t + \theta_0 + \frac{2\pi}{3})$$

In order to determine the rotor flux ψ_R, a similar calculation leads to:

$$\psi_R = \frac{3}{2} M\, I\sqrt{2}\cos(\theta_0 + \varphi) + L_R I_R$$

These expressions of the instantaneous flux within the different coils of the machine lead to the following comments:

– the rotor flux ψ_R does not depend on time, therefore there is no e.m.f. induced in the field winding;

– the total flux per stator phase is the sum of two sinusoidal terms with the same angular frequency ω ; it thus has an angular frequency ω itself. This will enable us to use complex notations.

If the complex number $\bar{I}_A = Ie^{-j\varphi}$ associated with the current i_A is introduced and if $\overline{\Psi}_A$ is similarly associated with flux ψ_A, we can write:

$$\overline{\Psi}_A = (L_S - M_S)\bar{I}_A + \frac{MI_R}{\sqrt{2}}e^{j\theta_0}$$

For phases B and C, similar expressions would be obtained, and it is therefore possible, in removing the suffixes, to unify the general expression of the total flux per stator phase:

$$\overline{\Psi} = (L_S - M_S)\bar{I} + \frac{MI_R}{\sqrt{2}}e^{j\theta_0}$$

that is to say:

$$\overline{\Psi} = L\bar{I} + \frac{MI_R}{\sqrt{2}}e^{j\theta_0} \qquad [3.4]$$

with $L = (L_S - M_S)$: synchronous inductance.

3.2.4.3. *Electrical equation of the cylindrical synchronous machine*

If the complex representation of the voltage per stator phase is $\overline{V}$, and the stator phase resistance is R, we can write:

$$\overline{V} = R\bar{I} + \frac{d\overline{\psi}}{dt} = R\bar{I} + j\omega\overline{\psi} = R\bar{I} + jL\omega\bar{I} + j\frac{M\omega I_R}{\sqrt{2}}e^{j\theta_0}$$

or also:

$$\overline{V} = (R + jL\omega)\,\overline{I} + \overline{E} \qquad [3.5]$$

with:

$$\overline{E} = j\frac{M\omega I_R}{\sqrt{2}}e^{j\theta_0}$$

$\overline{E}$ is the complex representation of the electromotive force per phase of the machine and Lω, the synchronous reactance. If

$$\delta = \theta_0 + \frac{\pi}{2}:$$

$$\overline{E} = \frac{M\omega I_R}{\sqrt{2}}e^{j\delta} \qquad [3.6]$$

δ is the power angle of the machine.

This expression emphasizes that the amplitude of the electromotive force E is proportional to the field system current I_R, and also to ω, and thus to the rotation speed Ω. Note the synchronous impedance:

$$\overline{Z} = R + jL\omega = Z\,e^{j\xi}$$

The electrical equation becomes:

$$\overline{V} = \overline{E} + \overline{Z}\,\overline{I}$$

3.2.4.4. *Equivalent diagram*

Equation [3.5] represents the equivalent per phase diagram of Figure 3.3, which is a diagram of an active dipole.

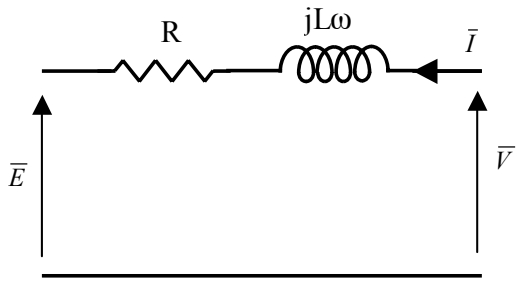

Figure 3.3. *Per phase equivalent circuit of the cylindrical synchronous machine*

3.3. Analysis of the synchronous machine connected to an infinite power network

We shall now consider that the synchronous machine (motor or AC generator) has its armature winding connected to a network. The power of this network is far superior to the power of the machine. Through a misuse of language, it is then called a network of "infinite power".

Assuming this, it is admitted that the network fixes the voltage at the terminals of the machine, as well as the stator angular frequency ω. It is then convenient to consider the voltage as the phase origin. The electrical equation per phase is written:

$$V = (R + jL\omega)\,\bar{I} + \bar{E}$$

where V is a real number.

3.3.1. *Phasor diagram*

The previous electrical equation can be illustrated by a vector diagram in the "voltages plane" (Figure 3.4), called a "voltage diagram".

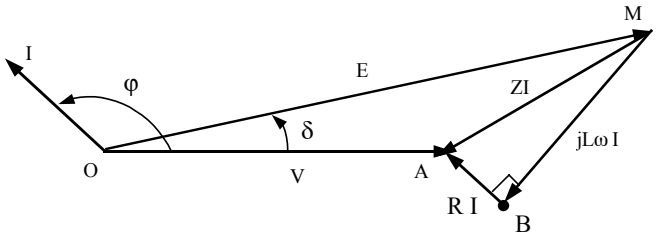

Figure 3.4. *Phasor diagram*

It can be noted that since V is assumed to be constant, points O and A are fixed and point M is representative of the "operating point" of the machine: active and reactive powers exchanged with the network, torque, mechanical power exchanged on the shaft, etc. We shall see in the following of this paragraph how it is possible to deduce those quantities from the position of point M.

3.3.2. *Active (P) and reactive (Q) graduation of the voltage diagram*

In order to deduce the powers exchanged with the network from the previous diagram, we shall graduate it in active power P and reactive power Q. We shall therefore determine the axes and the corresponding scale. First let us consider the complex apparent power:

$$\bar{S} = 3V\,\bar{I}^{*} = P + jQ$$

We have:

$$\bar{S}^{*} = 3V\,\bar{I} = P - jQ = 3V\,\frac{(V - \bar{E})}{\bar{Z}} = \frac{3V}{\bar{Z}}\,\overline{MA}$$

that is to say:

$$\bar{S}^{*} = \frac{3V}{Z}\,\overline{MA}\,e^{-j\xi} = P - jQ$$

The location of points M causing $\overline{S}^*$ to have positive real values provides the axis of the active power and its orientation. The previous expression shows that we must have:

$$Arg(\overline{AM}) = \pi + \xi$$

In the same way, $\overline{S}^*$ will be a negative imaginary number (and therefore $\overline{S}$ will be a positive imaginary number) if:

$$Arg(\overline{AM}) = \frac{\pi}{2} + \xi$$

which defines the axis of the reactive powers. We can therefore complete the diagram in making the axes of absorbed active and reactive powers appear (Figure 3.5). As the plane is initially graduated in voltages, the power scale will be obtained in multiplying the scale of the voltages by $\frac{3V}{Z}$.

If the projections of point M on the axes are considered: q on the reactive powers axis and p on the active powers axis, qM will measure power P, and pM, power Q absorbed in the network. This graduation will enable us to characterize the operating modes of the synchronous machine:

– if P < 0: generator mode (AC generator);

– if P > 0: receiver mode;

– if Q < 0: so-called “capacitive” state, through an analogy with capacitors which supply reactive power;

– if Q > 0: “inductive” state, in comparison to the inductances which absorb reactive power.

This enables us to characterize the four quadrants of the plane delimited by axes P and Q (Figure 3.5).

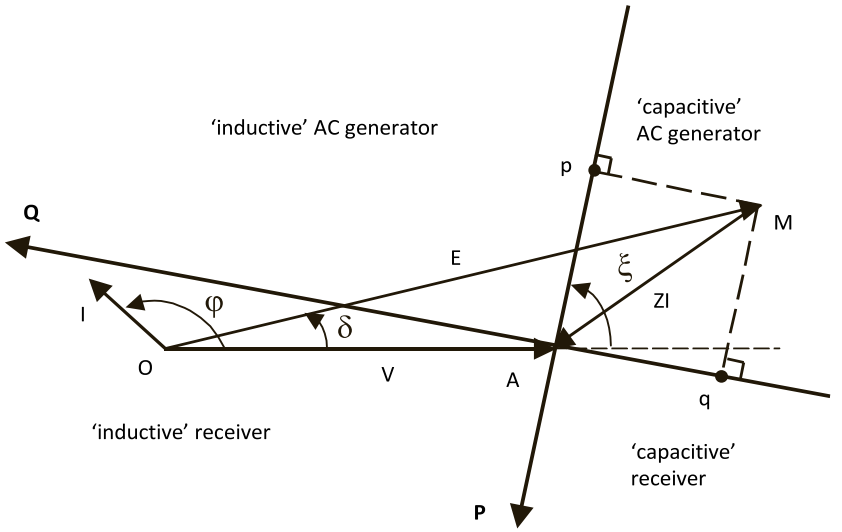

Figure 3.5. *Active (P) and reactive (Q) graduation of the phasor diagram*

3.3.3. *"Internal" powers*

In section 3.3.2, we emphasized a half-plane in which the machine absorbs active power. This can encourage us to consider that the machine works as a motor but, in order to establish it we have to calculate the mechanical power. With this end in view let us consider the expression of the torque P given by equation [3.1]:

$$\Gamma = -\frac{3}{2} p M I_R I\sqrt{2} \sin(\theta_0 + \varphi) = \frac{3}{2} p M I_R I\sqrt{2} \cos(\delta + \varphi) \quad [3.7]$$

Let us introduce the "internal apparent power" given by:

$$\bar{S}' = 3\bar{E}\,\bar{I}^* = P' + jQ'$$

that is to say:

$$\overline{S}' = \frac{3M\omega}{\sqrt{2}} I_R I \, e^{j(\delta+\varphi)}$$

hence the "internal active power":

$$P' = \frac{3}{2} M\omega I_R I\sqrt{2} \cos(\delta+\varphi) = \frac{3}{2} p\,\Omega\, M\, I_R I\sqrt{2} \cos(\delta+\varphi)$$

In bringing together this equation and the expression of the torque [3.7], we obtain:

$$P' = \Gamma\Omega$$

which shows that, considering the hypotheses made (neglected mechanical losses), the internal active power P' represents the mechanical power produced by the synchronous machine. In order to ensure that the machine operates as a motor, P' will have to be positive.

We shall now look for the locus of the points corresponding to P' > 0 in the plane previously introduced [Figures 3.4 and 3.5]. Let us consider the axis [Ax, Ay] in Figure 3.6 in which x and y are the coordinates of the point M:

$$\overline{AM} = x + jy$$

Calling (– a) the abscissa of point O in this coordinate system, leads to:

$$\overline{E} = V - \overline{Z}\,\overline{I} = \overline{OA} + \overline{AM} = a + x + jy$$

The expression of S' being:

$$\overline{S'} = 3\overline{E}\,\overline{I}^{*} = 3\overline{E}\frac{(\overline{Z}\,\overline{I})^{*}}{\overline{Z}^{*}}$$

with:

$\overline{Z}\,\overline{I} = \overline{MA} = -(x + jy)$, that is to say $(\overline{Z}\,\overline{I})^{*} = -(x + jy)$ and $\overline{Z}^{*} = \mathrm{Ze}^{-\mathrm{j}\xi}$

we get:

$$\overline{S}' = -\frac{3}{Z}(a + x + jy)(x - jy)e^{j\xi}$$

$$\overline{S}^{*} = -\frac{3}{Z}(x^2 + y^2 + ax - j\,ay)(\cos\xi + j\sin\xi)$$

hence:

$$P' = -\frac{3}{Z}\left[(x^2 + y^2 + ax)\cos\xi + ay\sin\xi\right]$$

The locus of the points corresponding to a constant mechanical power is therefore defined by:

$$-P'\frac{Z}{3} = (x^2 + y^2 + ax)\cos\xi + ay\sin\xi$$

expression which can be written as follows:

$$\left[(x + \frac{a}{2})^2 + (y + \frac{a}{2}tg\xi)^2\right]\cos\xi - \frac{a}{4\cos\xi} = -\frac{Z\,P'}{3}$$

which shows that the locus of points corresponding to P' = constant are circles centered on the point Ω_1 with coordinates:

$x = -\frac{a}{2}$ and $y = -\frac{a}{2} tg\xi$, and of radius $\left[\frac{a^2}{4\cos^2 \xi} - \frac{ZP'}{3\cos\xi}\right]^{1/2}$

It can be noted that Ω_1 is at the intersection of axis P with the median of segment OA. In the special case when P' = 0, circle (C_0) has the radius $\frac{V}{2\cos\xi}$ and goes through points O and A (Figure 3.6). The motor operating points (P' > 0) are therefore inside (C_0). It is then possible to distinguish the different operating modes of the synchronous machine in Figure 3.6.

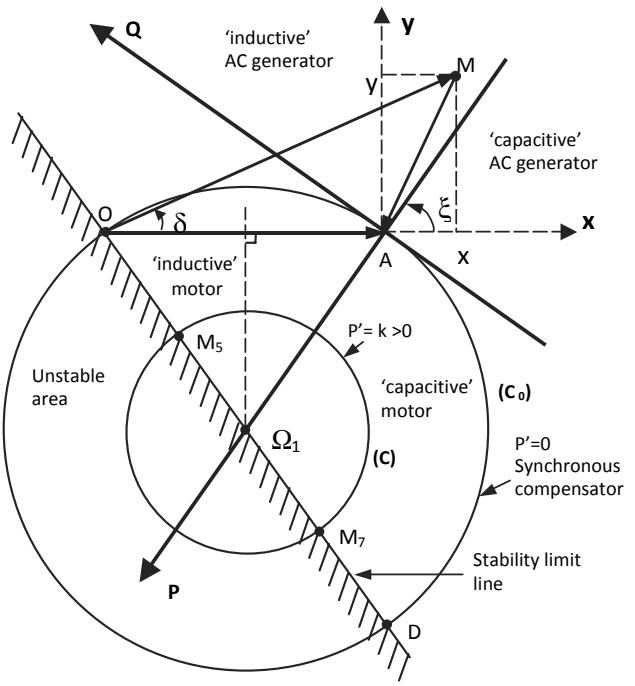

Figure 3.6. *Delimitation of the different operating modes on the phasor diagram*

A specific mode corresponds to the semicircle (C_0) located in the quadrant ($P > 0$, $Q < 0$): the machine works on a no-load motor (zero mechanical power) connected to a network from which it absorbs a little active power corresponding to the losses and to which is provides reactive power. This "synchronous compensator" state is commonly used to supply energy transport networks with the reactive power they need.

3.3.4. *Stability of the synchronous machine*

We have seen that the position of point M provides some information: active and reactive powers exchanged with the network, mechanical power (and therefore torque, too) on the shaft, etc. We are now going to see that all the operating points of this plane are not feasible.

Let us first remind ourselves that, in order to avoid excessive overheating, the field system current I_R and the rms value I of the stator current have to be lower than their nominal values, respectively called I_{RN} and I_N. Point M will therefore have to be inside two circles, the first centered in O and with a radius of $E_N = \frac{M\omega I_{RN}}{\sqrt{2}}$, and the second centered in A and with a radius of ZI_N.

Another limitation to the positioning of M within the plane exists: the stability of the machine. Indeed, at the beginning of this chapter we saw that the synchronous machine has a non-zero average torque only when it runs at the synchronous speed. If, for any reason (for example, a torque variation), this speed happens to be modified, it shall then be necessary for the machine to recover it.

In order to carry out this stability study, we shall start with the equation of the dynamic applied to rotating solids, or "mechanical equation" of the rotating machines:

$$J\frac{d\Omega}{dt} = \Gamma - \Gamma_C \qquad [1.15]$$

where J is the moment of inertia of all the rotating parts (rotor of the synchronous machine and associated "mechanical charge"), Γ the torque of the synchronous machine, and Γ_C, the torque of the associated machine (mechanical charge for a motor working or driving device for an AC generator working). And yet:

$$\Omega = \frac{d\Theta}{dt} = \frac{1}{p}\frac{d\theta}{dt}$$

with:

$$\theta = \omega t + \theta_0 = \omega t + \delta - \frac{\pi}{2}$$

Therefore:

$$\Omega = \frac{1}{p}\left(\omega + \frac{d\delta}{dt}\right)$$

Let us now assume that for a machine initially functioning in steady state (Ω constant, and therefore $\Gamma = \Gamma_0 = \Gamma_C$), with a voltage V and with a field current I_R both constant (and therefore with an electromotive force E constant in magnitude), an instantaneous variation of torque $\Delta\Gamma$ (or of power exchanged with the network) occurs. In Figure 3.7, it is expressed by a variation $\Delta\delta$ of the power angle δ.

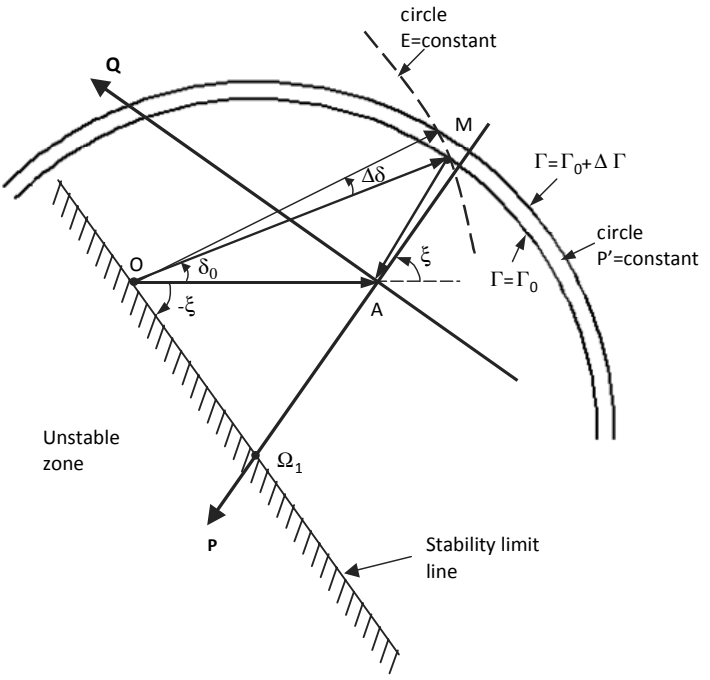

Figure 3.7. *Torque and power angle variation*

By calling δ_0 the initial value of this angle, we get:

$$\delta = \delta_0 + \Delta\delta$$

hence:

$$\Omega = \frac{1}{p}\left(\omega + \frac{d(\Delta\delta)}{dt}\right)$$

and:

$$\frac{d\Omega}{dt} = \frac{1}{p}\left(\frac{d^2(\Delta\delta)}{dt^2}\right)$$

With the machine working initially in steady state, it is possible to write:

$$\frac{J}{p}\frac{d^2(\Delta\delta)}{dt^2} = (\Gamma_0 + \Delta\Gamma) - \Gamma_{C0} = \Delta\Gamma$$

If only small variations about the starting point are taken into consideration, the torque characteristic in terms of δ can be assimilated to its tangent at the point under consideration. Therefore we can write:

$$\Delta\Gamma = \left(\frac{\partial\Gamma}{\partial\delta}\right)_{\delta_0} \Delta\delta$$

hence:

$$\frac{J}{p}\frac{d^2(\Delta\delta)}{dt^2} = \left(\frac{\partial\Gamma}{\partial\delta}\right)_{\delta_0} \Delta\delta \qquad [3.8]$$

This is a differential equation of the second order of variable $\Delta\delta$. If $\left(\frac{\partial\Gamma}{\partial\delta}\right)_{\delta_0} > 0$, $\Delta\delta$ has an exponential growth characterising an unstable functioning of the machine. The result is that a necessary condition of stability is:

$$\left(\frac{\partial\Gamma}{\partial\delta}\right)_{\delta_0} < 0$$

In order to be able to discuss this condition, a torque expression in which δ is the only variable has to be established. Let us look at the expression of apparent intern power $\overline{S'}$ again:

$$\overline{S'} = 3\overline{E}\,\overline{I}^* = 3\overline{E}\left(\frac{V-\overline{E}}{\overline{Z}}\right)^* = 3\overline{E}\left(\frac{V-\overline{E}^*}{\overline{Z}^*}\right) = 3\frac{\overline{E}V}{\overline{Z}^*} - 3\frac{E^2}{\overline{Z}^*}$$

that is to say:

$$\overline{S'} = \frac{3EV}{Z} e^{j(\delta+\xi)} - \frac{3E^2}{Z} e^{j\xi}$$

hence:

$$P' = \Gamma\Omega = \frac{3EV}{Z}\cos(\delta+\xi) - \frac{3E^2}{Z}\cos(\xi)$$

and therefore:

$$\Gamma = \frac{3p}{\omega}\left[\frac{EV}{Z}\cos(\delta+\xi) - \frac{E^2}{Z}\cos(\xi)\right] \qquad [3.9]$$

The necessary condition for stability established above becomes:

$$\frac{\partial\Gamma}{\partial\delta} = -3\frac{p}{\omega}\frac{EV}{Z}\sin(\delta+\xi) < 0$$

At starting point δ_0, we shall therefore have:

$$\sin(\delta_0+\xi) > 0$$

The necessary condition for stability is therefore written:

$$-\xi < \delta_0 < \pi - \xi \qquad [3.10]$$

We can deduce that the straight line OD (Figure 3.6) is the stability limit.

The previous condition does not constitute a necessary and sufficient condition for stability, because the solution of the differential equation [3.8] is then as follows:

$$\Delta\delta = \Delta\delta_{max} \sin \omega_0 t$$

with:

$$\omega_0^2 = \frac{3p^2}{J\omega}\frac{EV}{Z}\sin(\delta_0 + \xi)$$

$\Delta\delta_{max}$ is the maximum value of $\Delta\delta$. It is a sinusoidal variation of δ around initial value δ_0. In order for $\Delta\delta$ to tend toward zero, and therefore for the stability condition to become necessary and sufficient the differential equation [3.8] has to contain a damping term in $\frac{d(\Delta\delta)}{dt}$.

This can be obtained by providing the rotor of the machine with "damping windings"; this is usually a winding made of bars longitudinally inserted in the rotor and short-circuited at their two extremities in the same way as the cage of an induction motor. When the synchronous machine is in a steady state, this "damping cage" does not play any part because there is no current in it. On the other hand, as soon as the machine does not work at a strict synchronism, the damping cage is subjected to a flux varying at a frequency proportional to the relative speed difference of the rotor and of the air-gap field or "slip" (see Chapter 4, "Induction Machines"). If this slip is called g, it can be shown that the "asynchronous torque" which then appears can be written (if g is small):

$$\Gamma_a \approx Kg \qquad \text{(see section 4.5.3 and equation [4.19])}$$

where K is a constant, and:

$$g = \frac{\omega - \frac{d\theta}{dt}}{\omega} = \frac{\omega - \left[\omega + \frac{d(\Delta\delta)}{dt}\right]}{\omega} = -\frac{1}{\omega}\frac{d(\Delta\delta)}{dt}$$

In transferring this result into the mechanical equation:

$$\frac{J}{p}\frac{d^{2(\Delta\delta)}}{dt^2} + K\frac{d(\Delta\delta)}{dt} - \left(\frac{\partial\Gamma}{\partial\delta}\right)_{\delta_0}\Delta\delta = 0 \qquad [3.11]$$

If $-\xi < \delta_0 < \pi - \xi$, this equation has a damped sinusoidal solution which brings Δδ back to zero after a few oscillations. The synchronous machine is therefore stable in this part of the plane.

3.3.5. *V-curves called "Mordey curves"*

These are the characteristics of the variations of armature current I in terms of the field system current I_R for a load operating point at a constant internal power P' (that is to say at a constant torque Γ). Since the electromotive force is proportional to I_R, we can indiscriminately draw $I = f(I_R)$ or $I = f(E)$.

For this operating state, the machine can be considered as a system with one "input" I_R and two "outputs": the armature current I and its phase shift φ in relation to voltage V. Torque Γ (equal, in a steady state, to charge torque Γ_C) is considered as a "perturbation" (Figure 3.8).

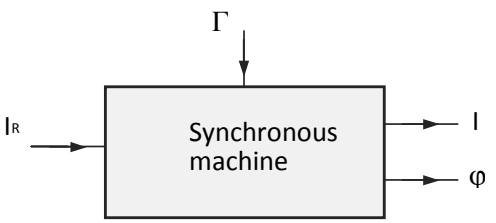

Figure 3.8. *"System" representation of the synchronous motor operating with constant P'*

In order to determine those curves, we shall refer to Figure 3.6. For a given power P', point M draws a semicircle bordered by the stability limit line. The corresponding Mordey curve is therefore the transform of this semicircle into the plane I(E). This curve does not usually have any simple analytical expression, we shall first attempt to establish the transforms, in the "Mordey plane", of particular curves of the voltages plane.

3.3.5.1. *Mordey curve for P'= 0*

Let us first assume that operating point M draws an arc AD corresponding to Q < 0. The following relationship can then be written:

$$V^2 = E^2 + Z^2 I^2 - 2E\,Z\,I\cos(\frac{\pi}{2} - \xi)$$

that is to say:

$$V^2 = E^2 + Z^2 I^2 - 2E\,Z\,I\sin\xi$$

a relationship which defines an elliptic arc limited at both points:

$$P_1 \begin{cases} I = 0 \\ E = V \end{cases} \qquad \text{and} \qquad P_2 \begin{cases} I = \dfrac{V}{Z} tg\xi \\ E = \dfrac{V}{\cos\xi} \end{cases}$$

If Q > 0, point M follows the arc AO, which leads to the relationship:

$$V^2 = E^2 + Z^2 I^2 - 2E\,Z\,I\cos(\frac{\pi}{2} + \xi)$$

that is to say:

$$V^2 = E^2 + Z^2 I^2 + 2E\,Z\,I \sin \xi$$

It is once again an elliptic arc limited at both points:

$$P_1 \begin{cases} I = 0 \\ E = V \end{cases} \qquad \text{and} \qquad P_3 \begin{cases} I = \dfrac{V}{Z} \\ E = 0 \end{cases}$$

3.3.5.2. *Stability limit curve*

If an operating point is located on segment OD of the stability limit, it can be written:

$$Z^2 I^2 = E^2 + V^2 - 2E\,V \cos \xi$$

This is a hyperbola arc limited by the two points:

$$\mathrm{P}_3 \begin{cases} I = \dfrac{V}{Z} \\ E = 0 \end{cases} \qquad \text{and} \qquad \mathrm{P}_2 \begin{cases} I = \dfrac{V}{Z} tg\xi \\ E = \dfrac{V}{\cos \xi} \end{cases}$$

3.3.5.3. *Locus of the armature currents minima*

When point M draws a semi-circle at constant P', the armature current is minimal when the absorbed reactive power Q is equal to zero. This corresponds to the operating point located on the intersection of axis P with the considered semi-circle.

The locus of currents minima is therefore the transform of straight line segment $A\Omega_1$ for which the relationship linking I to E can be written:

$$E^2 = V^2 + Z^2 I^2 - 2V\,Z\,I\cos\xi$$

it is therefore a hyperbola arc limited by points:

$$P_1 \begin{cases} I = 0 \\ E = V \end{cases} \qquad \text{and} \qquad P_4 \begin{cases} I = \dfrac{V}{2Z\cos\xi} \\ E = \dfrac{V}{2\cos\xi} \end{cases}$$

3.3.5.4. *General case, P'≠0*

The previous curves enable us to be more specific about the appearance of characteristic I(E) for a particular value of P' (Figure 3.9): it begins on a point P_5 homologue to point M_5 (see Figure 3.6) of intersection of circle P' = constant with the stability limit line, goes through a minimum of current in P_6 and ends in P_7, transform in Mordey plane of M_7, second intersection of the circle with the stability limit.

The general appearance of this characteristic justifies the name of "v-curve" which it is often called. It is interesting as it enables a choice, for a given mechanical power (or, likewise, a fixed torque), of the value of the excitation current: which is usually sought to be located around point P_6, in order to minimize the Joule losses.

A position slightly beyond this point enables us to provide the electrical network with reactive power without any major modification of current I, because of the relatively flat shape of the curve when nearing the current minimum.

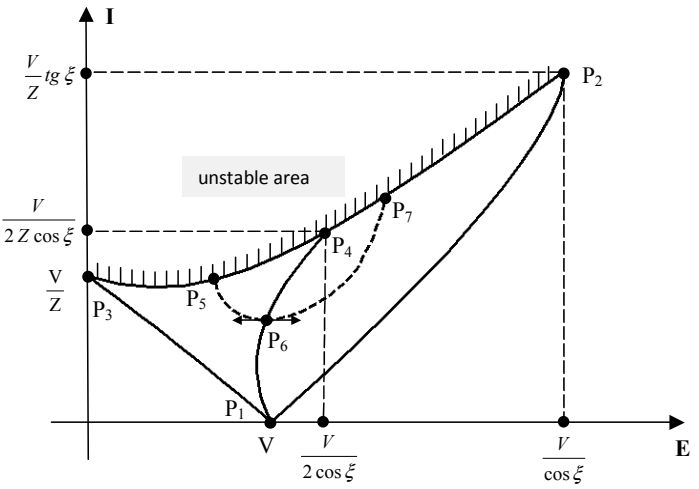

Figure 3.9. *Mordey curves. Machine 220 V, Z = 10Ω, ζ = 67.5°*

3.3.6. *Case when resistance R is negligible*

If stator resistance R is neglected, which generally is acceptable for high power machines, the synchronous inductance becomes equal to the synchronous reactance, and we have $\xi = \pi/2$.

The axis of the active powers becomes vertical and the axis of reactive powers becomes horizontal. Furthermore, as P' is now equal to P, the locuses of the points with constant mechanical power become horizontal straight lines, and the stability limit, a vertical straight line.

Figure 3.6 therefore transforms into Figure 3.10, and the two ellipse arcs P_1P_2 and P_1P_3 (Figure 3.9) then become straight line segments. The electromagnetic torque is written:

$$\Gamma = \frac{3}{2} pMI_R I\sqrt{2}\sin\gamma = \frac{3p}{\omega}\frac{EV}{Z}\sin\delta$$

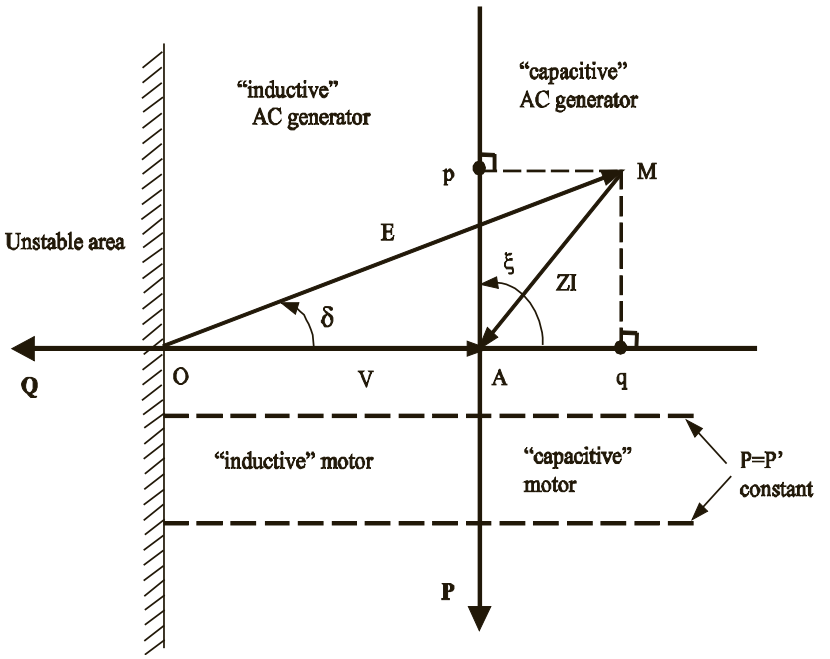

Figure 3.10. *Phasor diagram with R = 0*

3.4. Considerations about the salient pole synchronous machine

We have, from the beginning of this chapter, studied the behavior of cylindrical synchronous machines. However it has to be remembered that for many applications (low or medium speed motors and slow AC generators in hydraulic power stations, in particular), the rotor has salient poles.

These machines have a single-phase field system winding made of coils wound around ferromagnetic poles and connected in series in order to ensure an alternation of the poles. Action is taken on the shape of the polar shoe in order to obtain a repartition, close to a sinusoid, of the flux density within the air-gap. This structure is thus characterized by the simplicity of its making and of its maintenance.

Alternatively, for mechanical reasons, it is usually used for applications where speed does not exceed 1,000 rpm.

The major difficulty for the study of those machines is due to the geometric anisotropy (variable air-gap), and therefore magnetic anisotropy of the rotor, which leads to a dependence of the different mutuals and of most inductances, in position θ of the rotor, upon the stator. The armature reaction then varies according to the load state of the machine.

We shall, in this section, present a model of these machines overlooking the space harmonics (approximation at the first harmonic) and based on fields and corresponding flux density variations in the air-gap. These results are obtained using finite element computation.

3.4.1. *Torque and inductance matrix*

We consider a machine having a non-salient stator bearing a 3-phase armature winding and a salient pole rotor with the field system winding. Rotor and stator each have 2p poles.

This machine can be represented, as for the cylindrical machine, with three coils A, B and C representing the stator phases and with a coil R representing the rotor field system (Figure 3.2). The damping circuits (which are not in use in a steady state of the machine) are not taken into account. In what follows, magnetic saturation phenomena shall be neglected. The global expression of the flux is written:

$$\begin{bmatrix} \psi_A \\ \psi_B \\ \psi_C \\ \psi_R \end{bmatrix} = \begin{bmatrix} L_A & M_{AB} & M_{AC} & M_{AR} \\ M_{BA} & L_B & M_{BC} & M_{BR} \\ M_{CA} & M_{CB} & L_C & M_{CR} \\ M_{RA} & M_{RB} & M_{RC} & L_R \end{bmatrix} \begin{bmatrix} i_A \\ i_B \\ i_C \\ I_R \end{bmatrix} \qquad [3.12]$$

which can also be written:

$$\begin{bmatrix} M_{AR} \\ M_{BR} \\ M_{CR} \end{bmatrix} = \mathrm{M} \begin{bmatrix} \cos\theta \\ \cos(\theta - 4\pi/3) \\ \cos(\theta - 2\pi/3) \end{bmatrix}$$

The stator is considered to be non-salient, the reluctance met by the field system flux is independent from the position of the rotor. We deduce that L_R is independent from θ. The rotor reluctance being variable, the stator inductances depend on position θ. In limiting the study to the fundamental we get:

$$L_A = L_S + L_1 \cos 2\theta$$

$$L_B = L_S + L_1 \cos(2\theta - 2\pi/3)$$

$$L_C = L_S + L_1 \cos(2\theta - 4\pi/3)$$

this is the same for the mutuals between the stator phases:

$$M_{AB} = M_S + L_1 \cos(2\theta - 2\pi/3)$$

$$M_{AC} = M_S + L_1 \cos(2\theta - 4\pi/3)$$

$$M_{BC} = M_S + L_1 \cos 2\theta$$

Note that $L_1 = 0$ for a cylindrical rotor.

3.4.2. *Calculation of the flux*

We consider that the field system winding is supplied by a DC current I_R and that the three stator phases are supplied by a 3-phase current system:

$$i_A = I\sqrt{2}\cos(\omega t - \varphi)$$
$$i_B = I\sqrt{2}\cos(\omega t - \varphi - 2\pi/3)$$
$$i_C = I\sqrt{2}\cos(\omega t - \varphi + 2\pi/3)$$

Flux at the rotor given by:

$$\psi_R = M_{AR}\, i_A + M_{BR}\, i_B + M_{CR}\, i_C + L_R I_R = \frac{3}{2} M\, I\sqrt{2}\cos(\theta_0 + \varphi) + L_R I_R$$

has an expression identical to expression obtained for a cylindrical machine. Flux in phase A is given by:

$$\psi_A = \psi_{AS} + \psi_{AR}$$

$$\psi_{AR} = M_{AR} I_R$$

where ψ_{AR} is the flux generated by the rotor excitation current. This is expressed in the same way as for a cylindrical machine. Flux ψ_{AS} is the armature reaction flux, it corresponds to the flux generated by the stator currents:

$$\psi_{AS} = L_A\, i_A + M_{AB}\, i_B + M_{AC}\, i_C$$

Contrary to the cylindrical machine, this flux depends on the position of the rotor in relation to the stator. This is illustrated by Figures 3.11 to 3.13, which present the air-gap radial flux density $B_N(\theta)$ variation as well as the armature reaction field lines, for three positions of the rotor in relation to the stator electromotive force ε_S.

These figures correspond to a bipolar salient pole rotor machine with a 24 slot stator. Each stator phase therefore takes 4 “outward” slots and 4 “return” slots. We also assumed that this stator is supplied by a balanced 3-phase current system, considered at the one particular instant

when $i_A = -i_B$ and $i_C = 0$. The "outward" conductors are drawn in a shade darker than the "return" conductors.

On these figures, two axes are introduced: direct axis d, merged with the axis of the rotor, and axis q in quadrature. We can observe that, when mmf ε_s is colinear with axis d (Figure 3.11), the reluctance met with the flux is small. The corresponding inductance is then maximum; this is written L_d or direct axis synchronous inductance. Along the air-gap, the appearance of normal flux density Bn is almost sinusoidal, disturbed by the stator slots. The origin of the angles is the horizontal axis, Bn is at its maximum for $\theta = \pi/2$, that is to say along axis d.

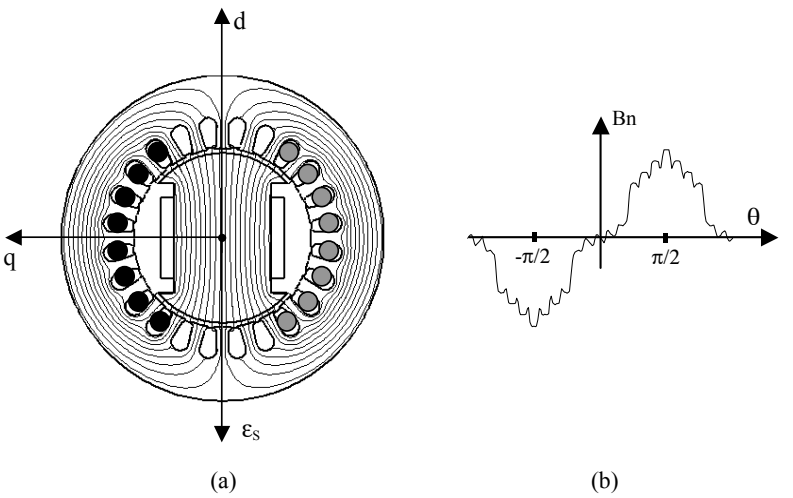

Figure 3.11. *No-load armature reaction field (load angle $\gamma = \pi$) : a) field lines; b) normal flux density in the air-gap*

When ε_s is aligned with axis q (Figure 3.12), the reluctance is important and the corresponding inductance is minimal. This inductance is written Lq or "synchronous inductance in quadrature". In accordance with the field lines, the normal induction in the air-gap decreases in the

neighborhood of axis q. When ε_s is shifted by a load angle γ in terms of axis d (Figure 3.13), the normal flux density in the air-gap presents a complex appearance depending on γ.

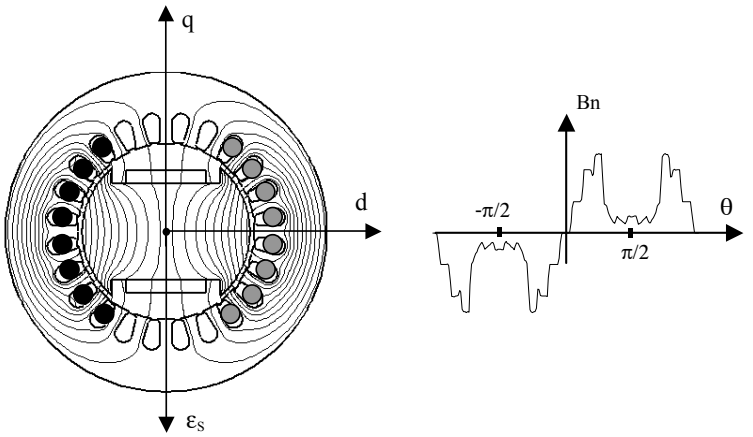

Figure 3.12. *Armature reaction field for a load angle $\gamma = \pi/2$: a) field lines; b) normal flux density in the air-gap*

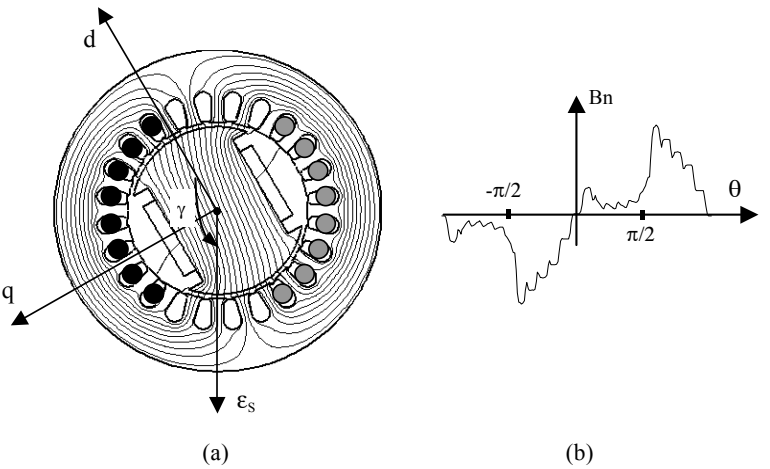

Figure 3.13. *Armature reaction field for a load angle γ: a) field lines; b) normal flux density in the air-gap*

If the magnetic saturation is neglected, the principle of superposition can be used to determine the armature reaction magnetic flux for any position γ in relation to the flux corresponding to the positions d ($\gamma = 0$ or π) and q ($\gamma = \pm \pi/2$).

ε_s is then decomposed into two mmf: one, ε_{sd}, in the direction of axis d, and the other, ε_{sq}, in quadrature (Figure 3.14).

$$\varepsilon_{sd} = \varepsilon_s \cos \gamma$$

$$\varepsilon_{sq} = \varepsilon_s \sin \gamma$$

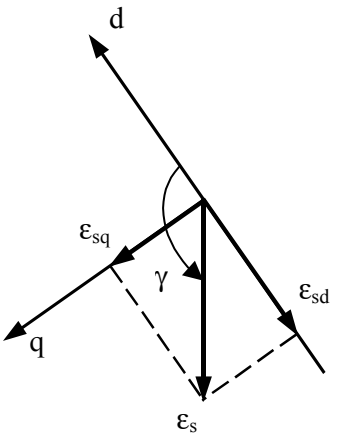

Figure 3.14. *Magnetomotive force following axes d and q*

Flux ψ_d corresponding to ε_{sd} is a direct axis flux; it is proportional to inductance L_d and is written:

$$\psi_d = L_d \, i_d$$

Flux ψ_q relative to ε_{sq} is the in-quadrature flux; it is proportional to L_q, with:

$$\psi_q = L_q\, i_q$$

i_d and i_q are then the components of current i_A following respectively axes d and q:

$$i_d = i_A \cos\gamma$$
$$i_q = i_A \sin\gamma$$

The armature reaction flux and the flux in phase A are therefore written:

$$\psi_{AS} = \psi_d + \psi_q = L_d\, i_d + L_q\, i_q$$

$$\psi_A = L_d\, i_d + L_q\, i_q + M_{AR}\, I_R$$

3.4.3. *Electrical equation and phasor diagram*

In adopting the sign covenants relative to a load operating mode, the electrical equation for phase A, with resistance R, is written:

$$v_A(t) = \frac{d\psi_A}{dt} + R\, i_A(t)$$

The total flux in phase A is the sum of the sinusoidal terms of similar angular frequencies ω. The complex notation can then be used. In phases B and C, similar expressions would be obtained, and it is therefore possible, by removing the indexes, to write the phase electrical equation as follows:

$$V = \bar{E} + R\bar{I} + jX_d\, \bar{I}_d + jX_q\, \bar{I}_q \qquad [3.13]$$

where $\bar{E}$ is the complex representation of the no-load emf. This is in back quadrature with current $\bar{I}_R$. $\bar{I} = \bar{I}_d + \bar{I}_q$ is the complex representation of the phase current. $X_d = L_d\,\omega$ is the direct reactance. $X_q = L_q\,\omega$ is the reactance in quadrature.

Regarding only the fundamental, it can be shown that:

$$X_d = (L_S - M_S + 3/2L_l)\,\omega$$

$$X_q = (L_S - M_S - 3/2L_l)\,\omega$$

By introducing the emf of "salience" $\overline{E}_S$ and the "resulting" emf $\overline{E}_t$:

$$\overline{E}_S = j(X_d - X_q)\,\overline{I}_d$$

$$\overline{E}_t = \overline{E} + \overline{E}_S$$

equation [3.13] becomes:

$$V = \overline{E}_t + R\overline{I} + jX_q\,\overline{I} \qquad [3.14]$$

An expression similar to this can be obtained for the cylindrical machine. This equation can be illustrated by the phasor diagram shown in Figure 3.15.

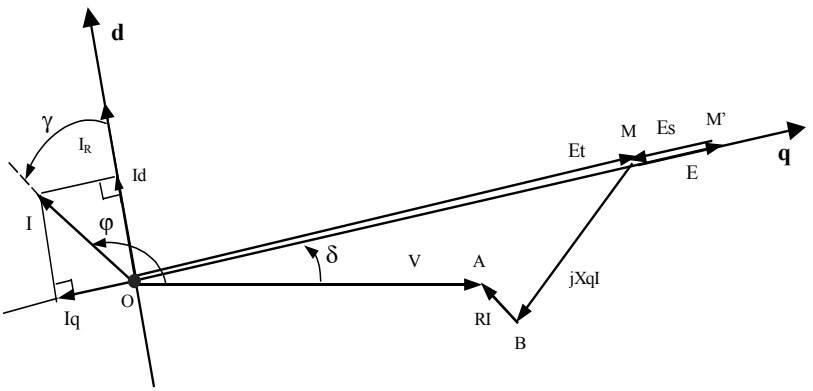

Figure 3.15. *Phasor diagram of the salient pole machine*

3.4.4. *Calculation of the torque and stability analysis*

Remember the general expression giving the instantaneous torque value of a rotating machine:

$$\Gamma = \frac{p}{2}[i]^t \left[\frac{\partial L(\theta)}{\partial \theta}\right][i]$$

matrix L is defined in equation [3.12].

It is considered that the three stator phases are supplied by a 3-phase current system, and it is stated that the machine rotates at speed Ω so that:

$$\theta = \mathrm{p}\,\Omega \mathrm{t} + \theta_0$$

It can then be shown that the average torque is different from zero only at the synchronism speed:

$$\Omega = \frac{\omega}{\mathrm{p}}$$

At this speed, it is equal to the instantaneous torque, and it is given by:

$$\Gamma = -\frac{3}{2}\sqrt{2}\,\mathrm{p}M\,I\,I_R \sin\gamma - 3\mathrm{p}(\mathrm{Ld}-\mathrm{Lq})\mathrm{I}^2 \sin 2\gamma = \Gamma_L + \Gamma_S \qquad [3.15]$$

The load angle is equal to $\gamma = \theta_0 + \varphi$.

The first term of this expression, Γ_L, is identical in form to that of a cylindrical machine. This term corresponds to the interaction of the stator and rotor currents. The second term,

Γ_S, is a salience torque (or reluctance torque) which depends on the square value of I; it is linked to the rotor geometry.

If the stator resistance is overlooked (case of high power machines), and we introduce internal angle δ given by:

$$\delta = \theta_0 + \pi/2 = \gamma - \varphi + \pi/2$$

the torque can be written:

$$\Gamma = -\,p\frac{3VE}{\omega X_d}\sin\delta - p\frac{3V^2}{2\omega}\left(\frac{1}{X_q} - \frac{1}{X_d}\right)\sin 2\delta \qquad [3.16]$$

In considering only the small variations in comparison with the initial equilibrium point, it can be shown that a condition necessary to the machine stability is written:

$$\left(\frac{d\Gamma}{d\delta}\right) < 0$$

Figure 3.16 shows the variation of the average torque given by [3.16] in terms of δ. In this example, the maximum value of the reluctance torque equals 30% of this, corresponding to the action of stator currents on the rotor current (cylindrical machine).

At a given stator voltage, when the internal angle increases, that is to say when the load increases, we can observe that the salience effect leads to a maximum torque Γ_{max} greater than this Γ_1 of an equivalent cylindrical machine. It is also observed that the stability limit is obtained for an absolute value of angle δ lower than $\pi/2$. This diagram shows the interest of salient poles synchronous motors.

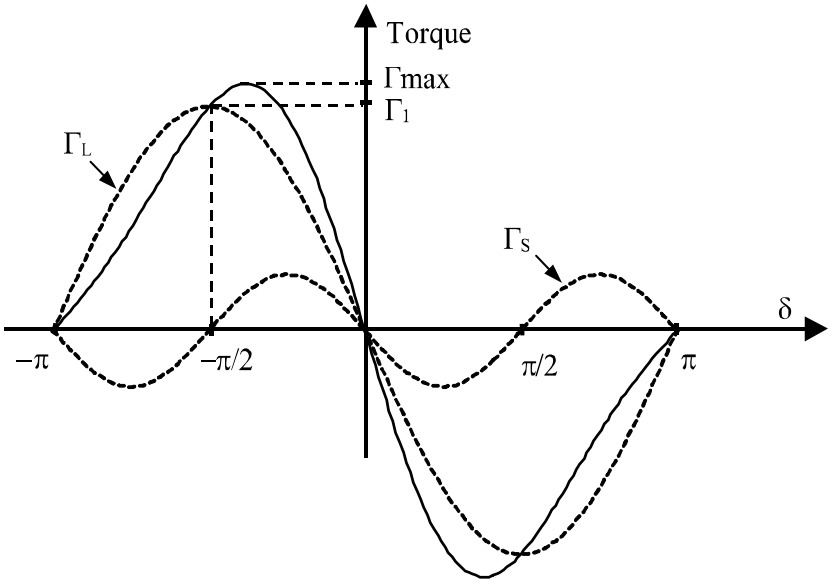

Figure 3.16. *Torques of a salient pole machine*

3.5. Consideration about permanent magnet machines

Several structures of permanent magnets synchronous machines can be encountered. We shall restrict ourselves to a non-exhaustive presentation of those with a cylindrical 3-phase stator similar to the machines studied in the previous sections.

The magnets are set in the rotor in order to generate the field necessary for the machine magnetization. Their magnetization can be radial (Figure 3.17), tangential (Figure 3.18), or mixed (Figure 3.19).

As in standard machines, we can distinguish:

– "sinusoidal distribution of ampere-turns machines" particularly appropriate to the continuous energy conversion when the stator currents are sinusoidal;

– “trapezoidal” emf machines or “DC brushless”, whose conductors are usually concentrated in one slot per pole and per phase, and are usually supplied by current commutators.

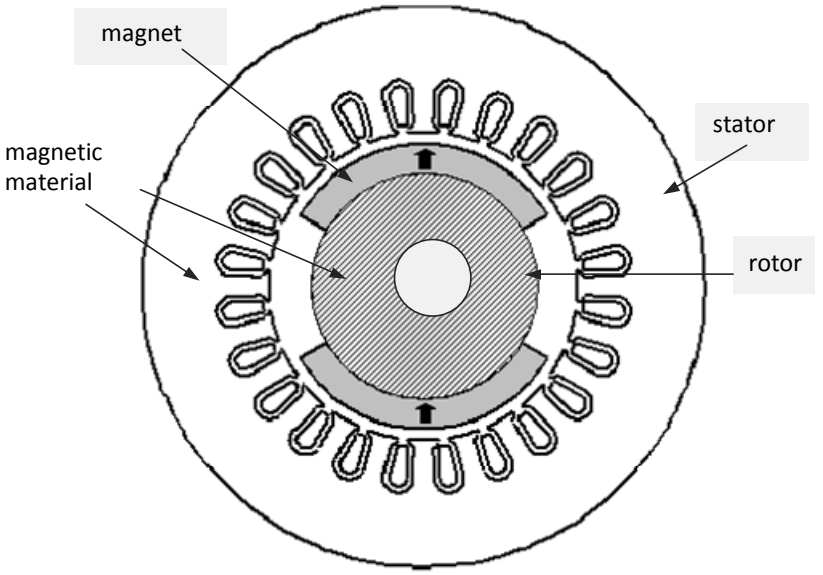

Figure 3.17. *Bipolar SPM synchronous machines: radial magnetization*

In the following we shall propose a classification of these structures according to the arrangement of the magnets. It is possible to distinguish machines with SPM (surface permanent magnets), INSET and IPM (intern permanent magnets).

3.5.1. *Surface permanent magnets machines*

The magnets are set on the surface of the rotor (Figures 3.17 and 3.19). This structure is largely used because of its simple manufacturing. In order to ensure their mechanical resistance to centrifugal forces, the magnets are often bound

by amagnetic binding bands. This causes an additional cost and also an increase of the air-gap.

It can be noted that the "magnetic" air-gap, that is to say the air-gap seen through the field generated by stator currents, is almost constant, and its value e_m is important because the magnets have a magnetic permeability close to that of air. We have:

$$e_m = e + h_a + e_f$$

where h_a is the magnets thickness (Figure 3.25), e is the "mechanical" air-gap, and e_f is the binding band thickness.

These machines are therefore cylindrical, characterized by relatively small stator inductances and mutuals because of the magnetic air-gap thickness. The armature reaction is therefore much smaller than the reaction of standard excitation machines.

3.5.2. *Machines with inserted magnets*

The magnets are set between magnetic parts as drawn in Figure 3.20. This figure introduces the direct axis d, joined to the axis of the excitation field, and the axis q in quadrature. Note that these are salient pole machines because the magnetic air-gap varies between a minimal value equal to e in the direction of the axis q and a maximum value equal to (e + h) in the direction of the axis d.

This variation of the air-gap leads to a so-called "inverted" structure because the reactance in quadrature is bigger than the direct reactance.

3.5.3. *Machines with embedded magnets*

The magnets are set inside the rotor (Figures 3.18 and 3.21), which protects them from mechanical stress and allows considerable rotation speeds. This arrangement leads to salient pole machines because the magnetic air-gap is not constant.

This structure enables us to channel the flux generated by the magnets in order to get the desired levels and variations of the flux density in the air-gap. The configuration given by Figure 3.18 is called "with flux concentration" configuration because the air-gap magnetic flux is almost equal to the sum of the flux generated by two successive magnets (Figure 3.22). Sufficient flux density values, around 0.7 T, can be obtained in the air-gap, by using, for example, ferrites, which are cheap magnets but in which the remanence flux density is quite small.

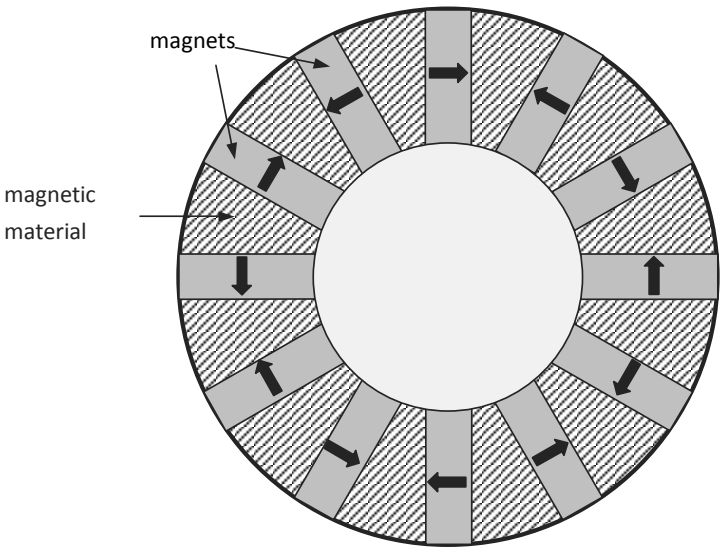

Figure 3.18. *Rotor of a 12-pole IPM synchronous machine with flux concentration: tangential magnetization*

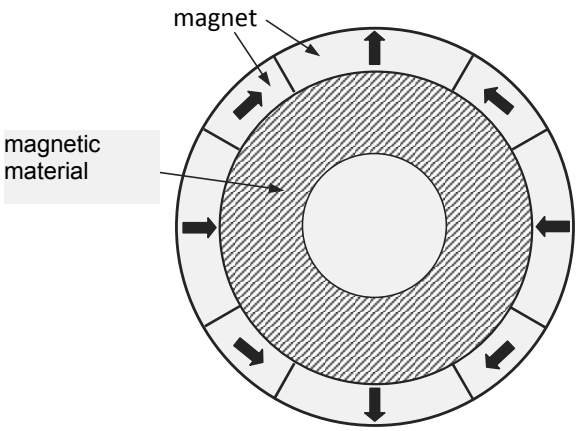

Figure 3.19. *Rotor of a 4-pole SPM synchronous machine: combined magnetization*

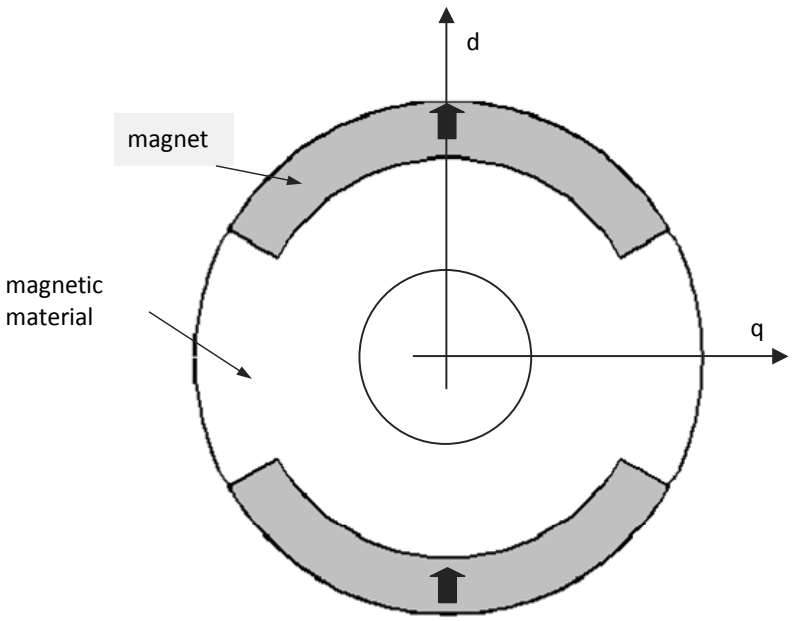

Figure 3.20. *Rotor of a 2-pole INSET synchronous machine: radial magnetization*

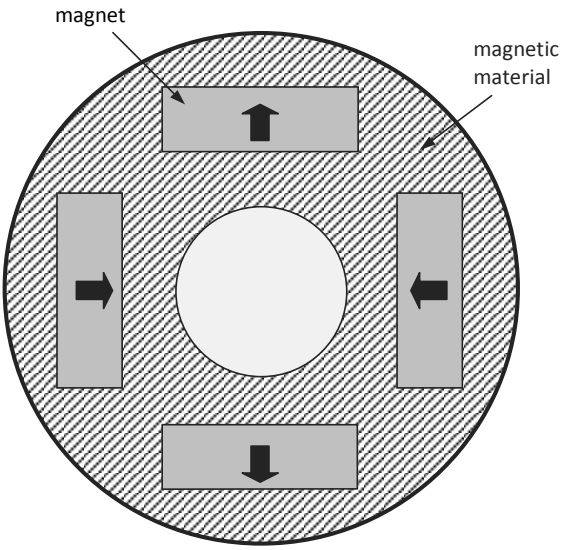

Figure 3.21. *Rotor of a 4-pole IPM synchronous machine: radial magnetization*

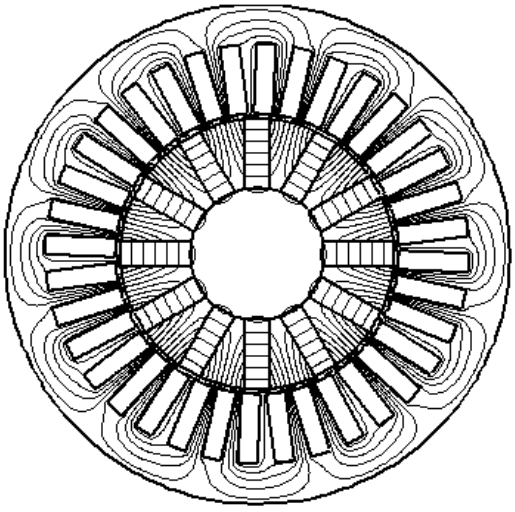

Figure 3.22. *Field lines due to the magnets in no-load operation of a 12-pole IPM synchronous machine with flux concentration: tangential magnetization*

3.5.4. *Modeling of permanent magnet machines*

A machine with a non-salient stator bearing the 3-phase armature winding and a salient rotor with permanent magnets is considered. The stator and the rotor each have 2p poles. This machine can be represented, as for the wound rotor machine, in the form of three coils A, B and C representing the stator phases of a magnet generating the rotor flux on the axis R (Figure 3.23).

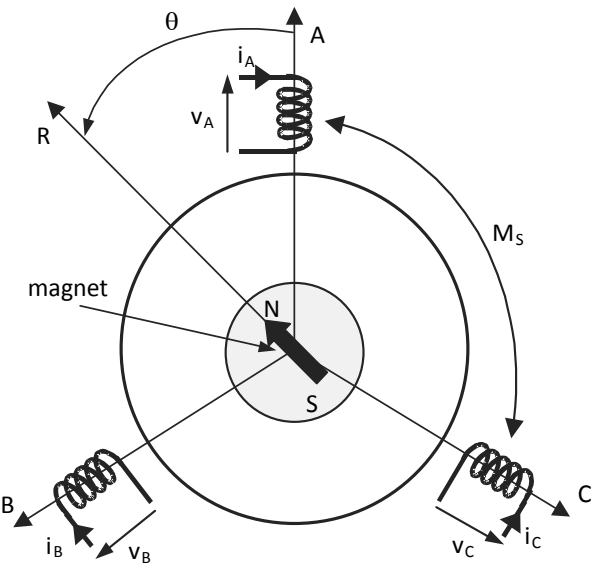

Figure 3.23. *Conventional representation of the permanent magnets synchronous machine*

The total flux in a stator phase can be written:

$$\{\psi_S\} = \begin{Bmatrix} \psi_A \\ \psi_B \\ \psi_C \end{Bmatrix} = \begin{bmatrix} L_A & M_{AB} & M_{AC} \\ M_{BA} & L_B & M_{BC} \\ M_{CA} & M_{CB} & L_C \end{bmatrix} \begin{Bmatrix} i_A \\ i_B \\ i_C \end{Bmatrix} + \begin{Bmatrix} \psi_{RA} \\ \psi_{RB} \\ \psi_{RC} \end{Bmatrix}$$

which can also be written as follows:

$$\left\{\psi_S\right\} = \left\{\mathcal{L}_S\right\}\left\{i_S\right\} + \left\{\psi_R\right\}$$

The co-energy of the system is then written:

$$\tilde{W}_{em} = \frac{1}{2}\left\{i_S\right\}^t\left\{\mathcal{L}_S\right\}\left\{i_S\right\} + \left\{i_S\right\}^t\left\{\psi_R\right\} + \tilde{W}_{em0}$$

$\tilde{W}_{em0}$ is the co-energy of the system when all the currents are zero. It can be shown that:

$$\tilde{W}_{em0} = -W_{em0}$$

W_{em0} is the electromagnetic energy stored in the machine when all the currents are zero.

The instantaneous torque is then obtained by differentiating, with constant currents, the co-energy. We have:

$$\Gamma_i = \frac{p}{2}\left\{i_S\right\}^t\left\{\frac{\partial \mathcal{L}_S}{\partial \theta}\right\}\left\{i_S\right\} + p\left\{i_S\right\}^t\left\{\frac{\partial \psi_R}{\partial \theta}\right\} + p\frac{\partial \tilde{W}_{em0}}{\partial \theta} \qquad [3.17]$$

The first term of expression [3.17] is the reluctance torque (or salience torque); it is linked to the rotor geometry. The last term is the cogging torque due to the interaction of the magnets with the stator slots. The second term of the expression is the “hybrid” torque; it corresponds to the interaction of the stator currents with the rotor flux. This is the main torque.

3.5.5. *Cylindrical machine modeling*

In the following, a symmetrical 3-phase machine with p pair of non-salient poles is considered (Figure 3.24). The inductances and the stator mutual inductances are therefore constant.

The magnetic saturation phenomena are neglected, as well as the space harmonics in restricting the study to the fundamental. The influence of stator slots is also neglected; the cogging torque is then considered to be zero.

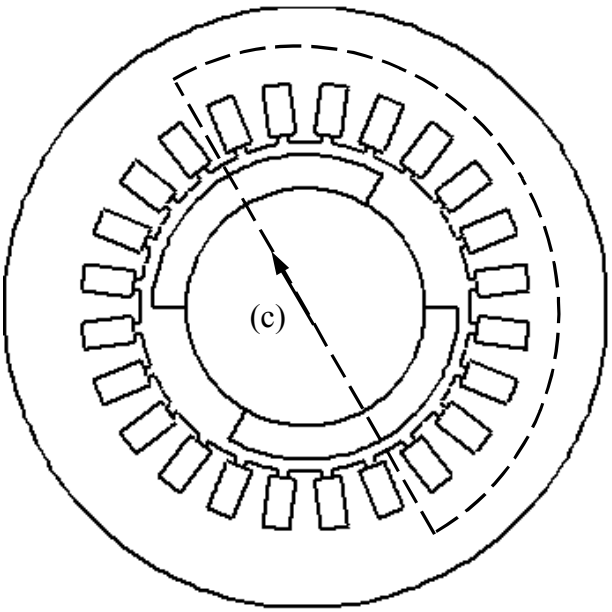

Figure 3.24. *Cylindrical synchronous machine and closed circuit of integration (c)*

Figure 3.25 shows the thickness h_a and the opening angle β of the magnets. θ_S and θ_R are the angles locating the position of a point P of the air-gap in relation to the stator axis S and the rotor axis R.

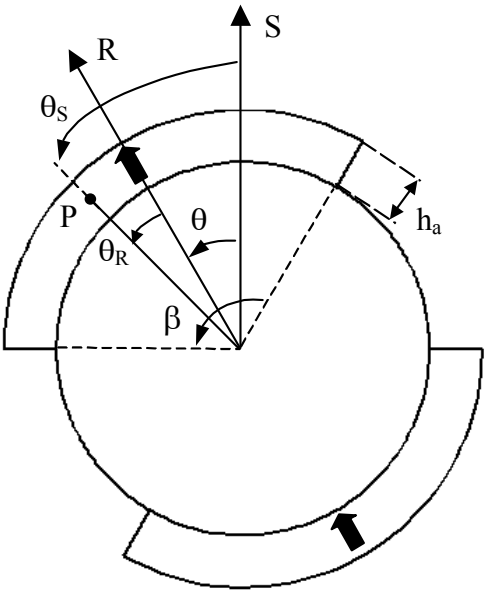

Figure 3.25. *Cylindrical rotor of SPM synchronous machine*

3.5.5.1. *Electrical equation of the synchronous machine*

Considering the adopted hypotheses, the flux caused by the magnets can be approximated by:

$$\{\psi_R\} = \begin{Bmatrix} \psi_{RA} \\ \psi_{RB} \\ \psi_{RC} \end{Bmatrix} = \psi_R \begin{Bmatrix} \cos\theta \\ \cos(\theta - 2\pi/3) \\ \cos(\theta + 2\pi/3) \end{Bmatrix} \qquad [3.18]$$

The total flux in a stator phase can be written:

$$\{\psi_S\} = \begin{bmatrix} \psi_A \\ \psi_B \\ \psi_C \end{bmatrix} = \begin{Bmatrix} L_S & M_S & M_S \\ M_S & L_S & M_S \\ M_S & M_S & L_S \end{Bmatrix} \begin{Bmatrix} i_A \\ i_B \\ i_C \end{Bmatrix} + \psi_R \begin{Bmatrix} \cos\theta \\ \cos(\theta - 2\pi/3) \\ \cos(\theta + 2\pi/3) \end{Bmatrix}$$

Assuming that stator currents are as follows:

$$i_A = I\sqrt{2}\cos(\omega t - \varphi)$$
$$i_B = I\sqrt{2}\cos(\omega t - \varphi - 2\pi/3))$$
$$i_C = I\sqrt{2}\cos(\omega t - \varphi + 2\pi/3))$$

we obtain, for phase A:

$$\psi_A = L_S\, i_A + M_S\,(i_B + i_C) + \psi_R \cos\theta$$

thus, in introducing the synchronous inductance $L = (L_S - M_S)$:

$$\psi_A = L\, i_A + \psi_R \cos\theta$$

The machine is considered to have the rotation speed:

$$\Omega = \frac{\omega}{p} = \frac{d\Theta}{dt} = \frac{1}{p}\frac{d\theta}{dt}$$

The position of the rotor in relation to the stator is $\theta = \omega t + \theta_0$. We have:

$$\psi_A = L\, I\sqrt{2}\cos(\omega t - \varphi) + \psi_R \cos(\omega t + \theta_0)$$

For phases B and C, we get:

$$\psi_B = L\, I\sqrt{2}\cos(\omega t - \varphi - 2\pi/3) + \psi_R \cos(\omega t + \theta_0 - 2\pi/3)$$
$$\psi_C = L\, I\sqrt{2}\cos(\omega t - \varphi + 2\pi/3) + \psi_R \cos(\omega t + \theta_0 + 2\pi/3)$$

The total flux per stator phase with the angular frequency ω and complex numbers $\bar{I}_A = Ie^{-j\varphi}$, with current i_A, and $\overline{\Psi}_A$, associated with flux Ψ_A are introduced. This can be written:

$$\overline{\Psi}_A = L\bar{I}_A + \frac{\psi_R}{\sqrt{2}} e^{j\theta_0}$$

For phases B and C similar expressions would be obtained, and therefore it is possible, by removing the indexes, to unify the general expression of the total flux per stator phase:

$$\overline{\Psi} = L\bar{I} + \frac{\psi_R}{\sqrt{2}} e^{j\theta_0}$$

If the complex representation of the voltage per stator phase is called $\overline{V}$ and the resistance of the stator phase is called R, we can write:

$$\overline{V} = R\,\bar{I} + \frac{d\overline{\psi}}{dt} = R\,\bar{I} + j\omega\overline{\psi} = R\,\bar{I} + jL\omega\,\bar{I} + j\frac{\psi_R\omega}{\sqrt{2}} e^{j\theta_0}$$

that is to say:

$$\overline{V} = (R + jL\omega)\,\bar{I} + \overline{E}$$

with:

$$\overline{E} = j\frac{\psi_R\omega}{\sqrt{2}} e^{j\theta_0} = \frac{\psi_R\omega}{\sqrt{2}} e^{j\delta} \qquad [3.19]$$

where $\overline{E}$ is the complex representation of the electromotive force per phase of the machine Lω, the synchronous reactance, and $\delta = \theta_0 + \pi/2$ is the power angle of the machine. This expression emphasizes the fact that the amplitude of the electromotive force E is proportional to flux ψ_R due to the magnets and to the rotation speed Ω.

In introducing the synchronous impedance $\overline{Z} = R + jL\omega = Z\,e^{j\xi}$, like the wound rotor cylindrical machine, we obtain the equation:

$$\overline{V} = \overline{E} + \overline{Z}\,\overline{I}$$

which can also be represented by the equivalent diagram per phase of Figure 3.3.

3.5.5.2. *Determination of the flux generated by permanent magnets*

The influence of the stator slots being neglected, it can be admitted that in the air-gap, the flux density is constant and equal to B_e for the whole width β of the magnet. The variation, along the air-gap, of this normal flux density is then given by Figure 3.26.

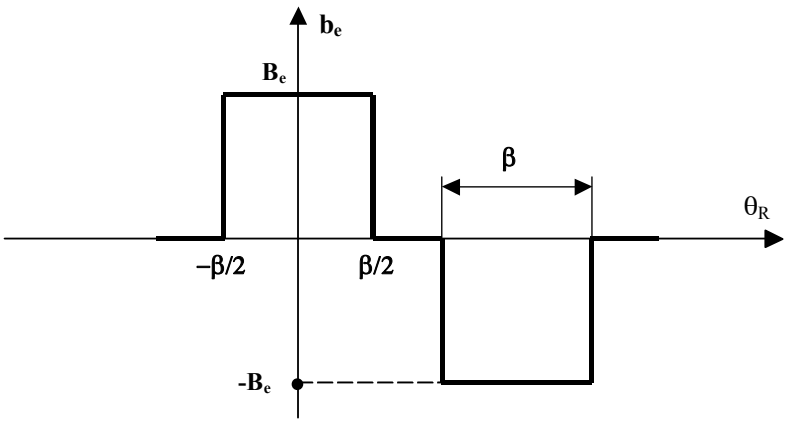

Figure 3.26. *Approximate form of the normal induction in the air-gap*

If this is restricted to the fundamental of its Fourier series, we get:

$$b_e = B_{e1}\cos\theta_R = B_{e1}\cos(\theta_S - \theta)$$

$$B_{e1} = \frac{4}{\pi} B_e \sin(\frac{\beta}{2})$$

Ampere's theorem, applied to the closed circuit (c), (Figure 3.24) is written:

$$\oint_{(c)} \vec{H}d\vec{l} = \int_{(air-gap)} \vec{H}d\vec{l} + \int_{(iron)} \vec{H}d\vec{l} + \int_{(magnet)} \vec{H}d\vec{l} = 0$$

If the magnetic field is neglected in the iron, and if it is admitted that fields H_e in the air-gap and H_a in the magnets are constant, we can write:

$$H_a h_a + H_e e = 0 \qquad [3.20]$$

where h_a and e are respectively the thicknesses of the magnets and of the air-gap. When the magnets are held by a binding band, e has to be increased by the thickness e_f of the binding band.

Flux densities B_a in the magnet and B_e in the air-gap are linked to the fields by:

$$B_a = \mu_a H_a + B_R$$
$$B_e = \mu_0 H_e \qquad [3.21]$$

B_R and μ_a are respectively the remanence flux density and the magnet permeability. In the following we shall state that $\mu_a = \mu_0$. In neglecting the leakage flux, we can state that B_a and B_e are equal. Equations [3.20] and [3.21] then lead to:

$$B_a = B_e = \frac{B_R}{1 + \frac{e}{h_a}} \qquad [3.22]$$

Flux ψ_{RA} generated by the magnets and crossing phase A with N_S turns is then given by:

$$\psi_{RA} = N_S \int_S b_e dS = N_S \int_S B_{e1} \cos(\theta_S - \theta) dS$$

with:

$$dS = R_i L_u d\Theta_S = R_i L_u \frac{d\theta_S}{p}$$

R_i is the internal radius of the stator, and L_u is the useful length of the machine. This can be written:

$$\psi_{RA} = \frac{1}{p} N_S R_i L_u \int_{-\pi/2}^{\pi/2} B_{e1} \cos(\theta_S - \theta)\, d\theta_S = \frac{2}{p} N_S R_i L_u B_{e1} \cos\theta$$

The maximum value is therefore equal to:

$$\psi_R = \frac{8 N_S}{p\pi} \frac{B_R}{1 + e/h_a} R_i L_u \sin(\frac{\beta}{2})$$

Using equation [3.19], the rms value of the phase emf becomes:

$$E = \frac{8 N_S}{\pi\sqrt{2}} \frac{B_R}{1 + e/h_a} R_i L_u \Omega \sin(\frac{\beta}{2})$$

3.5.5.3. *Determination of the electromagnetic torque*

The electromagnetic torque can be obtained from expression [3.17] where, considering the adopted hypotheses, only the hybrid torque plays a part. We have:

$$\Gamma_i = p\{i_S\}^t \left\{\frac{\partial \psi_R}{\partial \theta}\right\} = p\begin{bmatrix} i_A & i_B & i_C \end{bmatrix} \begin{bmatrix} \partial\psi_{RA}/\partial\theta \\ \partial\psi_{RB}/\partial\theta \\ \partial\psi_{RC}/\partial\theta \end{bmatrix}$$

Using expression [3.18], a torque independent from time is obtained:

$$\Gamma_i = \frac{3}{2}\psi_R I\sqrt{2}\sin(\theta_0 + \varphi) = \frac{3}{2}\psi_R I\sqrt{2}\sin\gamma$$

$\gamma = (\theta_0 + \varphi)$ is the load angle.

3.6. Inverted AC generators

The excitation of large synchronous machines is often carried out by smaller AC generators with inverted structures (rotor armature and stator field system) fixed on the same shaft as the main AC generator. It is then possible to connect the armature winding of the secondary AC generator to the field winding of the main AC generator through a static rectifier, often called "rotating diodes" (Figure 3.27). This prevents the field current from flowing through slippery contacts (slip ring-brushes) which are not very convenient, particularly when the field current is important.

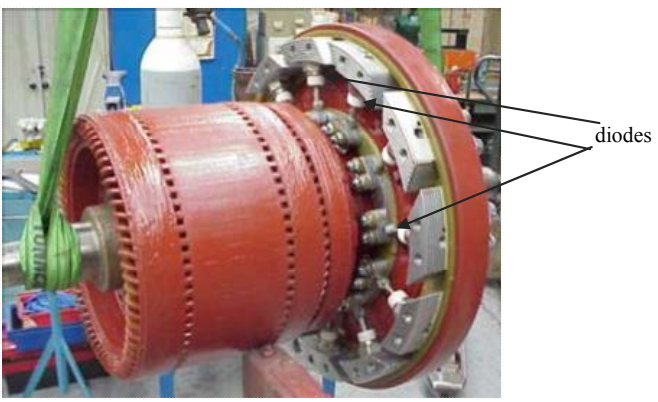

Figure 3.27. *Rotor of a "rotating diode" exciter, 155 kVA, 74 V, 3,000 rpm. On the right hand side of the photograph the semi-conductor components are distinctly visible enabling the armature currents of the inverted AC generator (ECA EN document) to be rectified*

3.7. Implementation of synchronous machines

The implementation of synchronous machines is very different depending on whether it is a motor or an AC generator; the analysis difficulties are also different.

AC generators usually work at a constant speed and supply networks with fixed voltages and frequencies. The problem to be solved is then to determine how to supply the network with the desired active and reactive powers using the adjustment parameters available: the field system current I_R and the drive turbine torque. In such conditions, the machine operates in sinusoidal state, but the difficulty of the study consists of the magnetic saturation phenomena.

Concerning the motor mode, the machine is usually a constituent of variable speed drives. In such conditions, it is essential to take into account the working of the static converters which generally supply the motor with non-sinusoidal currents. On the contrary, it is possible in an initial analysis to overlook the magnetic saturation phenomena.

Another working mode called "synchronous compensator" is also considered, for which the machine operates as a no-load motor (no mechanical charge) and supplies the network with reactive power only (Figure 3.6).

3.7.1. *Implementation of synchronous motors*

3.7.1.1. *Synchronous motor supplied by a current commutator*

Historically, the first item designed with that aim was the association of two thyristor bridges. One of them, P_1, supplied by the network, works as a rectifier and supplies the second one, P_2. The latter works as an inverter and supplies the stator of the machine (Figure 3.28).

An inductance L inserted between P_1 and P_2 enables the reduction of the harmonics of rectified current I, which is assumed to be constant. It can therefore be stated in an initial analysis that according to the state of conduction of the P_2 thyristors, the phases of the motor are supplied with currents of the values I, -I or zero. P_2 is thus called the "current inverter". The whole drive (thyristors bridges-synchronous motor) is often called a "self-synchronous controlled synchronous motor".

In fact, this drive usually uses salient pole motors; however, we shall make an analytical study assuming that it is a cylindrical machine in account of the simplicity of the equations. Furthermore, the qualitative conclusions remain valid whichever type of machine is under consideration.

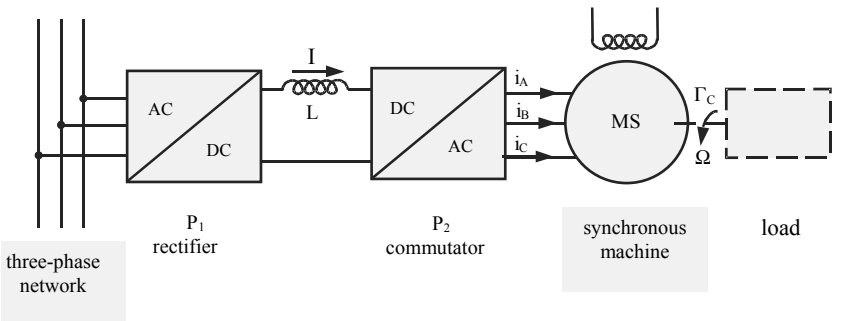

Figure 3.28. *Self-synchronous controlled synchronous motor*

3.7.1.1.1. Calculation of the instantaneous torque

The instantaneous torque of the synchronous machine is written as follows:

$$\Gamma_i = p\{i_S\}^t \left\{\frac{\partial \mathcal{L}_{SR}}{\partial \theta}\right\}\{i_R\}$$

with:

$$\{i_R\} = I_R, \qquad \{\mathcal{L}_{SR}\} = M_0 \begin{pmatrix} \cos\theta \\ \cos(\theta - 2\pi/3) \\ \cos(\theta + 2\pi/3) \end{pmatrix} \text{ and}$$

$$\{i_S\} = \begin{pmatrix} i_A \\ i_B \\ i_C \end{pmatrix}$$

Considering the machine supply mode (phase stator current equal to I, -I or 0), six different expressions for the instantaneous torque can be distinguished: Γ_{AB}, Γ_{AC}, Γ_{BC}, Γ_{BA}, Γ_{CA}, and Γ_{CB}, expressions in which, as a covenant, the first index indicates the phase where the current is worth + I, and the second index where the current is worth –I. Let us calculate, for example, Γ_{AC}:

$$\Gamma_{AC} = -pM_0 \begin{pmatrix} I & 0 & -I \end{pmatrix} \begin{pmatrix} \sin\theta \\ \sin(\theta - 2\pi/3) \\ \sin(\theta + 2\pi/3) \end{pmatrix} (I_R)$$

that is to say:

$$\Gamma_{AC} = -p\sqrt{3}M_0 I_R I \cos(\theta - 2\pi/3) = -\Gamma_{CA}$$

The other expressions of the instantaneous torque would be obtained in the same way:

$$\Gamma_{AB} = p\sqrt{3}M_0 I_R I \cos(\theta + 2\pi/3) = -\Gamma_{BA}$$

$$\Gamma_{BC} = p\sqrt{3}M_0 I_R I \cos(\theta) = -\Gamma_{CB}$$

Note that those elementary torques each have a sinusoidal expression in terms of θ, their average value is therefore zero (Figure 3.29).

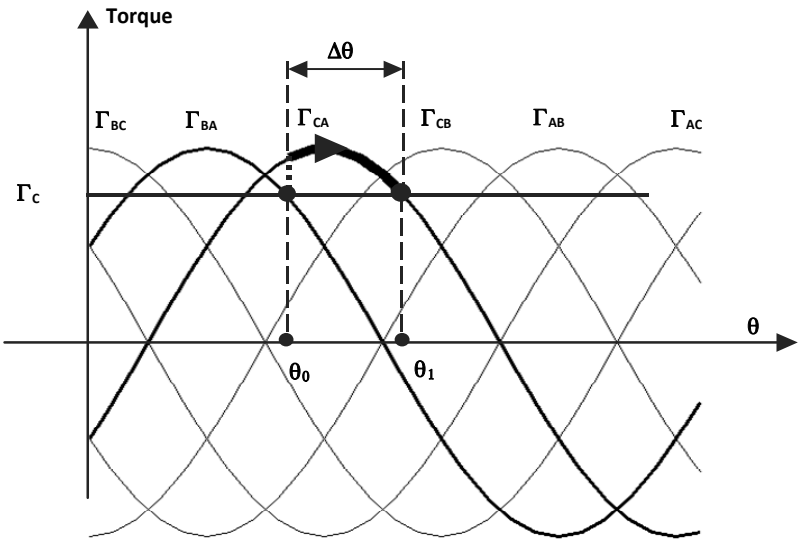

Figure 3.29. *Step by step operating*

3.7.1.1.2. Step by step operating

Let us consider the six instantaneous torque sinusoids again. Let us assume for example that the machine has phases A and B supplied with $I_A = -I$ and $I_B = I$, and that it is connected to a mechanical charge with a resistant torque Γ_C (Figure 3.29). The rotor of the motor shall therefore position itself at position θ_0 so that $\Gamma_{BA} = \Gamma_C$. If current I is commuted from phase B to phase C (to make the reasoning more convenient we shall assume an instantaneous commutation), the torque of the motor will become Γ_{CA}. Since, in θ_0, torque Γ_{CA} is greater than Γ_C, the motor will move until it reaches value θ_1 for which $\Gamma_{CA} = \Gamma_C$, position where it shall stabilize again (after some oscillations). For each commutation, the machine makes an incremental movement $\Delta\theta$ or "step". This device enables the use of the machine to make an incremental positioning of its charge, which is very interesting in various domains of electrical actuation.

For the positioning to be precise, it is important that $\Delta\theta$ is small. Machines with specific structures are generally used, mainly with variable reluctance, the study of which is outside the scope of this book.

3.7.1.1.3. Self-synchronous behavior

The set "rectifier-inverter" is usually used to make the synchronous machine work at a variable speed in various industrial domains. In this case, current I is successively commuted from one phase of the machine to the next, which also makes the motor torque "switched" to be worth successively Γ_{BC}, Γ_{BA}, Γ_{CA}, etc. (Figure 3.30).

If θ_j is the electrical angle, for which Γ_{BA} becomes greater than Γ_{BC} (Figure 3.30), it seems optimal to commute the current from one phase to the other for $\theta = \theta_j + k\pi/3$ ($k \in N$). However, in order to avoid the risk of commutation failure (see section 1.4.1.3.1), it is advisable to make these commutations with $\theta_C < \theta_j$. This leads to torque discontinuities that cannot be avoided, generating noises and vibrations.

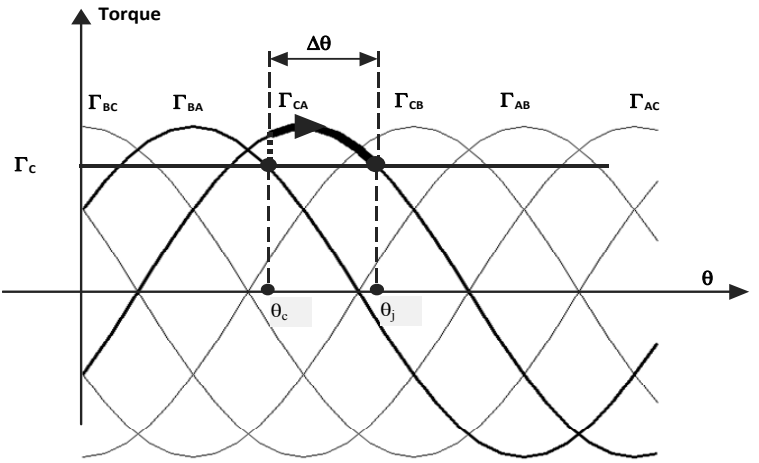

Figure 3.30. *Machine torque in self-synchronous state*

In order to reduce those discontinuities, which are very damaging in some industrial applications (rail traction and naval propulsion, in particular), it is useful to increase the number of phases. The most basic structure is the "double-star" synchronous machine in which the stator has two 3-phase coils (A_1, B_1, C_1 and A_2, B_2, C_2) shifted in space by an electric angle equal to $\pi/6$ (Figure 3.31). Each coil is supplied by a current commutator (Figure 3.32). The torque ripples are thus considerably reduced.

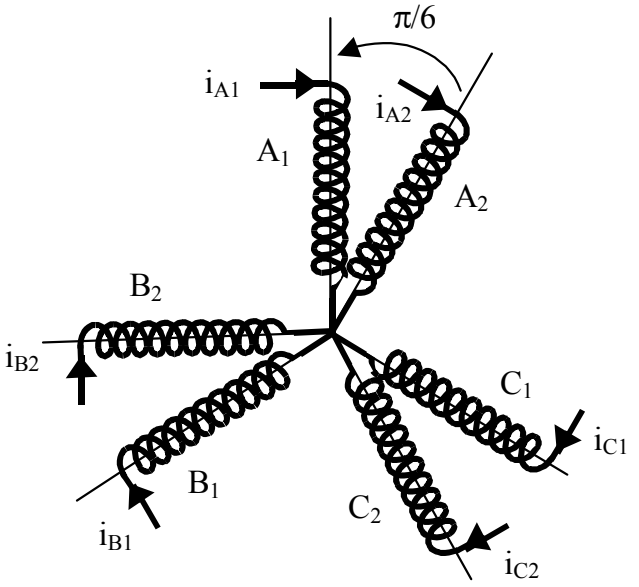

Figure 3.31. *Stator of the "double-star" synchronous machine*

The structure of "double-star" motors supplied by current commutators was developed during the 1980s for rail traction, then extended to more considerable powers (several MW) for naval propulsion (Figure 3.33). For this latter application, the motors are often located outside the ship's hull in pods (Figures 3.34) used for both propelling and

steering the ship. This device enables the simplification of motor maintenance.

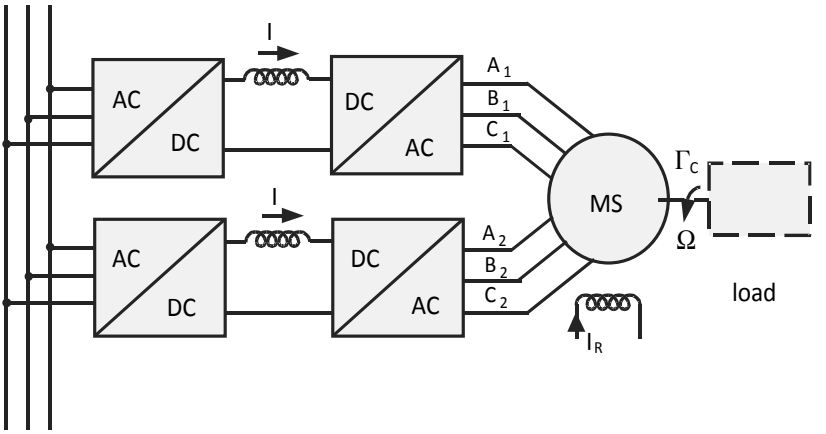

Figure 3.32. *Double-star machine supplied by current commutators*

Figure 3.33. *Cruise liner MSC Poesia, equipped with two inboard double-star synchronous motors driving the propellers through shafts. Each motor develops a power of 18 MW at around 170 rpm. These motors are supplied by current inverters (photograph Aker Yards Saint-Nazaire, Bernard Biger)*

Figure 3.34. *Motor in a pod fixed under the hull of a ship (photo source: Converteam)*

3.7.1.1.4. Concentrated winding machines

It has already been seen (Chapter 2) that the machines with sinusoidal repartition of ampere-turns are particularly well suited to continuous energy conversion when the stator currents are sinusoidal. In such a case, they are much more interesting than those for which conductors are concentrated in a single slot per pole and per phase (machines that we had called "basic"). Remember that, for those machines, the stator-rotor mutual inductances have triangular variation (Figure 3.35a).

Let us consider the general expression of the instantaneous torque again:

$$\Gamma = p\{i_S\}\left\{\frac{\partial \mathcal{L}_{SR}}{\partial \theta}\right\}\{i_R\}$$

with:

$$\{\mathcal{L}_{SR}\} = \begin{Bmatrix} M_{AR} \\ M_{BR} \\ M_{CR} \end{Bmatrix} \qquad \{i_S\} = \begin{Bmatrix} i_A \\ i_B \\ i_C \end{Bmatrix} \qquad \text{and} \qquad \{i_R\} = I_R$$

It is clearly visible that the triangular wave shape of the mutual inductances will lead to square waves for their derivatives (Figure 3.35b).

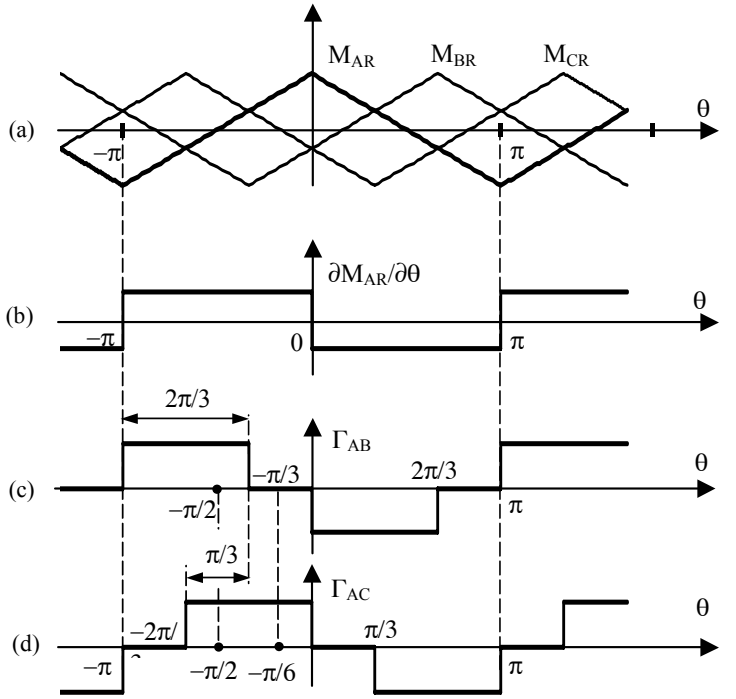

Figure 3.35. *a) Stator-rotor mutual inductances of a "non-distributed" synchronous machine; b) derivative of the mutual inductance M_{AR}; c) torque Γ_{AB}; d) torque Γ_{AC}*

If the machine is supplied by a current commutator, the three stator current values are +I, 0 or –I, and we obtain, as previously, six possible expressions for the instantaneous torque:

$$\Gamma_{AB} = -\Gamma_{BA} = pI_R I\left(\frac{\partial M_{AR}}{\partial \theta} - \frac{\partial M_{BR}}{\partial \theta}\right)$$

$$\Gamma_{BC} = -\Gamma_{CB} = pI_R I\left(\frac{\partial M_{BR}}{\partial \theta} - \frac{\partial M_{CR}}{\partial \theta}\right)$$

$$\Gamma_{CA} = -\Gamma_{AC} = pI_R I\left(\frac{\partial M_{CR}}{\partial \theta} - \frac{\partial M_{AR}}{\partial \theta}\right)$$

Figures 3.35c and d emphasize the evolution of the two elementary torques Γ_{AB} and Γ_{AC}. It is noticeable that they have a "flat" maximum for a duration of $2\pi/3$ electric and that these maxima overlap on a $\pi/3$ angle. If current –I is commuted from phase B to phase C during this overlap (for example, in $\theta = -\pi/2$), the electromagnetic torque will remain constant. Thus it can be seen that, with a current distribution such as the representation in Figure 3.36, the torques Γ_i will be constant (taking into account the simplifying assumptions).

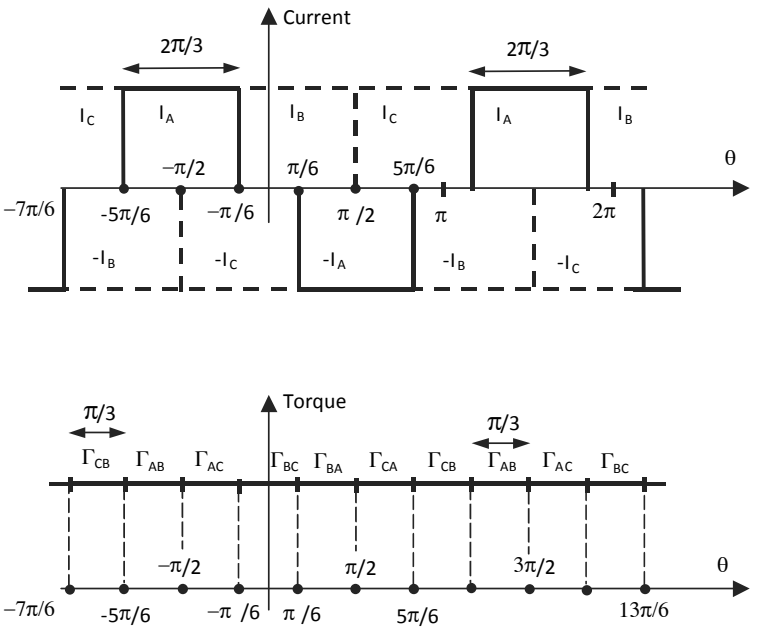

Figure 3.36. *Currents i_A, i_B and i_C and corresponding torques*

This relatively simple example enables us to illustrate a fundamental point of present electrical engineering: it is no longer possible to optimize a machine without knowing how it shall be used, and generally it is the whole drive (static converter-rotating machine set) which has to be optimized.

3.7.1.1.5. Principle of self-synchronous control

We have just seen that the inverter current has to be commuted from one phase of the machine to the following phase with judiciously chosen values of the electrical angle θ, that is to say for particular positions of the rotor.

A position sensor is used with this aim: it provides the control device of the inverter bridge with the order of the commutation components, thus the name of "self-synchronous controlled synchronous machine" given to the whole drive (bridges-synchronous machine-control) (Figure 3.37).

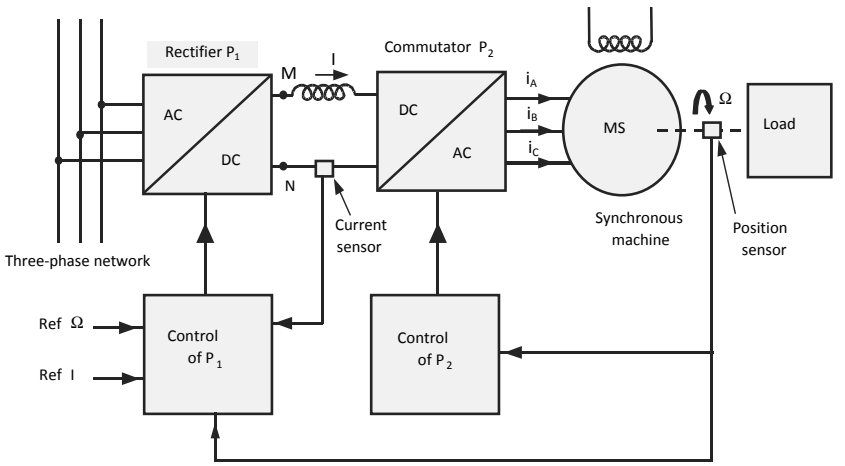

Figure 3.37. *General diagram of the self-synchronous machine control*

It can be shown that the model of the set commutator P_2-synchronous machine, observed between points M and N, is similar (in mean values and in stationary state) to a separated excitation DC machine. It has therefore been easy to transpose the methods of speed and current regulation. This device has quickly replaced the separated excitation DC machine from the 1970s.

The position sensor needed to control P_2 also gives through derivation, the "speed" information at P_1 control in charge of the current and speed regulation of the machine.

3.7.1.2. *PWM inverter synchronous motor drive*

The evolution of power electronics and the growth of the power of fully controllable switches allow to deal with the supply of high power synchronous motors (several megawatts) by PWM inverters (Figure 3.38). Without detailing the working of these converters, bear in mind that they enable to generate variable frequency stator currents with little harmonics (see section 1.3.5).

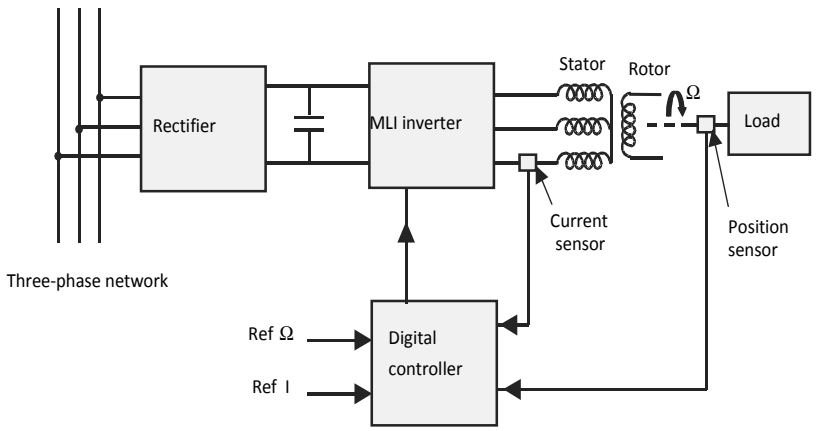

Figure 3.38. *Structural diagram of a vectorial controlled synchronous machine*

In a first approximation, those currents are therefore sinusoidal, and the motor turns at a speed proportional to their fundamental frequency; it produces a torque with a slight harmonic content.

This device, associated with digital controls (microprocessor, DSP, etc.), enabled the introduction of the vectorial command of synchronous machines. This command leans on a particular modeling of the machines in transient state (Park equations), which is beyond the scope of this book. Outstanding dynamic performance can thus be obtained. This device is now largely used in industry.

3.7.2. *Implementation of the AC generators taking into account the saturation phenomena*

In most cases, AC generators work connected to a network, which they have to supply with an active power P and a reactive power Q (Figure 3.39). With this end in view, it is possible to use two control parameters: the mechanical power supplied by the driving "motor" and the rotor excitation current I_R (voltage V, frequency f, and therefore speed Ω imposed by the network). Those control parameters or "inputs" therefore have to be predetermined. This is very different depending on whether the magnetic saturation can be neglected or not.

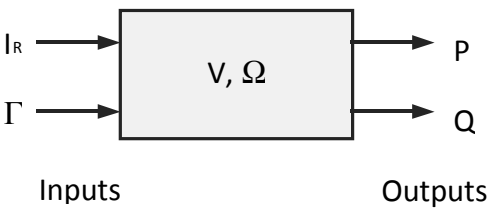

Figure 3.39. *"System" representation of an AC generator connected to a network*

3.7.2.1. *Analysis in a linear state*

When saturation can be neglected, the solution is immediate because the approach developed in section 3.3 is valid. Indeed, if P and Q are fixed, the position of operating point M in the phasor diagram is undoubtedly defined. Electromotive force E is immediately deduced and therefore current I_R to which E is proportional (Figure 3.5). In the same way, P' being known, the mechanical power and the torque needed are determined.

It is clear that, if the AC generator has to supply the network with active and reactive power (capacitive AC generator) the required value of E is linked to a very important field current I_R. In that case the AC generator cannot be in linear state. Figure 3.40 shows that when the field current is great, the electromotive force E is no longer proportional to I_R.

We shall therefore see how it is possible to take into account the saturation using a few physical considerations.

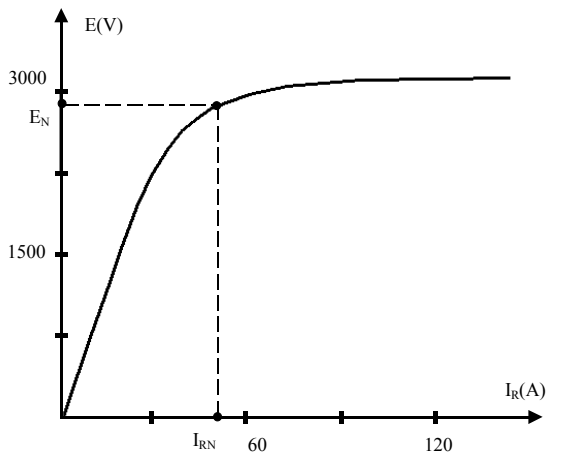

Figure 3.40. *Characteristic $E = f(I_R)$ or "no-load curve" of a 10 MVA machine, 50 Hz, Un = 5 000 V (composed voltage), I_N = 200 A, I_{RN} = 50 A*

3.7.2.2. *Physical considerations about magnetic saturation*

Magnetic saturation is a complex physics phenomenon linked with the non-linear behavior of ferromagnetic materials when they are excited by a magnetic field. The magnetic state of the machine then depends on the flux density in each point, and when it is important, there is no longer proportionality between the flux and the currents. Note that this flux density depends on the interaction of the whole of the fields and therefore on the rotor and stator currents.

The saturation in AC generators is taken into account using standard methods. In order to make these methods comprehensible we shall first point out some key phenomena. For that purpose we shall use field lines distribution and corresponding levels of flux densities. These are obtained by finite element computation.

3.7.2.2.1. Fields and inductances

In a ferromagnetic material, saturation is characterized by the fact that flux density B is not proportional to field H. For a synchronous machine working as a "no-load" AC generator (without any stator currents), this leads to the non-proportionality of the electromotive force E to I_R (Figure 3.40). When the machine is on-load, its magnetic state depends on the whole of the ampere-turns distributed in it: the field generated by the field system and the field linked to the stator currents or "magnetic armature reaction field". In the air-gap those two fields have amplitudes that can be described by sinusoidal progressive waves, and their phase shift depends on the operating point. Saturation therefore depends on various parameters, and particularly on I_R, I and φ.

Let us consider, for example, the cylindrical 3-phase machine represented by Figure 3.41. It is bipolar and has 18 slots in the rotor and 24 slots in the stator. Each stator

phase takes 4 “outward” slots and 4 “return” slots. Figure 3.41a shows the field lines in the machine during the no-load functioning, that is to say when only the field system is supplied by a current I_R corresponding to the mmf ε_R. In the Figure, the “outward” conductors of the rotor coil are represented in a darker shade than the “return” conductors.

It is observed that all the field lines do not go through all the parts of the machine uniformly. Thus, in an initial approximation, they go through the stator teeth located in front of the rotor poles only, and when I_R increases, those teeth are increasingly subject to saturation because the flux density becomes considerable there.

Figure 3.41b represents the local distribution of the flux density. It shows the parts of the machine likely to have the biggest magnetic saturation; they are the darkest parts. Note that those parts “move” with the rotor when it rotates.

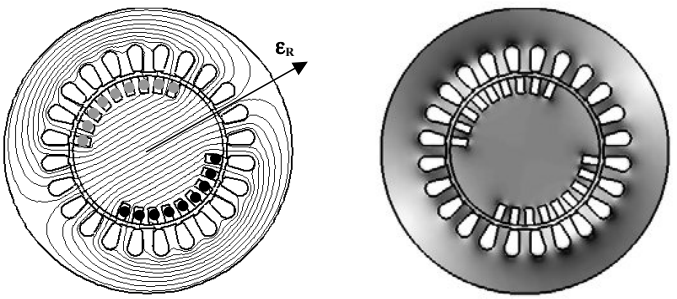

Figure 3.41. *No-load operating: a) field lines; b) flux density levels*

Figure 3.42a represents the on-load field lines, that is to say when the stator and the rotor are fed. In this example, the position of the rotor is the same as in Figure 3.41, and it is assumed that the stator is supplied by a balanced 3-phase current system considered at one particular instant when

$i_A = -i_B = I$ and $i_C = 0$. The "outward" stator conductors (represented in dark) are therefore located in 8 adjacent slots, and the "return" conductors (represented in a lighter shade) are located in 8 diametral slots. The corresponding mmf ε_S is shifted from mmf ε_R with load angle γ.

Figure 3.42b shows that the parts of the machine most subject to magnetic saturation (represented in a darker shade) do not exactly correspond to those of no-load operating. This saturation state, which varies with I_R, therefore depends on the amplitude of stator current I and of its shifting φ in terms of the voltage.

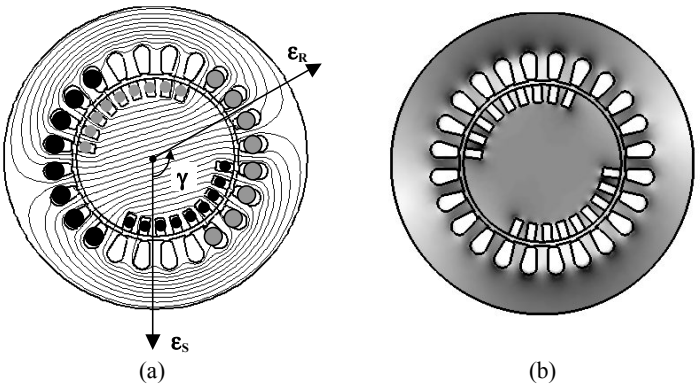

Figure 3.42. *On-load operating: a) field lines; b) flux density levels*

Figure 3.43 shows the armature reaction field lines, that is when only the stator is power supplied. The rotor is in the same position as in Figures 3.41 and 3.42. In Figure 3.43b, which is a zoom-in on a part of the machine, the field linked to the "useful" flux can be distinguished from the field linked to the leakage flux. The field determining the "useful" flux goes through the air-gap and through the ferromagnetic material constituting the stator and the rotor whereas the field lines corresponding to the leakage flux do not cross the air-gap and are mainly localized in materials with

permeability μ_0 (slots, air-gap, end winding, etc.). It can therefore be admitted that leakage inductance l associated with the leakage flux is constant and does not depend on the magnetic saturation.

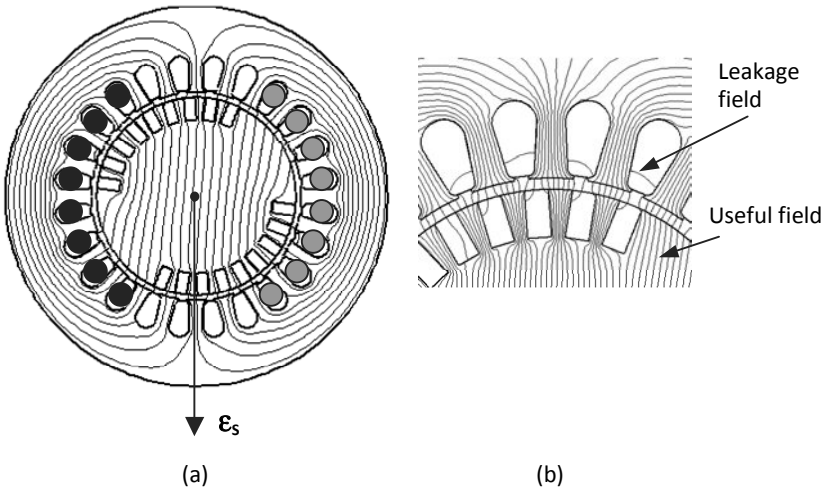

Figure 3.43. *Armature reaction field: a) field lines; b) zoom-in*

Synchronous inductance L is then broken up into two parts:

$$L = s + l \qquad [3.23]$$

Inductance s corresponds to the "useful" flux and varies with the saturation state of the machine.

3.7.2.2.2. Resulting electromotive force

Considering the electrical equation [3.5] of the synchronous machine again and if [3.23] is taken into account, we can write:

$$\bar{V} = \left(\bar{E} + js\omega\bar{I}\right) + \left(R + jl\omega\right)\bar{I}$$

that is to say:

$$\bar{V} = \bar{E}_\sigma + (R + jl\omega)\bar{I} \qquad [3.24]$$

with:

$$\bar{E}_\sigma = \bar{E} + js\omega\bar{I} \qquad [3.25]$$

$\bar{E}_\sigma$ is called the "resulting electromotive force" of the synchronous machine. It corresponds, for the stator phases, to the common flux coming from, on the one hand the field system, and on the other hand the armature currents. It is therefore representative of the overall saturation state of the machine.

When the machine is short-circuited (V = 0), there comes:

$$0 = \bar{E}_\sigma + (R + jl\omega)\bar{I}_{cc}$$

Since R is usually smaller than lω, we deduced that $\bar{E}_\sigma$ and $\bar{I}_{cc}$ are almost in quadrature. The flux generated by I_{CC} is then in direct opposition to the field system flux linked to I_R. The armature reaction is called "degaussing" and the resulting flux remains small. Characteristic $I_{CC} = f(I_R)$ or "short-circuit characteristic" can be approximated by a straight line, even for high values of I_R. In order to draw it, it is therefore possible to make one test only.

These various considerations lead to the methods used to answer the following question: what value shall be given to I_R in order to supply the network with an active power P and a reactive power Q (or, in the same way, set an armature current I with a phase φ)? Various methods exist in the literature, but we shall restrict ourselves to the two main ones: the Behn-Eschenburg method, which is the simplest to implement, and the Potier method, which is the more accurate.

3.7.2.3. *The Behn-Eschenburg method*

This method is quite elementary because it is based on large simplifying assumptions: the magnetic armature reaction is neglected, and the dipolar model of the machine is used assuming that E and L depend only on I_R. Let us draw on the same figure (Figure 3.44) the no-load curve $E(I_R)$ and the short-circuit straight line $I_{CC}(I_R)$.

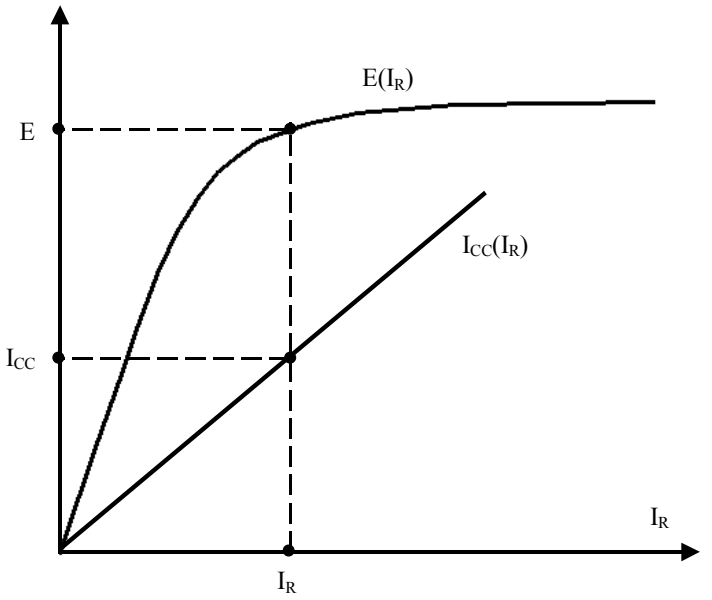

Figure 3.44. *No-load and short-circuit characteristics (same machine as Figure 3.40)*

If one value of field system current Ir is given, the corresponding values of E and of ICC (associated with this value of IR) can be determined. The value of the impedance is then deduced:

$$Z(I_R) = \frac{E(I_R)}{I_{CC}(I_R)}$$

In knowing the value of the stator resistance R, the phasor diagram can be drawn as follows (Figure 3.45). The stator current I is chosen as the phase origin and segment $OA = RI$ is positioned. Point B, the intersection of the perpendicular to OA in A and of circle of centre O and of radius *ZI*, is then determined. Let us consider the straight line going through B and making the angle φ with the direction of I; the intersection of this line with the circle of centre O and the radius E gives the point M.

Vector $\overrightarrow{BM} = \vec{V}$ verifies the equation:

$$\overline{E} = \overline{V} + \overline{ZI}$$

for the chosen value of current IR. The obtained value V therefore has *a priori* no reason for corresponding with the given voltage of the network.

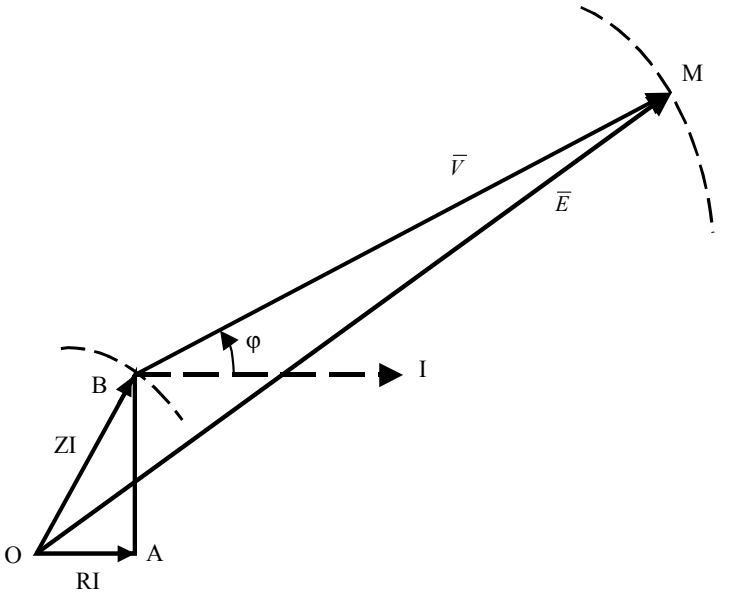

Figure 3.45. *Phasor diagram for the Behn-Eschenburg method*

The process is taken again for another value of IR (bigger than the previous one if too small a value of V was obtained, or smaller if a larger value of V was obtained). It is then possible, through successive approximations, to come closer to the value of IR leading to the desired value of V.

The interest of the method mainly resides in its great experimental simplicity. Indeed it requires only the knowledge of the no-load curve and the implementation of a short-circuit test. However it shall be noted that, considering the simplifying hypotheses adopted, it is unrealistic to hope for a good precision through this method.

3.7.2.4. *Potier method*

3.7.2.4.1. Theoretical foundations

This method is based on the model introduced in section 3.7.2.2: breaking up synchronous inductance L in a saturable part s and a non-saturable part l, and introduction of a "resulting electromotive force" Eσ.

Modification of the sign covenant: in order to find the standard Potier method again, we shall, for this section, leave the "motor" covenant to take the "AC generator" covenant of the synchronous machine. This consists of changing I into –I in the equations. Equations [3.24] and [3.25] become:

$$\bar{E}_\sigma = V + (R + j\lambda)\bar{I} \qquad [3.26]$$

$$\bar{E}_\sigma = \frac{M\omega I_R}{\sqrt{2}} e^{j\delta} - js\omega\bar{I} = \frac{M\omega}{\sqrt{2}}(I_R e^{j\delta} - j\frac{s\sqrt{2}}{M}\bar{I}) \qquad [3.27]$$

where $\lambda = l\omega$ is the leakage reactance.

Equation [3.27] highlights that the resulting electromotive force comes from the superposing of excitation ampere-turns and of armature reaction. We can set down:

$$\mu = \frac{s\sqrt{2}}{M}$$

This value has no size and is called "ampere-turns equivalence coefficient". It implies that μI amperes in the field system generate the same flux as a current I in the armature.

We can then set down:

$$\bar{I}_\sigma = jI_R e^{j\delta} + \mu\bar{I} \qquad [3.28]$$

$$\bar{E}_\sigma = -j\frac{M\omega}{\sqrt{2}}\bar{I}_\sigma \qquad [3.29]$$

These two equations amount to the consideration that the resulting electromotive force $\bar{E}_\sigma$ is produced by a resulting field system current I_σ which is the result of the superposing of current I_R and of an "equivalent" armature current $\mu\bar{I}$.

If equation [3.29] is put together with expression [3.6], it is evident that the magnitude dependence from E_σ to I_σ is the same as from E to I_R, coefficient M being representative of the saturation state of the machine. The "no-load curve" shall therefore be, at the same time, the image of $E = f(I_R)$ and of $E_\sigma = f(I_\sigma)$.

3.7.2.4.2. Potier diagram

Let us assume the "Potier coefficients" (μ and $\lambda = l\omega$), the resistance R and the no-load curve of the machine are known; equations [3.26] to [3.29] enable us to solve the formulated problem: if V, I and φ are given, the resulting electromotive force can be deduced from:

$$\bar{E}_\sigma = V + (R + j\lambda\bar{I}) \qquad [3.26]$$

where V, assumed constant, will be considered as a real number taken as the phase origin (Figure 3.46). It is then easy, in referring to the no-load curve, to obtain the value of the "resulting" current I_σ. We can then draw, on the same diagram, a "triangle of the currents" representative of equation [3.28].

In this vectorial diagram, the position of $\bar{I}_\sigma$ is defined in quadrature with $\bar{E}_\sigma$. The value of the sought excitation current $\bar{I}_R$ is thus obtained. Sometimes the figure is drawn by rotating the "triangle of the currents" by$(-\pi/2)$. Current I_σ is then in the same direction as E_σ, and μI is perpendicular to I.

3.7.2.4.3. Determining the Potier coefficients

The geometrical construction of Figure 3.46 assumes that λ and μ are known. These two coefficients are considered to be constant for a given machine. In order to determine them, let us examine what the diagram becomes for reactive currents, that is to say when $\varphi = \pi/2$ (Figure 3.47).

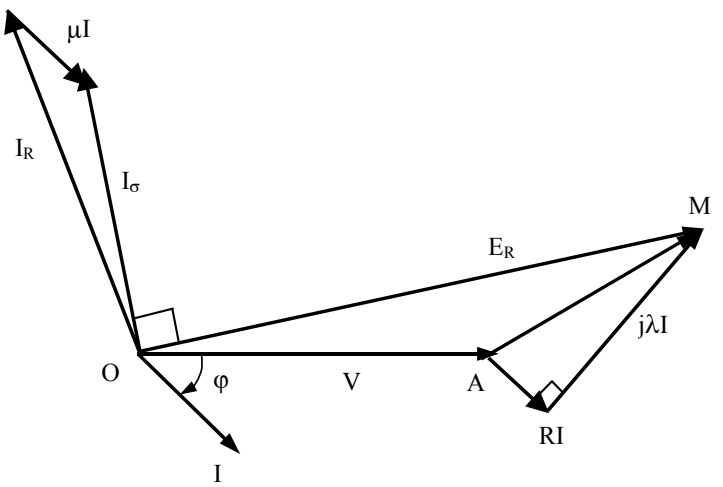

Figure 3.46. *Potier diagram*

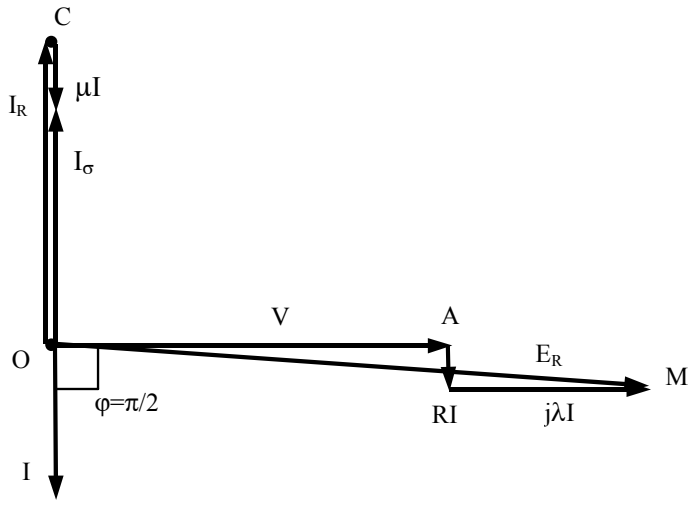

Figure 3.47. *Potier diagram for $\varphi = \pi/2$*

Since R is usually very small, it can be stated that V, $\lambda \bar{I}$ and E_σ are collinear and therefore $\bar{I}_\sigma$, $\bar{I}$ and $\bar{I}_R$ ($jI_R e^{j\delta}$) are collinear too, and orthogonal to the former, hence the two algebraic equations:

$$E_\sigma = V + \lambda I \quad I_\sigma = I_R - \mu I$$

The coefficients λ and μ can be deduced from these two equations: let us draw on the same diagram the no-load curve $E_\sigma = f(I_\sigma)$ and the "constant current of power factor zero" (p.f.z.) curve $V = f(I_R)$, drawn for the desired value of I (Figure 3.48). It can be considered that one point M on the "p.f.z." curve is related to one homologous point M_0 on the no-load curve through a translation ($-\mu I$ in the direction of the currents and λI in the direction of the voltages). If M and M_0 were known, λ and μ would be deduced immediately. If these two points are *a priori* unknown, M_0 can be deduced from M according to the following considerations.

If the Potier coefficients are assumed to be constant, any point on the p.f.z. curve is related to its homologue on the no-load curve through the same translation. This is therefore true for point P corresponding to V = 0 and its correspondent P_0 (Figure 3.48). Since P corresponds to a working short-circuit, the machine is not saturated at this point and P_0 is therefore located on the linear part of the no-load curve. This consideration enables us to determine M_0, because we can be consider that triangle POP_0 translates itself in the plane. So, if we set MO' = PO and at the point O', we draw the parallel to OP_0, this straight line crosses the no-load curve at M_0. In drawing M_0 the perpendicular to O'M, we get $HM_0 = \lambda I$ and $HM = \mu I$, which determine λ and μ.

Note that, since this determination is unique, there is no need to draw the whole curve; a single p.f.z. current point and the short-circuit point are enough.

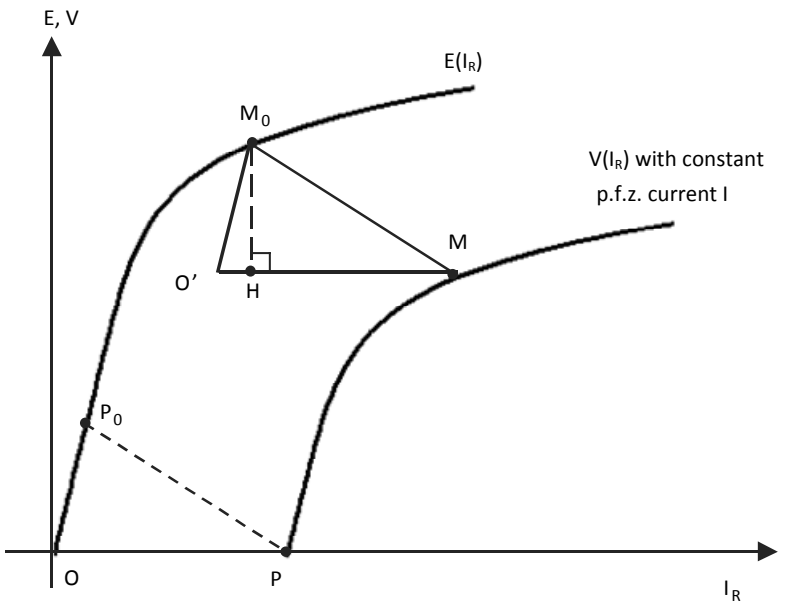

Figure 3.48. *No-load and p.f.z. characteristics*

3.8. Experimental determination of the parameters

The performances and characteristics of synchronous machines can be predetermined using the equivalent diagrams and the diagrams drawn above. This assumes, for a given machine, the knowledge of the parameters numerical values.

Depending on the case, we proceed as follows.

3.8.1. *Cylindrical machine in linear state*

It is a matter of identifying the parameters of the equivalent diagram in Figure 3.3. Resistance R is measured with a hot machine with DC current (nominal value) through an "ammeter-voltmeter" method. The value of reactance Lω is obtained from the no-load curve in its linear part and a short-circuit test with a field system current value of I_{RCC} corresponding to a supportable value (for example, the nominal value) of the armature current I.

We then obtain:

$$Z = \frac{E(I_{RCC})}{I(I_{RCC})}$$

and then we deduce $L\omega = \sqrt{Z^2 - R^2}$.

3.8.2. *Saturation of the cylindrical machine*

It is also necessary to draw the no-load curve $E = f(I_R)$ and to make a short-circuit test. Those two tests are enough to use the Behn-Eschenburg method (see section 3.7.2.3).

In order to use the Potier method, it is necessary to obtain a point with p.f.z. current. In order to do so, it is possible to

load the machine on a supposedly perfect 3-phase inductance, and to measure the phase voltage and current as well as the field current.

3.8.3. *Salient poles machine*

In order to determine reactances X_d and X_q, the "slip test" is used. The stator is supplied by a reduced value balanced 3-phase voltage system, with rms value V. The rotor, in open circuit, is driven in the direction of the stator field at a speed very close to the synchronous speed in order to reduce the effect of the damping windings.

During this test, when the stator mmf axis coincides with the rotor axis d, the reluctance met by the stator flux is at a minimum. This reluctance is maximum when those axes are in quadrature (position q). The current is therefore minimum in position d and maximum in position q (Figure 3.49). The variation of stator current i(t) is then recorded, the extreme values I_{min} and I_{max} are obtained and the direct and quadrature reactances are deduced:

$$X_{d1} = \frac{V\sqrt{2}}{I_{\min}}, \qquad X_{q1} = \frac{V\sqrt{2}}{I_{\max}}$$

Let us point out that during the short-circuit test the load angle is almost zero, which corresponds to position d. It is then preferred to determine X_d using the Behn-Eschenburg method (see section 3.7.2.3). Reactance X_q is then deduced in a more accurate way by:

$$X_q = X_d \frac{X_{q1}}{X_{d1}}$$

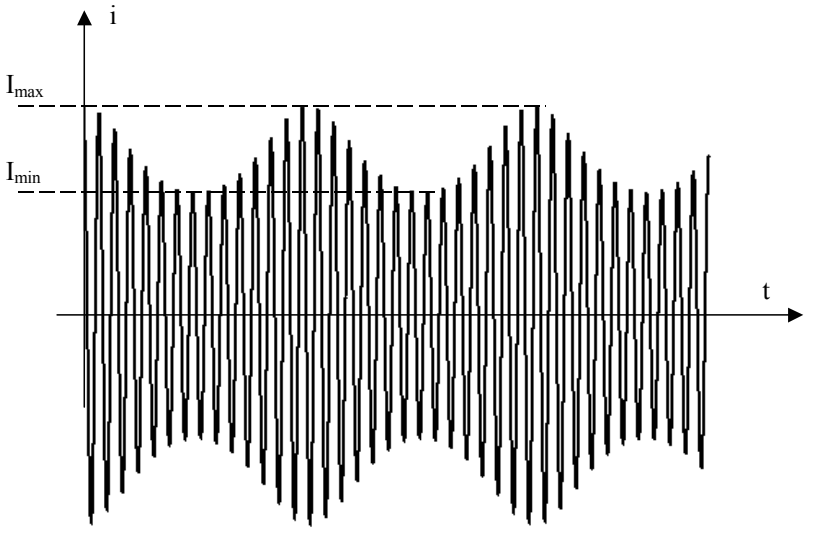

Figure 3.49. *Variation of the stator current: slip method*

Chapter 4

Induction Machines

4.1. Introduction

"Induction machines" are energy converters characterized by the fact that the rotation speed of their rotor is different from the synchronous speed, defined by:

$$\Omega_s = \frac{\omega}{p}$$

where ω is the angular frequency of the stator currents, and p is the number of pole pairs. These machines are called "induction machines" because their rotor currents are generally induced by the currents running through the stator coils.

These machines are rustic, robust and cheap. Formerly their use was restricted to simple and low performance applications when they were connected to constant frequency and constant voltage networks.

Now, induction machines have spread in every domain of industrial motorization, including high-tech applications, since the recent progress in power electronics and in digital control have made it possible to control them with good dynamic performance.

4.2. General considerations

4.2.1. *Structures*

4.2.1.1. *Stator*

The stator of induction machines is a 3-phase field spool with 2p non-salient poles identical to the stator of synchronous machines (Figure 4.1). It is connected, either with a 3-phase network, or with a static converter, and a 3-phase current system is produced.

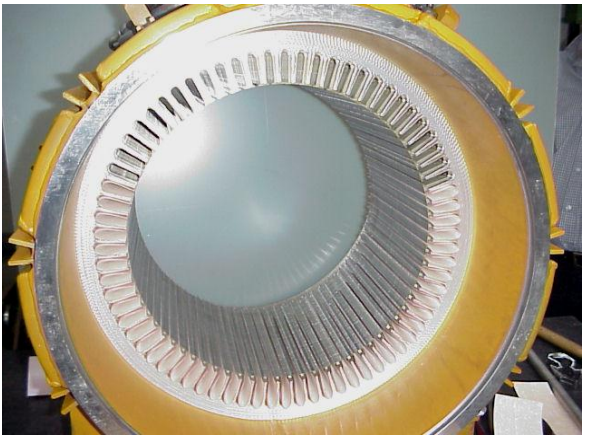

Figure 4.1. *Induction machine stator before winding, 45 kW, 440 V, 590 rpm (ECA EN document)*

4.2.1.2. *Rotors*

Two types of rotors exist: rotors called “wound rotors” and rotors called “squirrel rotors”.

4.2.1.2.1. Wound rotors

In this case, we have a 3-phase field spool with 2p non-salient poles, star connected, in which each phase is connected to a slip-ring on which a fixed brush is rubbing (Figure 4.2). This device makes it possible to connect the rotor coil to either a starting 3-phase rheostat, or to a static converter for some particular drives. In usual working, the 3-phases are short-circuited and 3-phase currents are induced by stator currents. This configuration is mainly found in high-power machines.

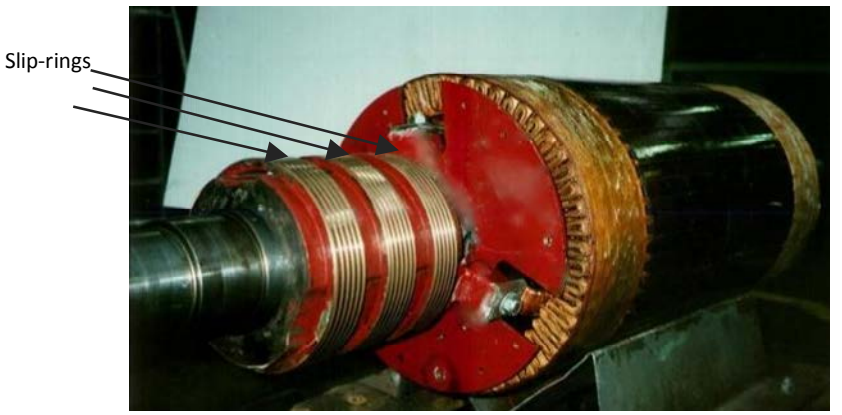

Figure 4.2. *Wound rotor of induction machine, 140 kW, 380 V, 800 rpm, shaft height: 355 mm (ECA EN document)*

4.2.1.2.2. Squirrel rotors

In this case, the rotor is hollowed out of longitudinal slots in which conductive bars are placed and short-circuited at each end by "short-circuit rings" (Figures 4.3 to 4.6). Those bars and rings are usually made of copper but, for small power machines, they can be made of aluminum alloy in order to reduce the cost price. This structure is not a 3-phase structure, but for each cage rotor, an equivalent 3-phase wound rotor can be determined.

As the external behavior of the two types of machines is similar, we shall consider, in this chapter, that we are dealing with wound-rotor machines for which equations are easier to set.

4.2.1.3. *Air-gaps*

In the two cases (wound rotor and squirrel rotor), it is possible to consider, in an initial approximation, that the air-gap is constant.

We shall see in the following that the induction machine performances are very dependent on the thickness of this air-gap, which is, as a consequence, as small as possible: it varies from a few tenths of a millimeter for the small power machines to a few millimeters for the high power machines.

Figure 4.3. *Squirrel rotor of induction machine, 6 kVA, 440 V, 60 Hz, 1 200 rpm. Note the skew of the slots (ECA EN document)*

Figure 4.4. *Piling up of steel sheets constituting the magnetic circuit of a squirrel rotor (photo source: Converteam)*

Figure 4.5. *Detail view of a squirrel rotor being built. Note the cooling holes (photo source: Converteam)*

Figure 4.6. *Squirrel rotor. The short-circuit ring connecting the bars to one another is visible as well as the fan on the shaft (photo source: Converteam)*

4.2.2. *Working principle*

Let us assume that the stator windings fed by 3-phase currents of angular frequency ω will correspond to an air-gap field rotating at angular speed:

$$\Omega_s = \frac{\omega}{p}$$

where Ω is the rotor speed. If $\Omega \neq \Omega_s$, the flux in the rotor phases are time variable and give rise to electromotive forces. Since the rotor phases are short-circuited, these electromotive forces generate currents, which, through an interaction with the stator field, give rise to a torque. On the contrary, if $\Omega = \Omega_s$, the rotor flux do not depend on time, and there are therefore neither electromotive force nor induced currents at the rotor. It is therefore clear that, with such machines, the energy conversion requires that the speeds of the rotor and of the air-gap field are different; that is the reason why they are also called “asynchronous machines”. The relative difference in speed between the field and the

rotor, or "slip", plays an important part in the study of induction machines. Slip g is defined by:

$$g = \frac{\Omega_s - \Omega}{\Omega_s}$$

thus: $\Omega = \frac{d\Theta}{dt} = (1-g)\Omega_s = (1-g)\frac{\omega}{p}$.

Θ measures the position of the rotor with regard to the stator. When introducing electrical angle θ, we write:

$$\theta = p\Theta = (1-g)\omega t + \theta_0$$

4.3. Equations

In this section, we are going to establish the external behavioral equations of the induction machines using the coupling matrixes of the stator and rotor phases.

4.3.1. *Main notations*

If the machines are assumed to be 3-phase at the rotor as well as at the stator, and the axis of phase A is chosen as the origin of the angles, we shall call:

– A, B, C: stator phases;

– a, b, c: rotor phases;

– g: slip;

– I_s: rms stator current value;

– I_r: rotor currents efficient value;

– J: moment of inertia;

– L_i: phase i self inductance;

– M_{ij}: mutual inductance between phases i and j;

– M_0: maximum value of the mutual inductance between a stator phase and a rotor phase;

– p: number of stator and rotor pole pairs;

– Θ : stator-rotor mechanical angle;

– $\theta = p\Theta$: electrical angle;

– ω : stator currents angular frequency;

– ω_r: rotor currents angular frequency;

– $\Omega = d\Theta/dt$: rotor speed;

– $\Omega_s = \omega/p$: synchronous speed;

– $\{i_s\}$: stator currents vector;

– $\{i_r\}$: rotor currents vector;

– $\{\mathcal{L}_s\}$: stator inductance matrix;

– $\{\mathcal{L}_r\}$: rotor inductance matrix;

– $\{\mathcal{L}_{sr}\} = \{\mathcal{L}_{rs}\}^t$: stator-rotor coupling matrix;

– $\{\Psi_s\}$: vector of the total flux per stator phase;

– $\{\Psi_r\}$: vector of the total flux per rotor phase.

4.3.2. *Sign covenants and working assumptions*

Throughout this chapter, we shall adopt the “motor” sign covenants for the machine, which means that the mechanical power will be considered as positive if it is produced, and the electrical power will be positive if it is absorbed. We shall therefore take, *a priori*, “receiver” sign covenants for each of the electrical circuits.

The coils are assumed to have a sinusoidal ampere-turns distribution, and we shall neglect the saturation and hysteresis phenomena.

4.3.3. *Conventional representation*

Figure 4.7 represents in a conventional way the stator and rotor windings.

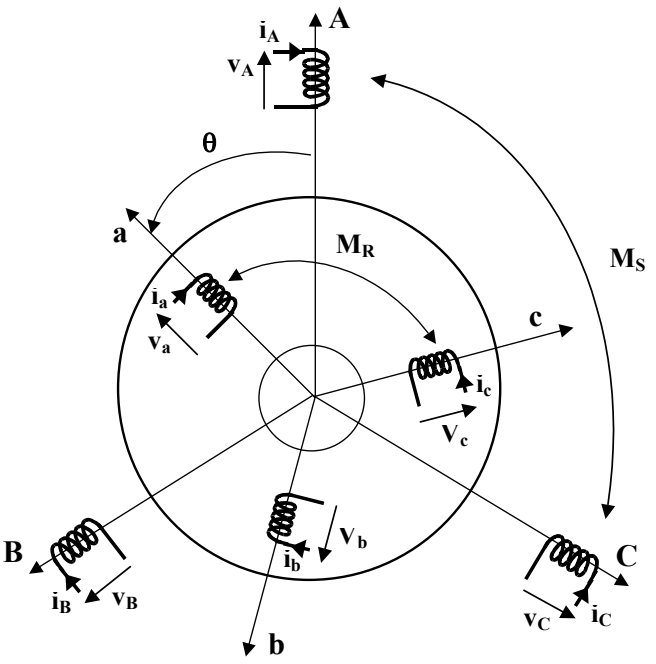

Figure 4.7. *Conventional representation of the machine*

4.3.4. *Flux analysis*

If the matricial general expression is considered again:

$$\{\Psi\} = \{L\}\{i\} \qquad [4.1]$$

or:

$$\begin{Bmatrix} \{\Psi_s\} \\ \{\Psi_r\} \end{Bmatrix} = \begin{bmatrix} \{L_s\} & \{L_{sr}\} \\ \{L_{rs}\} & \{L_r\} \end{bmatrix} \begin{Bmatrix} \{i_s\} \\ \{i_r\} \end{Bmatrix} \qquad [4.2]$$

with:

$$\{\Psi_s\} = \begin{Bmatrix} \Psi_A \\ \Psi_B \\ \Psi_C \end{Bmatrix}, \ \{\Psi_r\} = \begin{Bmatrix} \Psi_a \\ \Psi_b \\ \Psi_c \end{Bmatrix}, \ \{i_s\} = \begin{Bmatrix} i_A \\ i_B \\ i_C \end{Bmatrix} \text{ and } \{i_r\} = \begin{Bmatrix} i_a \\ i_b \\ i_c \end{Bmatrix}$$

the machine has non-salient poles both at the stator and at the rotor, only the stator-rotor coupling inductances depend on the position, and we can write;

$$\{L_s\} = \begin{Bmatrix} L_s & M_s & M_s \\ M_s & L_s & M_s \\ M_s & M_s & L_s \end{Bmatrix}; \qquad \{L_r\} = \begin{Bmatrix} L_r & M_r & M_r \\ M_r & L_r & M_r \\ M_r & M_r & L_r \end{Bmatrix}$$

where L_s and M_s are the self and mutual inductances of the stator phases, and L_r and M_r are the self and mutual inductances of the rotor phases. In the same way, we have:

$$\{L_{sr}\} = \{L_{rs}\}^t = M_0 \begin{Bmatrix} \cos\theta & \cos(\theta + \frac{2\pi}{3}) & \cos(\theta - \frac{2\pi}{3}) \\ \cos(\theta - \frac{2\pi}{3}) & \cos\theta & \cos(\theta + \frac{2\pi}{3}) \\ \cos(\theta + \frac{2\pi}{3}) & \cos(\theta - \frac{2\pi}{3}) & \cos\theta \end{Bmatrix}$$

Furthermore, we can write the stator and rotor currents in the vectorial form:

$$\{i_s\} = I_s\sqrt{2}\begin{Bmatrix}\cos(\omega t - \varphi_s)\\ \cos(\omega t - \frac{2\pi}{3} - \varphi_s)\\ \cos(\omega t + \frac{2\pi}{3} - \varphi_s)\end{Bmatrix}$$

and $$\{i_r\} = I_r\sqrt{2}\begin{Bmatrix}\cos(g\omega t - \varphi_r)\\ \cos(g\omega t - \frac{2\pi}{3} - \varphi_r)\\ \cos(g\omega t + \frac{2\pi}{3} - \varphi_r)\end{Bmatrix}$$

φ_s and φ_r are respectively the stator and rotor currents phases corresponding to the voltages taken as the phase origin. It is therefore possible to express the total flux per stator and rotor phase:

$$\{\Psi_s\} = \{L_s\}\{i_s\} + \{L_{sr}\}\{i_r\}$$

$$\{\Psi_r\} = \{L_{rs}\}\{i_s\} + \{L_r\}\{i_r\}$$

To simplify the calculations, we shall develop only the first line of these two equations for the determination of Ψ_A and Ψ_a:

$$\Psi_A = L_s i_A + M_s(i_B + i_C) + M_0\, i_a \cos\theta + M_0\, i_b \cos(\theta + \frac{2\pi}{3}) + M_0\, i_c \cos(\theta - \frac{2\pi}{3})$$

with $\theta = \theta_o + (1-g)\omega t$.

If the currents are replaced by their expressions in terms of time, we get:

$$\Psi_A = (L_s - M_s)I_s\sqrt{2}\cos(\omega t - \varphi_s) + \frac{3}{2}M_o I_r \cos(\theta_o + \omega t - \varphi_r) \quad [4.3]$$

In the same way, we obtain:

$$\Psi_a = \frac{3}{2}M_o I_s\sqrt{2}\cos(g\omega t - \theta_o - \varphi_s) + (L_r - M_r)I_r\sqrt{2}\cos(g\omega t - \varphi_r) \quad [4.4]$$

Expressions [4.3] and [4.4] show that the total flux per stator and rotor phase are sinusoidal values of respective angular frequencies ω and gω. It is therefore possible to use the complex notations associated with these sinusoidal values.

Given $\overline{\Psi}_A$, $\overline{\Psi}_a$, $\bar{I}_A$ and $\bar{I}_a$ the complex representations respectively associated with Ψ_A, Ψ_a, i_A and i_a; equations [4.3] and [4.4] lead to:

$$\overline{\Psi}_A = (L_s - M_s)\bar{I}_A + 3/2M_0\bar{I}_a e^{j\theta_o} \text{ (angular frequency } \omega) \quad [4.5]$$

$$\overline{\Psi}_a = (L_r - M_r)\bar{I}_a + 3/2M_0\bar{I}_A e^{-j\theta_o} \text{ (angular frequency } g\omega) \quad [4.6]$$

NOTE.– Since complex formalism makes angular frequencies disappear, we shall note them down separately in order to avoid any possible ambiguity.

It is obvious that, in the other stator and rotor phases, we would obtain similar expressions. It is therefore possible to unify the expression of the total flux per stator and rotor phase in making the following variable changes:

– $\bar{I}_A \Rightarrow \bar{I}_1$: stator current or “primary current”;

– $\bar{I}_a e^{j\theta_o} \Rightarrow \bar{I}_2$: “secondary” current;

– $\overline{\Psi}_A \Rightarrow \overline{\Psi}_1$: “primary” flux;

– $\overline{\Psi}_a e^{j\theta_o} \Rightarrow \overline{\Psi}_2$: “secondary” flux.

In setting down:

– $L_1 = L_s - M_s$: primary synchronous inductance;

– $L_2 = L_r - M_r$: secondary synchronous inductance;

– $M = 3/2 M_o$;

– $R_1 = R_s$;

– $R_2 = R_r$;

equations [4.5] and [4.6] become:

$$\overline{\Psi}_1 = L_1 \bar{I}_1 + M \bar{I}_2 \qquad \text{(angular frequency } \omega) \qquad [4.7]$$

$$\overline{\Psi}_2 = M \bar{I}_1 + L_2 \bar{I}_2 \qquad \text{(angular frequency g}\omega) \qquad [4.8]$$

4.3.5. *Electrical equations*

If the induction machine has its rotor short-circuited and its stator supplied by a balanced 3-phase voltage system of rms value per phase V_1, it can be written:

$$\bar{V}_1 = R_1 \bar{I}_1 + \frac{d\overline{\Psi}_1}{dt} \qquad \text{(angular velocity } \omega)$$

$$0 = R_2 \bar{I}_2 + \frac{d\overline{\Psi}_2}{dt} \qquad \text{(angular velocity g}\omega)$$

that is to say:

$$\bar{V}_1 = R_1 \bar{I}_1 + j\omega \overline{\Psi}_1$$

$$0 = R_2 \bar{I}_2 + jg\omega \overline{\Psi}_2$$

From the two equations [4.7] and [4.8], we get:

$$\bar{V}_1 = (R_1 + jL_1\omega)\bar{I}_1 + jM\omega\bar{I}_2 \qquad [4.9]$$

$$0 = jM\omega\bar{I}_1 + \left(\frac{R_2}{g} + jL_2\omega\right)\bar{I}_2 \qquad [4.10]$$

These two equations can be written under the matrix form:

$$\begin{Bmatrix} \bar{V}_1 \\ -\frac{R_2}{g}\bar{I}_2 \end{Bmatrix} = \begin{Bmatrix} R_1 + jL_1\omega & jM\omega \\ jM\omega & jL_2\omega \end{Bmatrix} \begin{Bmatrix} \bar{I}_1 \\ \bar{I}_2 \end{Bmatrix} \qquad [4.11]$$

4.3.6. *Change in the sign covenant*

Equation [4.11] is very similar to the equation of a single-phase transformer, without iron losses or secondary resistance, loaded on a resistance R_2/g. In order to make use of this similarity, it is natural to alter the sign covenant for the secondary current (rotor) and to choose, for induction machines rotors, the "generator" sign covenant (output current counted positively). It can be noted that, since the rotor windings are in short-circuit, this alteration has no energy consequences. In such conditions, equation [4.11] becomes:

$$\begin{Bmatrix} \bar{V}_1 \\ \frac{R_2}{g}\bar{I}_2 \end{Bmatrix} = \begin{Bmatrix} R_1 + jL_1\omega & jM\omega \\ jM\omega & jL_2\omega \end{Bmatrix} \begin{Bmatrix} \bar{I}_1 \\ -\bar{I}_2 \end{Bmatrix} \qquad [4.12]$$

4.4. Equivalent circuits

Equation [4.12] corresponds to an equivalent circuit per phase, identical to that of a single-phase transformer with stator Joule losses only (Figure 4.8).

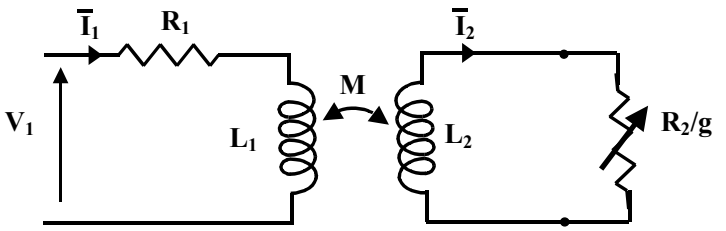

Figure 4.8. *Induction machine equivalent circuit*

The transformer appearing on this equivalent circuit has a voltage ratio $m = \frac{M}{L_1}$. The dispersion coefficient is also introduced:

$$\sigma = 1 - \frac{M^2}{L_1 L_2}$$

This diagram enables us to represent the energy flux in the machine. Term $3R_1I_1^2$ represents the Joule effect losses at the stator and $3\frac{R_2}{g}I_2^2$ corresponds to the overall power transmitted to the rotor. In order to separate the converted power from the rotor Joule losses, it is necessary to slightly modify the equations and the equivalent diagram of the machine. We shall therefore write:

$$\begin{Bmatrix} \bar{V}_1 \\ \frac{R_2(1-g)}{g}\bar{I}_2 \end{Bmatrix} = \begin{Bmatrix} R_1 + jL_1\omega & jM\omega \\ jM\omega & R_2 + jL_2\omega \end{Bmatrix} \begin{Bmatrix} \bar{I}_1 \\ -\bar{I}_2 \end{Bmatrix} \qquad [4.13]$$

which leads to the equivalent circuit given in Figure 4.9.

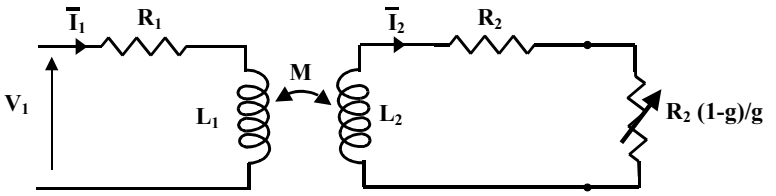

Figure 4.9. *Equivalent circuit separating the Joule losses from the converted power*

On the one hand, this diagram clearly shows the rotor Joule losses ($3R_2I_2^2$) appear and, on the other hand, the converted power $3\frac{R_2(1-g)}{g}I_2{}^2$.

In the following we shall see that it is sometimes convenient to use a transformer-less equivalent diagram based on a two-terminal network. We shall therefore set down:

– $I_2^{'} = \frac{M}{L_1} I_2$: rotor current referred to the stator;

– $R_2^{'} = \left(\frac{L_1}{M}\right)^2 R_2$: resistance of a rotor phase referred to the stator;

– $N_2{}^{'} = \left(\frac{L_1}{M}\right)^2 N_2$ with $N_2 = \sigma L_2 = L_2 - \frac{M^2}{L_1}$: total leakage inductance seen from the rotor.

In transferring these variable changes in equations [4.9] and [4.10] we finally have:

$$\bar{V}_1 = R_1\bar{I}_1 + jL_1\omega(\bar{I}_1 - \bar{I}_2^{'}) \qquad [4.14]$$

$$jL_1\omega\left(\bar{I}_1 - \bar{I}_2'\right) = jN_2'\omega\,\bar{I}_2' + \frac{R_2'}{g}\bar{I}_2' = jN_2'\omega\,\bar{I}_2' + (R_2' + R_2'\frac{1-g}{g})\bar{I}_2' \qquad [4.15]$$

These two equations correspond to the equivalent diagrams of Figures 4.10. Figure 4.10b separates the rotor Joule losses from the converted power.

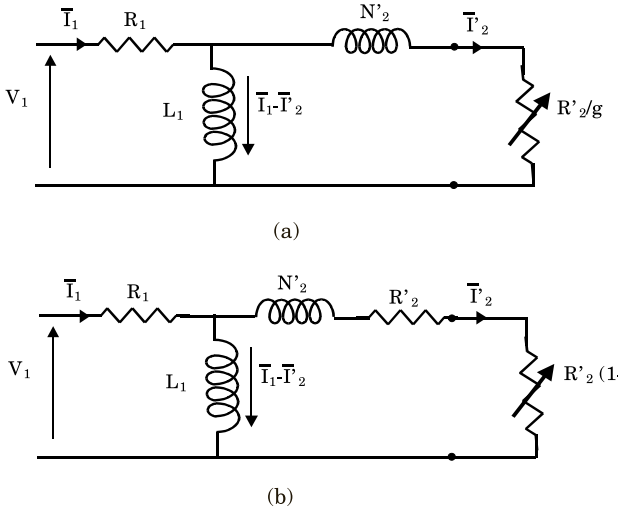

Figure 4.10. *Transformerless equivalent circuits*

4.5. Induction machine torque

4.5.1. *Instantaneous torque*

The expression of the induction machine instantaneous torque can be established from general expression [2.8a]:

$$\Gamma = p\{i_s\}^t \left\{\frac{dL_{sr}}{d\theta}\right\}\{i_r\}$$

The stator and rotor currents are assumed to be sinusoidal, in a balanced 3-phase system, with respective angular frequencies ω and gω, we shall set down:

$$\{i_s\} = I_s\sqrt{2}\begin{Bmatrix} \cos(\omega t - \varphi_s) \\ \cos(\omega t - \frac{2\pi}{3} - \varphi_s) \\ \cos(\omega t + \frac{2\pi}{3} - \varphi_s) \end{Bmatrix}$$

$$\{i_r\} = I_r\sqrt{2}\begin{Bmatrix} \cos(g\omega t - \varphi_r) \\ \cos(g\omega t - \frac{2\pi}{3} - \varphi_r) \\ \cos(g\omega t + \frac{2\pi}{3} - \varphi_r) \end{Bmatrix}$$

with:

$$\frac{d\{L_{sr}\}}{d\theta} = -M_o\begin{Bmatrix} \sin\theta & \sin(\theta + \frac{2\pi}{3}) & \sin(\theta - \frac{2\pi}{3}) \\ \sin(\theta - \frac{2\pi}{3}) & \sin\theta & \sin(\theta + \frac{2\pi}{3}) \\ \sin(\theta + \frac{2\pi}{3}) & \sin(\theta - \frac{2\pi}{3}) & \sin\theta \end{Bmatrix}$$

and:

$$\theta = \theta_o + (1 - g)\omega t$$

We finally get:

$$\Gamma = 3pMI_sI_r\sin(\theta_o + \varphi_s - \varphi_r) \qquad [4.16]$$

This expression shows that in sinusoidal steady state, the induction machine instantaneous torque is constant. It will therefore be possible to identify this instantaneous torque

with the average torque determined from global energy considerations.

Expression [4.16] is not convenient to use because it depends on values that are difficult to obtain, such as θ_o and φ_r; we shall therefore establish another torque formulation from the analysis of the energy transfer in the induction machine.

4.5.2. *Analysis of the energy transfer*

Let us assume that the machine is connected to a network having a phase voltage V_1. The absorbed active power is written P_a. The latter is partially dissipated in stator Joule losses p_{j1} and of stator iron losses p_{f1} (which had until now been neglected). The remaining power, which shall be called P_2, is transmitted to the rotor:

$$P_2 = P_a - p_{j1} - p_{f1} \qquad [4.17]$$

Referring to the equivalent diagram of Figure 4.8, it can also be written:

$$P_2 = 3\frac{R_2}{g} I_2^2$$

In the rotor, the frequency is small ($\omega_r = g\omega$), and it is therefore possible to neglect the rotor iron losses. After taking off the rotor Joule losses p_{j2}, P_2 is converted into mechanical power $P_m = \Gamma\Omega$.

Considering the equivalent diagram given in Figure 4.9, we get:

$$p_{j2} = 3R_2 I_2^2 = gP_2$$

$$P_m = 3R_2 \frac{1-g}{g} I_2^2$$

hence:

$$P_m = \Gamma\Omega = (1-g)P_2 = \Gamma(1-g)\frac{\omega}{p}$$

and therefore:

$$P_2 = \Gamma\frac{\omega}{p} = \Gamma\Omega_s \qquad [4.18]$$

This result shows that the power transmitted to the rotor is equal to the product of the torque by the synchronous speed. Furthermore, since $pj_2 = gP_2$, it is clear that the rotor Joule losses are proportional to the slip, and therefore inherent to the asynchronous energy conversion. This power transfer can be represented by Figure 4.11.

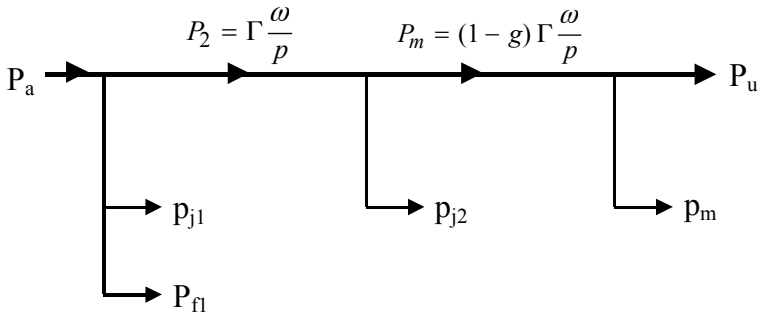

Figure 4.11. *Power transfer in the induction machine*

It is also deduced that if all losses except p_{j2} losses were neglected, the ideal efficiency would at the most be equal to:

$$\eta_{max} = 1 - g$$

This expression shows that in order to have a satisfying efficiency, an induction machine has to work with a small slip.

4.5.3. *Expression of the electromagnetic torque in terms of the slip*

For this study, we shall neglect all the stator losses. The equivalent circuit per phase of Figure 4.10a becomes that of Figure 4.12.

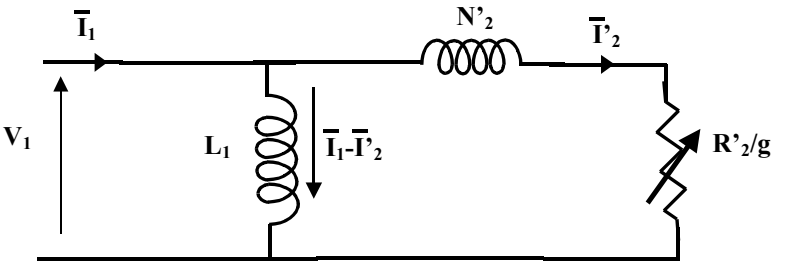

Figure 4.12. *Equivalent figure without stator losses*

The value of P_2 can be deduced from this diagram:

$$P_2 = 3\frac{R_2^{'}}{g} I_2^{'2}$$

We therefore have $\Gamma = \frac{p}{\omega} P_2 = \frac{3p}{\omega}\frac{R_2^{'}}{g} I_2^{'2}$, with:

$$I_2^{'2} = \frac{V_1^2}{\left(\frac{R_2^{'}}{g}\right)^2 + \left(N_2^{'}\omega\right)^2}$$

thus:

$$\Gamma = \frac{3p}{\omega} \frac{\frac{R_2^{'}}{g}}{\left(\frac{R_2^{'}}{g}\right)^2 + \left(N_2^{'}\omega\right)^2} V_1^2 \qquad [4.19]$$

Expression [4.19] makes it possible to study the variation of the torque of the induction machine in terms of the slip (Figure 4.13). This characteristic curve, drawn for a slip varying from $-\infty$ to $+\infty$, leads to the following remarks:

– if g is near zero, $\left(\frac{R_2^{'}}{g}\right)^2 >> N_2^{'2}\omega^2$ leads to $\Gamma \approx \frac{3p}{\omega}\frac{g}{R_2^{'}}V_1^2$.

We can deduce that curve $\Gamma(g)$ is almost linear when nearing the origin;

– if g is important, $N_2^{'2}\omega^2 >> \left(\frac{R_2^{'}}{g}\right)^2$ leads to $\Gamma \approx \frac{3p}{\omega}\frac{R_2^{'}}{gN_2^{'2}\omega^2}V_1^2$. The torque will therefore hyperbolically tend toward zero if g tends toward infinity;

– curve $\Gamma(g)$ has two extreme values $\pm\Gamma_m = \frac{3p}{\omega}\frac{V_1^2}{2N_2^{'}\omega}$ obtained for:

$$g = g_m = \pm\frac{R_2^{'}}{N_2^{'}\omega} = \pm\frac{R_2}{N_2\omega}$$

It is therefore clear that obtaining an important value of Γ_m will be linked to a small value of N'_2 corresponding to small stator-rotor leakage. This explains that induction machines have as small an air-gap as possible.

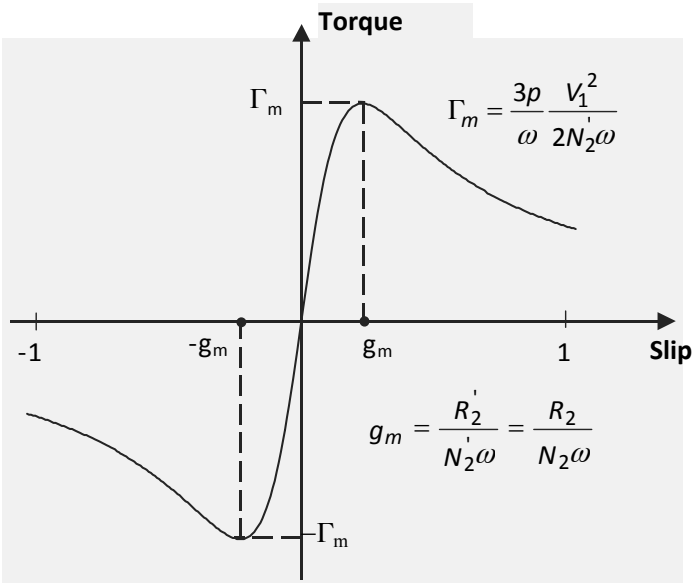

Figure 4.13. *Torque-slip characteristic*

Curve Γ(g) is symmetrical in relation to the origin. It is therefore clear that if g is negative ($\Omega > \Omega_s$), the electromagnetic torque is negative too, which characterizes a negative mechanical power. This shows the reversibility of the induction machine, which can operate as a generator or as a motor.

4.6. Study of the stability

Let us assume that the machine, working as a motor, drives a charge characterized by a resistant torque Γ_C (Figure 4.14). We observe that characteristics Γ(g) and Γ_C(g) have two intersections for working points corresponding to slips called g_C and g_C'. In order to show that only slip point g_c corresponds to an effective working point, we shall study the induction machine stability.

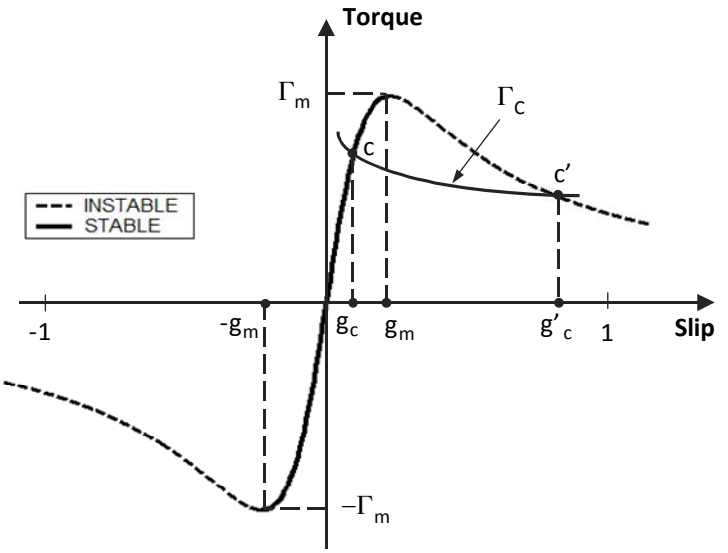

Figure 4.14. *Stable parts of the torque-slip characteristic*

Let us assume that the machine is in steady state with slip g_C and that a perturbation Δg occurs. If Δg is small enough, the characteristics $\Gamma(g)$ and $\Gamma_C(g)$ can be assimilated with their tangential lines in g_C:

$$J\frac{d\Omega}{dt} = \Gamma(g_c) - \Gamma_c(g_c) = 0$$

$$\Gamma(g) = \Gamma(g_c) + \left(\frac{d\Gamma}{dg}\right)_{g_C} \Delta g$$

and:

$$\Gamma_c(g) = \Gamma_c(g_c) + \left(\frac{d\Gamma_c}{dg}\right)_{g_C} \Delta g$$

Furthermore:

$$\Omega = (1 - g)\frac{\omega}{p} = (1 - g_c - \Delta g)\frac{\omega}{p}$$

hence:

$$\frac{d\Omega}{dt} = -\frac{d(\Delta g)}{dt}\frac{\omega}{p}$$

The mechanical equation therefore becomes:

$$-J\frac{\omega}{p}\frac{d(\Delta g)}{dt} = \left(\frac{d\Gamma}{dg} - \frac{d\Gamma_c}{dg}\right)_{g_C} \Delta g$$

Remember that in this equation, J represents the moment of inertia of all the rotating parts (rotor of the induction machine and load).

In order for the calculation to be stable, the machine must tend to get back to its initial working point, that is to say that g tends toward g_C and therefore that $\frac{d(\Delta g)}{dt}$ and Δg have opposite signs. It is then necessary to have:

$$\left(\frac{d\Gamma}{dg} - \frac{d\Gamma_c}{dg}\right)_{g_C} > 0 \qquad [4.20]$$

Generally the resistant torque increases with speed, consequently it decreases with slip. The condition for stability [4.20] can therefore be written:

$$\frac{d\Gamma}{dg} > 0 \qquad [4.21]$$

We can deduce that the stable part of characteristic $\Gamma(g)$ is the part located between $g = -g_m$ and $g = +g_m$, in the small slip area. In Figure 4.14, the stable operating point corresponds to g = g_C. The point corresponding to g'$_C$ is therefore unstable.

4.7. Circle diagram (or "Blondel" diagram)

4.7.1. *Introduction*

From its origins, electrical engineering has used graphic methods for the predetermination of the behavior of the machines, particularly that of AC machines. Indeed the latter are governed by equations that are difficult to treat in an analytical way.

Since digital calculation has been developed, diagrams have lost the part of "calculation instruments" that they had played for decades, to become mere support for qualitative reasoning, and for digital calculations that avoid the structural imprecision of the graphic methods.

This is true both for induction machines and for synchronous machines. That is why, in this book, we shall mainly use the simplified version of the circle diagram, called a "Blondel diagram". This diagram represents, in the complex plane, the locus of the vector of affix $\bar{I}_1$ when slip g varies from - ∞ to + ∞, with constant V_1 and ω. If matrix equation [4.13] is considered again and if current $\bar{I}_2$ is eliminated, we have:

$$\overline{V_1} = \left[R_1 + jL_1\omega + \frac{M^2\omega^2}{\frac{R_2}{g} + jL_2\omega} \right] \bar{I}_1 \qquad [4.22]$$

The stator phase impedance $\overline{Z}_1$ is then deduced:

$$\overline{Z}_1 = R_1 + jL_1\omega + \frac{M^2\omega^2}{\frac{R_2}{g} + jL_2\omega}$$

This impedance has two noticeable values:

– with g = 0, $\overline{Z}_1 = \overline{Z}_{10} = R_1 + jL_1\omega$;

– when g tends toward infinity, $\overline{Z}_1$ tends toward $\overline{Z}_{1\infty} = R_1 + jL_1\omega + \frac{M^2\omega^2}{jL_2\omega}$, that is to say:

$$\overline{Z}_{1\infty} = R_1 + j\sigma L_1\omega$$

σ is the stator-rotor dispersion coefficient defined by $\sigma = 1 - \frac{M^2}{L_1L_2}$.

Equation [4.22] gives the stator current:

$$\bar{I}_1 = \frac{\overline{V}_1}{R_1 + jL_1\omega + \frac{M^2\omega^2}{\frac{R_2}{g} + jL_2\omega}} \qquad [4.23]$$

It can be deduced (either geometrically, through inversion, or analytically from the properties of the Möbius transformation in the complex plane) that when g varies from –∞ to +∞, the locus of affix point $\bar{I}_1$ is a circle, called a "circle diagram" in the literature.

4.7.2. *g and in 1/g graduation of the circle*

We can also be deduced from equation [4.23] that a bijective transformation exists between the circle and any straight line Δ linearly graduated in slip (Figure 4.15). For

that purpose a transformation (inversion) pole A has to be chosen at the second intersection of the circle with the parallel to Δ going through point O_∞. The graduation origin is the intersection of Δ with straight line AO_0.

In order to obtain the graduation scale of Δ, we need only know the value of the slip corresponding to a point on the circle; point M_1 with slip g = 1 is often used because it is easy to obtain experimentally (locked rotor).

As $\bar{I}_1(g)$ is also a Möbius function of 1/g, it is possible to scale the circle in 1/g in the same way, providing that the roles of O_0 and O_∞ are exchanged (graduation of Δ' in Figure 4.16). The joint use of the two graduations makes determination of the value of the slip corresponding to any point of the circle possible.

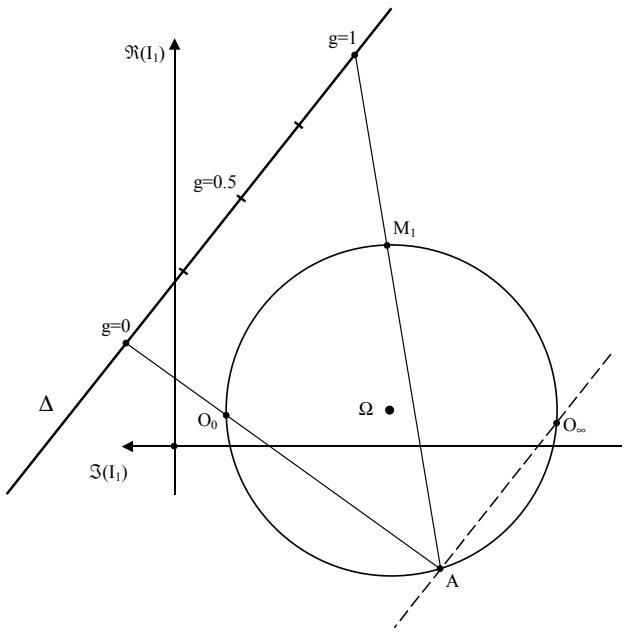

Figure 4.15. *Slip graduation of the circle diagram*

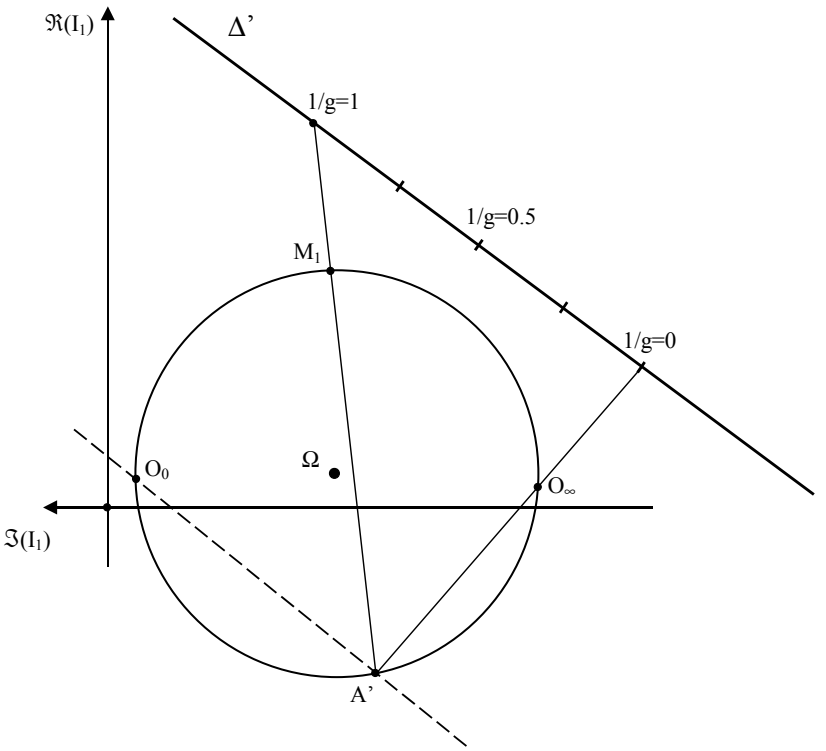

Figure 4.16. *1/g graduation of the circle diagram*

4.7.3. *Simplified circle diagram*

4.7.3.1. *General introduction*

This diagram is called "simplified" because it is based on the hypothesis that the stator Joule losses are negligible. It is therefore assumed that $R_1 = 0$ all along this section. The stator current is therefore written:

$$\bar{I}_1 = \frac{\bar{V}_1}{\bar{Z}_1} = \frac{\bar{V}_1}{jL_1\omega + \dfrac{M^2\omega^2}{\dfrac{R_2}{g} + jL_2\omega}} \qquad [4.24]$$

If the machine is assumed to be supplied by constant stator voltage $\bar{V}_1$, this voltage can be taken as the origin of the phases. The affixes of points O_0 and O_∞ respectively corresponding to g = 0 and to g infinite are:

$$\bar{I}_{10} = \frac{V_1}{jL_1\omega} = -j\frac{V_1}{L_1\omega} \qquad \text{and} \qquad \bar{I}_{1\infty} = \frac{V_1}{j\sigma L_1\omega} = -j\frac{V_1}{\sigma L_1\omega}$$

They are two imaginary negative numbers. The circle is then centered on the imaginary axis at point Ω, for which the affix is $-jV_1\frac{1+\sigma}{2\sigma L_1\omega}$.

4.7.3.2. *Drawing of the circle*

Experimentally, the circle is determined from two tests:

– a "no-load" test when the motor, supplied with its nominal voltage, drives no load: the slip is very small and the measured current will be assumed to be $\bar{I}_{10}$, and assumed to be $\frac{\pi}{2}$ lagging. Point O_o on the imaginary axis is then determined. For convenience reasons, the real axis is usually drawn vertically (Figure 4.17);

– a test at standstill, with a stator voltage V_{1C} reduced so that the corresponding current modulus $\bar{I}_{1c}$ does not exceed the nominal current. The machine impedance is assumed to be independent from the voltage, the stator current corresponding to voltage V_1 is calculated using $\bar{I}_{11} = \bar{I}_{1c}\frac{V_1}{V_{1c}}$. Point M_1 corresponding to g = 1 can therefore be set down (Figure 4.17).

Center Ω of the circle is then found at the intersection of the median O_oM_1 with the imaginary axis.

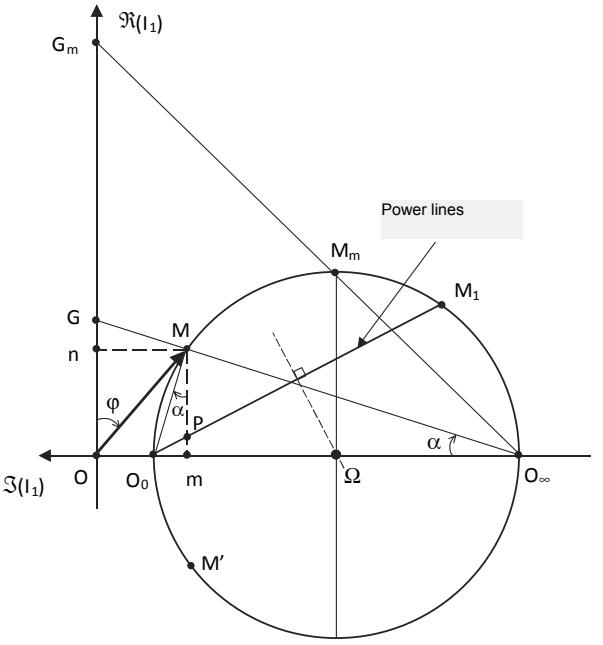

Figure 4.17. *Simplified circle diagram*

4.7.3.3. *Interpretation of the diagram*

Once the circle is drawn, it can be graduated in slip, as established above. We shall now show that it is possible to deduce from this diagram the main characteristics of the induction machine.

4.7.3.3.1. Absorbed powers

If we consider a point M on the circle, for which slip is g, vector OM represents the current $\bar{I}_1$, absorbed at the network, and for which the phase, with regard to the voltage, is φ (Figure 4.17). If n and m are respectively the projections of M on the real and imaginary axes, we obtain:

$$P_1 = 3V_1 I_1 \cos\varphi = 3V_1 \overline{On} = 3V_1 \overline{mM}$$

$$Q_1 = 3V_1 I_1 \sin\varphi = 3V_1 \overline{Om} = 3V_1 \overline{nM}$$

Segment mM therefore measures, providing the scale of the diagram is multiplied by $3V_1$, the active power absorbed at the network. This power is positive when point M is on the "upper" semi-circle ($g > 0$); it is negative for the "lower" semi-circle ($g < 0$).

In the same way, segment Mn represents the reactive power absorbed at the network, which is always positive.

4.7.3.3.2. Electromagnetic torque

As all stator losses are neglected, the absorbed power is fully transmitted to the rotor. Therefore we have:

$$P_1 = P_2 = \Gamma \frac{\omega}{p}$$

It is deduced:

$$\Gamma = 3 \frac{pV_1}{\omega} \overline{mM}$$

Thus, thanks to another scale change, $\overline{mM}$ also measures the electromagnetic torque. The latter is therefore positive for the upper semi-circle and, when g varies from zero to $+\infty$, the torque goes through its maximum Γ_m for point Mm corresponding to slip g_m (Figure 4.14). By calling α the angle $(O_o O_\infty M)$, we get $mM = O_o O_\infty \sin\alpha \cos\alpha$.

Point M_m relative to torque Γ_m corresponds to $\alpha = \frac{\pi}{2}$. It is deduced that:

$$\frac{\Gamma}{\Gamma_m} = 2\sin\alpha\cos\alpha = \sin 2\alpha = \frac{2tg\alpha}{1 + (tg\alpha)^2}$$

Furthermore, if the intersection of straight line $O_\infty M$ with the real axis is called G, segment OG is proportional to the slip (the real axis can be graduated in g with O_∞ as the pole). Given G_m the intersection of $O_\infty M_m$ with the real axis. We therefore get:

$$\frac{OG}{OG_m} = \frac{g}{g_m} = \frac{OO_\infty tg\alpha}{OO_\infty tg\frac{\pi}{4}} = tg\alpha$$

hence:

$$\frac{\Gamma}{\Gamma_m} = \frac{2\frac{g}{g_m}}{1+(\frac{g}{g_m})^2} = \frac{2}{\frac{g}{g_m}+\frac{g_m}{g}} \qquad [4.25]$$

Expression [4.25] is very convenient because, if Γ_m and g_m are known, it is very easy to calculate the torque corresponding to a given slip and *vice versa*.

4.7.3.3.3. Mechanical power

Absorbed power P_1, considering the above made hypotheses, is completely transmitted to the rotor. It is then divided, on the one hand, in rotor Joule losses p_{j2} and, on the other hand, in mechanical power P_M. It is therefore interesting to separate those two values on the diagram. If the straight line bearing mM is graduated in 1/g, the pole is O_o and the origin is m. If P is the intersection of this straight line with O_oM_1, this point corresponds to value 1 of the graduation. We therefore have:

$$\frac{\overline{mP}}{\overline{mM}} = \frac{1}{\frac{1}{g}} = g$$

Going back to the power graduation, we have:

$$\overline{mP} = g\,\overline{mM} = g\,P_2 = p_{j2}$$

and, as a consequence:

$$\overline{PM} = P_2 - p_{j2} = P_M$$

Segment $\overline{PM}$ therefore represents the mechanical power produced by the induction machine, and segment $\overline{nP}$, the rotor Joule losses. Straight line O_oM_1 that separates the mechanical power from the Joule losses is sometimes called "mechanical powers line".

4.7.3.3.4. Reversibility

The simplified circle diagram shows the reversibility of the induction machine: the half of the circle located below the imaginary axis corresponds to negative values of the slip and also negative values of the absorbed power P_1. It is therefore an asynchronous generator operating with a rotation speed Ω greater than Ω_S.

We shall come back to this working mode in more detail (section 4.9.2) but it is clear that, even when P_1 becomes negative (point M'), Q_1 remains positive, and the reactive power will therefore have to be supplied to the induction so that it is able to operate as a generator.

4.8. Induction machine characteristics

In order to illustrate the various curves of the following paragraphs, we shall consider a machine defined by:

– P_n = 1MW;

– U_n = 5,000 V phase-to-phase voltage;

– 2p = 8;

– f = 50 Hz;

– g_n = 1.2%;

– σ = 6.4%;

– R_1 = 0.0437 Ω;

– R_2 = 0.0437 Ω;

– L_1 = 0.263 H;

– L_2 = 0.0435 H.

M_n shall be placed on each curve point, corresponding to the nominal load of the machine. The characteristics of Figures 4.18 to 4.24 have been drawn numerically directly using the corresponding analytical equations.

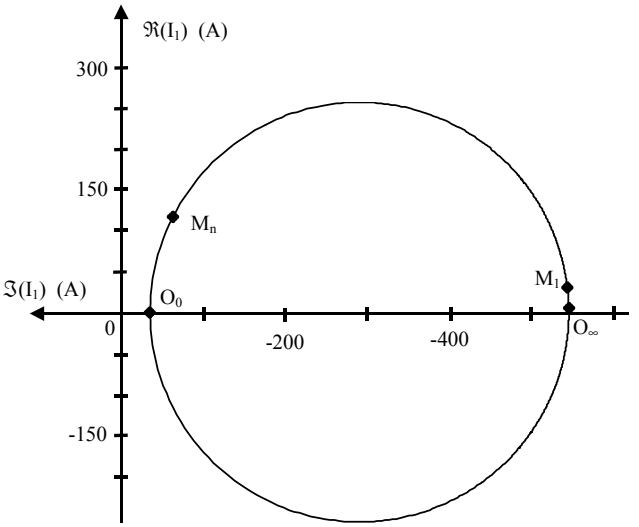

Figure 4.18. *Circle diagram. It can be noticed that for this machine, points M_1 and O_∞ are near the imaginary axis, and that the starting torque is clearly smaller than the nominal torque*

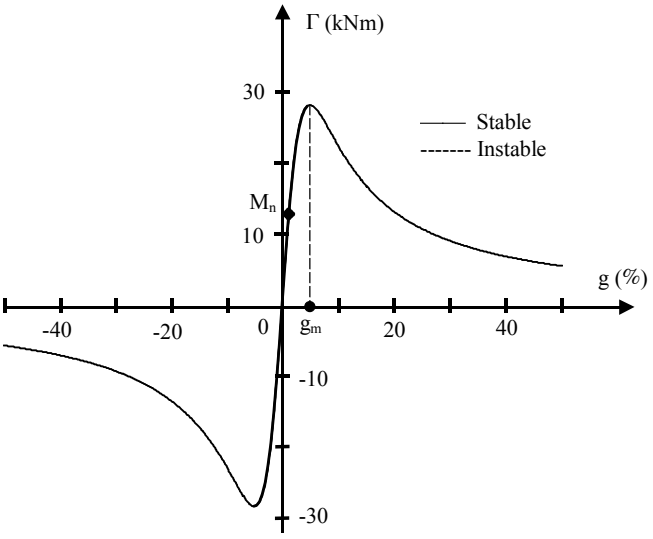

Figure 4.19. *Torque-slip characteristic. It can be noticed that slip g_m, which corresponds to the maximum torque value, is equal to 5% with g_n=1.2%*

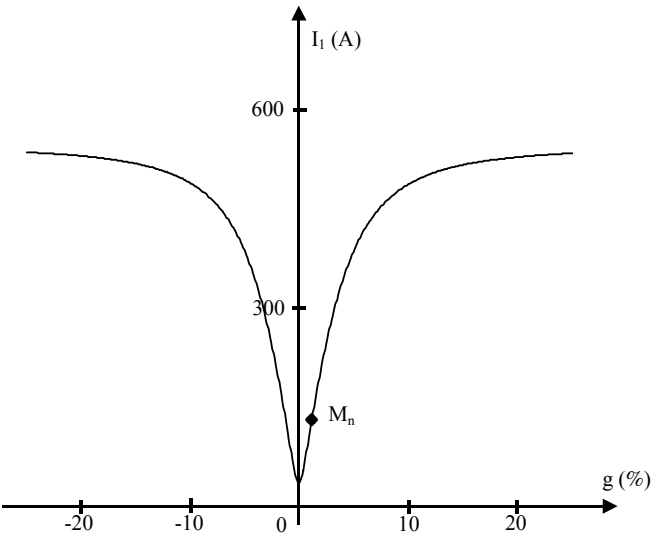

Figure 4.20. *Stator-slip current characteristic*

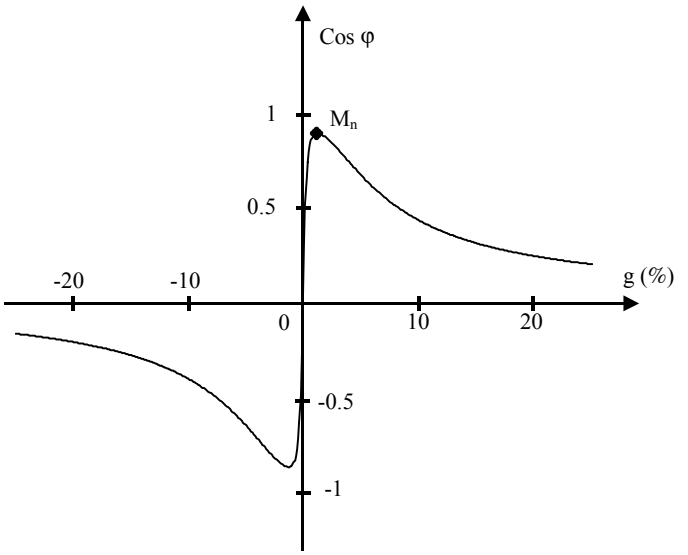

Figure 4.21. *Power-slip factor characteristic. Note that in this particular case the maximum power factor corresponds to the nominal power factor*

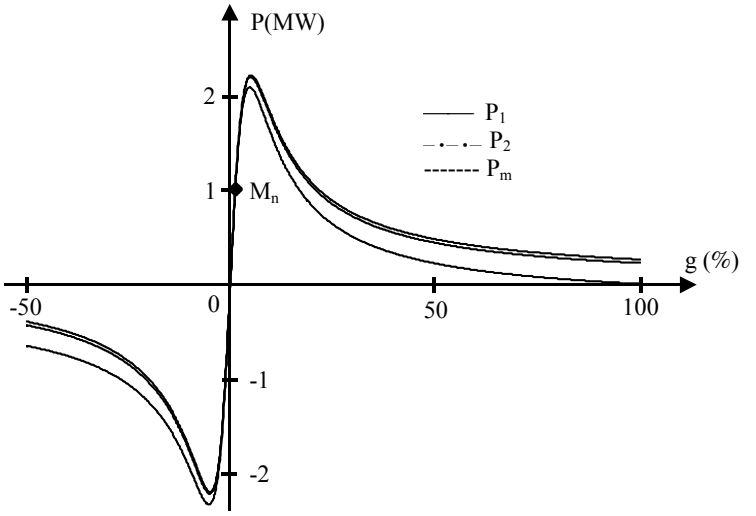

Figure 4.22. *Powers-slip characteristics (P_1: absorbed, P_2: converted, P_M: mechanical). Note that the 3 curves almost join one another on the useful part of these characteristics ($g \in [0, g_n]$)*

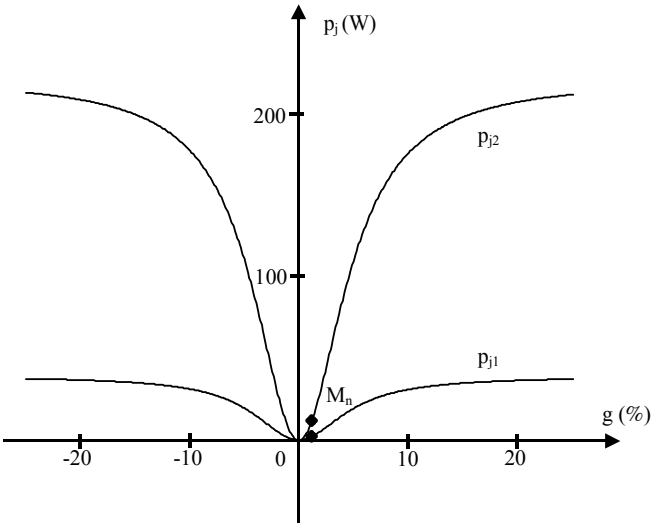

Figure 4.23. *Joule losses–slip characteristics (p_{j1}: at the stator, p_{j2}: at the rotor)*

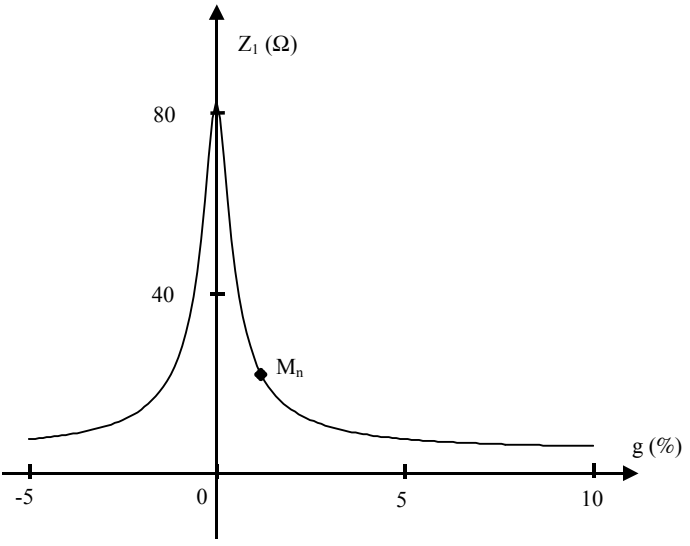

Figure 4.24. *Synchronous impedance-slip characteristic*

4.9. Implementation of induction machines

The use of induction machines has changed considerably over recent years. They are mainly used as motors but the number of induction generators is now increasing in the area of renewable energy particularly in wind power stations.

4.9.1. *Motor mode*

The induction motor is widely used in every industrial domain and for various applications, going from fixed-speed pumping (power supply by a constant frequency network) to rail traction and ship propulsion (power supply by static converters). We shall survey the various implementations starting with the most traditional one.

4.9.1.1. *Constant voltage and frequency power supply*

In this case, the induction motor is directly supplied by the network at an industrial frequency and drives a mechanical load the rotation speed of which is nearly constant, g being small. In such implementations, the only problem to be solved is the starting of the motor. For this analysis, the circle diagram is a good analysis support.

Referring to Figure 4.18, we can notice that when the motor is stopped ($g = 1$), torque $\Gamma(g = 1)$ is smaller than nominal torque Γ_n, and absorbed current $I_1(g = 1)$ is obviously greater than the stator nominal current. This example shows that it is usually impossible to start a loaded induction motor supplied with its nominal voltage.

In order to resolve this problem, solutions vary depending on whether we are dealing with a squirrel induction motor or with a wound-rotor induction motor.

4.9.1.1.1. Squirrel induction motors

Squirrel induction motors are very robust machines, likely to support a current largely greater than their nominal current during the few seconds necessary to their starting. It is possible to reduce this current in supplying the stator with reduced voltage (star-delta connection, use of a self-transformer or of an electronic AC power controller).

The star-delta start consists of star coupling (at the time of start) a motor designed for delta working. The phase voltage is thus reduced, and therefore the starting current with a ratio of $\sqrt{3}$.

Note that, since the electromagnetic torque is proportional to the square of the voltage, if the voltage is reduced (and therefore the current) in a k ratio, the torque is *ipso facto* reduced in a k^2 ratio. This process is therefore only to be used for no-load starting motors.

In order to improve the motor characteristics at starting, deep slots are used (Figure 4.25). Initially, the rotor frequency is equal to the supply frequency, and the skin-effect phenomenon leads to an induced current repartition concentrated at the surface of the rotor bars. This gives an increase of the apparent resistance of the bars, that is to say an increase in resistance R_2, and therefore a decrease in the starting current. On the circle diagram g_m moves and provides an increase of the starting torque. With the increase of speed, the rotor frequency decreases, the skin depth increases and leads to the reduction of the rotor resistance.

Various slot shapes can be used. It is clear that, for instance, in adopting trapezoid slots (Figures 4.25b), the variation effect of the resistance increases. At 50 Hz and for aluminum bars, it can be shown that this effect is noticeable only for bar heights over 2 cm.

Double-cage rotors are also used (Figure 4.26) in order to improve the starting performances of the machine. The first cage, or starting cage, is set near the air-gap. Its resistance is great due to the choice of the section and of the materials the bars are made from. Furthermore, its setting near the air-gap gives it a small leakage reactance. On the contrary, the second cage, or inside cage, is characterized by a smaller resistance and a greater leakage reactance.

Initially, both cage resistances are smaller than their reactances, and the induced currents are almost restricted to the outer cage, characterized by the smaller inductance. The starting torque is therefore great, and the current, reduced. In nominal working, the rotor frequency is small and the bars reactances become smaller than their resistances. The induced currents are then concentrated in the small resistance inner cage. The corresponding slip is then small, which leads to a good efficiency.

Figure 4.25. *Deep slots: a) rectangular; b) trapezoid*

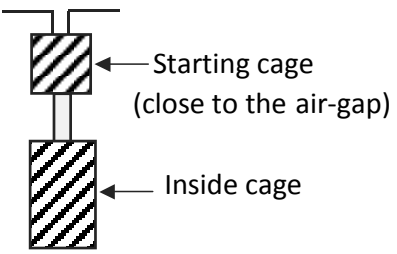

Figure 4.26. *Slot bearing a double cage*

4.9.1.1.2. Wound-rotor induction motors

When induction motors have wound rotors, it is possible to connect their rotor phases, star coupled, to external resistances through slip-rings and brushes (Figure 4.2). Those resistances called "starting rheostats" enable us to modify the apparent value of resistance R_2 (Figure 4.27) This starting method is almost not used any more. However we are introducing it because of its historical and pedagogical interest.

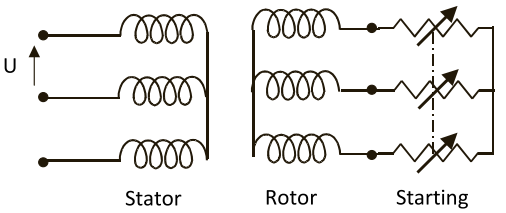

Figure 4.27. *Rotor starting rheostat*

The starting values of the motor (torque and absorbed current) can be modified in this way. Indeed, if the induction machine equations are considered, it is clear that (equation [4.23]) absorbed current I_1 depends on the slip through term $\frac{R_2}{g}$, that is to say that (V_1 and f being fixed) a working point is related to a $\frac{R_2}{g}$ ratio. Furthermore, maximum torque $\Gamma_m = \frac{3p}{\omega}\frac{V_1^{\,2}}{2N_2'\omega}$ does not depend on R_2, but the corresponding slip $g_m = \frac{R_2}{N_2\omega}$ is proportional to R_2.

The circle diagram is a good reasoning support to show the influence of the starting rheostat (Figure 4.28). Let us assume that the machine under consideration can endure a starting current kI_n and has to drive a load for which the

resistant torque is equal to nominal torque Γ_n. On the circle the corresponding points are respectively M_k and M_n. Point M_1 of slip g = 1 (without a rheostat) is also noted.

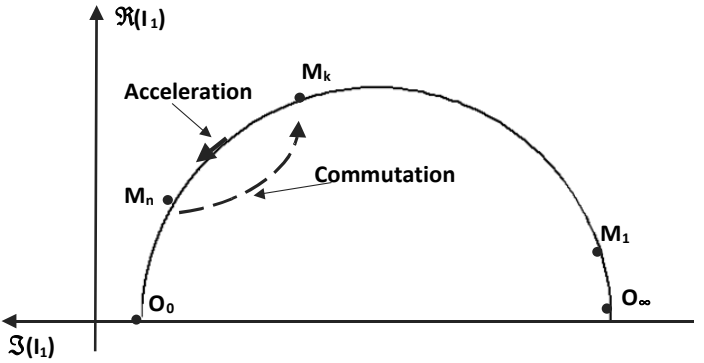

Figure 4.28. *Circle diagram*

Calling g_k the slip corresponding to M_k in normal working, it is possible to set down the starting point in M_k provided that a rheostat of resistance R_d is used:

$$\frac{g_k}{R_2} = \frac{1}{R_2 + R_d}$$

hence:

$$R_d = R_2 \frac{1 - g_k}{g_k} \qquad [4.26]$$

If the corresponding starting torque Γ_k is greater than Γ_n, the motor starts, accelerates, and its working point follows arc M_kM_n. Its speed stabilizes for a slip g'_n corresponding to point M_n (torque Γ_n). It can be written:

$$\frac{g'_n}{R_2 + R_d} = \frac{g_n}{R_2}$$

The previous calculation can be taken again in order to place the point with slip g'_n in M_k and to calculate the new rheostat resistance R'_d:

$$R'_d = R_2 \frac{g'_n - g_k}{g_k}$$

In commutating the rheostat from R_d to R'_d, the move from M_n to M_k is instantaneous and the motor accelerates again to go back to M_n, and so on and so forth. In plane $\Gamma(g)$, the characteristics of Figure 4.29 are obtained.

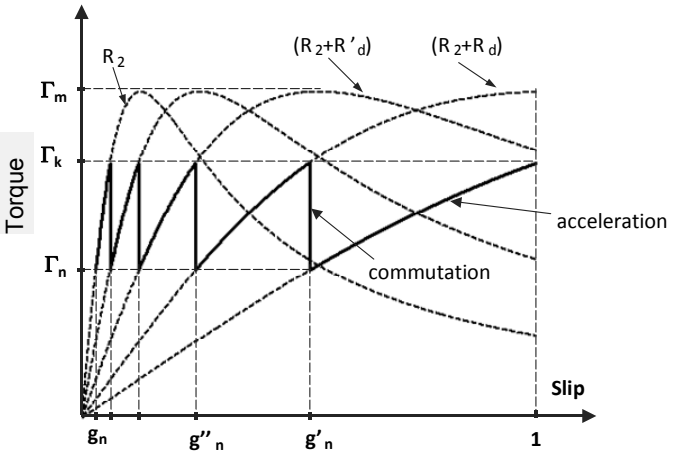

Figure 4.29. *Torque variation at starting*

4.9.1.2. *Variable voltage and fixed frequency supply*

We shall see in the following (section 4.9.1.3) that the most effective way to vary the speed of an induction motor consists of varying the frequency of the supply. However, for small power and low cost applications, another solution consists of varying the rms value of the supply voltage only.

In order to grasp the principle of this approach, it is suitable to refer to the torque-slip characteristic of the

machine (equation [4.19] and Figure 4.13). If it is assumed that, for example, the motor drives a load of torque $\Gamma_C(g)$, the working point will be at the stable intersection of those two characteristics (Figure 4.14). If these characteristics are drawn for various values of V_1, a family of curves $\Gamma(g)$ deduced by homothetic transformation and with their maxima for the same value g_m of g is obtained (Figure 4.30). Their intersections with torque Γ_C line therefore correspond to slips g, g', g", etc. which are larger when voltage V_1 is small. It is therefore possible in this way to vary, in a relatively small range, the induction motor speed. In order for this range to be as wide as possible, it is advisable to use motors with their maximum torque Γ_m for important values of the slip. Their rotor resistance R_2 therefore has to be significant. For this kind of application, machines with highly resistive cages are therefore used.

This variable voltage power supply is usually made using a 3-phase electronic AC power controller (Figure 4.31).

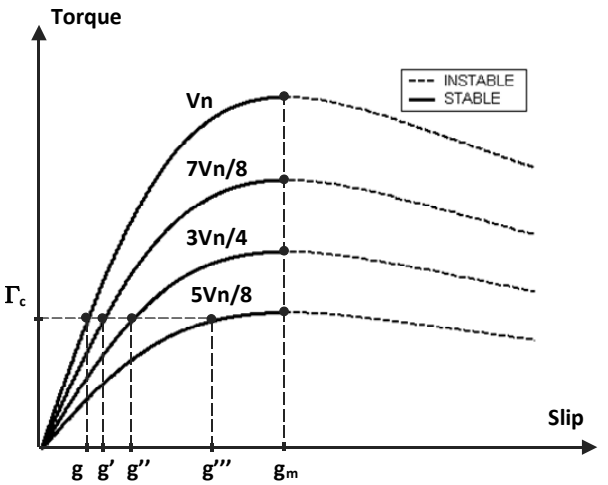

Figure 4.30. *Torque-slip characteristic for various stator voltages*

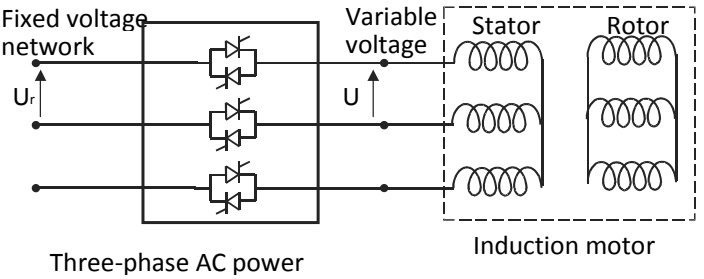

Figure 4.31. *3-phase electronic AC power controller supply*

It will be noted that, as this speed variation is based on a slip increase, it leads to a considerable decrease of efficiency η since $\eta < (1 - g)$. Moreover, electronic AC power controller supply generates non-sinusoidal currents, and harmonics contribute still further to reduce efficiency. That is why this way is only used for small power cage induction motors, destined to low-cost applications: pumps, fans, etc.

4.9.1.3. *Variable frequency and voltage supply*

This is the most modern and the most high-performance method of induction machine implementation. It was made possible by the emergence of voltage source inverters (Figure 4.32) at the end of the 1960s, then by their continued increase in power and performance. The principle of this implementation mode of induction motors follows from the expression:

$$\Omega = (1 - g)\frac{\omega}{p}$$

which shows that, if the slip is small, the speed is almost proportional to the stator angular frequency, and therefore to the frequency.

In supplying the stator with variable frequency voltages, it is therefore possible to control the machine speed. It is

however advisable to make these voltage amplitudes vary according to frequency.

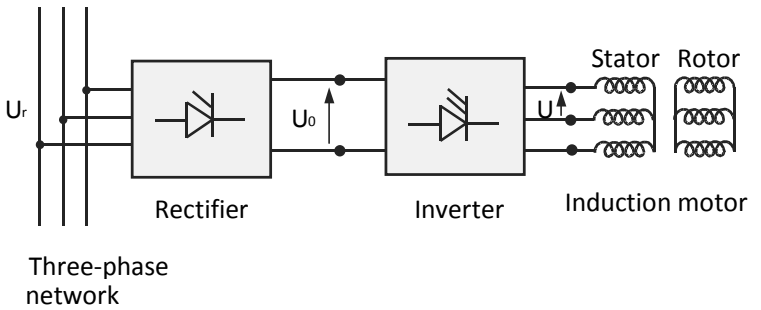

Figure 4.32. *Variable frequency drive*

We shall, in the following, first deal with the problem using a simplified approach overlooking the stator resistance.

4.9.1.3.1. Constant V_1/f supply

If R_1 is neglected, impedance $\bar{Z}_1$ is written:

$$\bar{Z}_1 = jL_1\omega + \frac{M^2\omega^2}{R_2/g + jL_2\omega} = (jL_1 + \frac{M^2}{R_2/\omega_r + jL_2})\omega$$

with $\omega_r = g\omega$.

The expression of the absorbed stator current can therefore be deduced:

$$\bar{I}_1 = \frac{V_1}{\omega} \frac{1}{jL_1 + \frac{M^2}{R_2/\omega_r + jL_2}} \qquad [4.27]$$

This expression shows that if a constant ratio V_1/ω is imposed when frequency varies, the current absorbed at the stator depends only on rotor angular frequency ω_r.

4.9.1.3.2. Circular diagram

Expression [4.27] defines, for a stator current, a Möbius function of variable ω_r in the complex plane. The extremity N of the vector with the affix $\bar{I}_1$ therefore describes a circle when ω_r varies from $-\infty$ to $+\infty$. This circle is centered on the imaginary axis in the middle Ω of segment N_0N_∞, points respectively corresponding to the rotor angular frequencies $\omega_r = 0$ and $\omega_r \to \infty$ (Figure 4.33).

This circle can, in the same way as the standard circle diagram, represent the powers exchanged with the source and the electromagnetic torque Γ. The result in particular is that segment nN represents both the absorbed active power and the torque. It is therefore deduced that characteristic $\Gamma(\omega_r)$ is unique. We have:

$$\Gamma = 3p\left(\frac{V_1}{\omega}\right)^2 \frac{R_2^{'}/\omega_r}{\left(R_2^{'}/\omega_r\right)^2 + \left(N_2^{'}\right)^2} \qquad [4.28]$$

The torque goes through a maximum (Figure 4.34) given by:

$$\Gamma_{max} = 3p\left(\frac{V_1}{\omega}\right)^2 \frac{1}{2N_2'}$$

for:

$$\omega_{rm} = \frac{R_2'}{N_2'} = \frac{R_2}{N_2}$$

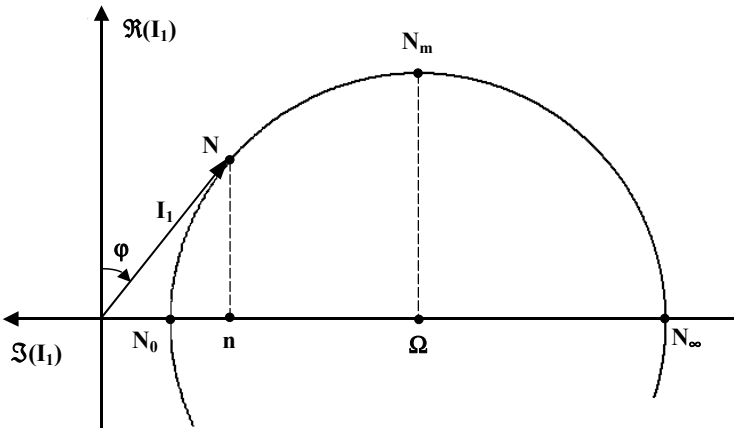

Figure 4.33. *Circular diagram of the stator current: V/f constant and ω_r variable*

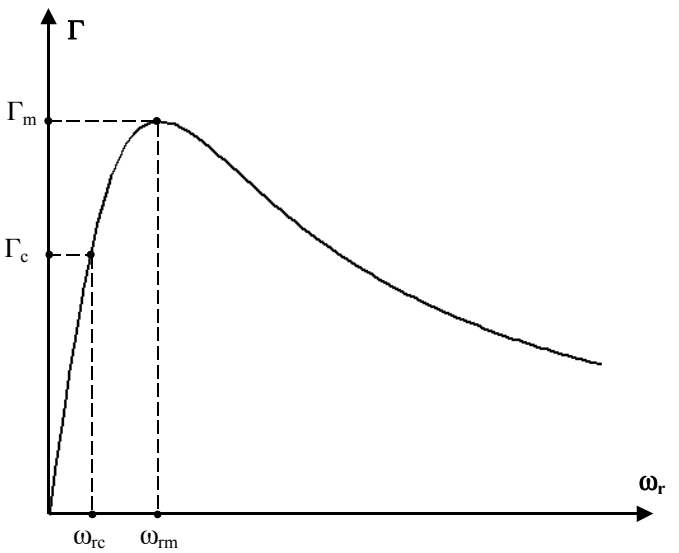

Figure 4.34. *Torque variation in terms of the rotor angular frequency. Supply at constant V/f*

Characteristic $\Gamma(\omega_r)$ being unique, load torque Γ_C fixes a value ω_r, and therefore one and only current I_1, regardless of

the frequency. This approach led to the development of rustic, sturdy variable speed drives that are satisfying when considerable dynamic performances are not sought.

However it is advisable to underline the limits of this study:

– first, it calls for a "permanent state" type model of the induction machine, which restricts its validity to slow frequency variations;

– then, the simplifying hypothesis, consisting of neglecting the stator resistances, is valid only for quite high frequencies. For low frequencies (particularly at starting), it is advisable to modify slightly the variation law of V_1 in terms of the frequency, in order to compensate the voltage drops due to the stator impedances. It is then called "constant flux" supply.

4.9.1.3.3. Introduction to vector control

The previous study (constant V/f or constant flux supply) is a matter for an "open loop" approach to speed variation, an approach from which it would be unrealistic to expect great accuracy and considerable dynamics. If this kind of performance is sought, it is necessary to rely on another theoretical approach, based on the exploitation of the induction machine transient equations (Park equations). Very high-performance speed and current regulations can then be developed, using pulse width modulation inverters (PWM) and digital control.

The principle of this implementation is represented by Figure 4.35 where Ref Ω and Ref I respectively represent the desired speed and the maximum admissible current. These systems, called "vector control drives", have been the subject of an abundant scientific literature over the past years. Their study goes beyond the scope of this book.

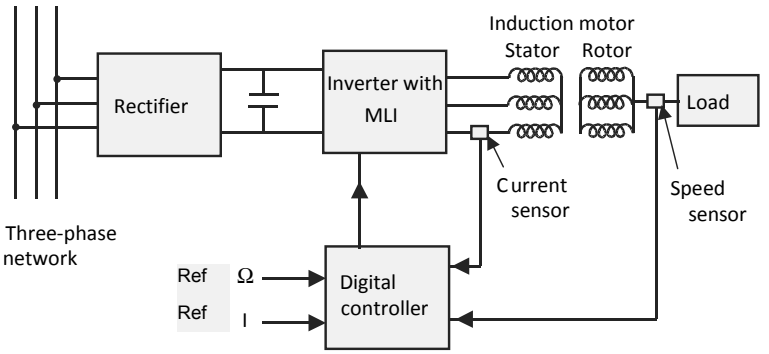

Figure 4.35. *Structural diagram of a vector-controlled induction machine*

4.9.2. *Generator mode*

Induction machines are mainly used as motors but, as with all rotating machines, they are reversible. Their use as generators has shown an increase in interest for a few years, particularly for the use of renewable energies such as wind energies.

4.9.2.1. *Induction generator connected to a network*

When an induction machine is connected to an electrical power network, the circle diagram is, as we have already seen, a good tool for a qualitative analysis.

Considering the diagram in Figure 4.36, it is clear that when the machine works with a negative slip (that is to say at a speed $\Omega > \Omega_s$) corresponding for instance to point M', the active power represented by $\overline{mM'}$ is negative. Angle φ is greater than $\pi/2$ and the electromagnetic torque (also represented by $\overline{mM'}$) is negative. All this characterizes a generator mode for which the machine absorbs the mechanical power (represented by $\overline{PM'}$) and supplies the network with electrical power (represented by $\overline{mM'}$).

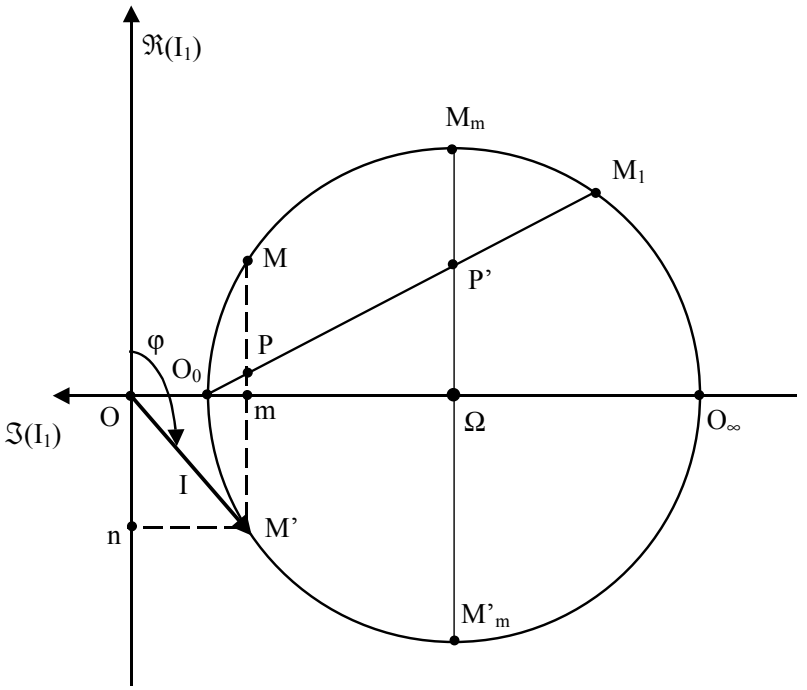

Figure 4.36. *Simplified circle diagram. Induction generator mode*

This diagram also makes a fundamental aspect of the induction machine appear: the reactive power represented by $\overline{Om} = \overline{nM'}$ had to be supplied to the machine for generator mode and for motor mode.

This operating mode is used to recover energy for cyclic working devices, for example service elevators: the induction machine operates as a motor on the way up and as a generator on the way down. On a way up-way down cycle, the overall energy consumption thus only represents losses.

Induction generators are also used in "micro-power plants" when the presence of a watercourse or of other primary energies (particularly wind energies) enables us to drive machines and supply the network.

4.9.2.2. *Self-excited induction generator*

The induction machine, unlike the synchronous machine, has no field winding; therefore it can produce energy only if an external source provides it with the reactive power needed for its magnetization. In isolated mode, this source is made of a capacitor bank C connected to the terminals of the stator windings (Figure 4.37).

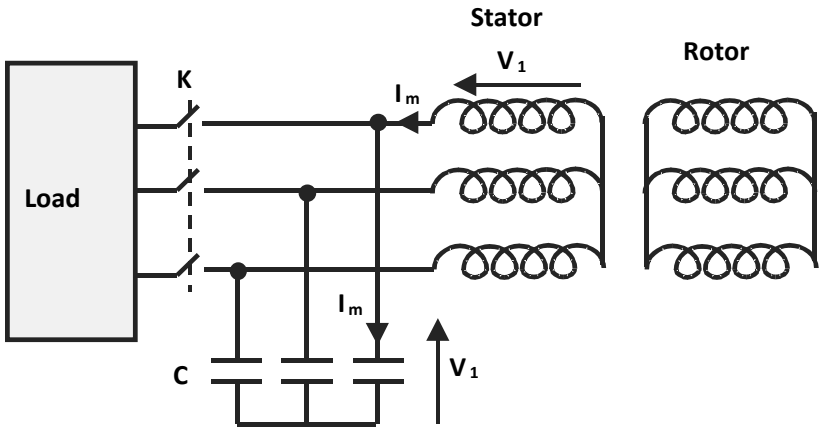

Figure 4.37. *Self-excited induction generator*

When the load is zero (switch K open), the equivalent diagram per phase is given in Figure 4.38.

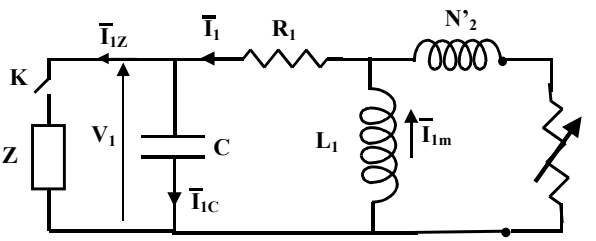

Figure 4.38. *Per phase equivalent circuit of a self-excited induction generator*

In driving the rotor at speed Ω, the self-voltage build-up is possible if capacitor C provides a reactive energy Q_C equal to the sum of Q_{L1} and $Q_{N'2}$ absorbed by inductances L_1 and N'_2. If the voltage drop in stator resistance R_1 is neglected, Q_C and Q_{L1} can be written in terms of V_1:

$$Q_C = \frac{1}{2} C\omega V_1^2 \qquad Q_{L1} = \frac{1}{2} \frac{V_1^2}{L_1\omega}$$

$Q_{N'2}$ is usually small, hence the necessary condition of no-load self-voltage build-up:

$$Q_C > Q_{L1}$$

which leads to $L_1C\omega^2 > 1$. The minimum values of C in terms of L_1 can thus be determined. Angular frequency ω is almost equal to pΩ.

In order to explain the self-voltage build-up phenomenon, it is necessary to take into account the saturation as well as the remanence field in the magnetic circuit. Those phenomena are complex, and we shall restrict to qualitative explanations in the following analysis.

Figure 4.39 shows that when the machine is driven by an external device, the remanence field of the rotor generates an emf V_R at the terminals of each stator phase, leading to the creation of a reactive current I_{m0}. This magnetizing current increases the flux in the machine, which increases the voltage of phase V_1. In a no-load state, the modulus of V_1 is related to the magnetizing current I_m through the specific internal magnetic characteristic of the machine $V_1(I_m)$ (Figure 4.39, curve a), and also through external characteristic $V_1 = \frac{I_m}{C\omega}$ (curve b_1). The operating point is therefore obtained by the intersection of these two characteristics.

Figure 4.39, representing the evolution of current I_m during the self-voltage build-up, shows that the value of C can be chosen so that the working point corresponds to nominal voltage V_{1N} (curve b_1). It also shows that when the value of C is important (leading to a low slope of the external characteristic), the working point corresponds to a great voltage V_{12} that can be dangerous for the machine (curve b_2). It is furthermore deduced that if the value of C is too small, there cannot be any self-voltage build-up (curve b_3).

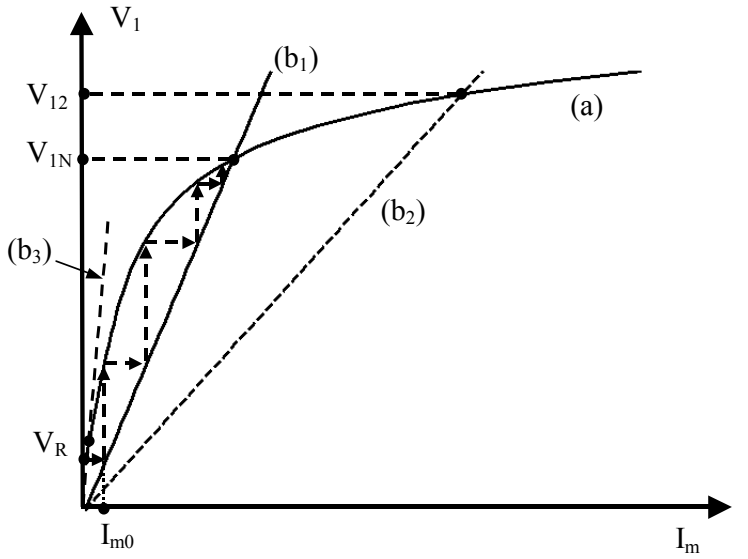

Figure 4.39. *Voltage build-up in a self-excited induction generator*

Let us consider the case when the generator supplies an inductive load Z (Figure 4.38, switch K closed). When the load increases, the capacitor value has to increase in order to maintain the desired frequency and voltage because, on the one hand, the reactive energy needed by the machine increases, and, on the other hand, C also has to provide the reactive energy for Z.

The value of the capacitor needed for the working can be obtained by writing the two equations relative to energy conservation:

– the reactive energy generated by the capacitor bank is equal to this absorbed by inductances L_1, N'_2 and the imaginary part of Z;

– active energy $\frac{R'_2}{g} I'^2_R$ is consumed in resistances R_1 and the real part of Z.

We shall not develop this calculation in this book.

Figure 4.40 shows, at a given frequency, the evolution of the phase voltage in terms of the active power P provided by the generator for various values of capacitor C, with $C_1 < C_2 < C_3$.

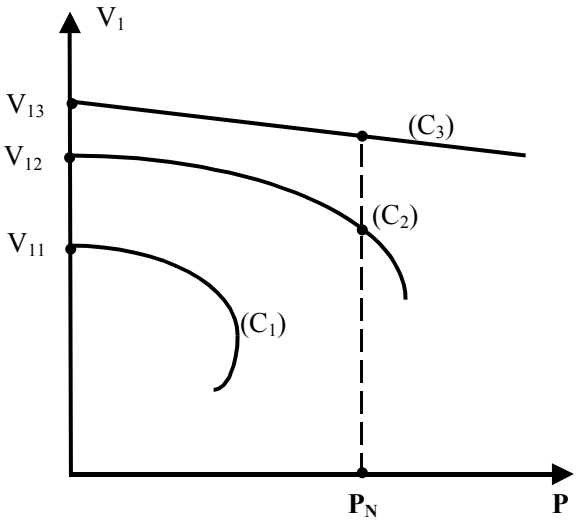

Figure 4.40. *Voltage-power characteristics for various capacitors ($C_1 < C_2 < C_3$)*

In order to maintain a fixed frequency when the load increases, that is to say when the slip increases, the generator speed Ω has to be increased slightly:

$$\Omega = (1 - g)\frac{\omega}{p} \qquad g<0$$

Note that when P increases, the voltage given by the machine decreases faster for smaller values of C. For a small capacitor value, for example C = C_1, note that power P goes through a maximum and then diminishes. In this case, if the call for power is maintained it can bring about the demagnetization of the generator and lead to its working stop.

Figure 4.40 also shows that, in order to regulate the voltage at the load terminals, when P increases, the reactive power issued by capacitor bank C has to increase.

4.9.2.3. *Doubly-fed induction machine*

So far we have considered that the rotor currents were induced in the short-circuited coils. It is obvious that for cage motors, there is no alternative, but for the wound rotor machines, it is possible to inject a 3-phase AC current system of fundamental frequency f_r into the rotor. These rotor currents are produced by an inverter working in pulse width modulation while the machine stator is connected to the network of angular frequency ω. It is then called a "doubly-fed induction machine" or a "DFIM" (Figure 4.41).

This system working principle and its uses can be deduced from expression [2.12], which is revised here:

$$\omega_s = \omega_r + p\Omega \text{ with } \omega = \omega_s$$

If ω is considered to be constant, we can note that in fixing angular frequency ω_r, speed $\Omega = \frac{\omega - \omega_r}{p}$ is set. This is used for quite economical rotation speed variators because the static converters only have to supply the rotor power.

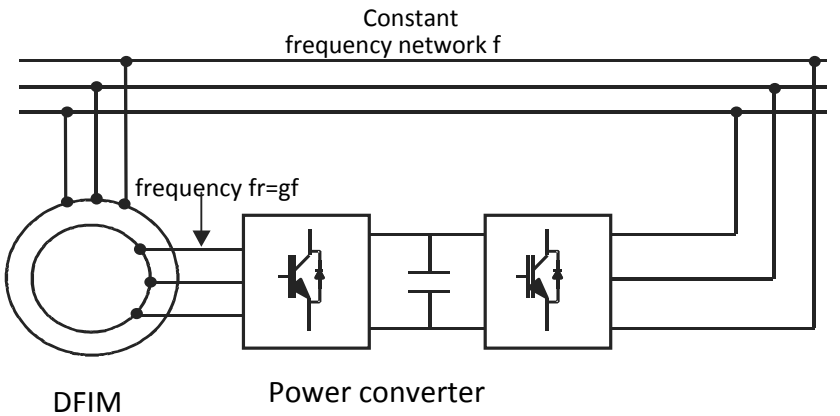

Figure 4.41. *Doubly-fed induction machine principle*

The main application of this drive is energy production made from wind energy. Indeed, in this case, rotation speed Ω is linked to the speed of the wind, and therefore is highly variable. If AC generators are used, the frequency of the obtained voltages is therefore also variable, which does not allow us to connect them directly to the network.

On the contrary, for the DFIM, the rotor windings only have to be supplied with an angular frequency $\omega_r = \omega - p\Omega$ in order to obtain the desired stator frequency regardless of the rotor rotation speed. It is therefore possible to connect the DFIM directly on the network.

Figure 4.42. *Doubly-fed induction machine wind turbine (parc de Bouin, Vendée, France). 2.5 MW, 660 V machines. The three-bladed turbine has a diameter of 80 m, and its speed is between 11 and 19 rpm. The generator rotation speed is near 1,500 rpm. The induction machine is connected to the blades by a mechanical device multiplying the speed*

4.9.3. *Single-phase induction motor*

When a 3-phase source is not available, single-phase induction motors are often called upon to drive small-power devices (pumps, fans, compressors, etc.).

4.9.3.1. *Structure*

A single-phase induction motor is a cage induction motor, for which the stator has the same structure as the stator of a 3-phase motor, but where only 2/3 of the slots are used to make a single-phase winding. The additional 1/3 enables the

winding of a so-called "auxiliary" phase, used for starting, as we shall see in the following.

In an initial analysis, a single-phase induction machine can be considered as a 3-phase machine supplied by a single-phase current at the stator with voltage U (Figure 4.43).

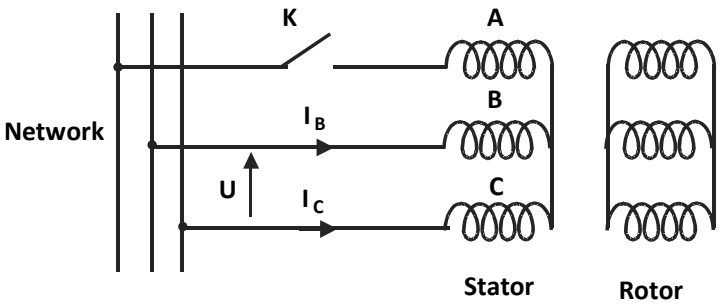

Figure 4.43. *Single-phase power supply of the induction machine*

4.9.3.2. *Equations*

According to the previous section, it can be considered, for example, that the current in phase A is equal to zero and that $\bar{I}_B = -\bar{I}_C = \bar{I}$. Furthermore it is also possible to write $\bar{U} = \bar{V}_B - \bar{V}_C$.

We are in the presence of a problem with an induction machine in an unbalanced operating mode, and Fortescue's symmetrical components method is very convenient for analyzing it (see section 1.2.4).

4.9.3.3. *Stator current calculation*

The stator supply voltage U is assumed to be known, and the machine impedances in direct, inverse and zero-sequence modes are called Z_d, Z_i and Z_o. We therefore have the six expressions, on the one hand:

$$\bar{I}_A = 0$$

$$\bar{I} = \bar{I}_B = -\bar{I}_C$$

$$\overline{U} = \overline{V}_B - \overline{V}_C$$

in the phase value scale, and on the other hand:

$$\overline{V}_d = -\overline{Z}_d \, \bar{I}_d$$

$$\overline{V}_i = -\overline{Z}_i \, \bar{I}_i$$

$$\overline{V}_0 = -\overline{Z}_0 \, \bar{I}_0$$

in Fortescue's component space.

It is advisable to incorporate the previous equations when using the passage expressions:

$$\begin{bmatrix} \overline{V}_A \\ \overline{V}_B \\ \overline{V}_C \end{bmatrix} = \begin{bmatrix} 1 & 1 & 1 \\ 1 & a^2 & a \\ 1 & a & a^2 \end{bmatrix} \begin{bmatrix} \overline{V}_o \\ \overline{V}_d \\ \overline{V}_i \end{bmatrix} \quad \text{and} \quad \begin{bmatrix} \bar{I}_A \\ \bar{I}_B \\ \bar{I}_C \end{bmatrix} = \begin{bmatrix} 1 & 1 & 1 \\ 1 & a^2 & a \\ 1 & a & a^2 \end{bmatrix} \begin{bmatrix} \bar{I}_o \\ \bar{I}_d \\ \bar{I}_i \end{bmatrix}$$

We therefore obtain:

$$\begin{aligned} \overline{U} &= (a^2 - a)(\overline{V}_d - \overline{V}_i) \\ \bar{I}_0 &= 0 \\ \bar{I}_d &= \bar{I}_i \end{aligned} \qquad [4.29]$$

After calculation, the three currents and the three voltage expressions in Fortescue's space are deduced:

$$\begin{cases} \bar{I}_0 = 0 \\ \bar{I}_d = -\bar{I}_i = \dfrac{\overline{U}}{(a^2 - a)(\overline{Z}_d - \overline{Z}_i)} \end{cases} \qquad [4.30]$$

$$\begin{cases} \overline{V}_0 = 0 \\ \overline{V}_d = \overline{Z}_d \dfrac{\overline{U}}{(a^2 - a)(\overline{Z}_d - \overline{Z}_i)} \\ \overline{V}_i = \overline{Z}_i \dfrac{\overline{U}}{(a^2 - a)(\overline{Z}_d - \overline{Z}_i)} \end{cases} \quad [4.31]$$

If the inverse transformation is used to calculate the phase values, we finally obtain:

$$\bar{I} = \frac{\overline{U}}{\overline{Z}_d - \overline{Z}_i} \quad [4.32]$$

This expression enables us to calculate the absorbed stator current, providing $\overline{Z}_d$ and $\overline{Z}_i$ are known.

4.9.3.4. *Positive and negative sequence impedances of the induction machine*

$\overline{Z}_d$ and $\overline{Z}_i$ are, by definition, the impedances presented by the induction machine to respectively positive and negative sequence current systems. The words “positive sequence” and “negative sequence” can be interpreted in relation to the rotor rotation direction.

It is therefore possible, by respectively naming g_d and g_i the rotor slips corresponding to the positive sequence and negative sequence rotating fields, to write:

$$g_d = g \qquad \text{and} \qquad g_i = 2 - g$$

If the phase impedance expression is considered again, we obtain:

$$\overline{Z}_d = \overline{Z}(g) = (R_1 + jL_1\omega) + \frac{M^2\omega^2}{R_2 / g + jL_2\omega} \quad [4.33]$$

$$\overline{Z}_i = \overline{Z}(2-g) = (R_1 + jL_1\omega) + \frac{M^2\omega^2}{R_2 /(2-g) + jL_2\omega} \quad [4.34]$$

If these expressions are transferred into expression [4.32], the variation of stator current I in terms of slip g can be deduced.

4.9.3.5. *Single-phase induction machine torque*

The single-phase induction machine torque is the resultant of torque Γ_d due to the positive sequence currents component and to torque Γ_i linked to the negative sequence component. Γ_i is a braking torque:

$$\Gamma = \Gamma_d - \Gamma_i = \Gamma(g) - \Gamma(2-g)$$

In referring to expression [4.19] and to Figure 4.12, we get:

$$\Gamma_d = \frac{3p}{\omega} \frac{\dfrac{R_2'}{g}}{\left(\dfrac{R_2'}{g}\right)^2 + \left(N_2'\omega\right)^2} V_d^2 \quad [4.35]$$

$$\Gamma_i = \frac{3p}{\omega} \frac{\dfrac{R_2'}{(2-g)}}{\left(\dfrac{R_2'}{(2-g)}\right)^2 + \left(N_2'\omega\right)^2} V_i^2 \quad [4.36]$$

If expressions [4.35] and [4.36] in connection with [4.31], [4.33] and [4.34] are considered, it is clear that torque Γ has a symmetrical formulation in terms of g and (2 – g). The characteristic of Figure 4.44 shows the variation in terms of the slip of positive sequence and negative sequence torques. The resultant torque can then be deduced. This characteristic $\Gamma(g)$ emphasizes:

– the symmetry in terms of the point corresponding to g = 1. The motor therefore has no favorite rotation direction;

– the cancellation of the torque for two values of the slip, one slightly below 0, and the other, worth 2;

– a value of the torque developed by the single-phase motor, for a given slip, smaller than this of the 3-phase motor;

– cancellation of the resultant torque for g = 1. The single-phase asynchronous motor therefore does not start by itself. Specific methods are needed for it to start.

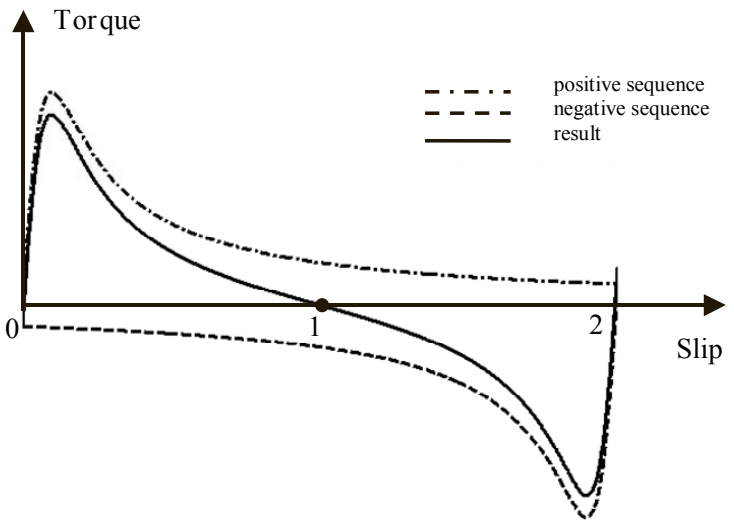

Figure 4.44. *Single-phase induction machine torque*

4.9.3.6. *Capacitive single-phase motor*

The stator winding of the single-phase induction machine usually takes only 2/3 of the slots. It is therefore possible to use the remaining slots to make an auxiliary coil P_A shifted of $\pi/2$ electrical in terms of the main winding called P_P.

In supplying the main winding with a single AC current I_{pp}, the motor cannot start because the corresponding field is pulsating. We then seek to generate a rotating field in the motor in supplying simultaneously P_A and P_P, so that current I_{pa} in the auxiliary winding is shifted from I_{pp}.

This phase-shift can be obtained by adding an impedance in series with the auxiliary winding. This impedance can be, in some cases, a resistance or an inductance, but a capacitor is usually used.

The aim is to obtain (or to approach) the equivalent of a balanced 2-phase motor that produces a circular rotating field. Coils P_P and P_A being shifted in space of $\pi/2$ electrical, it would be necessary that for all the rotation speeds, magnetomotive forces $N_{pp}I_{pp}$ and $N_{pa}I_{pa}$ (N_{pp} and N_{pa} respectively being the number of turns of phases P_P and P_A) are equal and shifted in time of $\pi/2$ electrical. This constraint is very hard to achieve in practical terms.

Let us consider the diagram of the capacitive motor given by Figure 4.45a. Voltage V_1 is applied to main phase P_P and to auxiliary phase P_A in series with capacitor Cp.

When speed varies the impedances of coils P_P and P_A also vary, leading to the variations of the magnitudes and the phases of currents I_{pa} and I_{pp}. Thus, for example, if a value of C provides a circular rotating field at the start of the motor is chosen, the mmf $N_{pp}I_{pp}$ and $N_{pa}I_{pa}$ will no longer be equal and shifted by $\pi/2$ electrical for a speed that is different from zero. For this speed, the corresponding field would therefore

not be circular. It is called elliptic, because the locus of the vector representing at every instant the maximum field is an ellipse.

The elliptic field can be broken into two circular fields rotating in opposite directions. The field rotating in the positive sequence direction (rotation direction) produces the useful torque while the negative sequence field generates a harmful braking torque.

Single-phase induction motors are used to drive devices for which power usually does not go over a few kW. Permanent capacitor motors Cp (Figure 4.45a), start capacitor motors Cd (Figure 4.45b) or start capacitor and permanent capacitor motors (Figure 4.45c) are encountered.

The standard permanent capacitor motor is reserved for small-power uses enabling a starting torque smaller than the nominal torque. The auxiliary phase is permanently in series with capacitor Cp.

In order to increase the starting torque, a capacitor of larger capacity is used for an “intermittent duty”. When speed reaches about 2/3 of the nominal speed, a centrifugal contactor K (or electric relay) connected in series with the auxiliary phase opens and cuts the starting circuit. The nominal working is then solely single-phase (only one coils is power-supplied) and characterized, as we have seen previously, by the presence of an inverse braking torque and a poor power factor.

At the same time, in order to improve the starting torque, the power factor and the efficiency, start capacitor and permanent capacitor motors (Figure 4.45c) are adopted. At the start, the two capacitors Cd and Cp are connected in parallel and the total capacity (Cd + Cp) is chosen so that the motor produces a torque about twice the nominal torque.

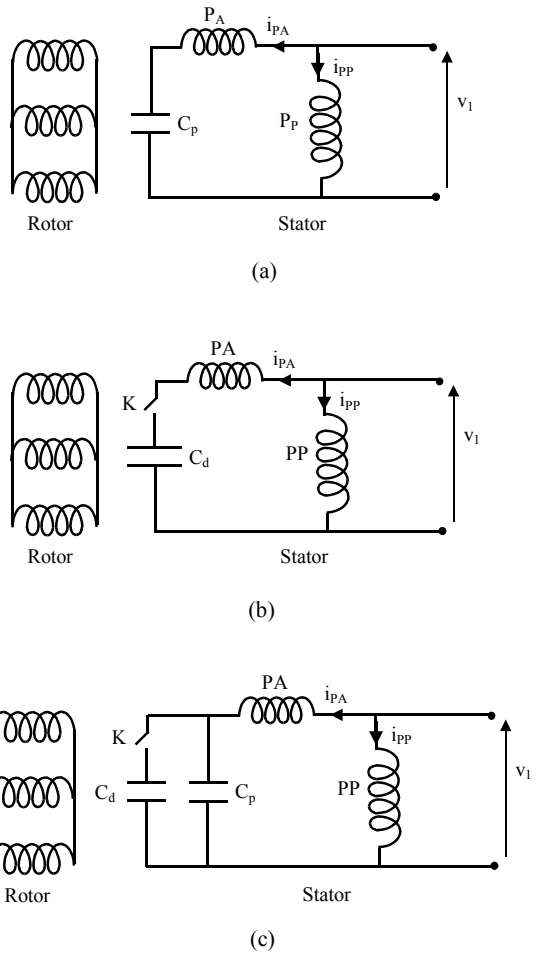

Figure 4.45. *Single-phase motor: a) permanent capacitor; b) start capacitor; c) permanent capacitor and start capacitor*

After the start, the "intermittent" capacitor Cd is disconnected beyond a particular speed thanks to Switch K. Permanent capacitor Cp is chosen so that the permanent working is almost of the same as a balanced two-phase motor characterized by a small slip (that is to say a good efficiency) and a good power factor.

For these three kinds of motors, the inversion of the rotation direction is obtained by changing the connections of one phase.

4.10. Principle of the experimental determination of the parameters

The determination of the parameters appearing on the equivalent diagrams is necessary for the predetermination of the machine characteristics. This determination is quite different depending on whether it is a wound rotor induction machine or a cage induction machine, especially concerning the rotor parameters. Let us consider the equivalent figure given in Figure 4.46. This corresponds to Figure 4.10a to which a resistance R_f representing the iron losses is added.

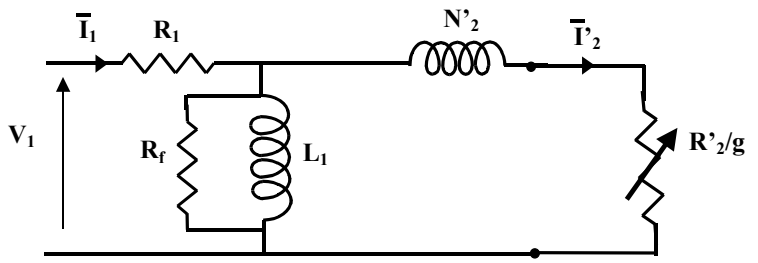

Figure 4.46. *Equivalent diagram per phase including iron losses*

4.10.1. *Case of wound rotor induction machines*

In this case, all the parameters can be obtained through direct measurement. Stator and rotor resistances are measured in DC current using an "ammeter-voltmeter" method (nominal temperature and current).

Stator leakage inductance L_1 can be measured directly by leaving the rotor circuit open. It is usually preferable to make a no-load test, with a "zero" slip motor.

Voltage and phase current V_{10} and I_{10}, are measured as well as active and reactive powers P_{10} and Q_{10} absorbed by the machine. L_1 and R_f are then deduced using:

$$L_1 \approx \frac{3V_{10}^2}{\omega Q_{10}} \qquad \text{and} \qquad R_f \approx \frac{3V_{10}^2}{P_{10}}$$

In the same way, inductance L_2 can be obtained via a test by supplying the rotor with a 3e-phase system, when the stator is in open circuit. The value of the induced voltage on the non-supplied side gives two measurements of the "transformation ratio", $\frac{M}{L_1}$ or $\frac{L_2}{M}$, enabling us to determine M.

4.10.2. *Case of cage induction machines*

It is neither possible to directly access the rotor parameters nor to leave the rotor in open circuit. Stator resistance R_1 is measurable directly in DC current, and inductance L_1 is deduced from a no-load test (g ~ 0).

As for the wound rotor induction machine, L_1 and R_f are determined from the measurement of voltage and phase current, V_{10} and I_{10}, and from the active and reactive powers P_{10} and Q_{10} absorbed by the machine.

Concerning the rotor parameters, determination can only be indirect. A test with a locked rotor (g = 1), under reduced voltage, enables (knowing L_1 and R_1 which can often be neglected) us to determine elements $N'_2\omega$ and R'_2 appearing on the equivalent diagram of Figure 4.46. With g = 1, it can indeed be admitted that:

$$N_2'\omega \approx \frac{Q_{1c}}{3I_{1c}^2} \qquad \text{and} \qquad R_2' \approx \frac{P_{1c}}{3I_{1c}^2} - R_1$$

I_{1c}, P_{1c} and Q_{1c} are respectively the current and the active and reactive powers absorbed by the machine.

Chapter 5

Direct Current Machines

5.1. Introduction

The so-called “direct current machines” are electromechanical energy converters in which the electrical energy is exchanged with their environment (supply or load) under the form of direct voltages and currents. This is possible due to the brush-commutator systems which plays the part of a “mechanical rectifier”. That is the reason why these machines are sometimes called “commutator machines”.

Like all rotating machines, DC machines are reversible and can operate as a motor or as a generator (they are sometimes called “dynamos” in this case). However it can be noted that the development of power electronics, and particularly of diode and thyristor rectifiers, from the 1960s onwards, has gradually marginalized the use of DC generators. Today the generator function of these machines is restricted to the recovery of kinetic energy during braking and slowing down, we shall therefore focus this chapter on the motor mode.

5.2. Main notations

In the remainder of this chapter, we shall allot the index "1" to the field system, and the index "2" to the armature. We shall also set down:

– e: air-gap thickness;

– E: electromotive force;

– J: moment of inertia of all of the rotating parts;

– L_i: self inductance of the winding i;

– M: mutual inductance between the field system and the armature;

– R_i: resistance of the winding i;

– U: supply voltage;

– μ_0: free space permeability ($\mu_0 = 4\pi\ 10^{-7}$ H/m);

– Ω: angular speed of the rotor;

– Γ: machine torque;

– Γ_C: "load" torque.

5.3. DC machine structure

5.3.1. *Constituents*

Figure 5.1 represents a bipolar DC machine. It is composed of:

– a solid stator bearing a field system, usually a salient-pole system. It bears the field coil intended to produce the excitation magnetic field. Each pole is made of a core and of a pole shoe allowing the concentration of the field along the air-gap. For small machines, the excitation field coil is sometimes replaced by permanent magnets;

– a non-salient laminated rotor bearing the armature winding. The armature conductors are set down in slots and linked so that they make an unbroken winding fully closed on itself;

– a commutator rotating with the rotor and made of conductive segments insulated from one another. The armature conductors are linked to the commutator segments;

– fixed brushes rubbing on the commutator segments and making up the armature terminals (Figure 5.2).

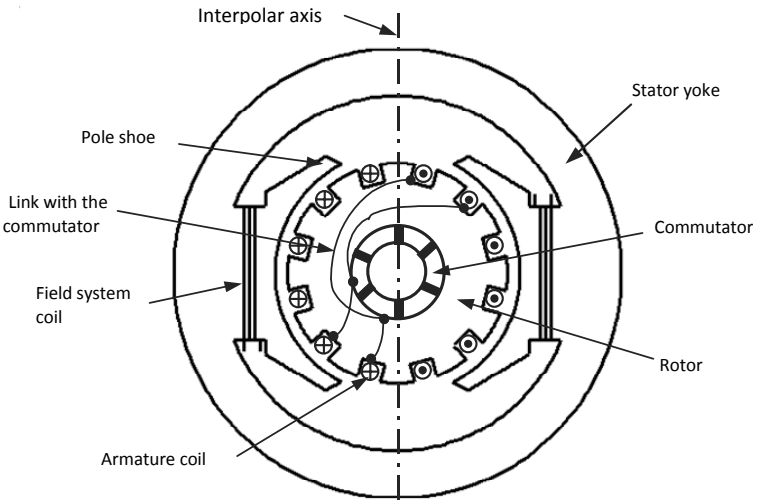

Figure 5.1. *Bipolar DC machine*

The brush-commutator set allows the selection of the armature coils so that the "outward" conductors are separated from the "return" conductors by the stator interpolar axis (Figure 5.1). We shall demonstrate later on in this chapter that this spatial distribution of the currents is fixed during the rotation, and that the armature winding can be modeled by a fixed axis stationary coil.

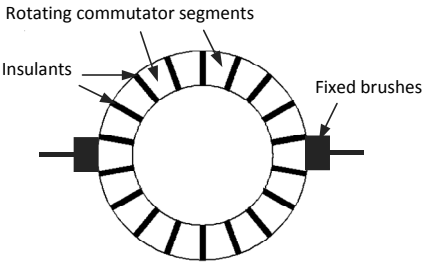

Figure 5.2. *Brushes-commutator set*

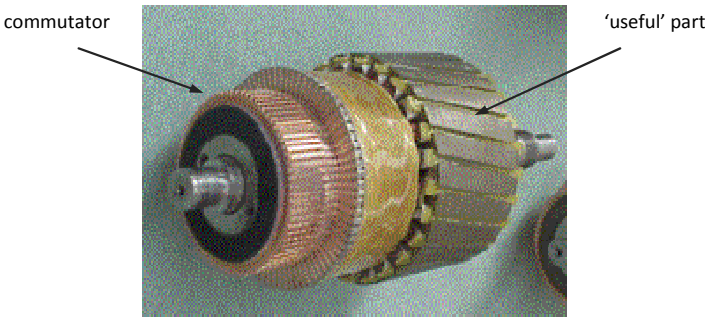

(a)

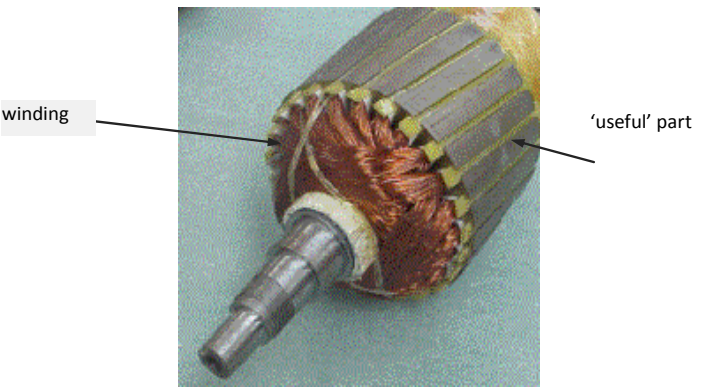

(b)

Figure 5.3. *Armature of a DC machine, 180 W, 960 rpm: a) commutator side, b) end windings side (ECA EN document)*

Figures 5.3a and b show the rotor of a small DC machine. Note that the "useful" length of the conductors is quite small compared to the overall length because of the size of the end winding and of the commutator.

Figure 5.4 shows the brushes and the commutator of a four-pole machine. Note the important length of the commutator segments; the brush-commutator contact surface indeed has to be enough in order to limit the current density going through them.

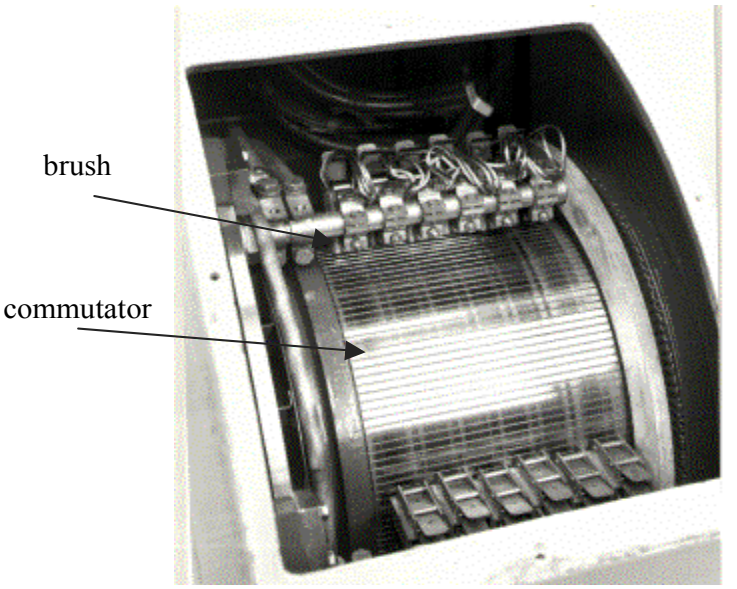

Figure 5.4. *Brush-commutator set. Note the important length of the commutator segments. To allow a good contact quality, the brushes are divided in several parts (ECA EN document)*

Figure 5.5 shows the arrangement of the outward and return conductors in the armature slots of a four-pole machine.

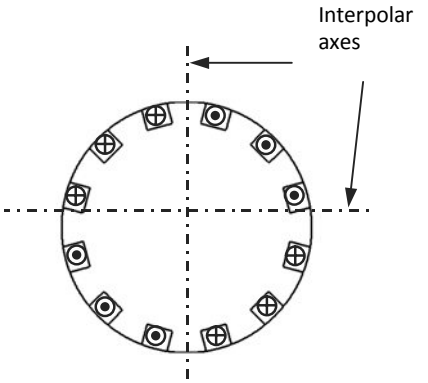

Figure 5.5. *Armature of a four-pole machine*

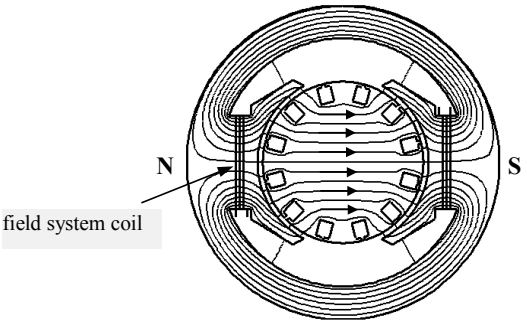

Figure 5.6. *Field lines. Bipolar machine*

5.3.2. *Analysis of the field winding*

Figure 5.6 shows the field lines obtained when only the field winding is supplied. These lines rotate around excitation currents; they cross the air-gap, then the rotor, and finally close through the stator. We can observe that on a first approximation, these lines only cross the part of the air-gap, of small thickness e, located under the pole shoes.

Figure 5.7a shows the variation of the normal flux density along the air-gap. The origin $\theta = 0$ corresponds to the

interpolar axis. The influence of the slots is observed but it can be admitted in a first approximation that the flux density is constant over the whole width of a pole (Figure 5.7b) and is zero around the interpolar axis. It is assumed to be positive under a north pole, and negative under a south pole.

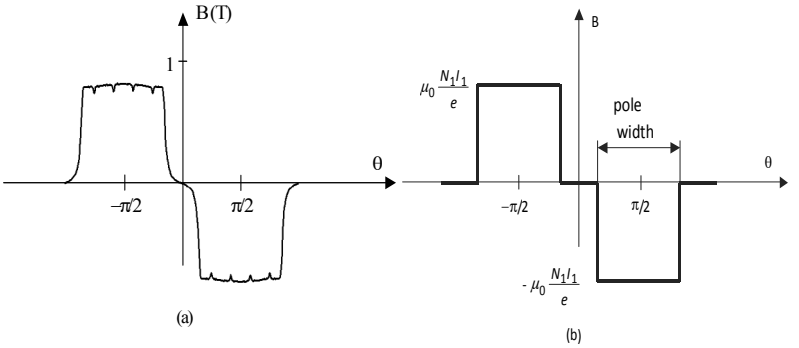

Figure 5.7. *Normal flux density in the air-gap: a) finite element calculation; b) simplified form*

The Ampere theorem used along any field line (closed circuit (c)) is written:

$$2N_1 I_1 = \oint_{(c)} \vec{H} d\vec{l} = \int_{(air-gap)} \vec{H} d\vec{l} + \int_{(iron)} \vec{H} d\vec{l}$$

where N_1 is the number of turns per pole, and I_1, the field current.

The magnetic field circulation along the air-gap is always dominating compared to the magnetic field in the iron side, particularly when the magnetic circuit is not saturated. Furthermore, along the air-gap, the normal flux density can be considered to be constant since the air-gap is very small (a few millimeters for the most important machines). It can therefore be written:

$$B = \mu_0 H = \mu_0 \frac{N_1 I_1}{e}$$

where e is the air-gap thickness, and μ_0, the free space permeability. The normal flux density is usually between 0.7 and 1 T.

5.3.3. *Analysis of the armature winding*

The armature winding is obtained by connecting in series and/or in parallel several "coil sections". One coil is made of several insulated conductors connected in series (Figure 5.8a). The active part, with a useful length L, is distinguished from the end windings. Figure 5.8b shows its schematic representation. The armature winding can be wound in a complex way, but we shall consider only the simplest windings, which can be "lap windings" or "wave windings" (Figures 5.9 and 5.10).

Figure 5.9a shows a lap winding made of the series connection of two identical coil sections. It is preferred to represent it as if each section had only one turn (Figure 5.9b). Figure 5.10 shows the series connection of two coil sections in order to make a wave winding.

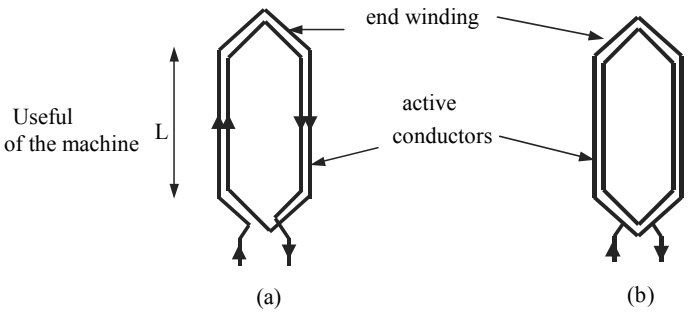

Figure 5.8. *a) 2-turn coil section; b) simplified representation*

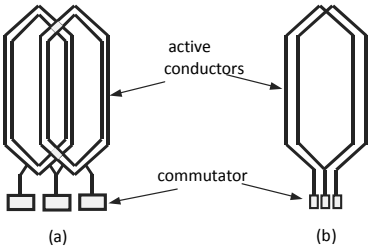

Figure 5.9. *Lap winding: a) series connection of 2 coil sections, b) simplified representation*

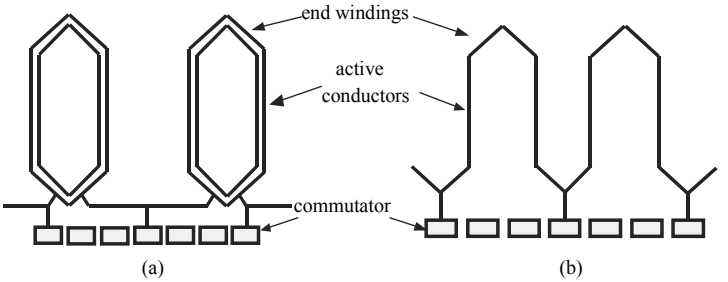

Figure 5.10. *Wave winding: a) series connection of 2 coil sections; b) simplified representation*

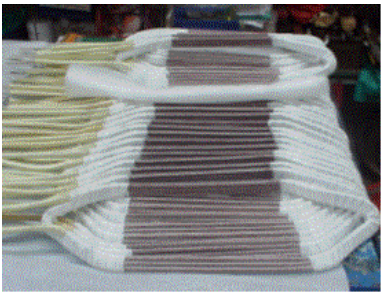

Figure 5.11. *Coil sections for a 155 kVA machine; useful length: 150 mm (ECA EN document)*

Let us consider the armature of the machine in Figure 5.1, with 12 slots. In a real winding, each slot has at least

two independent bundles of conductors. In order to simplify the study, we shall assume that a slot has only one bundle of conductors crossed by the same current. Its commutator then has only 6 segments.

Figure 5.12 represents the corresponding lap winding, presented in a developed form. In motor operating, a direct voltage is applied to the terminals of the two brushes and generates a current I that crosses segment A of the commutator, divides into two "ways" (pairs of armature circuits in parallel) and comes back through segment D. Each conductor bundle is therefore crossed by current I/2. The adjacent conductors located in slots 1 to 6 are thus crossed by "positive" currents while slots 7 to 12 carry the return conductors crossed by "negative" currents.

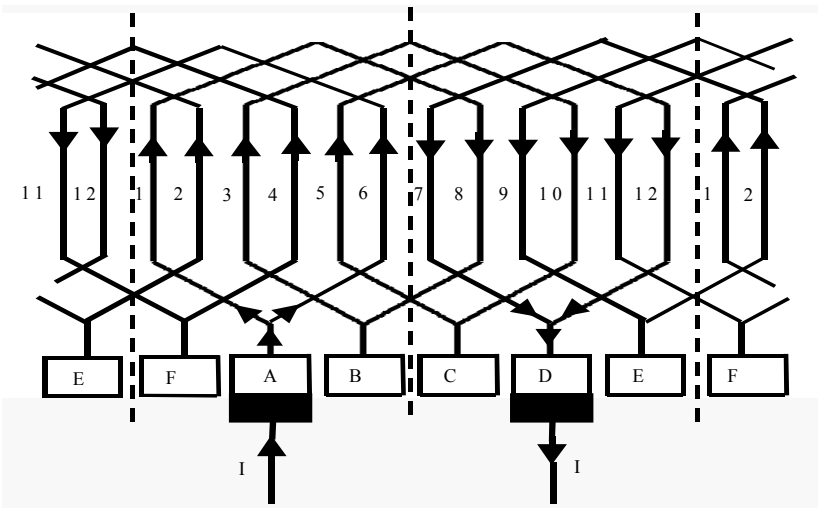

Figure 5.12. *Simplified lap winding, 12 slots, 2 poles, 2 "ways", 6 commutator segments*

The position of the stator poles in terms of the armature conductors is specified in Figure 5.13 for two positions of the rotor. For both positions we can notice that the current is the

same in the rotor slot conductors in front of each stator pole. In the position given by Figure 5.13b, current I crosses commutator segment F and comes back via segment C. Slots 5 to 10 then contain the return conductors; the outward conductors are therefore located in the other slots.

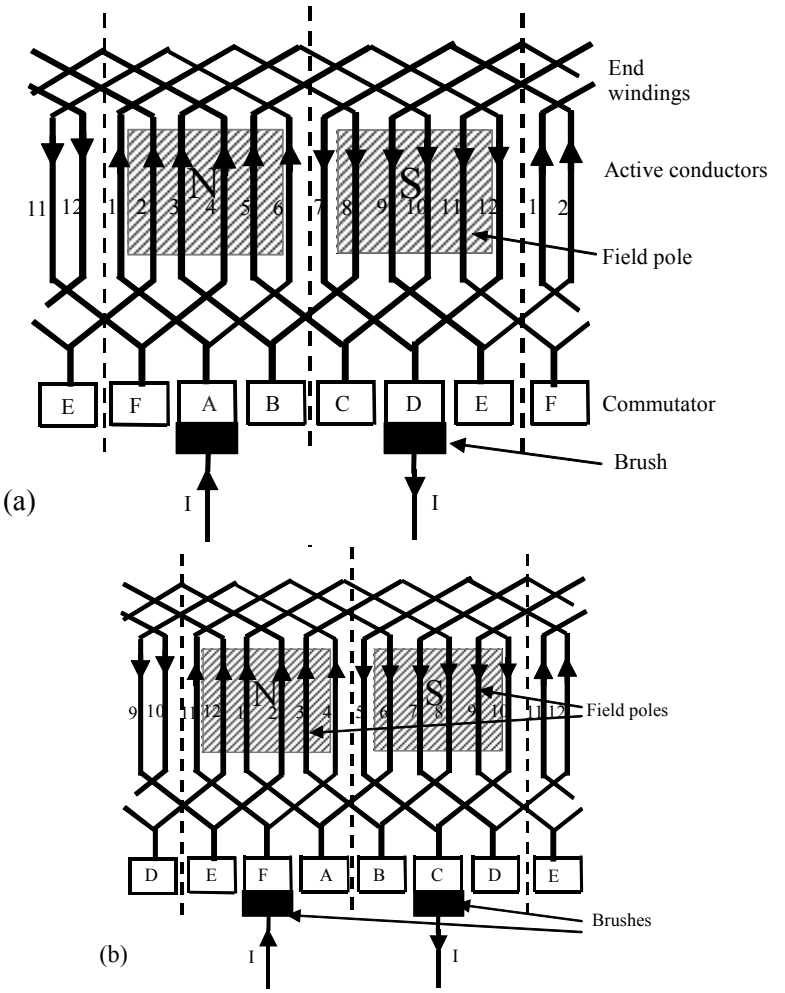

Figure 5.13. *Distribution of the armature currents for two positions of the rotor. The same current runs through the conductors in the rotor slots in front of each stator pole*

If the armature keeps on rotating, current I will successively cross segments E, D, C, etc. and will respectively get out through segments B, A, F, etc., so that, in terms of the stator, the armature spatial distribution will remain unchanged. Thus the brush-commutator system makes it possible to impose on the rotor a current distribution, fixed in space and dependent on the position of the brushes. The rotor winding can therefore be modeled in a fixed axis stationary winding. This specific characteristic of DC machines will therefore be extremely useful in order to establish their equations (section 5.4.2).

We mentioned before that in practice, each slot has two conductor bundles, one taking up the top, and the other, the bottom of the slot (Figure 5.14).

An example of two-layer bipolar lap winding is given in Figure 5.15. It has 12 slots and the commutator has 12 insulated segments. In each slot, the conductor bundle corresponding to the first layer takes up the top of the slot and is represented by a continuous line. The second layer is located at the bottom of the slot and is represented by a broken line. Note that each coil section is made by the series connection of a conductor bundle taking up the top of a slot with a conductor bundle located at the bottom of another slot.

Figure 5.16 shows the field lines obtained when only the armature winding is supplied (field called “armature reaction field”). These lines turn around rotor currents; they cross the air-gap, then the stator, and then close through the rotor. In a first approximation, these lines cross only the small air-gap located under the poles.

Figure 5.17 shows the variation of the armature normal flux density along the air-gap. Origin $\theta = 0$ corresponds to the interpolar axis. The flux density is equal to zero for $\theta = \pm\pi/2$ (field system poles axis), and it can be admitted that

it varies in a linear way within the pole width. Around the interpolar axis, its value is small and can be assumed to be constant.

When both rotor and stator windings are supplied, the resulting field is obtained by superimposing the excitation winding and the armature fields. An example of the drawing of field lines is given by Figure 5.18. The influence of the armature reaction can be observed, which leads to a concentration of the field lines in one horn of each polar shoe.

For each pole, this phenomenon leads to the increase of the normal flux density under one horn and its decrease under the other horn (Figure 5.19). It thus leads to the magnetic saturation of the horn and of the stator teeth, subjected to the field concentration. Thus the magnetic field crossing the armature winding decreases and leads to a reduction of the electromotive force. We shall see later that this reduction can be compensated by using an extra winding at the stator, called "compensating winding" (Figure 5.47).

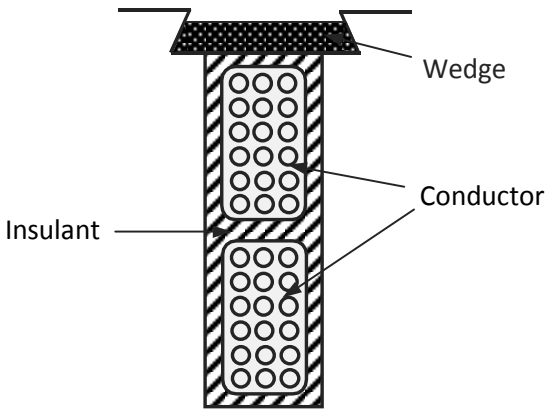

Figure 5.14. *Armature slot having 2 conductor bundles*

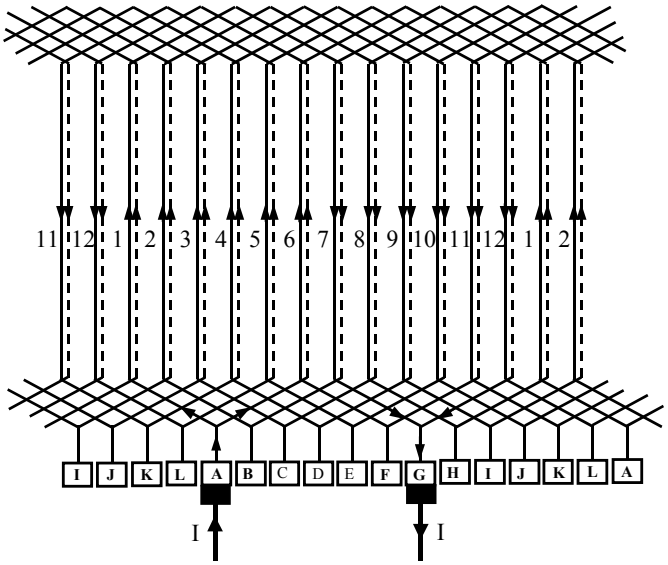

Figure 5.15. *Lap winding, 12 slots, 2 poles, 2 layers, 2 "ways", 12 commutator segments*

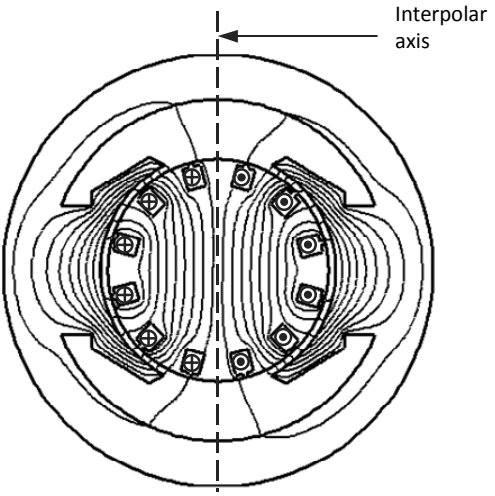

Figure 5.16. *Armature field lines: bipolar machine*

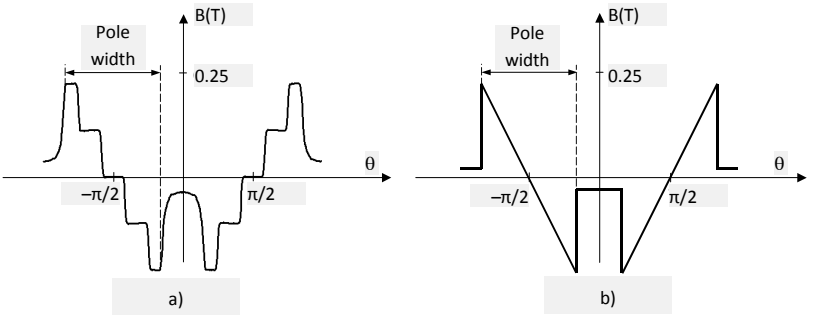

Figure 5.17. *Normal flux density in the air-gap: a) finite element calculation; b) simplified form*

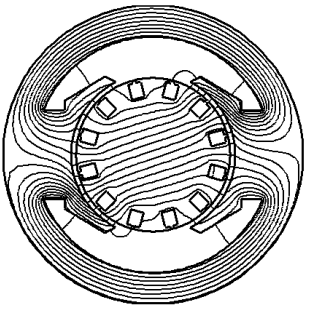

Figure 5.18. *Distortion of the on-load field lines: bipolar machine*

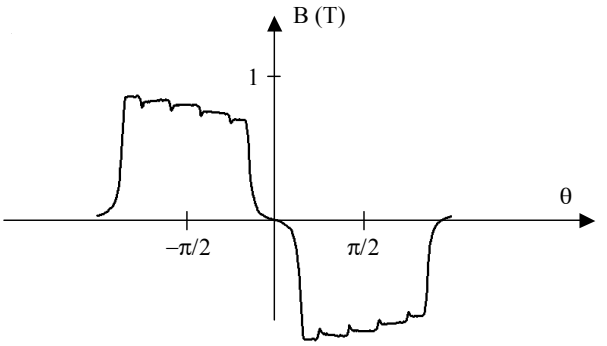

Figure 5.19. *Normal on-load flux density: finite element calculation*

5.4. DC machine equations

5.4.1. *Hypotheses and covenants*

We shall, in a first analysis, neglect all the losses except the Joule losses, as well as the magnetic saturation and hysteresis phenomena. The current commutation when the brushes go from one commutator segment to the next shall be assumed to be instantaneous. These various phenomena shall be the subject of a specific study at the end of the chapter.

Furthermore, since we shall assume field system current I_1 and armature current I_2 are perfectly constant, the field system and armature self inductances shall not take part in the equations. These parameters will have an influence only in dynamic operating or when the machines are supplied by static converters. Except if especially mentioned, we shall use the "motor" sign covenants (mechanical power considered as positive when it is supplied to a load) and, as a consequence, the two electrical circuits (armature and field system) are considered as receivers.

5.4.2. *Equations*

The example of simplified winding presented in Figures 5.12 and 5.13 enables us to establish a fundamental result for DC machines: the distribution of rotor currents is fixed in space and depends only on the brushes position.

The rotor coil (or the armature coil) of the machine shall therefore be likened to a fixed coil, the position of which with regard to the stator coil (or the field system coil) depends only on the brushes position. These two field systems (index 1) and armature (index 2) coils have respective self-inductances L_1 and L_2 and a mutual inductance M.

The DC machine has non-salient rotor poles and salient stator poles. Thus, only M and L_2 depend on the respective position of the two coils, positions represented by the angle α of their respective axes (Figure 5.20). It is thus wise to derive the electromagnetic co-energy in terms of α in order to calculate the electromagnetic torque of the DC machine.

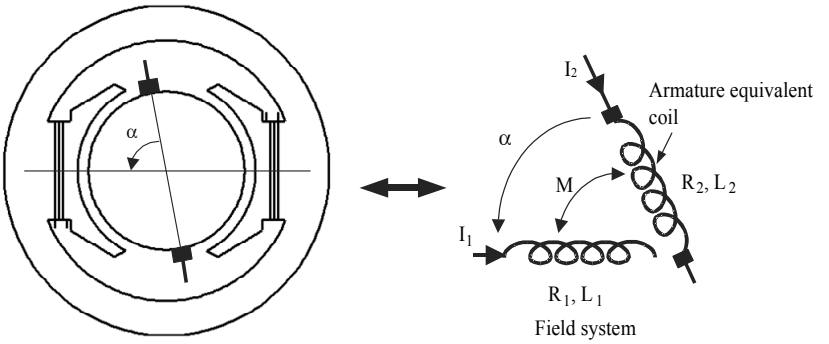

Figure 5.20. *Bipolar DC machine: a) cross-section; b) schematic external representation*

The general formulation of the torque (equation [2.7]) leads to:

$$\Gamma = \frac{\partial \omega_{em}}{\partial \alpha} = \frac{\partial}{\partial \alpha}\left[M(\alpha)\, I_1\, I_2 + \frac{1}{2} L_1\, I_1^2 + \frac{1}{2} L_2(\alpha)\, I_2^2 \right]$$

We thus obtain:

$$\Gamma = \frac{\partial M(\alpha)}{\partial \alpha} I_1 I_2 + \frac{1}{2} \frac{\partial L_2(\alpha)}{\partial \alpha} I_2^2 \qquad [5.1]$$

Let us now consider Ohm's law applied to the rotor circuit:

$$U = R_2\, I_2 + E$$

where E is the electromotive force, and R_2, the armature winding resistance measured between the brushes. The power absorbed by the armature is equal to:

$$U\ I_2 = R_2 I_2^2 + E\ I_2$$

This power is transformed, besides Joule losses $R_2 I_2^2$, in mechanical power $P_m = \Gamma\ \Omega$. If all the losses except for the rotor Joule losses are neglected, we have:

$$\Gamma\Omega = EI_2$$

an expression characterizing the power conservation. We obtain:

$$\left[\frac{\partial M(\alpha)}{\partial \alpha} I_1\ I_2 + \frac{1}{2}\frac{\partial L_2(\alpha)}{\partial \alpha}\ I_2^2\right]\Omega = E\ I_2$$

hence:

$$E = \left[\frac{\partial M(\alpha)}{\partial \alpha} I_1 + \frac{1}{2}\frac{\partial L_2(\alpha)}{\partial \alpha}\ I_2\right]\Omega$$

This expression shows the difference between the machine no-load electromotive force ($I_2 = 0$), $\frac{\partial M(\alpha)}{\partial \alpha} I_1\ \Omega$, and on-load electromotive force E. However, in most cases, term $\frac{1}{2}\frac{\partial L_2(\alpha)}{\partial \alpha} I_2$ can be neglected compared to $\frac{\partial M(\alpha)}{\partial \alpha} I_1$. In all the following, it shall therefore be neglected.

Let us now see how to choose α. Assume that only the fundamental of $M(\alpha)$ is taken into account (see Chapter 1):

$$M(\alpha) = M \cos \alpha$$

where, in order to avoid multiplying notations, M is the maximum value of mutual inductance M(α). In this hypothesis, the expression:

$$E = \frac{\partial M(\alpha)}{\partial \alpha} I_1 \Omega$$

leads, in modulus, to:

$$E = M \Omega I_1 \sin \alpha$$

with the electromagnetic torque:

$$\Gamma = M \ I_1 \ I_2 \ \sin \alpha$$

In order to obtain the maximum torque or the maximum emf, it is necessary to have $\alpha = \pi / 2$, that is to say $M(\alpha) = 0$. The brushes are then said to be "settled on the neutral line". In such conditions, the electrical equations of the machine are obtained:

$$U = E + R_2 \ I_2 \qquad [5.2]$$

$$E = M \ \Omega \ I_1 \qquad [5.3]$$

$$\Gamma = M \ I_1 \ I_2 \qquad [5.4]$$

These equations correspond to the schematic representation of Figure 5.21, where the field system is assumed to be supplied by a current source. The mechanical equation is written:

$$J \frac{d\Omega}{dt} = \Gamma - \Gamma_c \qquad [2.15]$$

In steady state (Ω constant) Γ = ΓC. Hence in the following we shall write indiscriminately Γ or ΓC.

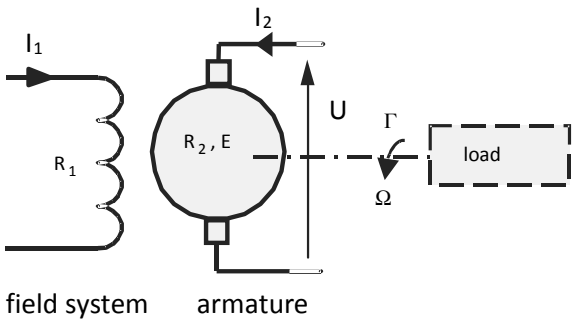

Figure 5.21. *Conventional representation of the DC machine*

5.4.3 *Determination of the parameters*

Equations [5.2] to [5.4] enable us to study the steady state of DC machines, providing their supply and implementation modes are known: separate excitation machine or series excitation machine. In order to predetermine the working of a particular machine, it is therefore necessary to determine parameters R2, R1 and M.

5.4.3.1. *Resistance measurement*

The measurement of R1, static coil resistance, is not particularly a problem. A standard "ammeter-voltmeter" method enables us to determine its value with satisfying precision. Alternately, the determination of R2 is more difficult.

Let us consider Figures 5.13 and 5.15. The current goes from one brush to another by circulating through a number

of conductors connected in series and in parallel. When the rotor turns, this conductor repartition is modified because the brushes are successively in contact with one or several commutator segments. The result is that the value of resistance R_2 depends on the rotor position. Furthermore, at the brush-commutator contact, there is a voltage drop Δu depending on the contact surfaces, on the pressure and on the value of the current.

R_2 therefore appears to be a very simple model for the representation of complex phenomena; strictly speaking, its dependency upon Θ and I_2 should be taken into account. In order to take into account the dependence on R_2 in relation to Θ, it is advisable to make measurements with various rotor positions and to take the average. For the dependence on I_2, it is advisable to repeat the previous measurement for various values of the armature current and to tabulate the obtained results. For simplicity's sake, this determination is generally only achieved with the nominal current and under the normal operating temperature. This induces an acceptable lack of precision.

5.4.3.2. *Measurement of M*

Expression [5.3] shows that if E, Ω and I_1 are known, it can be deduced:

$$M = \frac{E}{\Omega\ I_1} \qquad [5.5]$$

For this, a "no-load generator" test is achieved: the studied machine is driven by an auxiliary motor (Figure 5.22), a current I_1 is injected in the excitation circuit and voltage U = E is measured at the armature terminals, in which no current circulates. So that mutual M may be considered to be constant, it is advisable to restrict the value of I_1 ($I_1 < I_{11}$) in order to avoid magnetic saturation (Figure 5.23).

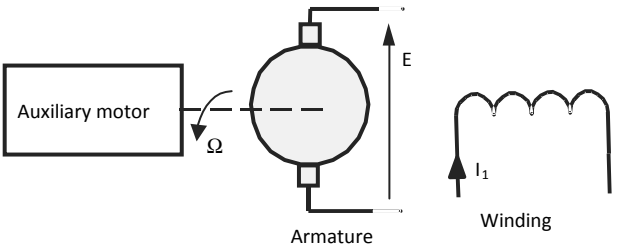

Figure 5.22. *No-load generator test*

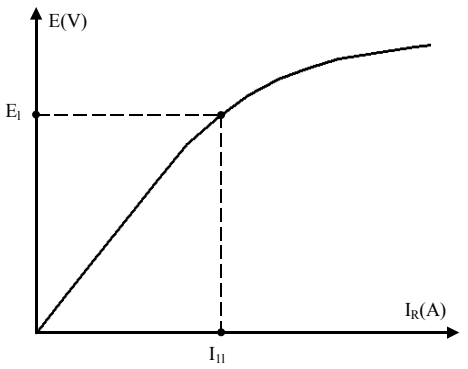

Figure 5.23. *Independent excitation no-load generator characteristic*

5.5. Separately excited motor

5.5.1. *Introduction*

This is the most common use of the DC motor. The field system and the armature are supplied separately by two supposedly distinct sources, which allows us to separately impose field system current I_1 and voltage U to the armature terminals.

We shall now analyze how the various variables appearing in equations [5.2] to [5.4] vary according to the different operating modes of the machine. A "system" approach of the machine highlights (Figure 5.24) two

"inputs" U and I_1 (supposedly controllable values), a "perturbation" $\Gamma = \Gamma_C$ imposed by the environment (Γ_C is the load resistant torque that the motor has to drive) and two "outputs" Ω and I_2, values for which evolutions in terms of the inputs and of the perturbation are determined by the machine equations.

The characteristics are therefore the curves representative of the output variations in terms of one of the three other values, the other two supposedly being constant. It is therefore advisable to formulate the two output expressions in terms of the inputs and of the perturbation.

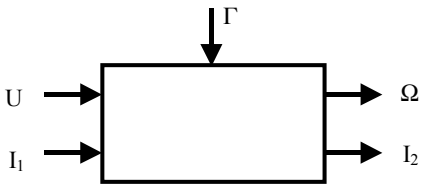

Figure 5.24. *"System" representation of the separately excited motor*

We therefore have:

$$I_2 = \frac{\Gamma}{MI_1} \qquad [5.6]$$

and:

$$\Omega = \frac{U}{MI_1} - \frac{R_2\Gamma}{(MI_1)^2} \qquad [5.7]$$

Those two expressions make it possible to draw the separately excited machine characteristics. In the following paragraphs we shall determine these characteristics by considering a "model machine" for which the parameters are the following:

– nominal power: P_n = 4 kW;

– nominal armature voltage: U = 220 V;

– nominal armature current: I_{2n} = 22 A;

– nominal field system current in motor operating: I_{1n} = 1.1 A;

– nominal field system current in generator operating: I_{1n} = 1.6 A;

– armature resistance: R_2 = 0.5 Ω;

– field system resistance: R_1 = 133 Ω;

– mutual inductance: M = 1.27 H;

– nominal speed: Ω_n = 157 rd/s.

5.5.2. *External characteristics*

5.5.2.1. *Characteristic $I_2 = f(\Gamma)$ with constant U and I_1*

Equation [5.6] corresponds to a straight line going through the origin and to slope $1/(MI_1)$ (Figure 5.25).

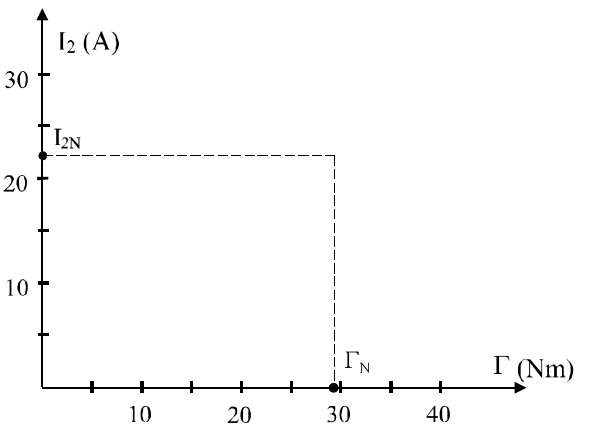

Figure 5.25. *Characteristic $I_2(\Gamma)$ with constant armature voltage and field current*

5.5.2.2. *Characteristic $\Omega = f(\Gamma)$ with constant U and I_1*

The motor speed is given by expression [5.7]. Note that, as U and I_1 are fixed, Ω varies linearly in terms of Γ (Figure 5.26). It is a straight line of origin $\Omega = \frac{U}{M\ I_1}$ and of slope $-\frac{R_2}{(M\ I_1)^2}$. This straight line with a small slope, and we deduce that the rotation speed of a separately excited motor is almost independent of the load torque value.

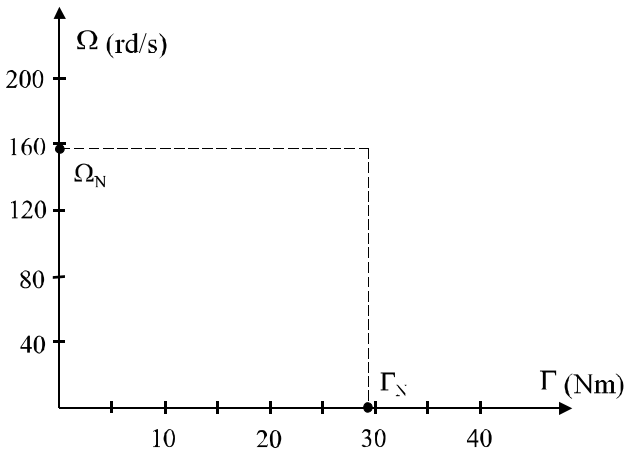

Figure 5.26. *Characteristic $\Omega(\Gamma)$ with constant armature voltage and field current*

5.5.2.3. *Characteristic $\Omega = f(U)$ with fixed Γ and I_1*

This is an important characteristic for separately excited DC motors. Equation [5.7] represents a straight line of slope $1/(MI_1)$ which starting abscissa depends on Γ (Figure 5.27). As the term $\frac{R_2\ \Gamma}{(M\ I_1)^2}$ is usually small, we deduce that in a first approximation, the rotation speed of this kind of motor is proportional to the armature voltage.

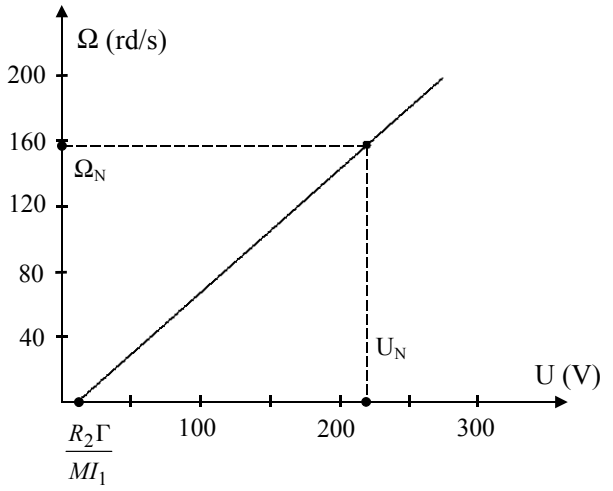

Figure 5.27. *Characteristic Ω(U) with constant torque and field current*

This property is largely used for industrial variable speed drives, where separate excitation motors are supplied by static converters.

5.5.2.4. *Characteristic $I_2 = f(U)$ with fixed Γ and I_1*

With Ω = 0, we can be write:

$$U = R_2 \, I_2 = \frac{R_2 \, \Gamma}{M \, I_1}$$

It is therefore necessary to have $U > \frac{R_2 \, \Gamma}{M \, I_1}$ for the motor to start. Below this value, the armature behaves as a resistance, and therefore $I_2 = U/R_2$. Above this limit, $I_2 = \Gamma/(MI_1)$ is constant (Figure 5.28).

5.5.2.5. *Characteristic $I_2 = f(I_1)$ with fixed Γ and U*

If Γ is fixed, equation [4.6] shows that current I_2 hyperbolically varies in terms of I_1 (Figure 5.29). If I_1 tends

toward zero, I_2 therefore tends toward infinity, and it can thus be dangerous to reduce the field system current too much.

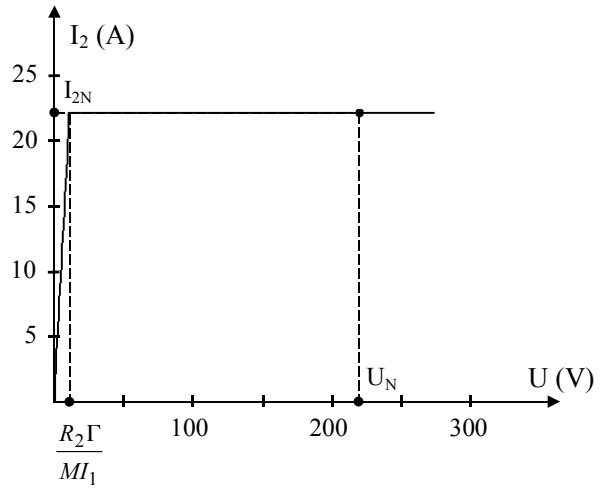

Figure 5.28. *Characteristic $I_2(U)$ with constant torque and field current*

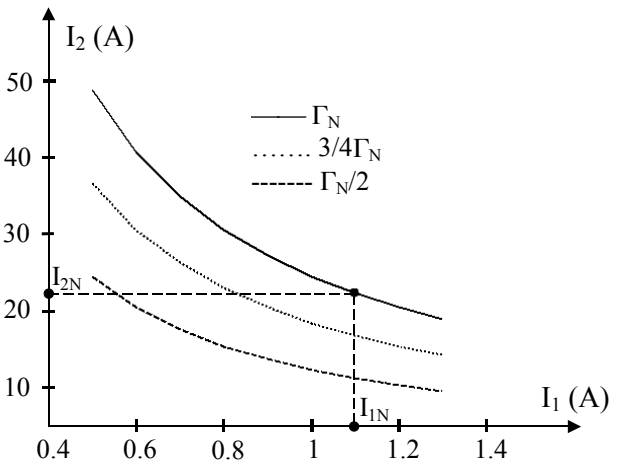

Figure 5.29. *Characteristic $I_2(I_1)$ with constant armature voltage and torque*

5.5.2.6. *Characteristic* $\Omega = f(I_1)$ *with fixed* Γ *and* U

Equation [4.7] shows that, in order to obtain $\Omega > 0$, it is necessary to have $I_1 > \frac{R_2 \Gamma}{M U}$. It is also clear that if I_1 tends toward infinity, the rotation speed Ω tends toward zero. Furthermore, note that if I_1 tends toward zero, Ω tends toward $-\infty$. This result, which corresponds to the curves of Figure 5.30, has to be considered with caution. Indeed when these curves are considered, note that when I_1 decreases, speed goes through a maximum ($\Omega_{max} = \frac{U^2}{4R_2\Gamma}$) with $I_1 = \frac{2R_2\Gamma}{MU}$.

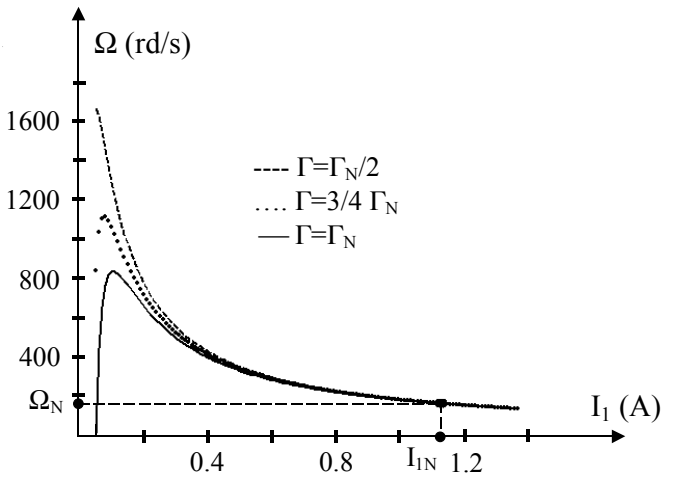

Figure 5.30. *Characteristic* $\Omega(I_1)$ *with constant voltage and torque*

This theoretical maximum is much higher than the actual speed the machine can tolerate, hence the usual expression: "if the field system current is lowered too much, the machine races". If current I_1 is accidentally switched off, the machine behavior will depend on the load. If the motor does not have any mechanical load, it will have a tendency to race ($\Omega \rightarrow \infty$

if $I_1 \rightarrow 0$, with $\Gamma = 0$). On the contrary, if the load torque exists, mechanical equation [2.15] shows that the speed is cancelled when Γ is zero; the machine will then "stall" and there is a risk of damage due to an excessive armature current. It is obvious that it is very important to avoid any accidental switching off of the field system current.

All of these characteristics show that the separately excited DC machine gives a very interesting possibility for the design of variable speed drives. It is indeed very convenient to control it with the armature voltage, the great simplicity of the equations linking U to Ω and to I_2 allowing the use of very simple speed and current controllers.

The influence of I_1 on the speed variation is more complex and hazardous. In practice, the adjustment of Ω by I_1 is only used to obtain a speed increase beyond the maximum value of U. I_1 is then decreased to accelerate the motor. It is important to note that this can only be done if the torque is smaller than the nominal torque (see equation [5.4]).

5.5.3. *Energy recovery: generator operating*

In the past, separately excited machines were used to produce direct current. This working mode has almost disappeared with the rise of static rectifiers. This machine however enables it to recover kinetic energy during braking or slowing down, within the devices where they mostly play the part of motors.

Figure 5.31 schematizes the generator working of the separately excited machine. In this case, it is judicious to modify the sign covenant for the armature, which shall be considered as a generator.

If the "system" analysis is used again, note (Figure 5.32) that, in this case, I_1 and U remain inputs, and I_2, an output.

Rotation speed Ω is usually imposed by the mechanical environment and has to be considered as a perturbation. Conversely, torque $\Gamma = M\ I_1\ I_2$ is an output.

By adopting the "generator" sign covenants (electrical power considered as positive when it is supplied to a load), equations [5.2] to [5.4] become:

$$U = E - R\,I_2 \qquad [5.2']$$

$$E = M\ \Omega\ I_1$$

$$\Gamma = M\ I_1\ I_2$$

The output expressions become:

$$I_2 = \frac{M\,\Omega\,I_1 - U}{R_2} \qquad [5.8]$$

$$\Gamma = M\,I_1\,\frac{M\,\Omega\,I_1 - U}{R_2} \qquad [5.9]$$

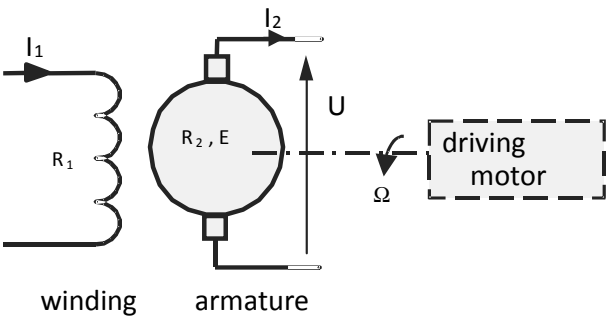

Figure 5.31. *Conventional representation for generator mode*

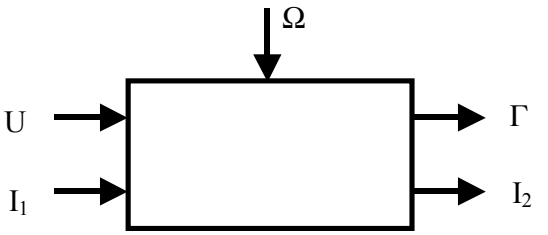

Figure 5.32. *System inputs and outputs*

In the following we shall outline the characteristics by referring to the "model" machine defined in section 5.5.1.

5.5.3.1. *Operating mode with fixed U and Ω*

Equations [5.8] and [5.9] highlight a minimum value of field system current $I_1 = U/(M\Omega)$ enabling the energy recovery. Characteristic $I_2 = f(I_1)$ is a straight line starting from this minimum value and of slope $M\Omega/R_2$ (Figure 5.33). The torque variation in terms of I_1 is a parabola (Figure 5.34).

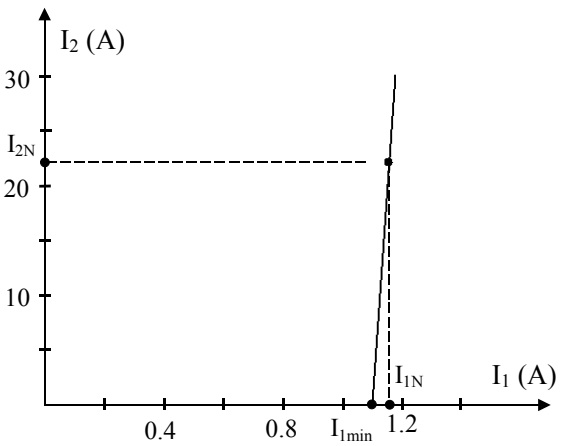

Figure 5.33. *Characteristic $I_2(I_1)$ with constant voltage and speed*

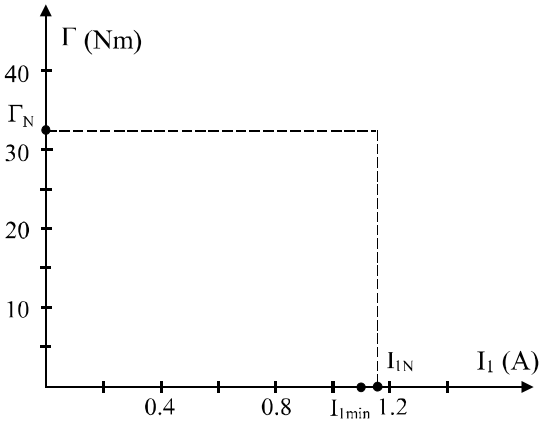

Figure 5.34. *Characteristic Γ(I₁) with constant voltage and speed. Note that the useful part of the parabola is almost linear*

5.5.3.2. *Variable voltage operating*

Characteristics $I_2(U)$ and $\Gamma(U)$ are straight lines that cut the axes in points $U = M\Omega I_1$ and respectively $I_2 = \frac{M\ \Omega I_1}{R_2}$ and $\Gamma = \frac{(M\ I_1)^2}{R_2}$ (Figures 5.35 and 5.36).

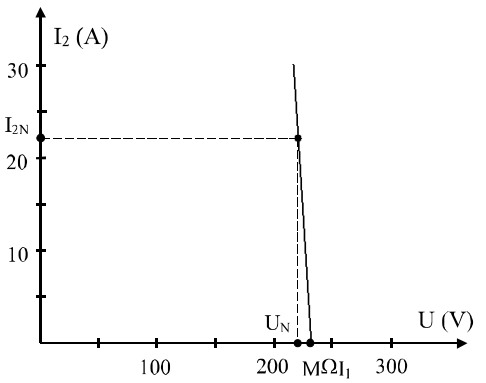

Figure 5.35. *Characteristic $I_2(U)$ with constant excitation and speed. Point ($U = 0$, $I_2 = M\Omega I_1 / R_2$) is out of the frame of the figure*

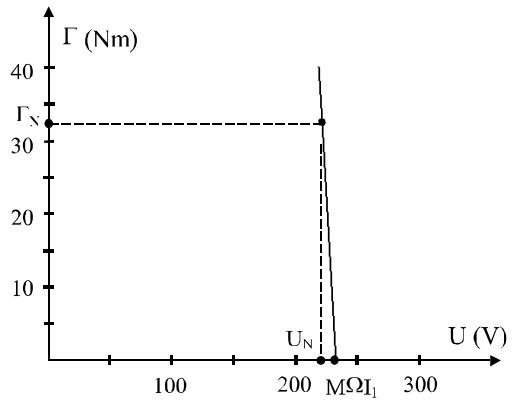

Figure 5.36. *Characteristic Γ(U) with constant excitation and speed. Point (U = 0, Γ=(MI₁)²Ω / R₂) is out of the frame of the figure*

5.6. Series excited motor

5.6.1. *Introduction*

In a "series excited" DC motor, or "series motor", the field system and the armature are connected in series and supplied by the same continuous voltage source. This brings a constraint on the field system which, as it is travelled by the armature current, has to have a small enough resistance to prevent a reduction of the global efficiency. The field coil is therefore made of quite a small number of turns of important section conductors. Note that this increases the machine inductance, which is favorable when it is supplied by power converters.

Figure 5.37 shows the conventional representation of the machine. In this case, the machine equations become:

$$\begin{cases} I_1 = I_2 = I \\ E = M\ \Omega\ I \\ U = \left(R_1 + R_2 + M\ \Omega\right) I \\ \Gamma = M\ I^2 \end{cases}$$

In order to simplify, we set down $R = R_1 + R_2$.

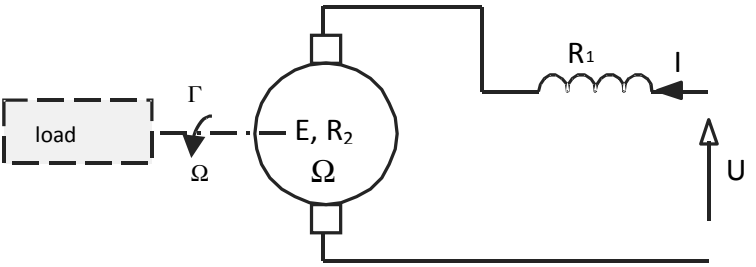

Figure 5.37. *Conventional representation of the series excited machine*

This system has one degree of freedom less than the separately excited motor; the supply voltage U is now the only "input" (Figure 5.38).

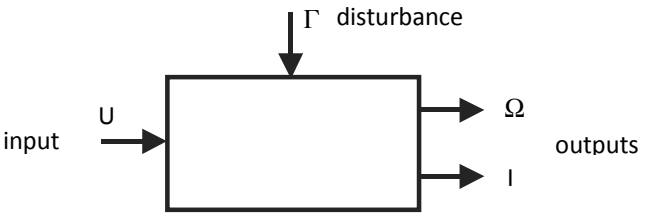

Figure 5.38. *"System" representation of the series excited machine*

The characteristics of this motor are therefore the variation curves of Ω and I in terms of U or to Γ, the other value remaining constant. Let us then write the expressions of I and Ω:

$$I = \sqrt{\frac{\Gamma}{M}} \qquad [5.10]$$

$$\Omega = \frac{U}{\sqrt{\Gamma M}} - \frac{R}{M} \qquad [5.11]$$

5.6.2. *External characteristics*

In order to outline the characteristics of series motors we shall use the parameters of the following "model" machine:

– nominal power: P_n = 4 kW;

– nominal armature voltage: U = 220 V;

– nominal current: I_n = 22 A;

– armature resistance: R_2 = 0.5 Ω.

– field coil resistance: R_1 = 0.375 Ω;

– mutual inductance: M = 58.1 mH;

– nominal speed: Ω_n = 157 rd/s.

5.6.2.1. *Characteristic I(Γ) with U = constant*

Current I is given by [5.10], its variation in terms of Γ is represented by Figure 5.39. It is a parabola going through the origin.

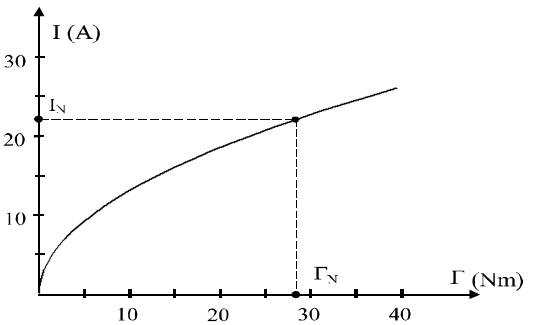

Figure 5.39. *Characteristic I(Γ) with constant voltage, U = U_N*

5.6.2.2. *Characteristic Ω = f(Γ) with fixed U*

The expression of speed is given by equation [5.11]. If U is assumed to be constant, and Γ variable, we obtain a curve with hyperbolic appearance (Figure 5.40) emphasizing that if

Γ tends toward 0, the motor races (speed tends toward infinity). This is a fundamental feature of the series motor, for which no-load operation is not allowed in order to prevent it from racing.

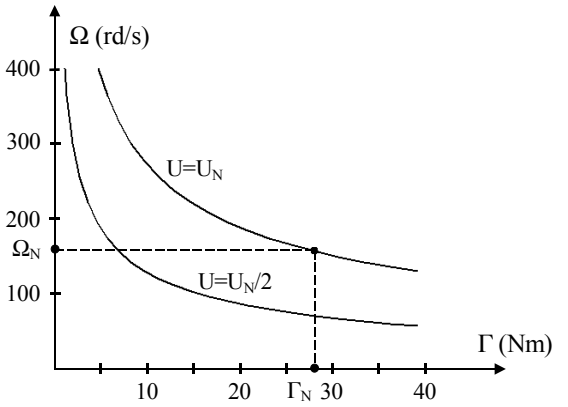

Figure 5.40. *Characteristic Ω(Γ) with constant voltages, U =UN and UN /2*

It is however noted that speed has an important variation in terms of the load torque. Theoretically Ω would be zero when $\Gamma = M\,(U/R)^2$; this very important value corresponds to a current I = U/R much greater than the nominal current. This however characterizes the ability of the series motor to provide a very important starting torque.

5.6.2.3. *Characteristic Ω = f(U) with constant Γ*

This characteristic (Figure 5.41) is a straight line going through the point with the coordinates $\Omega = 0$ and $U = RI = R\sqrt{\frac{\Gamma}{M}}$. Note that the motor only starts for a voltage higher than $R\sqrt{\frac{\Gamma}{M}}$.

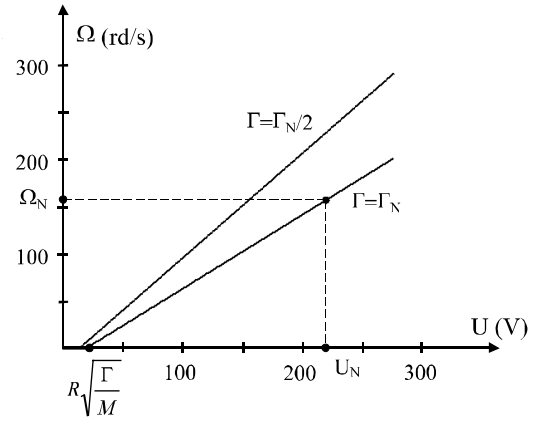

Figure 5.41. *Characteristic Ω(U) with constant torque, Γ=ΓN and ΓN /2*

5.6.2.4. *Characteristic* $I = f(U)$ *with constant* Γ

Current I given by equation [5.10] is constant when the motor works, that is to say for $U > R\sqrt{\frac{\Gamma}{M}}$. Below this value, the motor behaves like a resistance R and the current is worth I = U/R (Figure 5.42).

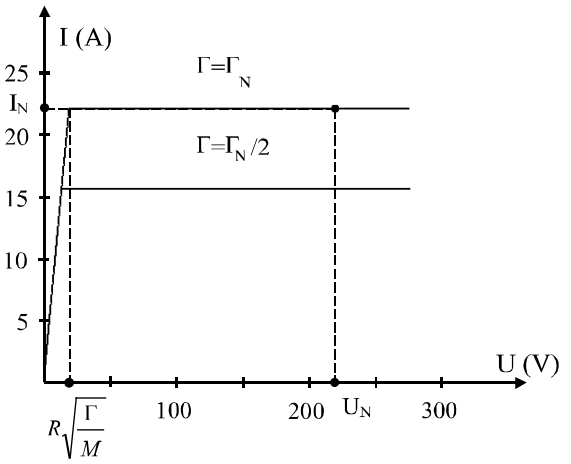

Figure 5.42. *Characteristic I(U) with a constant torque, Γ=ΓN and ΓN /2*

5.7. Special case of the series motor: the universal motor

A universal motor is a series machine capable of being supplied in direct current as well as in alternative current. We have indeed seen that the series machine torque is proportional to the square current; it is therefore independent from the direction of the current circulation and can thus be supplied with alternative current.

However, comparative to the standard series motor, this kind of motor has to have a laminated stator in order to minimize the iron losses (see Chapter 2). The number of turns in the field winding has to be reduced in order to restrict the stator inductance. In order to compensate for the reduction of the excitation flux, the rotor turns number increases accordingly.

As with all series motors, the universal motor races at no-load and its speed is very dependent on its load. It is used in devices requiring a good starting torque: traction, domestic appliances, etc.

5.8. Commutation phenomena

The commutation phenomenon appears when a brush goes from one commutator segment to the next because the current has to reverse in one coil section. The latter being inductive and submitted to induced electromotive forces, the reversal of the current is not instantaneous. We shall restrict the study to the case of "simple" commutation, that is to say when the brush width is equal to the commutator segment width.

Let us consider the example given in Figure 5.43, representing an armature with 12 slots, 12 commutator segments, 2 poles and 2 conductor layers. In Figure 5.43a,

each brush covers a single commutator segment. At this instant, the current in the coil section made of conductors 1 and 7 is considered to be positive and worth I/2.

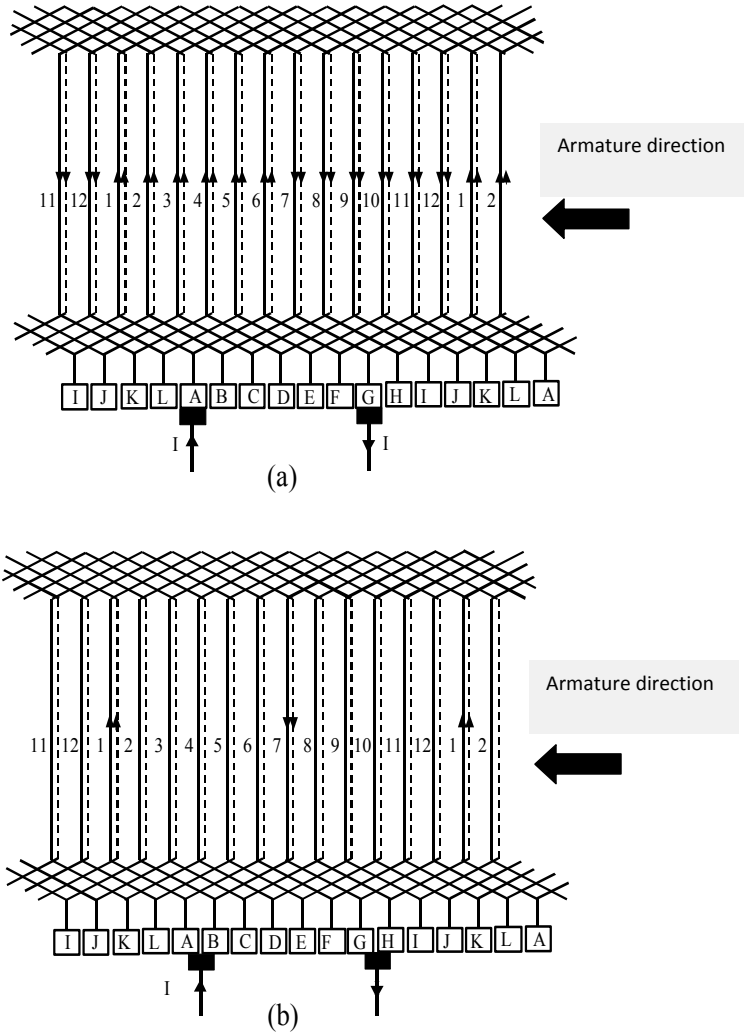

Figure 5.43. *Transition of the brushes from a commutator segment to the next: a) brush in contact with a single segment; b) brush short-circuiting two segments*

In Figure 5.43b, which shows a later instant, the brushes, overlapping two segments, short-circuit two coil sections. A still later instant, when the brushes leave left segments A and G of the commutator to position themselves on segments B and H, the current in coil section 1-7 changes its sign and goes from I/2 to –I/2.

If the armature diagram is simplified (Figure 5.44), it is noticed that when the brush overlaps 2 commutator segments, the corresponding coil section (noted "S" on the figure) is short-circuited. Current I_S in this coil section will therefore vary according to the flux that crosses it and to its impedance.

Depending on the cases, the variation of I_S (from I/2 to –I/2) can have various aspects (Figure 5.45):

– on curve (1), I_S varies linearly, which corresponds to a current density constant on brush-commutator contact. This constitutes the ideal commutation;

– on curve (2), the current does not vary linearly, but naturally reaches –I/2 when the brush leaves commutator segment A;

– for curves (3) and (4), the current does not reach –I/2 when the brush leaves commutator segment A. There is therefore a current discontinuity on brush-commutator contact, which has to go instantly from (I_S + I/2) to zero. This current discontinuity generates an arc at the moment when the brush leaves the commutator segment. If this discontinuity is important, the arc can damage the commutator and the brushes. In any case, these arcs are ageing factors that are prejudicial to the brush-commutator set life duration.

Without going into detail, it is advisable to point out at this stage that the commutation phenomena are even more complex when the armature current is alternative (universal

motors) or, to a lesser extent, have an important harmonic content (case of static converter supply).

In order to improve the commutation, the flux in the short-circuited section has to be reduced. This can be obtained either by shifting the brushes (for small power motors), or by using an extra winding called "commutation winding". This commutation winding is set down between the main poles and supplied with the armature current (Figures 5.46 and 5.47).

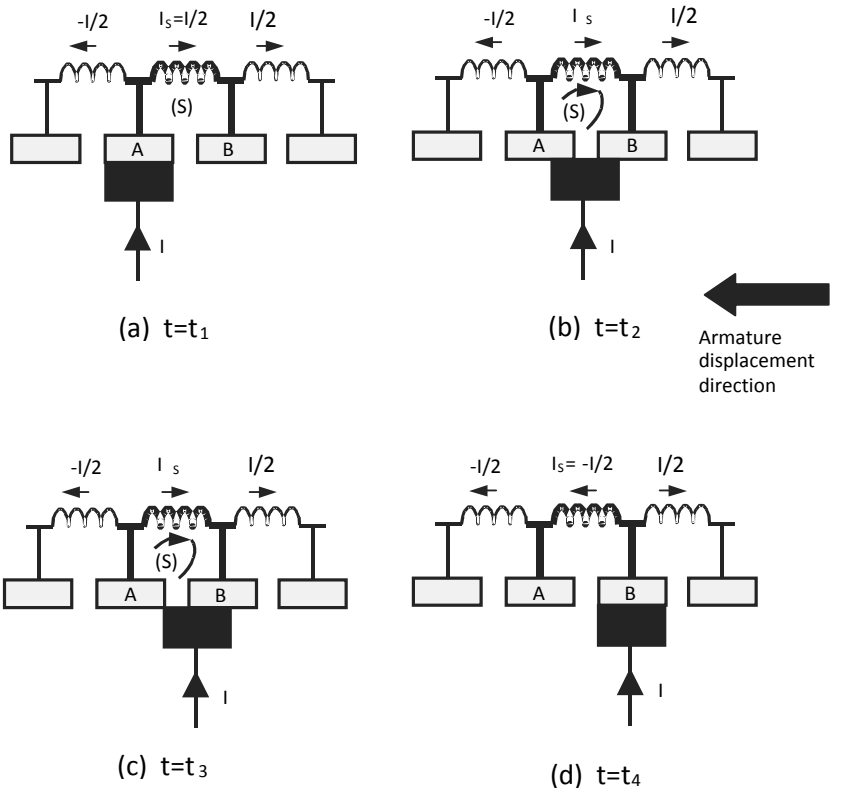

Figure 5.44. *Schematic representation of the moving of a brush from one segment to the next*

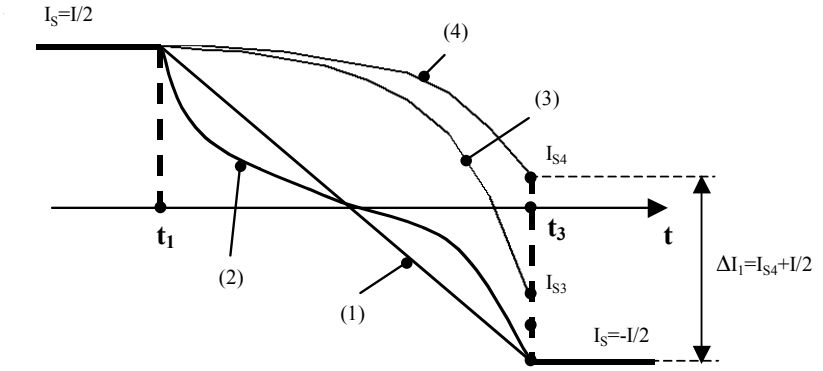

Figure 5.45. *Evolution of the current in a coil section in commutation. On t_1, the brush comes into contact with the second commutator segment B, and on t_3, it leaves initial segment A*

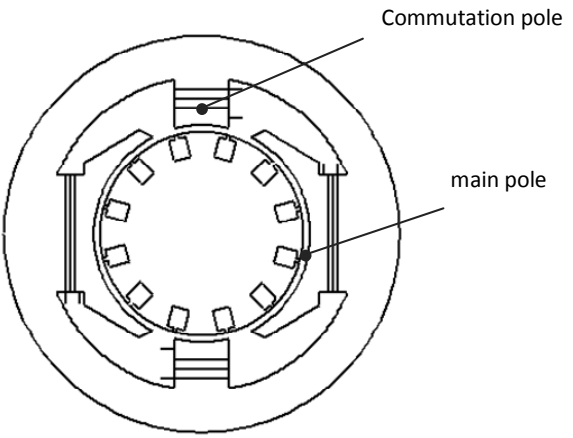

Figure 5.46. *Main poles and commutation poles of a bipolar machine*

5.9. Saturation and armature reaction

As for all electromechanical converters, DC machines are subjected to the magnetic saturation phenomenon. This leads to a non-linear no-load characteristic E = f(I_1) (Figure 5.23). This phenomenon is amplified by the armature

reaction effect. Indeed, we have seen in paragraph 5.3.3, by considering Figure 5.18, that the field lines concentrate in one of the polar horns to the detriment of the other horns. This leads to a local saturation and to the reduction of the useful flux.

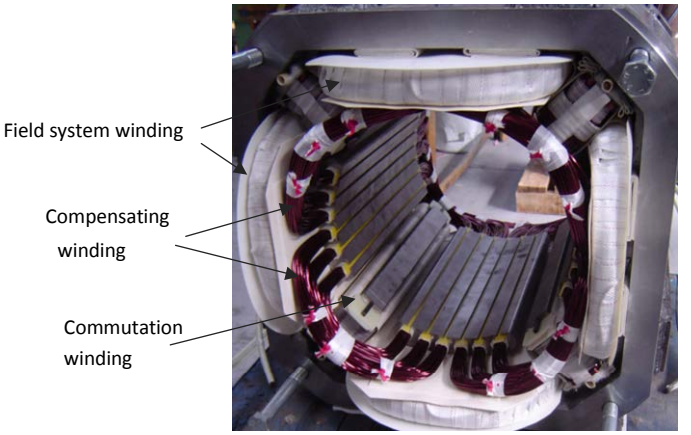

Figure 5.47. *Stator of a four-pole machine, 220 kW, 440 V, 2,800 to 7,000 rpm. The field system windings, commutation windings and compensation windings can be distinguished (ECA EN document)*

To overcome this problem, a winding called "compensation winding" is used. It is located in slots gouged into the stator pole pieces and supplied with the armature current. This leads to the stator structure represented in Figure 5.47, where the field winding, the commutation winding and the compensation winding are visible.

5.10. Implementation of DC motors

Nowadays it is necessary to distinguish, on the one hand, the traditional implementation with constant voltages (it has a historical and a pedagogical interest), and on the other hand, the present implementation using static converters.

5.10.1. *Constant voltage implementation*

When a DC machine, either a separate or series excited machine, is supplied with constant voltage, the main difficulty is to ensure it starts. Indeed, when at standstill, the machine has no electromotive force and the absorbed current is limited only by small value resistances (R_2 in the case of separate excitation or $R_1 + R_2$ in the case of series excitation). The aim is therefore to restrict the absorbed current to a value acceptable for the machine, while maintaining a torque sufficient for the start. Since the thermal time constants are noticeably greater than the mechanical time constants, it is acceptable to have, during transient states, and in particular during starting, a current greater than the nominal current. If the starting current is called I_d we have:

$$I_d = k I_n$$

"Over-current" coefficient k is usually around 2.

5.10.1.1. *Separately excited motor start*

In order to study the start, we shall admit that the armature electrical time constants can be overlooked compared to the mechanical time constants. This will enable us to assume that the armature current variations are instantaneous.

Let us consider a machine supplied with its armature nominal voltage and with its nominal field current. It is mechanically connected to a load for which the resistant torque Γ_c is equal to the motor nominal torque. In order to reduce the current absorbed during the start, a "starting rheostat" R_d is inserted between the source and the motor armature (Figure 5.48)

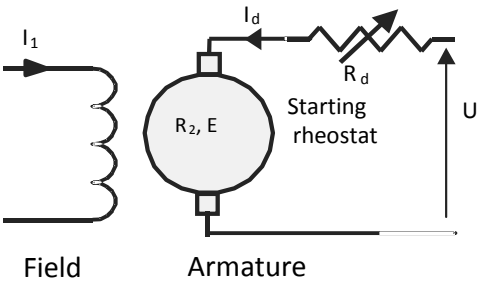

Figure 5.48. *Rheostatic starting*

By calling R_{d0} the value of R_d necessary for current I_2 to be equal to $k\,I_n$ at standstill we get:

$$U = \left(R_2 + R_{d0}\right) k\, I_{2n}$$

thus:

$$R_{d0} = \frac{U}{k\, I_{2n}} - R_2$$

At the switching on of the armature, motor torque Γ will therefore be equal to $k\, M\, I_{1n}\, I_{2n}$, which leads to the equation:

$$J\frac{d\Omega}{dt} = k\,\Gamma_n - \Gamma_n > 0$$

The machine will therefore start and will generate an electromotive force $M\Omega I_{1n}$ with:

$$U = M\,\Omega\, I_{1n} + \left(R_2 + R_{d0}\right) I_2$$

thus:

$$I_2 = \frac{U - M\,\Omega\, I_{1n}}{R_2 + R_{d0}}$$

The armature current will therefore decrease with the machine acceleration. The motor torque given by:

$$\Gamma = M\,\frac{U - M\,\Omega\,I_{1n}}{R_2 - R_{d0}}\,I_{1n}$$

is therefore variable in terms of the rotation speed. The equation of the dynamic:

$$J\,\frac{d\Omega}{dt} = M\,\frac{U - M\,\Omega\,I_{1n}}{R_2 + R_{d0}}\,I_{1n} - \Gamma_c$$

shows that the motor accelerates until $\Gamma = \Gamma_c$, value obtained for $I_2 = I_{2n}$. The corresponding rotation speed Ω_1 is:

$$\Omega_1 = \frac{U - \left(R_2 + R_{d0}\right) I_{2n}}{M\,I_{1n}}$$

The value of the starting resistance can then be modified to a value R_{d1} defined by:

$$U = M\Omega_1\,I_{1n} + \left(R_2 + R_{d1}\right) k\,I_{2n}$$

The motor will accelerate again to:

$$\Omega_2 = \frac{U - \left(R_2 + R_{d1}\right) I_{2n}}{M\,I_{1n}}$$

The process is then iterated until complete cancellation of the starting resistance.

Figure 5.49 represents the time variations of the armature current and of the speed of the “model machine” presented in section 5.5.1 during a nominal torque start.

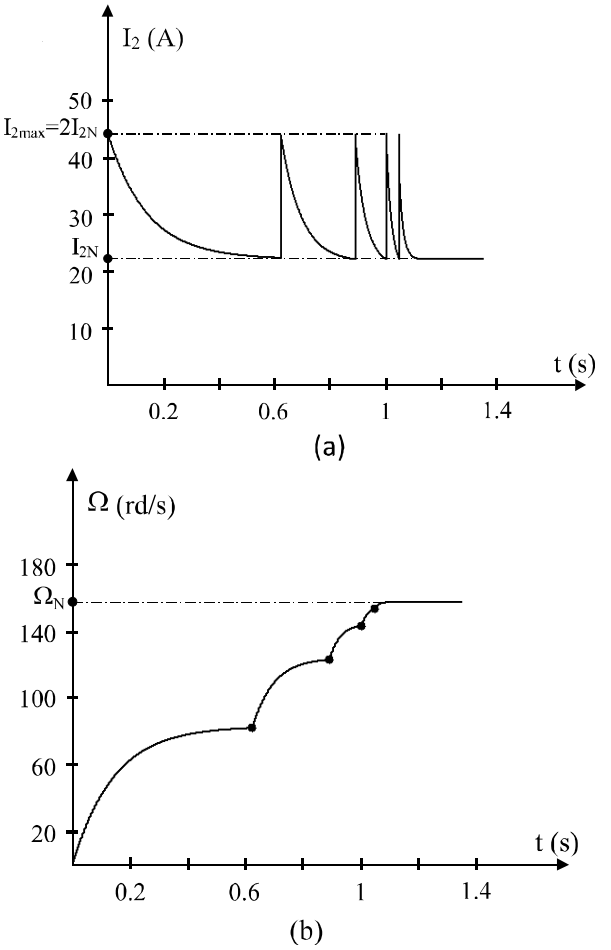

Figure 5.49. *Starting of the separately excited motor (example motor): a) armature current variation b) speed variation*

5.10.1.2. *Particular case of the separately excited motor: DC shunt motor*

When there is only one voltage source, the armature and the field system are connected in parallel to this source, the armature through the starting resistance, and the field

system through another rheostat called a "field rheostat" and noted R_h in Figure 5.50.

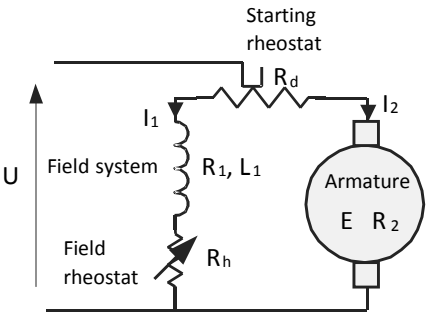

Figure 5.50. *Shunt motor implementation*

During starting, R_h is usually short-circuited in order to have maximum I_1 and the greatest possible torque. Voltage source U is applied to the cursor of the starting rheostat so that, when R_d is short-circuited, its resistance adds to the resistance of the field system. Current I_1 decreases and reaches $I_1 = I_{1n}$ at the end of the starting. R_h then enables us to make I_1 decrease in order to increase speed Ω.

5.10.1.3. *Series motor starting*

A starting rheostat is also used to reduce the current to kI_n and the iterative process leading to the progressive removal of R_d is identical. The only notable difference is that Γ is proportional to the square of I, the starting torque is multiplied by k^2 which gives, for the series motor, a great starting torque.

5.10.2. *Present implementation of DC motors*

5.10.2.1. *Separately excited motor*

Figure 5.51 represents a separately excited motor for which the armature is supplied by a 3-phase thyristor

bridge. The control variable V_C of the pulse generators (not represented in order to avoid complicating the figure) is the output of a current and speed controller. This controller receives on the one hand current reference (Ref I) and speed reference (Ref Ω), and on the other hand the signals given by the corresponding sensors. The current reference usually corresponds to the maximum value acceptable by the motor: Ref I = kI_2.

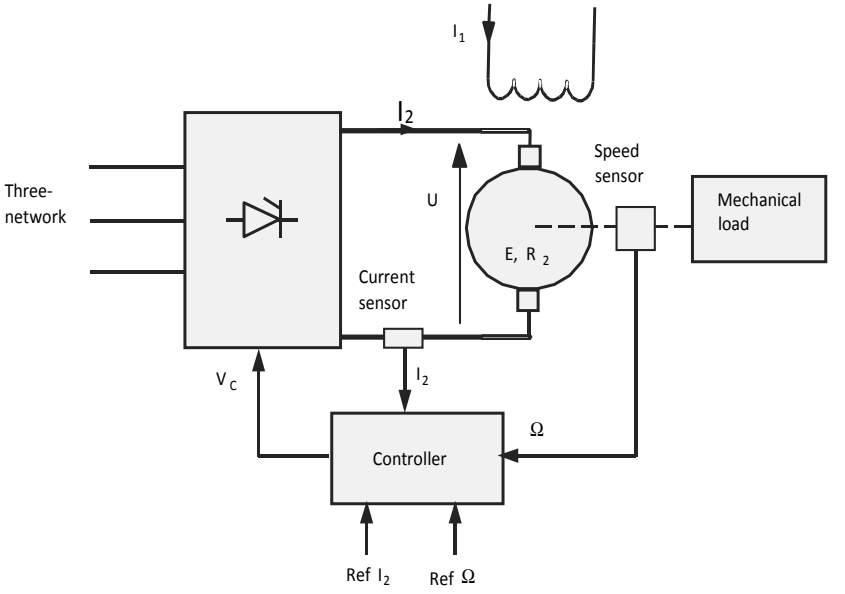

Figure 5.51. *Separately excited motor implementation*

Without going into the details of the control, a fast internal loop is used to control the current and prevent it from being greater than the fixed limit during transients and particularly during starting.

Since, in a first approximation, output voltage U of the thyristor bridge is proportional to V_c, and rotation speed Ω is also proportional to U, the speed controller of the motor is

simple to implement. If we want the motor to turn in both directions (reversibility in Ω and in Γ), a two-bridge "back to back" structure is used, as represented in Figure 1.26.

5.10.2.2. *Series motor implementation*

Figure 5.52 represents a series motor supplied by a step-down chopper. The fully controllable switch T_c (it can be turned on and off at will) is a power transistor, an IGBT, even a GTO for very high powers.

The variation of the duty cycle α (see Chapter 1) makes it possible to impose the average value of voltage U applied to the motor ($U = \alpha U_0$), and therefore its average speed in steady state. The control has two loops: an internal "fast" loop for current control enabling us to limit I under kIn in dynamic operating mode, and a slower external loop for speed control. In order to recover the kinetic energy during slowing down and motor braking, it is necessary to use a reversible chopper (see section 1.3.3).

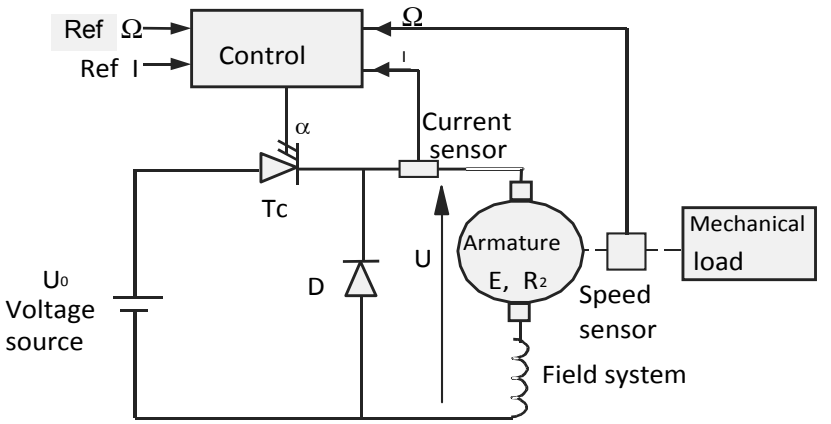

Figure 5.52. *Implementation of a series motor supplied by a chopper*

Bibliography

[BAU 92] BAUSIÈRE R., LABRIQUE F., SÉGUIER G., *Les convertisseurs de l'électronique de puissance. La conversion continu-continu*, vol. 3, Lavoisier, Paris, 1992.

[BON 71] BONNEFILLE R., ROBERT J., *Principes généraux des convertisseurs directs d'énergie,* Dunod, Paris, 1971.

[BOU 96] BOUCHARD R.P., OLIVIER G., *Electrotechnique*, Presses Internationales Polytechniques, Montreal, 1996.

[BUH 97] BUHLER H., *Réglage de systèmes d'électronique de puissance*, vol. 1 and 2, Presses polytechniques et universitaires romandes, Lausanne, 1997.

[DUR 68] DURAND E., *Magnétostatique*, Masson, Paris, 1968.

[FOU 85] FOURNET G., *Electromagnétisme à partir des équations locales*, Masson, Paris, 1985.

[GRE 01] GRENIER D., BUYSE H., LABRIQUE F., MATAGNE E., *Electromécanique – Convertisseurs d'énergie et actionneurs,* Dunod, Paris, 2001.

[IVA 94] IVANES M., PERRET R., *Éléments de génie électrique – Connaissances de base et machines statiques*, Hermes, Paris, 1994.

[JUF 79] JUFER M., *Électromécanique,* Dunod, Paris, 1979.

[KOS 69] KOSTENKO M., PIOTROVSKI L., *Machines électriques,* vol I and II, Mir, Moscow, 1969.

[LAB 95] LABRIQUE F., SÉGUIER G., BAUSIÈRE R., "Les convertisseurs de l'électronique de puissance", *La conversion continu-alternatif,* vol. 4, Lavoisier, Paris, 1995.

[LES 81] LESENNE J., NOTELET F., SÉGUIER G., *Introduction à l'électrotechnique approfondie,* Technique and documentation, Paris, 1981.

[LEO 97] LEONHARD W., *Control of Electrical Drives*, Springer, Berlin, 1997.

[NAS 87] NASAR S.A., *Handbook of Electric Machines*, McGraw-Hill, New York, 1987.

[PER 97] PEREZ J.P., CARLES R., FLECKINGER R., *Électromagnétismes. Fondements et applications*, Masson, Paris, 1997.

[PIE 03] PIERRON G., *Introduction au traitement de l'énergie électrique*, École des mines de Paris, Les Presses, 2003.

[ROM 91] ROMBAUT C., SÉGUIER G., "Les convertisseurs de l'électronique de puissance", *La conversion alternatif-alternatif*, vol. 2, Lavoisier, Paris, 1991.

[SAI 76] SAINT-JEAN B., *Électrotechnique et machines électriques*, Eyrolles, Paris, 1976.

[SEG 92] SÉGUIER G., "Les convertisseurs de l'électronique de puissance", *La conversion alternatif-continu*, vol. 1, Lavoisier, Paris, 1992.

[SEG 77] SÉGUIER G., NOTELET F., *Électrotechnique industrielle*, Technique et documentation, Paris, 1977.

[SEG 99] SÉGUIER G., *Électronique de puissance*, Lavoisier, Paris, 1999.

Index